

**The role of Solute Carrier Family 7 Member 8 (*SLC7A8*) in adipogenesis in vitro and  
in a murine model of obesity**

Submission by

Reabetswe Pitere

Student number: 10228188

Submitted in partial fulfilment of the requirements for the degree

**Doctor of Philosophy (Medical Immunology)**



UNIVERSITEIT VAN PRETORIA  
UNIVERSITY OF PRETORIA  
YUNIBESITHI YA PRETORIA

Supervisor: Dr Melvin A. Ambele

Co-supervisor: Prof Michael S. Pepper

**2023**

# DECLARATION

UNIVERSITY OF PRETORIA

## DECLARATION OF ORIGINALITY

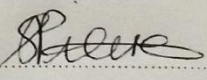
This document must be signed and submitted with every essay, report, project, assignment, dissertation and / or thesis.

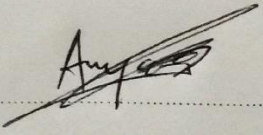
Full names of student: Reabetswe Rost Pitere

Student number: 10228188

### Declaration

1. I understand what plagiarism is and am aware of the University's policy in this regard.
2. I declare that this thesis (eg essay, report, project, assignment, dissertation, thesis, etc) is my own original work. Where other people's work has been used (either from a printed source, Internet or any other source), this has been properly acknowledged and referenced in accordance with departmental requirements.
3. I have not used work previously produced by another student or any other person to hand in as my own.
4. I have not allowed, and will not allow, anyone to copy my work with the intention of passing it off as his or her own work.

SIGNATURE OF STUDENT: 

SIGNATURE OF SUPERVISOR: 

## THESIS OUTPUTS

### Peer-reviewed publications

1. **Reabetswe R. Pitere**, Marlene B. van Heerden, Michael S. Pepper and Melvin A. Ambele. *Slc7a8* deletion is protective against diet-induced obesity and attenuates lipid accumulation in multiple organs. *Biology*. 2022; 11(2), 311; <https://doi.org/10.3390/biology11020311>
2. Priyanka Dhanraj, **Reabetswe Pitere**, Michael Pepper. The impact of obesity on the cellular and molecular pathophysiology of COVID-19. *South African Medical Journal*. 2021;111(3):211-214. DOI:10.7196/SAMJ.2021v111i2.15398.

### Manuscript/s under review

1. **Reabetswe R. Pitere**, Michael S. Pepper, Melvin A. Ambele. Investigating the possible mechanism of *Slc7a8* deletion on the prevention of adipocyte hypertrophy and its effect on plasma metabolite levels. Under review in *Genes* (Manuscript ID: genes-2302882)

### Conference presentations

#### International

1. **Reabetswe Pitere**, Marlene Van Heerdan, Melvin Ambele, Michael Pepper. Investigating the mechanism of lipid transport and plasma metabolic profile in Solute Carrier Family 7 Member 8 (SLC7A8) knockout mice. 14th International Congress of Human Genetics (Cape Town, 22nd February - 26th February 2023).
2. **Reabetswe Pitere**, Marlene Van Heerdan, Melvin Ambele, Michael Pepper. "Solute Carrier Family 7 Member 8 (SLC7A8) as a Potential Target for Combating Obesity". ObesityWeek 2022 (San Diego, 1st November - 4th November 2022).

3. **Reabetswe Pitere**, Melvin Ambele, Michael Pepper. The role of the *SLC7A8* gene in a murine model of diet-induced obesity". 13th Conference of the African Society of Human Genetics & 1st Conference of the Tanzania Society of Human Genetics (Virtual conference, 30th August – 5th September 2021).

### **National**

1. **Reabetswe Pitere**, Melvin Ambele, Michael Pepper. The title was "The role of the *SLC7A8* gene in a murine model of diet-induced obesity". 18th Biennial Congress of the Southern African Society for Human Genetics (Cape Town, 3rd – 6th August 2019).

## DEDICATION

To my day ones, my clan, my being: Mama, Papa, Mpho, Olerato and Rakgadi. Motho ke motho ka batho - I am because you are. Thank you for being my source of inspiration. Your unwavering love and support have carried me through this journey, ke le rata ke sa ikhutse. To my friends, thank you for walking this journey with me; the fun, the laughter and sometimes the tears have made this road feel short – ke leboga go menagane... le kamoso. I love you all!

Pula!

## ACKNOWLEDGEMENTS

I would like to express my deepest gratitude to the following individuals and organisations who have contributed immensely to this body of work:

- My supervisors, Dr Melvin Ambele and Prof Michael Pepper. Thank you for your unwavering support, guidance, patience, lessons, and commitment. Your leadership and expertise have led me and the project to this point and for that, I am utterly grateful.
- Muchavengwa Chovheya and Ilse van Rensburg at the Onderstepoort Veterinary Animal Research Unit (OVARU), for assisting with animal care, housing, and experiments.
- Mrs Marlene B. van Heerden and Rene Sutherland at the Department of Oral and Maxillofacial Pathology for all your assistance with tissue processing.
- The Department of Anatomy for kindly allowing us to use their facilities, including the light microscope.
- Dr Luyanda Kwofie at the Department of Immunology for assisting with the ELISA and TaqMan assays.
- Dr Chrisna duRandt at the Institute for Cellular and Molecular Medicine for always availing herself to assist with flow cytometry, quantitative PCR, cell culture and many other laboratory-related queries.
- All my colleagues at the Institute for Cellular and Molecular Medicine for the constant support, laughter, and love.
- To all the funding bodies; this project would not have been possible without your support
  - National Research Foundation (NRF) Competitive Support for Unrated Researchers (NRF CSUR)
  - National Health Laboratory Service Development Grant (NHLS development grant)
  - Institute for Cellular and Molecular Medicine
  - South African Medical Research Council (SAMRC) University Flagship Project
  - SAMRC Extramural Unit for Stem Cell Research and Therapy
  - NRF Postgraduate Scholarships
  - University of Pretoria Postgraduate bursaries
  - Ninety-One bursary

## ABSTRACT

Obesity is a pandemic affecting both adults and children with an increasing annual prevalence. Adipogenesis, a process in which adipocyte precursors differentiate into mature adipocytes, is considered an important process in identifying molecular determinants that could be targeted to modulate lipid accumulation and adipocyte hypertrophy, thereby combating obesity. Over the past two decades various studies have been conducted to investigate genes that are central to the adipogenesis process. The one limitation has been that most of the studies used animal models and cell lines for this purpose which may possibly be different to how the process is regulated in humans. To overcome this challenge, Ambele et al., 2016 performed an in vitro transcriptome analysis of human adipose-derived stromal cells (ASCs) undergoing adipogenic differentiation. Various genes at various phases of differentiation were identified but one gene of interest was the *SLC7A8* which was transiently expressed and was highly upregulated in the early phases of adipogenesis. The *SLC7A8* gene encodes LAT2 which is a neutral amino acid transporter. It belongs to a superfamily of proteins that have been implicated in obesity and/or adipogenesis. Since *SLC7A8* had not been previously described in the context of adipogenesis and obesity, -it was necessary to elucidate its function in this context using a murine model of diet-induced obesity (DIO). Wildtype and knockout *Slc7a8* mice fed on high-fat and control diets were monitored over a 14-week period and various analyses were performed at different time points. Further, human ASCs were differentiated into mature adipocytes in the presence/absence of 2-aminobicyclo-(2,2,1)-heptane-2-carboxylic acid (BCH), an inhibitor of LAT2/SLC7A8. The results obtained from the study showed that in conditions of DIO, *Slc7a8* knockout mice had significantly reduced weight gain, improved glucose tolerance, reduced inflammation due to macrophage infiltration and decreased adipocyte hypertrophy in different adipose depots when compared with the wildtype. Lipid accumulation in other peripheral non-lipid storage tissues and organs such as the liver was reduced in the knockout model. Further, the possible mechanism of hypotrophy prevention in *Slc7a8* knockout mice was investigated by measuring the expression of genes involved in lipid transport and metabolism and the effect on different plasma metabolites. The observations demonstrated that attenuation of adipocyte hypertrophy in knockout mice differed across the adipose tissue depots, i.e., hypotrophy in the perigonadal (pWAT) and brown adipose tissues (BAT) is due to increased lipolysis, in addition to browning (in BAT), with reduced lipid uptake in the mesenteric adipose tissue (mWAT). Adipocyte hypotrophy in *Slc7a8* knockout mice resulted to a

significantly lower and higher leptin and adiponectin levels, respectively, as well as reduced plasma levels of the proinflammatory cytokines IL- $\alpha$ , IL-6, IL-7, MIP-1 $\alpha$ , and elevated levels of the anti-inflammatory cytokines IL-5, IL-13, and G-CSF in comparison to the wildtype. The inhibition of SLC7A8 function in human ASCs undergoing adipogenic differentiation led to reduced adipogenic capacity with a reduction in lipid droplet formation in mature adipocytes. This was accompanied by downregulation of important adipogenic genes such as *PPARY*, *FABP4* and *CD36* in response to SLC7A8 function inhibition. Moreover, the timing of inhibition of SLC7A8 function appeared to be critical as inhibition on the day of induction (day 0) suppressed white adipogenesis while inhibition on day 3 post adipogenic induction both suppressed white adipogenesis and promoted white adipose tissue browning activity through increase expression of *PRDM16*. Overall, this study demonstrates that *SLC7A8* is important in obesity development and that its function is important in the production and maturation of adipocytes. Furthermore, the results suggest that *SLC7A8* may serve as a potential therapeutic target for anti-obesity drug development with great promise for improving metabolic health.

Keywords: SLC7A8, obesity, high-fat diet, adipogenesis, adipocyte hypertrophy, adipose tissue, inflammation, gene expression, adipose-derived stromal cells, adipogenic differentiation



# TABLE OF CONTENTS

DECLARATION.....	i
THESIS OUTPUTS .....	ii
Peer-reviewed publications.....	ii
Manuscript/s under review .....	ii
Conference presentations.....	ii
DEDICATION .....	iv
ACKNOWLEDGEMENTS .....	v
ABSTRACT .....	vi
TABLE OF CONTENTS.....	viii
LIST OF FIGURES .....	xii
LIST OF TABLES .....	xiv
LIST OF ABBREVIATIONS.....	xv
Chapter 1.    General Introduction .....	1
1.1    Problem statement and rationale for study.....	1
1.1.1    The <i>SLC7A8</i> gene .....	2
1.2    Research questions and hypotheses.....	3
1.2.1    Research question .....	3
1.2.2    Hypotheses .....	3
1.3    Aims and objectives.....	3
1.3.1    Aim.....	3
1.3.2    Objectives .....	4
1.4    General methodology.....	4
1.4.1    Ethical approval .....	4
1.4.2    Mouse acclimatisation and breeding .....	4
1.4.3    DNA extraction and genotyping .....	5
1.4.4    Agarose gel electrophoresis .....	7
1.4.5    Study design.....	8
1.5    Thesis layout.....	9
Chapter 2.    Literature review .....	10
2.1    Causes of obesity.....	10
2.1.1    Environmental/lifestyle factors.....	11
2.1.2    Genetics and epigenetic factors .....	11
2.1.3    Gut microbiome.....	13
2.2    Therapeutic options for obesity .....	13

2.2.1	Lifestyle modifications.....	13
2.2.2	Pharmacological interventions.....	13
2.2.3	Bariatric surgery .....	14
2.2.4	Faecal microbiome transplant.....	14
2.3	Adipose tissue types and their function in obesity .....	15
2.4	Changes in plasma biochemistry seen in obesity .....	16
2.5	The role of Solute Carrier transporters in obesity and/or adipogenesis.....	19
2.6	Adipogenesis and obesity .....	21
2.7	Animal models of obesity .....	23
2.8	Rationale for study .....	24
2.9	References .....	24
Chapter 3.	<i>Slc7a8</i> deletion is protective against diet-induced obesity and attenuates lipid accumulation in multiple organs .....	38
3.1	Abstract .....	39
3.2	Introduction.....	40
3.3	Materials and methods .....	42
3.3.1	Animals .....	42
3.3.2	Histology and immunohistochemistry of mouse tissues and organs.....	42
3.3.3	Statistical and image analyses.....	43
3.4	Results .....	44
3.4.1	Deficiency in <i>Slc7a8</i> protects against diet-Induced Obesity .....	44
3.4.2	Deficiency in <i>Slc7a8</i> Has No Effect on Glucose and Insulin Metabolism but Significantly Improves Glucose Tolerance When on HFD.....	46
3.4.3	<i>Slc7a8</i> Deletion Attenuates Adipocyte Hypertrophy in White and Brown Adipose Depots...	47
3.4.4	Deletion of <i>Slc7a8</i> Reduces Liver Steatosis in Diet-Induced Obese Mice .....	51
3.4.5	Deficiency in <i>Slc7a8</i> Decreases Lipid Accumulation in Gastrocnemius Muscle .....	52
3.4.6	Deficiency in <i>Slc7a8</i> Reduces Accumulation of Epicardial Adipose Tissue.....	53
3.4.7	Deficiency in <i>Slc7a8</i> Reduces Lipid Accumulation in the Ganglion Layer in Diet-Induced Obese Mice	54
3.4.8	Deficiency in <i>Slc7a8</i> Reduces Lipid Accumulation in the Kidney.....	55
3.4.9	Deficiency in <i>Slc7a8</i> Reduces Adipose Tissue Accumulation in the Lungs .....	55
3.4.10	Deficiency in <i>Slc7a8</i> Reduces White Adipose Tissue Inflammation in DIO .....	56
3.4.11	Deficiency in <i>Slc7a8</i> Reduces Inflammation in the Liver .....	58
3.4.12	Deficiency in <i>Slc7a8</i> Has No Effect on the Presence of Macrophages in the Kidney or Gastrocnemius Muscle in DIO .....	58
3.5	Discussion .....	59
3.6	Conclusions.....	63

3.7	Supplementary data .....	64
3.7.1	Supplementary methods .....	64
3.7.2	Supplementary figures .....	65
3.8	References .....	71
Chapter 4. Investigating the possible mechanism of <i>Slc7a8</i> deletion on the prevention of adipocyte hypertrophy and its effect on plasma metabolite levels .....		75
4.1	Abstract .....	76
4.2	Introduction.....	77
4.3	Materials and Methods .....	79
4.3.1	Animal model.....	79
4.3.2	RNA isolation and RT-qPCR.....	80
4.3.3	Measurement of plasma hormones and lipid .....	81
4.3.4	Measurement of plasma chemokines and cytokines .....	81
4.3.5	Statistical analysis.....	82
4.4	Results .....	82
4.4.1	Expression of genes involved in lipid metabolism and adipogenesis across various adipose tissue depots.....	82
4.4.2	Plasma leptin .....	85
4.4.3	Plasma adiponectin .....	86
4.4.4	Plasma total cholesterol .....	86
4.4.5	Effect of <i>Slc7a8</i> deletion on the kinetics of cytokine and chemokine production as measured in plasma <sup>87</sup>	
4.5	Discussion .....	94
4.6	Conclusions.....	97
4.7	Supplementary data .....	98
4.8	References .....	100
Chapter 5. Inhibition of SLC7A8 function decreased adipogenic differentiation capacity of human adipose derived stromal/stem cell.....		105
5.1	Abstract .....	106
5.2	Introduction.....	107
5.3	Materials and methods .....	108
5.3.1	Ethics statement.....	108
5.3.2	Adipocyte isolation .....	108
5.3.3	Microscopy imaging of differentiated adipocyte .....	111
5.3.4	RNA isolation and RT-qPCR.....	113
5.3.5	Statistical analysis.....	114
5.4	Results .....	114

5.4.1	ASC characterisation and adipocyte differentiation.....	114
5.4.2	Semi-quantification of lipid droplet formation .....	116
5.4.3	RT-qPCR .....	117
5.5	Discussion .....	119
5.6	References .....	122
Chapter 6.	General discussion and conclusion.....	125
6.1	Discussion .....	125
6.2	Conclusion .....	127
6.3	Limitations of the study.....	127
6.4	Future studies.....	128
6.5	References .....	129
Appendix 1.	Research ethics certificate .....	131
Appendix 2.	Animal ethics certificate.....	132
Appendix 3.	Proof of manuscript submission.....	134

## LIST OF FIGURES

Figure 1-1: Agarose gel electrophoresis image depicting the different genotypes. ....	8
Figure 1-2: A summary of the study design. ....	9
Figure 3-1: Effect of <i>Slc7a8</i> deletion on body weight and caloric intake. ....	45
Figure 3-2: Effect of genotype on glucose tolerance and insulin sensitivity tests. ....	46
Figure 3-3: Glucose tolerance and insulin sensitivity tests of animals on experimental diet. ....	47
Figure 3-4: Adipocyte size distribution across the various adipose tissue depots. ....	51
Figure 3-5: Lipid accumulation in the liver. ....	51
Figure 3-6: Effect of <i>Slc7a8</i> deletion on adipose tissue accumulation and myocyte atrophy in gastrocnemius muscle. ....	53
Figure 3-7: Effect of <i>Slc7a8</i> on epicardial adipose tissue accumulation in the heart. ....	54
Figure 3-8: Effect of <i>Slc7a8</i> deletion on lipid droplet accumulation in brain tissue. ....	54
Figure 3-9: Effect of <i>Slc7a8</i> deletion on lipid accumulation in the kidneys. ....	55
Figure 3-10: Effect of <i>Slc7a8</i> deletion on lipid accumulation in the lungs. ....	55
Figure 3-11: Effect of <i>Slc7a8</i> deletion on macrophage infiltration in adipose tissue. ....	57
Figure 3-12: Effect of <i>Slc7a8</i> deletion on the presence of macrophages in the liver. ....	58
Figure 3-13: Effect of <i>slc7a8</i> on macrophage infiltration profiles of the kidney and gastrocnemius muscle. ....	59
Figure 4-1: Effect of <i>Slc7a8</i> deletion on gene expression profiles in perigonadal, mesenteric and brown adipose depots. ....	84
Figure 4-2: Effect of <i>Slc7a8</i> deletion on plasma leptin concentrations. ....	85

Figure 4-3: Effect of <i>Slc7a8</i> deletion on plasma adiponectin levels. ....	86
Figure 4-4: Effect of <i>Slc7a8</i> deletion on plasma total cholesterol concentrations. ....	87
Figure 4-5: Effect of <i>Slc7a8</i> deletion on plasma cytokine production.....	93
Figure 5-1: Nomenclature of adipocyte-derived stromal cell (ASC) cultures. ....	109
Figure 5-2: Inhibition of SLC7A8 function with BCH treatment in differentiating ASCs.....	111
Figure 5-3: The fluorescent microscopy images of the differentiated adipocytes.....	112
Figure 5-4: Immunophenotype data of the ASCs. ....	115
Figure 5-5: Microscopic images of ASCs differentiated into adipocytes. ....	116
Figure 5-6: Semi-quantification of number of lipid droplets formed in differentiated adipocytes.....	117
Figure 5-7: Gene expression in adipogenic differentiated BCH-treated ASCs. ....	118

## LIST OF TABLES

Table 1-1: The components, concentrations and volumes used to extract DNA from the mouse tail tissues.....	5
Table 1-2: The oligonucleotide sequences used to detect the Slc7a8 genotypes in mice.....	6
Table 1-3: The components, concentrations and volumes used to prepare the PCR reaction to identify the Slc7a8 genotypes in the mice.....	6
Table 1-4: The thermal cycling conditions used to amplify the mice DNA to determine Slc7a8 genotypes.....	7

## LIST OF ABBREVIATIONS

%	Percent
+3DI BCH	BCH treatment three days after induction
-3DI BCH	BCH treatment three days before adipogenic induction
ANOVA	Analysis of variance
AP2	Adipocyte fatty-acid binding protein
ARHL	Age-related hearing loss
ASC	Adipose-derived stromal cell
ATGL (Human)	Adipocyte triglyceride lipase - human
Atgl (Mouse)	Adipocyte triglyceride lipase - mouse
ATGL	Adipose triglyceride lipase
AUC	Area under curve
AXIN2	Axis inhibition protein 2
BAT	Brown adipose tissue
BCAA	Branched-chained amino acid
BCH	2-Aminobicyclo-(2,2,1)-heptane-2-carboxylic acid
BMI	Body mass index
BMP4	Bone morphogenetic protein 4
Bp	Base pairs
°C	Degree Celsius



C/EBP $\alpha$	CCAAT/enhancer-binding protein alpha
C/EBP $\beta$	CCAAT/enhancer-binding protein beta
C/EBP $\delta$	CCAAT/enhancer-binding protein delta
CD	Control diet
CD36 (Human)	Cluster of differentiation 36 - human
Cd36 (Mouse)	Cluster of differentiation 36 - mouse
cDNA	Complementary deoxyribonucleic acid
DOI BCH	BCH treatment on day 0 of adipogenic induction
DAB	3,3' Diaminobenzidine
DAPI	4',6-Diamino-2-phenylindole, dihydrochloride
DIO	Diet-induced obesity
DKK	Dickkopf
DMEM	Dulbecco's Modified Eagle's Medium
DNA	Deoxyribonucleic acid
DPX	Distyrene, plasticiser, xylene
EDTA	Ethylenediaminetetraacetic acid
EPEC	Enteropathogenic <i>Escherichia coli</i>
EPO	Erythropoietin
ER+	Oestrogen receptor positive
EtBr	Ethidium bromide
FABP4 (Human)	Fatty acid binding protein 4 - human

Fabp4 (Mouse)	Fatty acid binding protein 4 - mouse
FBS	Foetal bovine serum
FDA	Food and Drug Administration
FFA	Free-fatty acid
FFPE	Formalin fixed paraffin embedded
FMT	Faecal microbiome transplant
g	Gram
GADPH	Glyceraldehyde-3-phosphate dehydrogenase
G-CSF	Granulocyte colony stimulating factor
GLUT4	Glucose transporter type 4
GM-CSF	Granulocyte-macrophage colony stimulating factor
GREM-1	Gremlin-1
GSH	Glutathione
GTT	Glucose tolerance test
H&E	Haemotoxylin and eosin
HFD	High-fat diet
HRP	Horse radish peroxidase
ICMM	Institute for Cellular and Molecular Medicine
IGF2	Insulin-like growth factor 2
IGT	Impaired glucose tolerance
IL-10	Interleukin-10

IL-4	Interleukin-4
IL-6	Interleukin-6
INF- $\gamma$	Interferon gamma
IP-10	Interferon- $\gamma$ inducible protein 10
IRS-1	Insulin receptor substrate-1
IST	Insulin sensitivity test
iWAT	Inguinal subcutaneous white adipose tissue
KC	Keratinocyte chemoattractant
kcal	Kilocalories
kg/m <sup>2</sup>	Kilogram per square meter
KO	Knockout
KOCD	Knockout mice on control diet
KOHFD	Knockout on high-fat diet
LAT1	Large amino acid Transporter 1
LAT2	Large neutral amino acid transporter small subunit
LDL	Low-density lipoprotein
L-DOPA	Levodopa
LEP	Leptin
LEPR	Leptin receptor
LPI	Lysinuric protein intolerance
LPL	Lipoprotein lipase

MAIT	Mucosal-associated invariant T (MAIT)
MC4R	Melanocortin 4 receptor
MCP-1	Monocyte chemoattractant protein 1
mg/g	Milligram per gram
MIP-1 $\alpha$	Macrophage inflammatory protein 1 alpha
MIP-1 $\beta$	Macrophage inflammatory protein 1 beta
MIP-2	Macrophage inflammatory protein 2
miRNA	MicroRNA
mM	Millimolar
mRNA	Messenger RNA
MSC	Mesenchymal stem cell
mTORC1	Mammalian target of rapamycin complex 1
mU/g	Milliunits per gram
mWAT	Mesenteric white adipose tissue
NAFLD	Non-alcoholic fatty liver disease
ng/ $\mu$ l	Nanogram per microlitre
NH <sub>4</sub> OH	Ammonium hydroxide
OVARU	Onderstepoort Veterinary Animal Research Unit
PCR	Polymerase chain reaction
PCSK1	Proprotein convertase subtilisin/kexin Type 1
PDGF- $\alpha$	Platelet-derived growth factor alpha

PDGF-β	Platelet-derived growth factor beta
Pen/strep	Penicillin/streptomycin
pH	Potential hydrogen
PPARY (Human)	Peroxisome proliferator-activated receptor γ - human
<i>Pparγ</i> (Mouse)	Peroxisome proliferator-activated receptor γ - mouse
PRDM16	PR domain containing 16
pWAT	Perigonadal white adipose tissue
RANTES	Regulated on activation normal T cell expressed and secreted
RIST	Rapid insulin sensitivity test
RNA	Ribonucleic acid
RT-qPCR	Reverse transcriptase quantitative polymerase chain reaction
SAT	Subcutaneous adipose tissue
SEM	Standard error of mean
SLC	Solute Carrier
SLC3A2	Solute carrier family 3 member 2
SLC7A10	Solute carrier family 7 member 10
SLC7A11	Solute carrier family 7 member 11
SLC7A5	Solute carrier family 7 member 5
SLC7A8 (Human)	Solute carrier family 7 member 8 - human
<i>Slc7a8</i> (Mouse)	Solute carrier family 7 member 8 - mouse
SMAD4	SMAD family member 4

STEC	Shigatoxin-producing <i>Escherichia coli</i>
SVF	Stromal vascular fragment
T2D	Type 2 diabetes
TAE	Tris-Acetate-EDTA
TNF- $\alpha$	Tumor necrosis factor alpha
Tris-HCL	Tris (hydroxymethyl) aminomethane hydrochloric acid
<i>UCP1</i> (Human)	Uncoupling protein 1 - human
Ucp1 (Mouse)	Uncoupling protein 1 - mouse
UP	University of Pretoria
UV	Ultraviolet
V	Volts
VAT	Visceral adipose tissue
WAT	White adipose tissue
WHO	World Health Organization
WISP	WNT1-inducible-signalling pathway protein 2
WNT	Wing-less related integration site
WOF	World Obesity Federation
WT	Wildtype
WTCD	Wildtype mice on control diet
WTHFD	Wildtype mice on high-fat diet
ZNF423	Zinc-finger protein 423

## **Chapter 1. General Introduction**

Obesity is a chronic, multifactorial pandemic, affecting over 1 billion people globally; at least 650 million adults, 39 million children and 340 million adolescents<sup>1</sup>. The prevalence of obesity is increasing progressively, and it is postulated that at least 167 million new cases of overweight obesity will be reported by 2025<sup>1</sup>. The primary defects in obesity and obesity-related comorbidities are adipocyte and adipose tissue expansion<sup>2</sup>. Expansion of adipose tissue in obesity occurs either by hypertrophy, an increase in adipocyte size or hyperplasia, an increase in adipocyte number<sup>3</sup>. Adipogenesis is a process in which new adipocytes are formed and it is thus, a result of adipose tissue hyperplasia<sup>3-4</sup>. Adipose tissue dysfunction can be caused by many factors including adipocyte hypertrophy, leading to a range of metabolic complications, chronic inflammation, and disruptions in energy homeostasis<sup>5-6</sup>. Therefore, it is important to understand the molecular mechanisms underlying adipogenesis as this may aid in resolving the surge of obesity.

### **1.1 Problem statement and rationale for study**

Many research studies conducted to further understand the process of adipogenesis make use of preadipocyte cells and cell lines from animal models such as mice to identify molecular factors affecting this process<sup>7-10</sup>. This may sometimes pose a potential challenge as adipogenic differentiation process in the mice cell lines may not entirely reflect what occurs in human cells. Although mice share a majority of their protein-coding sequence with humans, the two organisms still differ significantly in their cellular and regulatory mechanisms, and much still remains to be uncovered in a systemic comparison at the cellular level of both organisms<sup>11</sup>. Using primary cells or cell lines derived from human tissues to identify molecular factors involved in adipogenesis is thus pertinent as this may provide a more accurate representation of adipogenesis in the human body.

A previous study in our lab at the Institute for Cellular and Molecular Medicine (ICMM), University of Pretoria, performed an unbiased genome-wide transcriptomic analysis of adipose-derived stromal cells (ASCs) isolated from human tissue undergoing adipogenic differentiation over a period of 21 days<sup>12</sup>. This led to the identification of several genes including transcription factors that shared common pathways with some obesity-related pathophysiological conditions. Another important finding was the identification of novel genes not previously described in adipogenesis

such as the Solute Carrier Family 7 Member 8 (*SLC7A8*) gene which was up-regulated from day 1 of differentiation up until day 7 and thereafter, the expression of which dropped significantly, indicating a possible role in the early stages of adipogenesis<sup>12</sup>.

### 1.1.1 The *SLC7A8* gene

The *SLC7A8* gene is localised on chromosome 14q11.2, in the lysinuric protein intolerance (LPI) critical region<sup>13</sup>. It encodes a large neutral amino acid transporter small subunit (LAT2) which is composed of 535 amino acids. It is highly expressed in the kidneys, brain, intestines, placenta, skeletal muscle, and spinal cord<sup>13-14</sup>. The protein functions to transport small and large neutral amino acids (i.e., valine, leucine, isoleucine, histidine, lysine, methionine, threonine, tryptophan, and tyrosine) across the cell membrane when associated with Solute Carrier Family 3 Member 2 (*SLC3A2*) in a heterodimer<sup>15</sup>. In addition, *SLC7A8* facilitates thyroid hormone and dopamine precursor, levodopa (L-DOPA) transport<sup>16-17</sup>. Furthermore, *SLC7A8* mediates amino acid exchange and plays a role in the reabsorption of neutral amino acids<sup>14,18</sup>.

Not many research studies have been done to investigate the role of *SLC7A8* in complex biological processes or conditions. One study has reported on a role of *SLC7A8* in age-related hearing loss (ARHL) in mice<sup>19</sup>. Also, in human patients with ARHL, rare variants were identified which either inhibited or caused tyrosine transport, correlating to the ARHL phenotype<sup>19</sup>. Another study reported that the ablation of LAT2 led to cataract formation in older female mice<sup>20</sup>. Further investigation of *SLC7A8* in a family of patients diagnosed with congenital or age-related cataract, identified a homozygous single nucleotide deletion segregating in the family<sup>20</sup>. Knockout of *Slc7a8* has also been shown to be associated with aminoaciduria, a urinary loss of small amino acids<sup>21</sup>. In a recent study, *SLC7A8* was found to be overexpressed in oestrogen receptor positive (ER+) low proliferative breast cancer tumours<sup>22</sup>. The overexpressed *SLC7A8* seem to have tumour suppressive characteristics and the authors suggested that *SLC7A8* may serve as a potential prognostic factor for the breast cancer ER+ subtype<sup>22</sup>. The important role of *SLC7A8* reported in diverse biological conditions may reflect its importance in the transport of small and large neutral amino acids that are critical in the pathophysiological development of these conditions.



Despite the reported findings on the function of *SLC7A8*, none have previously described the role of this gene in the context of adipogenesis and/or obesity, for which expression of this gene was identified for the first time to play a key role in adipogenesis in vitro.

## **1.2 Research questions and hypotheses**

### **1.2.1 Research question**

Does the *SLC7A8* gene product, identified to be an important molecule in adipogenesis in vitro, play a significant role in obesity development?

### **1.2.2 Hypotheses**

*1.2.2.1 Null hypothesis: The SLC7A8 gene is not a significant molecular role player in obesity development.*

*1.2.2.2 Alternate hypothesis: The SLC7A8 gene is a significant molecular role player in obesity development.*

## **1.3 Aims and objectives**

### **1.3.1 Aim**

To investigate the functional role of the *SLC7A8* gene in obesity development using a murine model of diet-induced obesity.

### 1.3.2 Objectives

1.3.2.1 *To assess weight gain or loss, glucose tolerance and insulin sensitivity in Slc7a8 knockout and wildtype mice fed with either high-fat or control diets over a 14-week period.*

1.3.2.2 *To perform histological and immunohistochemical analyses on various tissues isolated from Slc7a8 knockout and wildtype mice fed on both high-fat and control diets.*

1.3.2.3 *To evaluate plasma analytes (i.e., leptin, adiponectin, insulin, cholesterol, and cytokines) in Slc7a8 knockout and wildtype mice fed on both high-fat and control diets.*

1.3.2.4 *To determine the expression levels of genes involved in adipocyte differentiation, lipid metabolism and lipid transport in mice tissues.*

1.3.2.5 *To differentiate adipose-stromal cells (ASCs) to mature adipocytes and to perform gene expression analysis on the differentiating cells.*

## 1.4 **General methodology**

This section outlines the basic methodology employed in this study. A more detailed and comprehensive description of the methodologies used to achieve the different study objectives will be provided in the subsequent chapters which are presented as published articles or manuscript format.

### 1.4.1 Ethical approval

This study was approved by the Research Ethics Committee, Faculty of Health Sciences, and the Animal Ethics Committee at the University of Pretoria (Ref. No.: 474/2019).

### 1.4.2 Mouse acclimatisation and breeding

*Slc7a8* (*Slc7a8<sup>tm1Dgen</sup>*) heterozygous and wildtype mice of the C57BL/6J strain were obtained from The Jackson Laboratory (*Bar Harbor, Maine, United States of America*). The mice were housed at the Onderstepoort Veterinary Animal Research Unit (OVARU) at the University of Pretoria (UP) and qualified Veterinarians and Veterinary Technologists were present to confirm the health

status of the mice to ensure that only healthy mice were admitted into the study. Prior to the start of the study, the mice were acclimatised for a period of 21 days at a room temperature between 22°C and 24°C and a humidity ranging between 40% and 60%. The mice were kept in ventilated housing cages sourced from Tecniplast (*Tecniplast S.p.A, Buguggiate, Varese, Lombardy, Italy*). Wood shavings were used as bedding and standard enrichment aids such as tissues, egg containers and toilet rolls were sterilised in an autoclave prior to being placed in the cages. Reverse osmosis water and erythropoietin (EPO) diet (composed of 43.90% protein, 29.26% moisture, 6.10% fat, 14.63% fibre, 4.39% calcium, 1.71% phosphorus (*Epol Pretoria Mill, Pretoria Industrial, Pretoria, 0183*)) were provided to animals *ad libitum*. Cage changing was conducted weekly for the duration of the study to make sure that the microenvironment conditions of the mice were hygienic to prevent any health complications that may arise. Mice were mated and allowed to breed to produce pups from which the *Slc7a8* wildtype (WT) and knockout (KO) genotypes were selected through genotyping.

### 1.4.3 DNA extraction and genotyping

#### 1.4.3.1 DNA extraction

A tail biopsy of the mouse pups was used to extract genomic DNA (gDNA). The KAPA Mouse Genotyping Kit (*Kapa Biosystems, Wilmington, Massachusetts, United States of America*) and the KAPA Express Extract Protocol (*Kapa Biosystems, Wilmington, Massachusetts, United States of America*) was used. The extractions were performed in a 100 microlitre (µl) volume and they were set up as follows with the polymerase chain reaction (PCR) components outlined in Table -1.

**Table 1-1:** The components, concentrations and volumes used to extract DNA from the mouse tail tissues.

Component	Final concentration	100 µl reaction
PCR grade water	-	88 µl
10 x KAPA Express Extract buffer	1 x	10 µl
1U/µl KAPA Express Extract enzyme	2 U/µl	2 µl
Mouse tail tissue (biopsy)	2mm section	Add section to solution

The PCR reaction was performed in the Applied Biosystems 9700 thermal cycler (*Applied Biosystems, Waltham, Massachusetts, United States, United States of America*). Enzymatic lysis

was conducted at 75°C for 10 minutes followed by enzymatic inactivation at 95°C for 5 minutes. The extracted gDNA was diluted 10-fold in 10 micromolar (mM) TRIS-HCL at a pH of 8.5.

#### 1.4.3.2 Genotyping

To determine the *slc7a8* wildtype, heterozygous and knockout genotypes, the gene-specific primer sequences in Table 1-2 recommended by The Jackson Laboratory were used for genotyping. The oligonucleotides sequenced used in the study were synthesised by Integrated DNA Technologies (IDT) (*Integrated DNA Technologies, Coralville, Iowa, United States of America*).

**Table 1-2:** The oligonucleotide sequences used to detect the *Slc7a8* genotypes in mice.

Primer orientation	Target allele	Primer sequence
Forward	Wildtype	5'-CAAATGCCAGCTGTCCTGACCTCAC-3'
Forward	Knockout	5'-GGGTGGGATTAGATAAATGCCTGCTCT-3'
Common reverse	Wildtype and knockout	5'-CAGACTTAGGGATGGTGACGCCTAG-3'

The PCR amplification reaction was performed using the KAPA2G Fast Genotyping buffer (*Kapa Biosystems*) in a total volume of 25 µl using the Applied Biosystems 9700 thermal cycler. The components of PCR used for the reaction are shown in Table 1-3, while the thermal cycling conditions are detailed in Table 1-4. The primer concentrations used for the reaction were 10 µM and the amplicon concentrations were 10 nanograms per microlitres (ng/µl). The amplicon concentrations were quantified using the Nanodrop ND-1000 Spectrophotometer (*Thermo Fisher Scientific, Waltham, Massachusetts, United States of America*).

**Table 1-3:** The components, concentrations and volumes used to prepare the PCR reaction to identify the *Slc7a8* genotypes in the mice.

PCR component	Final concentration	25 µl reaction
PCR grade water	n/a	6.5 µl
KAPA2G Fast Genotyping buffer	1 X	12.5 µl
10 µM Wildtype forward primer	0.5 µM	1.25 µl
10 µM Mutant forward primer	0.5 µM	1.25 µl
10µM Common reverse primer	0.5 µM	2.5 µl
DNA amplicon	10 ng/µl	1 µl

The thermal cycling conditions used for the amplification were as follows:

**Table 1-4:** The thermal cycling conditions used to amplify the mice DNA to determine Slc7a8 genotypes.

Conditions	Temperature (°C)	Time
Initial denaturation	95	3 mins
Denaturation	95	15 sec
Annealing	60	15 sec
Extension	72	15 sec
Final extension	72	2 min
Hold	10	∞

#### 1.4.4 Agarose gel electrophoresis

After amplification, 10 µl of each amplicon was separated on a 2% agarose gel stained with Ethidium Bromide (EtBr) solution, Molecular Grade (*Promega Corporation, Madison, Wisconsin, United States of America*). The amplicons were separated using gel electrophoresis alongside a Thermo Scientific FastRuler Low Range DNA ladder with a size range of 50 base pairs (bp) to 1500bp (*Thermo Fisher Scientific, Waltham, Massachusetts, United States of America*). Electrophoresis was performed in 1xTAE (Tris-Acetate-Ethylenediaminetetraacetic acid (EDTA)) buffer (*ThermoFischer Scientific, Waltham, Massachusetts, United States of America*) at 120 volts (V) for 40 minutes. The gel was viewed under ultraviolet (UV) light using the Molecular Imager Gel Doc XR System (*Bio-Rad, Hercules, California, United States of America*). The expected amplicon sizes were 206 bp for the wildtype allele and 390bp for the knockout allele. Only wildtype and knockout mice for the *Slc7a8* gene were used in the study. Figure 1-1 shows the expected *Slc7a8* genotypes and amplicon sizes; lanes 1 and 3 indicate the heterozygous genotype with both the wildtype and knockout allele present with sizes 206bp and 390bp, respectively. Lane 2 depicts the homozygous wildtype genotype with a single band of 206bp size and lane 4 shows the homozygous knockout genotype with a single band size of 390bp.

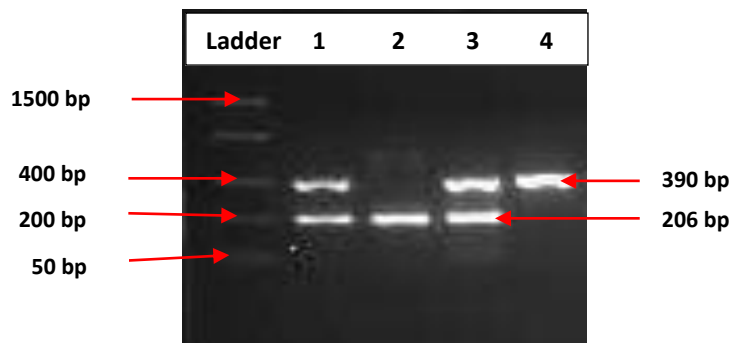


**Figure 1-1: Agarose gel electrophoresis image depicting the different genotypes.** Lanes 1 and 3 are indicative of the heterozygous genotype, with amplicon sizes of 206bp and 290bp representing the wildtype and knockout alleles, respectively. Lane 2 is the homozygous wildtype genotype illustrated by the 206bp band. Lane 4 is the homozygous knockout genotype characterised by the single 390bp band.

#### 1.4.5 Study design

After genotyping, 48 WT and 48 KO *Slc7a8* mice (8 weeks old) were selected and used in the study. The sample comprised of 30 wildtype males and 18 wildtype females, and 21 knockout females and 27 knockout males. For each genotype, 24 mice were fed with either a control diet with 10% kilocalories (kcal) of fat and energy of 3.84 kcal/g (CD; D12450J) or a high- fat diet with 60% kcal of fat and energy of 5.61 kcal/g (HFD; D12492) from Research Diets (*Research Diets, Inc., New Brunswick, New Jersey, USA*) for a period of 14 weeks, with different termination time points at weeks 5, 8, 10 and 14. At every termination time point, 6 mice from each group were terminated and analysed further as described in the chapters ahead. The nomenclature used to specify the different genotypes on either a CD or HFD were WTCD (wildtype mice on control CD), WTHFD (wildtype mice on HFD), KOCD (knockout mice on control CD), and KOHFD (knockout mice on HFD). Figure 1-2 provides a summary of the study design.

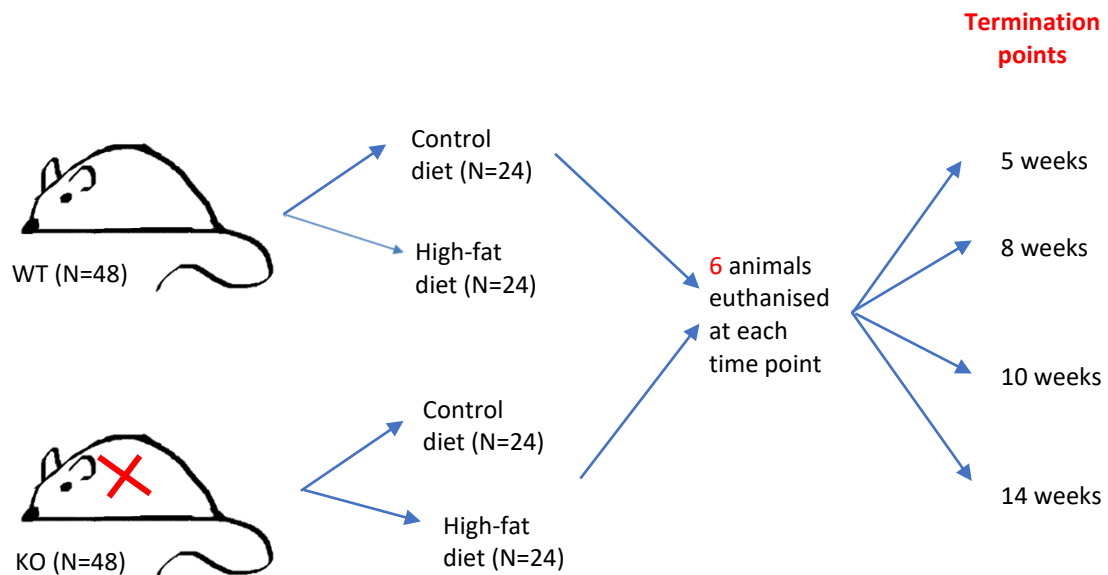


**Figure 1-2: A summary of the study design.** 48 WT and 48 KO *Slc7a8* mice were selected to be used in the study, and they were divided into four subgroups of 24 mice each. Each subgroup from both WT and KO were fed with a control or high-fat diet. Six mice from each group were euthanised at 5, 8, 10 and 14 weeks and used further analyses.

## 1.5 Thesis layout

Chapter 1 of this thesis presents the background and rationale of the study. Additionally, it provides the aim and objectives achieved in the study, and the basic methodology performed to achieve the said objectives. Chapter 2 is the literature review section which outlines the current and relevant available literature on obesity and adipogenesis in relation to the work conducted in this study. Chapter 3 presents the published data from the study which report the findings on weight, energy intake, histology, and immunohistochemistry findings. This section will address the objectives shown under Chapter 1, sections 1.3.2.1 and 1.3.2.2. Chapter 4 will present the manuscript which describes the plasma biochemistry and gene expression findings, addressing the objectives highlighted under Chapter 1, sections 1.3.2.3, 1.3.2.4 and 1.3.2.5. Finally, Chapter 5 will provide the discussion which will annotate key findings from the study and how it advances the knowledge in this field, as well as some strengths and limitations of the study. A conclusion which aims to provide a new body of knowledge by answering the research question posed in Chapter 1.2.1 will also be presented in this chapter. Furthermore, potential future work, suggestions and recommendations will be included in Chapter 5.

## Chapter 2. Literature review

Obesity is a pandemic, and its prevalence has almost tripled in the past five decades<sup>1,23</sup>. Obesity as defined by the World Health Organization [WHO], is disproportionate fat accumulation which can potentially impair one's health. Adults with a body mass index (BMI) of 25 kilograms per square meter ( $\text{kg}/\text{m}^2$ ) are regarded as overweight, while those with a BMI of 30  $\text{kg}/\text{m}^2$  or greater are regarded as obese<sup>24</sup>. The number of obesity-affected individuals is continuously increasing, and it is postulated that if the increasing trend continues, 18% of men and more than 21% of women will be affected by obesity by the year 2025<sup>24</sup>. Excessive weight gain in childhood and adolescence is also a global health concern, and its prevalence from 4% in 1975 to 18% in 2016. In 2016, at least 124 million children and adolescents were reported to have obesity<sup>24</sup>. The 2019 Atlas of Childhood Obesity by the World Obesity Federation (WOF) predicted that more than 250 million children and adolescents will be obese by 2030<sup>25</sup>. However, these predicted figures were surpassed by 2022 with nearly 380 million children and adolescents being reported as obese<sup>1</sup>.

The WHO and the Africa Health Organization (AHO) have reported that the prevalence of obesity is rising in Africa at an alarming rate<sup>26-27</sup>. Data from the AHO estimates that one in five adults and one in ten children and adolescents will be obese December 2023<sup>27</sup>. It is further estimated that the obesity prevalence in high-burden countries will range between 13.6% and 31% in adults whilst ranging between 5% and 16.5% in children and adolescents<sup>26-27</sup>. Some of the listed high-burden countries to be affected by this surge in obesity prevalence include South Africa, Zimbabwe, Eswatini, Mauritius and Libya<sup>27</sup>. AHO attributes this increase in obesity statistics to a lack of physical activity, changing modes of transportation and a shift from consuming fresh food to high-energy processed foods which are high in calories<sup>27</sup>.

### 2.1 Causes of obesity

The regulation of caloric utilisation is important in the pathogenesis of obesity. When energy intake is equal to expenditure, body fat levels are maintained. However, increases in body mass are a consequence of a positive energy balance where the energy intake far exceeds energy expenditure, leading to weight gain and obesity development<sup>2,28</sup>. Several factors have been implicated in adipose tissue accumulation and the pathogenesis of obesity, and these include genetic and environmental/lifestyle factors<sup>5</sup>.



### 2.1.1 Environmental/lifestyle factors

The influence of westernisation and globalisation has been implicated as one of the main factors driving the increase of body weight and obesity in low to middle income and high-income countries worldwide<sup>29-30</sup>. Researchers postulate that this is due to a nutritional transition where a large shift in diet exists with many people globally abandoning traditional, local cuisines for processed foods which are associated with weight gain and chronic diseases<sup>29-30</sup>. These processed, obesogenic foods are easily accessible, inexpensive and are high in sugar, saturated fats, sodium, and refined carbohydrates while low in fibre<sup>29-30</sup>. A study conducted on approximately 3000 young adults showed that high fast food consumption correlated with increased BMI in comparison to individuals with lower fast food intake<sup>31</sup>. Furthermore, there is a global decline in water intake which is replaced by the intake of high-caloric and sugar-sweetened beverages, contributing to increasing body mass<sup>29-30</sup>. The increase in sedentary lifestyle and a decline in physical activity due to technological advances and screen media exposure contributes to maintaining an obesogenic environment<sup>32-33</sup>. Medication-induced weight gain has been noted as a side effect associated with taking certain drugs<sup>34</sup>. Antidepressants, antipsychotics, and anti-epileptic drugs (i.e., valproate) have been reported in literature to induce weight gain and sometimes transitioning to overweight or obese<sup>35-37</sup>. Corticosteroids, antidiabetic drugs and oral contraceptives are also common drugs known to cause weight gain<sup>34,38-41</sup>.

### 2.1.2 Genetics and epigenetic factors

#### 2.1.2.1 *Genetic factors*

Genetic causes of obesity can be classified as either monogenic or polygenic<sup>42</sup>. Monogenic obesity is inherited in a Mendelian pattern, and it arises due to a single gene mutation; it is described as rare, early-onset and severe. This form of obesity has a strong genetic contribution with high penetrance and little to no environmental influences<sup>42-43</sup>. Monogenic obesity emerges primarily as a result of genetic disruptions in the leptin-melanocortin signalling pathway which regulates food intake<sup>42</sup>. One of the first genes to be discovered in this pathway with a strong association to severe, early-onset obesity was leptin (*LEP*)<sup>44</sup>, which is pertinent in regulating appetite. Mutations in the leptin receptor gene (*LEPR*) were later identified and associated to obesity<sup>45</sup>. Genes which encode various components of the melanocortin pathway and resulting in severe early-onset

obesity include melanocortin 4 receptor (*MC4R*) which regulates energy, glucose and lipid homeostasis<sup>42,46-47</sup>; proopiomelanocortin (*POMC*) which regulates body weight<sup>48-49</sup> and Proprotein Convertase Subtilisin/Kexin Type 1 (*PCSK1*) which functions in processing polypeptide hormones and neuropeptides precursors<sup>50-52</sup>.

Polygenic obesity is common and has little genetic contribution, with environmental influences playing a key role in the onset of disease<sup>43</sup>. Genetic predisposition to obesity is due to several low penetrance susceptibility variants in many genes, with each variant contributing a small genetic effect to the overall obesity phenotype<sup>43,53</sup>.

#### 2.1.2.2 Epigenetic factors

Physical alterations of DNA by epigenetic modifications have been associated with obesity development<sup>53-54</sup>. Some studies reported that the duration of breastfeeding negatively correlated with DNA methylation of the *LEP* gene and childhood obesity<sup>55-56</sup>. DNA methylation levels in the adiponectin (*ADIPOQ*) gene located in the subcutaneous adipose tissue were positively associated with BMI and low-density lipoprotein (LDL) cholesterol in severely obese individuals<sup>57</sup>. Reduced expression of the insulin receptor substrate-1 (*IRS-1*) gene and increased *IRS-1* promoter methylation were seen in the subcutaneous and visceral adipose tissues of individuals with obesity. Furthermore, *IRS-1* promoter methylation was associated with waist circumference, increased body mass and glucose intolerance<sup>58</sup>. Hypomethylation of insulin-like growth factor 2 (*IGF2*) was associated with paternal obesity in newborns and it is suggested to potentially affect the health status of the child in the future<sup>59</sup>. MicroRNAs (miRNAs), which are short, noncoding RNA sequences involved in gene regulation by repressing target messenger RNA (RNA), have been implicated in obesity<sup>53,60</sup>. A childhood obesity study revealed that increasing body mass, waist circumference, body fat distribution and percentage were significantly correlated with high levels of miRNAs miR-486-3p, miR-142-3p, miR-486-5p, miR-423-5p and low levels of miR-221 and miR-28-3p<sup>61</sup>. In a separate study, circulating miR-519d, miR-122 and miR-31 were associated with significant weight gain<sup>62</sup>. A study conducted using obese rats to evaluate the expression of miRNAs in different tissues such as adipose tissue, liver and skeletal muscle showed that upregulation of miR-342-3p and 335-5p and downregulation of miR-200a and miR-200b were only observed in the white adipose tissue of these animals, suggesting that differential expression of miRNAs occurs in different cell types and may possibly affect the function of white adipose tissue in obesity<sup>63</sup>.

### 2.1.3 Gut microbiome

The link between the gut microbiome and obesity has been described in various studies. In one study, overweight or obesity was shown to be closely associated with a low bacterial diversity in the faeces<sup>64</sup>. The faecal samples showed that obese mice had a high percentage of Firmicutes and low Bacteroidetes content when compared with their non-obese, lean counterparts<sup>65</sup>. These results correspond to a twin study conducted using faecal samples, which revealed that obesity-associated genes were from Firmicutes, while lean-enriched genes were from Bacteroidetes genomes<sup>66</sup>. John and Mullin, 2016 suggest that the effect of the gut microbiota on obesity is complex and not necessarily the balance between the presence of different bacteria in the gut. They further postulate that modulating the gut microbiome through various measures such as diet, antibiotics, faecal transplantation, and surgery may aid in managing obesity<sup>67</sup>.

## **2.2 Therapeutic options for obesity**

### 2.2.1 Lifestyle modifications

Lifestyle modifications are the first-line treatment for individuals with obesity<sup>68</sup>. According to the WHO, most causes of obesity can be reversed and prevented through modifying lifestyle habits<sup>24</sup>. The WHO proposes that managing the risk of obesity development includes decreasing caloric intake from sugar and fats while increasing intake of fruits, vegetables, nuts, whole grains, and legumes. They also recommend regular physical activity for approximately 60 minutes per week for children and 150 minutes for adults<sup>24</sup>. It is suggested that people living with obesity lose approximately 5-10% of their weight through diet, physical activity, and behavioural therapy (i.e. food intake and weight monitoring, setting goals and collaboration with an interventionist)<sup>69</sup>. It is also recommended that screen time and sedentary behaviour are limited to potentially increase physical activity, and promote weight loss whilst reducing obesity risk<sup>70</sup>.

### 2.2.2 Pharmacological interventions

Guidelines recommend that pharmacological treatment be used as second-line therapy for obesity, in conjunction with lifestyle modifications<sup>71</sup>. The use of anti-obesity drugs is recommended for individuals with a BMI  $\geq 30$  or BMI  $\geq 27$  with comorbidities, who are incapable

of losing weight using lifestyle modifications alone<sup>72-74</sup>. Several drugs that can be used to manage obesity have been approved by the Food and Drug Administration (FDA) and these include Orlistat, Naltrexone-Bupropion, Liraglutide, Phentermine-Topiramate, Plenity, Setmelatonin, Tirzepatide and Semaglutide<sup>53,74-77</sup>. Some drugs (i.e., Lorcaserin, Fenfluramine, Phenylpropanolamine, Amphetamines, Rimonabant and Sibutramine) which have been previously used for obesity management have been withdrawn from the market due to clinical and safety concerns<sup>53,74,78</sup>.

### 2.2.3 Bariatric surgery

Bariatric surgery is effective in the treatment of severe obesity, and it is performed in patients with a BMI  $\geq 40\text{kg/m}^2$  or BMI  $\geq 35\text{kg/m}^2$  with comorbidities and unable to lose weight by modification of lifestyle or pharmacological treatment<sup>72-74</sup>. Research has shown that patients who undergo bariatric surgery can lose at least 20 to 35% of their body weight<sup>53,79-80</sup>. Studies have also reported that in addition to weight loss, bariatric surgery reduces chronic inflammation associated with obesity and long-term remission of type 2 diabetes in approximately 80% of the patients<sup>81-83</sup>. Significant changes in the gut microbiota following bariatric surgery were observed; these could be attributed to changes in gastric pH (potential hydrogen), status of malabsorption and metabolism of bile acids and hormones<sup>84-85</sup>.

### 2.2.4 Faecal microbiome transplant

Faecal microbiome transplant (FMT) entails transplanting faecal matter of a healthy donor to a patient, with the sole purpose of treating disease<sup>86-87</sup>. FMT has the potential to remodel the gut microbiome of the host to improve physiological function<sup>88</sup>. A study performed by transferring the human faecal microbiota of obese and lean individuals to mice fed on low-fat diet demonstrated that mice that received faecal microbiota from obese individuals had increased body weight when compared with mice that received faecal microbiome of the lean individual<sup>89</sup>. In a human study, faecal samples were collected from lean males with BMI  $\leq 23$  and transplanted in obese patients. After six weeks of infusion, insulin sensitivity was increased in the obese patients<sup>90</sup>. In 2020, however, the FDA warned against the use of FMT and the likelihood of serious adverse effects following the development of Enteropathogenic *Escherichia coli* (EPEC) and Shigatoxin-producing *Escherichia coli* (STEC) infections in several patients, and the death of two patients after FMT<sup>91</sup>.

### 2.3 Adipose tissue types and their function in obesity

Adipose tissue, primarily constituted of adipocytes, can be categorised into white adipose tissue (WAT), brown adipose tissue (BAT) and beige adipose<sup>92-93</sup>. BAT is mainly characterised by multilocular lipid droplets and numerous mitochondria which is responsible for producing heat through non-shivering thermogenesis<sup>94</sup>. It is abundant in neonates but has also been found to be metabolically active in adults. BAT in humans is in the kidneys, adrenal glands, thorax, cervical muscles, and abdomen. In rodents, the interscapular region is the major site of BAT<sup>95-96</sup>.

Beige adipose tissue has also been described in humans and rodents and is dispersed in WAT<sup>93</sup>. Beige adipocytes can differentiate from white to brown adipocytes in a process called browning. Like BAT, beige adipose tissue has high mitochondrial content and is important in thermogenesis<sup>93</sup>. WAT on the contrary is made up of large adipocytes with a single lipid droplet and consists of fewer mitochondria. WAT is also composed of stromal vascular fraction (SVF) which contains pre-adipocytes, stem cells, immune cells, endothelial cells, and fibroblasts<sup>97</sup>. The key role of WAT is to store energy in the form of triglyceride lipids and to secrete it during periods of energy deprivation<sup>2</sup>. In addition, they secrete endocrine molecules which are important in regulating metabolism<sup>92</sup>.

WAT is classified by its location in the body; subcutaneous adipose tissue (SAT) which is located beneath the skin and visceral adipose tissue (VAT) which is intra-abdominal<sup>3</sup>. VAT is comprised of omental (lies over the stomach and organs), mesenteric (on the mesentery of the intestines), gonadal (surrounding ovaries and testes), retroperitoneal (surrounding the kidneys) and epicardial (between heart and pericardium) adipose tissue<sup>92</sup>. Excessive accumulation of VAT has been implicated in obesity. In contrast, high SAT depots are most abundant in lean subjects, making up approximately 80% of all adipose tissue<sup>98</sup>. Additionally, an increase in VAT mass leads is associated with a deterioration in metabolic function and is complicit in the onset of metabolic syndrome/s compared with SAT<sup>3,92,99</sup>.

Obesity is characterised by expanding adipose tissue and when adipose tissue becomes dysfunctional, it is unable to store excess fat efficiently. This causes lipids to be deposited in non-adipose tissues such liver, heart, kidneys, and skeletal muscle; an event known as lipotoxicity<sup>2,92</sup>. This contributes to the development of metabolic syndromes such as insulin resistance<sup>2,6</sup>. Insulin

maintains blood glucose levels by prompting glucose uptake into insulin-target tissues such as adipose tissue, skeletal muscle, and liver<sup>100</sup>. A defect in the insulin signalling pathway causes an insulin resistance occurs and this results in a failure of glucose uptake to target tissues and consequently, an increase in blood glucose levels<sup>100</sup>. Obesity-related insulin resistance is key in the pathogenesis of type 2 diabetes, a chronic and persistent elevation of circulating glucose levels<sup>101</sup>. During obesity, pancreatic  $\beta$ -cells are dysfunctional and unable to secrete high enough insulin to maintain normal glucose homeostasis<sup>2,102</sup>. This, in turn, produces elevated fatty acids in plasma, preventing the efficient uptake of glucose by peripheral tissues and leading to increased hepatic glucose production and hyperglycaemia<sup>100-101</sup>. Hypertrophic adipocytes which have reached their capacity to store additional lipids are sufficient to cause insulin resistance due to defects in glucose transporter type 4 (GLUT4) signalling<sup>2</sup>. GLUT4 is a glucose transporter protein which is important in maintaining blood glucose levels. It is primarily expressed in adipose tissue and skeletal muscle and mediates insulin-stimulated glucose transport into muscle and adipose tissue<sup>103</sup>. During obesity, there are high FFA levels in circulation and a downregulation of GLUT4 in adipose tissue. This results in an impairment in insulin-stimulated glucose uptake by adipocytes and thus, hyperglycaemia<sup>103-104</sup>. Some of the obesity-associated comorbidities include dyslipidaemia, hyperlipidaemia, hypertension, cardiovascular disease, non-alcoholic fatty liver disease (NAFLD)<sup>5-6</sup>.

## **2.4 Changes in plasma biochemistry seen in obesity**

Previous research shows that adipose tissue secretes over 50 hormones and signalling proteins, collectively termed adipokines (cytokines secreted by adipose tissue), which are important in various physiological processes such as regulating energy and glucose metabolism, and immunity. Adipokines can either display pro-inflammatory or anti-inflammatory properties, contributing to insulin resistance development<sup>3,105-106</sup>.

Adipose tissue from lean individuals secretes anti-inflammatory adipokines such as interleukin 4 (IL-4), and adiponectin which play a vital role in improving insulin sensitivity<sup>3,107</sup>. IL-4 is important in regulating haematopoiesis and inflammation. It was shown to inhibit fat cell formation and lipid accumulation in adipose tissue, while promoting lipolysis. This in turn, reduces weight gain, prevents obesity development and improves insulin sensitivity<sup>108</sup>. In obesity, low levels of IL-4 have been associated with an increase in lipid accumulation and insulin resistance<sup>108-109</sup>.

Adiponectin regulates lipid and glucose metabolism, and it is present at high concentrations in lean and obese individuals at high and low concentrations, respectively. It is hypothesised that adiponectin alleviates free-fatty acids (FFA) in circulation, improving insulin sensitivity<sup>110-111</sup>. Elevated FFA levels in plasma have been shown to cause defects in the insulin signalling pathway. The low levels of adiponectin in obesity leads to high FFA concentrations thereby causing the development of insulin resistance<sup>3,111</sup>.

**2.5 In obesity, adipose tissue mainly secretes pro-inflammatory cytokines IL-6 and tumour necrosis factor- $\alpha$  (TNF- $\alpha$ ) at elevated levels. Other proinflammatory cytokines released from obese adipose tissue include MCP-1 and leptin<sup>2,105</sup>. TNF- $\alpha$  is mainly produced by adipose tissue but is secreted by many other cell types in the body. TNF- $\alpha$  levels are positively correlated to an increase in fat accumulation<sup>3,112</sup>. In human obese subjects, higher levels of TNF- $\alpha$  have been observed in plasma and adipose tissue when compared with lean subjects<sup>113</sup>. In rodent studies, TNF- $\alpha$  was shown to be overexpressed in obese mice and obese mice deficient of TNF- $\alpha$  were protected against the development of insulin resistance<sup>114</sup>. Adipocyte TNF- $\alpha$  has been previously shown to induce insulin resistance by increasing Serine/Threonine phosphorylation of the insulin receptor substrate-1 (IRS-1) which inhibits IRS-1 from interacting with the insulin receptor and thereby interfering with insulin signaling<sup>115</sup>. TNF- $\alpha$  stimulates the secretion of interleukin 6 (IL-6) by adipose tissue, liver, and skeletal muscle. In healthy, lean individuals, adipocytes account for at least one-third of circulating IL-6<sup>105</sup>. IL-6 expression in plasma and adipose tissue correlates with an increase in body mass. When adipose tissue expands, there is excessive adipocyte lipolysis and elevated levels of FFA is observed, which promotes IL-6 secretion. IL-6 expression is thus observed to be higher in individuals with obesity when compared with lean individuals<sup>2,105,112</sup>. VAT expresses at least 2-fold more IL-6 than SAT, implicating IL-6 as a potential marker of visceral adiposity<sup>116</sup>. MCP-1, a chemokine secreted by adipocytes recruits monocytes which are differentiated macrophages during adipose tissue expansion. The macrophages secrete MCP-1 to further recruit more monocytes and macrophages into adipose tissue<sup>3,117</sup>. An increase in adiposity correlates positively with expression of MCP-1, while MCP-1 levels have been seen to decrease with weight loss<sup>118</sup>. Diet-induced obese mice have been shown to display increased MCP-1 circulating levels when compared with their lean counterparts<sup>117</sup>. Leptin is another pro-inflammatory adipokine strongly associated with obesity. It is a hormone that regulates biological processes such as reproduction, body weight, appetite, and metabolism<sup>119-120</sup>. Plasma leptin levels correspond to adipose tissue mass and are thus elevated in obesity<sup>121</sup>. Previous research suggests that leptin stimulates the production of pro-inflammatory cytokines and recruits macrophages into adipose tissue in obesity-related inflammation<sup>106</sup>. Obese individuals are susceptible to developing a leptin resistance due to an excessive amount of circulating leptin levels. This impairs leptin signalling and leptin is not efficiently**



transported past the blood-brain barrier to regulate appetite and reduce weight gain<sup>106,122</sup>. In obese humans, triglycerides go past the blood-brain barrier<sup>123</sup>. In addition, leptin resistance can occur due to mutations in the leptin (*LEP*) or leptin receptor (*LEPR*) genes resulting in hyperphagia and excessive eating, which subsequently leads to severe obesity<sup>124-125</sup>. Furthermore, frameshift mutations which produce truncated LEPR protein which lacks the transmembrane or intracellular domains inhibit leptin from binding to the receptor and achieving its function, giving rise to leptin resistance and an obese phenotype<sup>126-127</sup>. Impairments in leptin signalling have also been associated to leptin resistance. Activation of inhibitors such as suppressor of cytokine signaling-3 (*SOCS3*) and protein tyrosine phosphatase 1B (*PTP1B*) interfere with leptin signalling, contributing to leptin resistance in obese subjects<sup>128-129</sup>. Selective leptin resistance has also been described in the obese phenotype. This phenomenon suggests that in some obese states such as diet-induced obesity (DIO), there is a resistance to leptin function in controlling appetite and weight loss, however, the sympathetic nerve activation and regulation of blood pressure by leptin is preserved<sup>130-132</sup>. The role of Solute Carrier transporters in obesity and/or adipogenesis

The Solute Carrier (SLC) proteins are transporters which facilitate the influx and efflux of various molecules across the intracellular and plasma membranes<sup>133</sup>. Some of the molecules transported across the membranes include sugars, amino acids, nucleotides, drugs, and vitamins<sup>133</sup>. SLC proteins exist as SLC superfamily which currently consists of over 400 genes and more than 60 families<sup>134</sup>. Categorisation of genes into the SLC superfamily is based on biological function, while members of each family harbour approximately 20 to 25% sequence similarity<sup>133-134</sup>. The SLC proteins are highly expressed in the liver, kidneys, intestines, and the brain<sup>133-135</sup>. The expression of these proteins in metabolically active organs identifies their role in metabolism and their association to diseases. Some of the diseases described due to defective SLC proteins are neurological disorders, neuropathic disorders, and metabolic disorders such as type 2 diabetes and obesity<sup>135</sup>.

LAT1/SLC7A5 (Large Amino Acid Transporter 1/Solute Carrier Family 7 Member 5), a transporter of neutral amino acids, is one of the SLC proteins which has been associated with obesity development<sup>136-137</sup>. SLC7A5 is an activator of the mammalian target of rapamycin complex 1

(mTORC1) which is important in cellular metabolism and signalling of nutrients such as amino acids and glucose<sup>136,138</sup>. When nutrients are abundant in the cell, mTORC1 promotes processes such as lipid, protein, and nucleotide biosynthesis. Upon nutrient starvation, the activity of mTORC1 is halted. Dysregulation of the mTOR signalling pathway has been implicated in ageing, cancer, neurodegenerative and metabolic diseases like obesity<sup>139-140</sup>. Mucosal-associated invariant T (MAIT) cells are innate cells involved in immune defence and have been previously shown to be dysregulated in obesity<sup>137</sup>. A study conducted on MAIT cells isolated from obese patients showed defective mTORC1 signalling. In addition, glycolysis, which is dependent on the mTORC1 signalling was impaired. Further investigation revealed that there was reduced SLC7A5-mediated amino acid transport. Overall, the results show that dysregulation in obesity is due to a reduction in the influx of amino acids by SLC7A5, leading to defective mTORC1 signalling in the cells<sup>137</sup>. In other studies, the rs113883650 variant in the *SLC7A5* gene was associated with the risk of obesity in infants<sup>141-142</sup>.

The Solute Carrier Family 7 Member 11 (*SLC7A11*) is important in glutamine metabolism and the extracellular uptake of cysteine for glutathione (GSH) biosynthesis<sup>143-144</sup>. The knockdown of *SLC7A11* was conducted to determine its role in the adipogenic differentiation of mesenchymal stem cells (MSCs). The results obtained demonstrated that adipogenesis was reduced in knockdown cells when compared with the control cells. Additionally, silencing of *SLC7A11* was shown to decrease the expression of PPAR $\gamma$ , which is a key regulator of adipogenesis<sup>145</sup>. DIO was shown to cause ferroptosis (iron-dependent programmed cell death) and cardiac injury in mice<sup>146</sup>. The ferroptosis and cardiac injury was promoted by overexpressed miR-140-5p in adipose tissue macrophages (ATMs) and ATM-derived exosome from the obese mice. The study revealed that miR-140-5p targeted and silenced *SLC7A11*, inhibiting the synthesis of GSH by *SLC7A11*<sup>146</sup>.

Solute Carrier Family 7 Member 10 (*SLC7A10*) is a transporter of small neutral amino acids (i.e., alanine, serine, cysteine)<sup>147</sup>. In a recent study of severely obese adults who underwent bariatric surgery, *SLC7A10* was shown to be upregulated in the visceral and subcutaneous adipose tissues following fat loss, and significantly higher in the visceral adipose in comparison to the subcutaneous depot. *SLC7A10* was inversely associated with waist-to-hip ratio, adipocyte hypertrophy and insulin resistance. To further elucidate the role of *SLC7A10* in obesity, the authors obtained zebrafish with a splice-site, loss of function mutation. Following 8 weeks of

overfeeding, the mutant zebrafish gained approximately 38% of their body weight when compared with their wildtype counterparts, further demonstrating the inverse proportion between *SLC7A10* and adiposity. Upon histological analyses, the adipose tissue of the mutant zebrafish displayed about 49% larger adipocytes in comparison to the wildtype, while the liver tissue showed no obvious differences between the loss-of-function and wildtype zebrafish<sup>147</sup>.

Considering the above-mentioned roles of the SLC transporters, the *SLC7A8* gene identified in an unbiased genome-wide transcriptomic study of human ASC undergoing adipogenesis by Ambele et al., 2016, is a SLC protein not previously described in this context which may play a critical role in the development of obesity.

## **2.6 Adipogenesis and obesity**

In addition, to excess and/or dysfunctional adipose tissue, adipogenesis can produce obesity-related metabolic effects. Adipogenesis is the process in which mature adipocytes are formed from the proliferation and differentiation of adipocyte precursor cells<sup>4</sup>. The process of adipogenesis is divided into stages which entail mesenchymal precursor cells going through commitment phase, becoming growth-arrested preadipocytes, going through clonal expansion, undergoing terminal differentiation and finally, becoming mature adipocytes. Although a paucity of literature remains pertaining to the underlying biological and molecular processes in adipogenesis, several transcription factors and stimulators which are important in the differentiation of preadipocytes to mature adipocytes have been identified<sup>2,148-150</sup>.

Mesenchymal stromal/stem cells (MSCs) are multipotent cells which can differentiate into various lineages such as adipocytes, osteoblasts, chondrocytes, and myoblasts<sup>2,150-151</sup>. The MSC adipocyte progenitor cells express platelet-derived growth factor alpha and/or beta (PDGF- $\alpha$  and/or PDGF- $\beta$ )<sup>4,152</sup>. The mesenchymal progenitors undergo a phase of commitment in which cells become restricted to the adipogenic lineage<sup>4,150</sup>. It was previously postulated that the preadipocyte to adipocyte transition is irreversible<sup>4,150</sup>. Recent studies, however, provide contrary evidence, indicating that mature adipocytes can de-differentiate and return to their adipocyte precursor state<sup>153-154</sup>.

The commitment phase is facilitated by bone morphogenetic protein 4 (BMP4) and due to BMP4 signalling, the committed preadipocytes precursors express the transcription activator zinc-finger

protein 423 (ZNF423), an important protein in determining cell fate of preadipocytes<sup>2,4</sup>. During the commitment phase, several pathways such as the wing-less related integration site (WNT) and WNT1-inducible-signalling pathway protein 2 (WISP2) are inhibited<sup>2,155</sup>. The WNT pathway plays a key role during embryonic development and in adults as well. Additionally, the pathway is significant in maintenance and control of stem cells<sup>155</sup>. Signalling by WNT pathways is mediated through canonical and non-canonical pathway. During adipogenesis, the canonical WNT pathway maintains uncommitted and undifferentiated precursor cells, preventing adipogenic differentiation<sup>2,4</sup>. Dickkopf (DKK) and axis inhibition protein 2 (AXIN2) are expressed during preadipocyte differentiation, inhibiting the WNT pathway and thus, inducing commitment and differentiation of preadipocytes into mature adipocytes<sup>2,155</sup>.

The canonical WNT pathway activates the WISP2 pathway. The activation of WISP2, like WNT pathway, suppresses commitment of preadipocytes into adipocytes<sup>156</sup>. WISP2 inhibits adipocyte commitment by preventing the ZNF423 transcription co-activator from entering the nucleus by forming a protein complex with ZNF423, which blocks ZNF423 from activating preadipocytes from undergoing commitment. BMP4 through its SMAD binding complex dissociates the WISP2-ZNF423 complex, allowing entry of ZNF423 into the nucleus and inducing commitment<sup>156</sup>.

Following commitment, the preadipocytes go into growth arrest and differentiate into an adipocyte<sup>4</sup>. After induction of adipogenesis, preadipocytes go through several rounds of cell division during mitotic clonal expansion to permanently leave the cycle<sup>150</sup>. BMP4 binds to its receptors and signals the activation of a downstream transcription factor, SMAD family member 4 (SMAD4) which induces transcription of peroxisome proliferator-activated receptor- $\gamma$  (PPAR $\gamma$ ) in the differentiating adipocyte<sup>2</sup>.

Adipogenic induction is initiated by CCAAT/enhancer-binding protein beta and delta (C/EBP $\beta$  and C/EBP $\delta$ ), followed by the main adipogenesis transcription factors PPAR $\gamma$  and C/EBP alpha (C/EBP $\alpha$ )<sup>150</sup>. Induction of PPAR $\gamma$  and C/EBP $\alpha$  can be suppressed by the WNT pathway, preventing differentiation of adipocytes<sup>150</sup>. PPAR $\gamma$  transcription factor is regarded the master regulator of adipogenesis as it plays a major role in the differentiation of adipocyte precursor cells to mature adipocytes. Its expression is also required for the maintenance of mature adipocytes<sup>4,150</sup>. PPAR $\gamma$  has two isoforms; PPAR $\gamma$ -1 whose function is not well documented, while PPAR $\gamma$ -2 is required for adipogenesis<sup>150</sup>. PPAR $\gamma$  is coordinated in synergy with C/EBP $\alpha$  to activate differentiation; that is,

PPARY binds to the *C/EBPα* gene promoter, activating its expression and vice versa, creating a positive feedback loop to facilitate adipogenic differentiation<sup>2,4,148</sup>. At least 90% of PPARY deoxyribonucleic (DNA) binding motifs can also bind *C/EBPα*, suggesting that adipocyte differentiation by PPARY and *C/EBPα* involves binding of these factors to adjacent gene targets<sup>157</sup>. Activation of PPARY and *C/EBPα*, and lipid accumulation, induce the expression of GLUT4 and adipocyte fatty-acid binding protein (AP2), which are markers adipocytes in the early stages of differentiation and is important in maintaining insulin sensitivity in normal adipocytes<sup>2,4,150</sup>. Upon completion of adipocyte differentiation, the mature adipocyte expresses all markers of adipocyte differentiation and hormones leptin and adiponectin, and lipases such as adipose triglyceride lipase (ATGL) and lipoprotein lipase (LPL)<sup>2,4</sup>.

In obesity, adipogenic capacity is reduced, contributing to the metabolic decline observed in obese individuals<sup>150</sup>. Gremlin-1 (GREM1) was found to be an antagonist of BMP4, and it was expressed at high levels in hypertrophic obesity. This results in a defect during commitment phase of preadipocyte formation, potentially reducing adipogenic capacity<sup>158</sup>. Hypertrophic obese individuals exhibited great hypermethylation at the CpG islands in the *ZNF423* gene which correlated to reduced expression of the gene in the preadipocytes. The results obtained from the study indicate that changes in the epigenetic profile and transcriptional regulation may explain impairments observed in adipogenesis of obese individuals<sup>159</sup>. The WISP2 protein was shown to be highly upregulated in preadipocytes and in individuals of hypertrophic obesity, thereby inhibiting adipogenic differentiation and the activation of PPARY<sup>160</sup>.

## **2.7 Animal models of obesity**

Most studies conducted to understand obesity and the process of adipogenesis use cell lines or preadipocyte precursor cells from animal models such as rodents<sup>4,161</sup>. Mice models have also been shown to be susceptible to developing obesity, hyperglycaemia and insulin resistance when fed on a HFD<sup>161-162</sup>. Gene differences that exist between different mouse strains influence their susceptibility to developing DIO. Similarly, the susceptibility of rats to DIO is dependent on the strain. However, the most utilised rat strains are outbred and thus, exhibit great genetic variation<sup>163</sup>. The SWR/J and A/J inbred mouse strains are resistant to developing obesity and associated metabolic complications when fed on an obesogenic diet<sup>163</sup>. The C57BL/6J mouse strain, however, is typically used as it is a good model to mimic metabolic disorders associated

with obesity. In this strain, the body mass of mice increases with age as observed in humans<sup>164</sup>. In contrast to mice on HFD, mice fed on a control diet do not develop obesity nor obesity-related metabolic disorders<sup>163,165</sup>. Furthermore, these models of DIO are useful for studying chronic inflammation<sup>166</sup>. C57BL/6J mice fed on a high-fat diet are increasingly susceptible to developing obesity, hyperglycaemia, hyperinsulinaemia, prediabetes and impaired glucose tolerance (IGT)<sup>4,161,167-168</sup>.

## 2.8 Rationale for study

The *SLC7A8* gene was identified to be a potential role player in the early stages of adipogenesis<sup>12</sup>. However, a paucity of literature exists on the role of *SLC7A8* in adipogenesis and obesity development. Therefore, this study aims to contribute new knowledge on *SLC7A8* in the context of obesity and adipogenesis by investigating the function of the gene in obesity development using C57BL/6J mouse model of diet-induced obesity as well as its functional role in human adipose derived stromal/stem cell (ASC) adipogenesis in vitro.

## 2.9 References

1. (WHO) WHO. World obesity day 2022 – accelerating action to stop obesity. <https://www.who.int/news/item/04-03-2022-world-obesity-day-2022-accelerating-action-to-stop-obesity>. 2022; Accessed 25 July 2023
2. Longo M, Zatterale F, Naderi J, Parrillo L, Formisano P, Raciti GA, et al. Adipose tissue dysfunction as determinant of obesity-associated metabolic complications. *International Journal of Molecular Sciences*. 2019; 20(9):2358.
3. Chait A, den Hartigh LJ. Adipose tissue distribution, inflammation and its metabolic consequences, including diabetes and cardiovascular disease. *Frontiers in Cardiovascular Medicine*. 2020; 7:22. doi:10.3389/fcvm.2020.00022
4. Ghaben AL, Scherer PE. Adipogenesis and metabolic health. *Nature Reviews Molecular Cell Biology*. 2019; 20(4):242-58. doi:10.1038/s41580-018-0093-z
5. Apovian CM. Obesity: Definition, comorbidities, causes, and burden. *American Journal of Managed Care* 2016; 22(7 Suppl):s176-85.
6. Tang P, Virtue S, Goie JYG, Png CW, Guo J, Li Y, et al. Regulation of adipogenic differentiation and adipose tissue inflammation by interferon regulatory factor 3. *Cell Death & Differentiation*. 2021; 28(11):3022-35. doi:10.1038/s41418-021-00798-9

7. Morrison S, McGee SL. 3t3-l1 adipocytes display phenotypic characteristics of multiple adipocyte lineages. *Adipocyte*. 2015; 4(4):295-302. doi:10.1080/21623945.2015.1040612
8. Czumaj A. Optimization of the differentiation of 3t3-l1 cells to adipocytes. [https://www.researchgate.net/publication/311810027\\_Optimization\\_of\\_the\\_differentiation\\_of\\_3\\_T3-L1\\_cells\\_to\\_adipocytes](https://www.researchgate.net/publication/311810027_Optimization_of_the_differentiation_of_3_T3-L1_cells_to_adipocytes), editor2016.
9. Huang H-Y, Hu L-L, Song T-J, Li X, He Q, Sun X, et al. Involvement of cytoskeleton-associated proteins in the commitment of c3h10t1/2 pluripotent stem cells to adipocyte lineage induced by bmp2/4. *Molecular & cellular proteomics*. 2011; 10:M110.002691. doi:10.1074/mcp.M110.002691
10. Lane JM, Doyle JR, Fortin JP, Kopin AS, Ordovás JM. Development of an op9 derived cell line as a robust model to rapidly study adipocyte differentiation. *PLoS One*. 2014; 9(11):e112123. doi:10.1371/journal.pone.0112123
11. Yue F, Cheng Y, Breschi A, Vierstra J, Wu W, Ryba T, et al. A comparative encyclopedia of DNA elements in the mouse genome. *Nature*. 2014; 515(7527):355-64. doi:10.1038/nature13992
12. Ambele MA, Dessels C, Durandt C, Pepper MS. Genome-wide analysis of gene expression during adipogenesis in human adipose-derived stromal cells reveals novel patterns of gene expression during adipocyte differentiation. *Stem Cell Research & Therapy* 2016; 16(3):725-34. doi:10.1016/j.scr.2016.04.011
13. Bassi MT, Sperandeo MP, Incerti B, Bulfone A, Pepe A, Surace EM, et al. Slc7a8, a gene mapping within the lysinuric protein intolerance critical region, encodes a new member of the glycoprotein-associated amino acid transporter family. *Genomics*. 1999; 62(2):297-303. doi:10.1006/geno.1999.5978
14. Pineda M, Fernández E, Torrents D, Estévez R, López C, Camps M, et al. Identification of a membrane protein, lat-2, that co-expresses with 4f2 heavy chain, an l-type amino acid transport activity with broad specificity for small and large zwitterionic amino acids. *Journal of Biological Chemistry*. 1999; 274(28):19738-44. doi:10.1074/jbc.274.28.19738
15. Rossier G, Meier C, Bauch C, Summa V, Sordat B, Verrey F, et al. Lat2, a new basolateral 4f2hc/cd98-associated amino acid transporter of kidney and intestine \*. *Journal of Biological Chemistry*. 1999; 274(49):34948-54. doi:10.1074/jbc.274.49.34948
16. Wu Y, Yin Q, Lin S, Huang X, Xia Q, Chen Z, et al. Increased slc7a8 expression mediates l-dopa uptake by renal tubular epithelial cells. *Molecular Medicine Reports*. 2017; 16(1):887-93. doi:10.3892/mmr.2017.6620
17. Braun D, Kinne A, Bräuer AU, Sapin R, Klein MO, Köhrle J, et al. Developmental and cell type-specific expression of thyroid hormone transporters in the mouse brain and in primary brain cells. *Glia*. 2011; 59(3):463-71. doi:10.1002/glia.21116
18. Park SY, Kim JK, Kim IJ, Choi BK, Jung KY, Lee S, et al. Reabsorption of neutral amino acids mediated by amino acid transporter lat2 and tat1 in the basolateral membrane of proximal tubule. *Archives of Pharmacal Research*. 2005; 28(4):421-32. doi:10.1007/bf02977671

19. Espino Guarch M, Font-Llitjos M, Murillo-Cuesta S, Errasti-Murugarren E, Celaya AM, Giroto G, et al. Mutations in I-type amino acid transporter-2 support slc7a8 as a novel gene involved in age-related hearing loss. *Elife*. 2018; 7 doi:10.7554/eLife.31511
20. Knöpfel EB, Vilches C, Camargo SMR, Errasti-Murugarren E, Stäubli A, Mayayo C, et al. Dysfunctional lat2 amino acid transporter is associated with cataract in mouse and humans. *Frontiers in Physiology*. 2019; 10(688) doi:10.3389/fphys.2019.00688
21. Braun D, Wirth EK, Wohlgemuth F, Reix N, Klein MO, Gruters A, et al. Aminoaciduria, but normal thyroid hormone levels and signalling, in mice lacking the amino acid and thyroid hormone transporter slc7a8. *Biochemical Journal*. 2011; 439(2):249-55. doi:10.1042/BJ20110759
22. El Ansari R, Alfarsi L, Craze ML, Masisi BK, Ellis IO, Rakha EA, et al. The solute carrier slc7a8 is a marker of favourable prognosis in er-positive low proliferative invasive breast cancer. *Breast Cancer Research and Treatment*. 2020; 181(1):1-12. doi:10.1007/s10549-020-05586-6
23. Collaboration NCDRF. Trends in adult body-mass index in 200 countries from 1975 to 2014: A pooled analysis of 1698 population-based measurement studies with 19.2 million participants. *Lancet*. 2016; 387(10026):1377-96. doi:10.1016/S0140-6736(16)30054-X
24. (WHO) WHO. Obesity and overweight. <https://www.who.int/news-room/fact-sheets/detail/obesity-and-overweight>. 2021; Accessed 25 July 2023
25. World Obesity Federation W. Global atlas on childhood obesity. <https://www.worldobesity.org/membersarea/global-atlas-on-childhood-obesity>. 2022; Accessed 16 May 2022
26. (WHO) WHO. Obesity rising in africa, who analysis finds. <https://www.afro.who.int/news/obesity-rising-africa-who-analysis-finds>. 2022; Accessed 26 July 2023
27. (AHO) AHO. Africa plagued by obesity, warns africa health organisation aho. <https://aho.org/news/africa-plagued-by-obesity-warned-africa-health-organisation-aho/>. 2022; Accessed 26 July 2023
28. Hill JO, Wyatt HR, Peters JC. The importance of energy balance. *European endocrinology*. 2013; 9(2):111-5. doi:10.17925/EE.2013.09.02.111
29. Fox A, Feng W, Asal V. What is driving global obesity trends? Globalization or “modernization”? *Globalization and Health*. 2019; 15(1):32. doi:10.1186/s12992-019-0457-y
30. Popkin BM, Ng SW. The nutrition transition to a stage of high obesity and noncommunicable disease prevalence dominated by ultra-processed foods is not inevitable. *Obesity Reviews*. 2022; 23(1):e13366. doi:<https://doi.org/10.1111/obr.13366>
31. Duffey KJ, Gordon-Larsen P, Jacobs DR, Jr, Williams OD, Popkin BM. Differential associations of fast food and restaurant food consumption with 3-y change in body mass index: The coronary artery risk development in young adults study. *The American Journal of Clinical Nutrition*. 2007; 85(1):201-8. doi:10.1093/ajcn/85.1.201



32. Robinson TN, Banda JA, Hale L, Lu AS, Fleming-Milici F, Calvert SL, et al. Screen media exposure and obesity in children and adolescents. *Pediatrics*. 2017; 140(Suppl 2):S97-S101. doi:10.1542/peds.2016-1758K
33. Haghjoo P, Siri G, Soleimani E, Farhangi MA, Alesaeidi S. Screen time increases overweight and obesity risk among adolescents: A systematic review and dose-response meta-analysis. *BioMed Central (BMC) Primary Care*. 2022; 23(1):161. doi:10.1186/s12875-022-01761-4
34. Singh S, Ricardo-Silgado ML, Bielinski SJ, Acosta A. Pharmacogenomics of medication-induced weight gain and antiobesity medications. *Obesity (Silver Spring)*. 2021; 29(2):265-73. doi:10.1002/oby.23068
35. Musil R, Obermeier M, Russ P, Hamerle M. Weight gain and antipsychotics: A drug safety review. *Expert Opinion on Drug Safety*. 2015; 14(1):73-96. doi:10.1517/14740338.2015.974549
36. Gafoor R, Booth HP, Gulliford MC. Antidepressant utilisation and incidence of weight gain during 10 years' follow-up: Population based cohort study. *British Medical Journal*. 2018; 361:k1951. doi:10.1136/bmj.k1951
37. Chukwu J, Delanty N, Webb D, Cavalleri GL. Weight change, genetics and antiepileptic drugs. *Expert Review of Clinical Pharmacology*. 2014; 7(1):43-51. doi:10.1586/17512433.2014.857599
38. Berthon BS, MacDonald-Wicks LK, Wood LG. A systematic review of the effect of oral glucocorticoids on energy intake, appetite, and body weight in humans. *Nutrition Research*. 2014; 34(3):179-90. doi:10.1016/j.nutres.2013.12.006
39. Lopez LM, Ramesh S, Chen M, Edelman A, Otterness C, Trussell J, et al. Progestin-only contraceptives: Effects on weight. *Cochrane Library: Cochrane Reviews*. 2016; 2016(8):Cd008815. doi:10.1002/14651858.CD008815.pub4
40. Endalifer ML, Diress G, Addisu A, Linger B. The association between combined oral contraceptive use and overweight/obesity: A secondary data analysis of the 2016 ethiopia demographic and health survey. *British medical journal (BMJ) Open*. 2020; 10(12):e039229. doi:10.1136/bmjopen-2020-039229
41. Kalra S, Kalra B, Unnikrishnan A, Agrawal N, Kumar S. Optimizing weight control in diabetes: Antidiabetic drug selection. *Diabetes, Metabolic Syndrome and Obesity*. 2010; 3:297-9. doi:10.2147/dmsott.S11941
42. Yeo GSH, Chao DHM, Siegert A-M, Koerperich ZM, Ericson MD, Simonds SE, et al. The melanocortin pathway and energy homeostasis: From discovery to obesity therapy. *Molecular Metabolism*. 2021; 48:101206. doi:<https://doi.org/10.1016/j.molmet.2021.101206>
43. Loos RJF, Yeo GSH. The genetics of obesity: From discovery to biology. *Nature Reviews Genetics*. 2022; 23(2):120-33. doi:10.1038/s41576-021-00414-z
44. Zhang Y, Proenca R, Maffei M, Barone M, Leopold L, Friedman JM. Positional cloning of the mouse obese gene and its human homologue. *Nature*. 1994; 372(6505):425-32. doi:10.1038/372425a0

45. Clément K, Vaisse C, Lahlou N, Cabrol S, Pelloux V, Cassuto D, et al. A mutation in the human leptin receptor gene causes obesity and pituitary dysfunction. *Nature*. 1998; 392(6674):398-401. doi:10.1038/32911
46. Huszar D, Lynch CA, Fairchild-Huntress V, Dunmore JH, Fang Q, Berkemeier LR, et al. Targeted disruption of the melanocortin-4 receptor results in obesity in mice. *Cell*. 1997; 88(1):131-41. doi:[https://doi.org/10.1016/S0092-8674\(00\)81865-6](https://doi.org/10.1016/S0092-8674(00)81865-6)
47. Yeo GSH, Farooqi IS, Aminian S, Halsall DJ, Stanhope RG, O'Rahilly S. A frameshift mutation in *mc4r* associated with dominantly inherited human obesity [1]. *Nature Genetics*. 1998; 20(2):111-2. doi:10.1038/2404
48. Krude H, Biebermann H, Luck W, Horn R, Brabant G, Grüters A. Severe early-onset obesity, adrenal insufficiency and red hair pigmentation caused by *pomc* mutations in humans. *Nature Genetics*. 1998; 19(2):155-7. doi:10.1038/509
49. Lindberg I, Fricker LD. Obesity, *pomc*, and *pomc*-processing enzymes: Surprising results from animal models. *Endocrinology*. 2021; 162(12) doi:10.1210/endo/bqab155
50. Jackson RS, Creemers JWM, Ohagi S, Raffin-Sanson ML, Sanders L, Montague CT, et al. Obesity and impaired prohormone processing associated with mutations in the human prohormone convertase 1 gene. *Nature Genetics*. 1997; 16(3):303-6. doi:10.1038/ng0797-303
51. Stijnen P, Ramos-Molina B, O'Rahilly S, Creemers JW. *Pcsk1* mutations and human endocrinopathies: From obesity to gastrointestinal disorders. *Endocrine Reviews*. 2016; 37(4):347-71. doi:10.1210/er.2015-1117
52. Philippe J, Stijnen P, Meyre D, De Graeve F, Thuillier D, Delplanque J, et al. A nonsense loss-of-function mutation in *pcsk1* contributes to dominantly inherited human obesity. *International Journal of Obesity*. 2015; 39(2):295-302. doi:10.1038/ijo.2014.96
53. Lin X, Li H. Obesity: Epidemiology, pathophysiology, and therapeutics. *Frontiers in Endocrinology (Lausanne)*. 2021; 12:706978. doi:10.3389/fendo.2021.706978
54. Mahmoud AM. An overview of epigenetics in obesity: The role of lifestyle and therapeutic interventions. *International Journal of Molecular Sciences*. 2022; 23(3) doi:10.3390/ijms23031341
55. Sherwood WB, Bion V, Lockett GA, Ziyab AH, Soto-Ramírez N, Mukherjee N, et al. Duration of breastfeeding is associated with leptin (*lep*) DNA methylation profiles and bmi in 10-year-old children. *Clinical Epigenetics*. 2019; 11(1):128. doi:10.1186/s13148-019-0727-9
56. Obermann-Borst SA, Eilers PHC, Tobi EW, de Jong FH, Slagboom PE, Heijmans BT, et al. Duration of breastfeeding and gender are associated with methylation of the leptin gene in very young children. *Pediatric Research*. 2013; 74(3):344-9. doi:10.1038/pr.2013.95
57. Houde AA, Légaré C, Biron S, Lescelleur O, Biertho L, Marceau S, et al. Leptin and adiponectin DNA methylation levels in adipose tissues and blood cells are associated with bmi, waist girth and ldl-cholesterol levels in severely obese men and women. *BioMed Central (BMC) Medical Genetics*. 2015; 16:29. doi:10.1186/s12881-015-0174-1

58. Rohde K, Klös M, Hopp L, Liu X, Keller M, Stumvoll M, et al. Irs1 DNA promoter methylation and expression in human adipose tissue are related to fat distribution and metabolic traits. *Scientific Reports*. 2017; 7(1):12369. doi:10.1038/s41598-017-12393-5
59. Soubry A, Schildkraut JM, Murtha A, Wang F, Huang Z, Bernal A, et al. Paternal obesity is associated with igf2 hypomethylation in newborns: Results from a newborn epigenetics study (nest) cohort. *BioMed (BMC) Medicine*. 2013; 11:29. doi:10.1186/1741-7015-11-29
60. Cruz KJC, de Oliveira ARS, Morais JBS, Severo JS, Marreiro PDdN. Role of micrnas on adipogenesis, chronic low-grade inflammation, and insulin resistance in obesity. *Nutrition*. 2017; 35:28-35. doi:<https://doi.org/10.1016/j.nut.2016.10.003>
61. Prats-Puig A, Ortega FJ, Mercader JM, Moreno-Navarrete JM, Moreno M, Bonet N, et al. Changes in circulating micrnas are associated with childhood obesity. *The Journal of Clinical Endocrinology and Metabolism*. 2013; 98(10):E1655-60. doi:10.1210/jc.2013-1496
62. Zhao H, Shen J, Daniel-MacDougall C, Wu X, Chow WH. Plasma microrna signature predicting weight gain among mexican-american women. *Obesity (Silver Spring)*. 2017; 25(5):958-64. doi:10.1002/oby.21824
63. Oger F, Gheeraert C, Mogilenko D, Benomar Y, Molendi-Coste O, Bouchaert E, et al. Cell-specific dysregulation of microrna expression in obese white adipose tissue. *The Journal of Clinical Endocrinology & Metabolism*. 2014; 99(8):2821-33. doi:10.1210/jc.2013-4259
64. Le Chatelier E, Nielsen T, Qin J, Prifti E, Hildebrand F, Falony G, et al. Richness of human gut microbiome correlates with metabolic markers. *Nature*. 2013; 500(7464):541-6. doi:10.1038/nature12506
65. Ley RE, Bäckhed F, Turnbaugh P, Lozupone CA, Knight RD, Gordon JI. Obesity alters gut microbial ecology. *Proceedings of the National Academy of Sciences of the United States of America*. 2005; 102(31):11070-5. doi:10.1073/pnas.0504978102
66. Turnbaugh PJ, Hamady M, Yatsunencko T, Cantarel BL, Duncan A, Ley RE, et al. A core gut microbiome in obese and lean twins. *Nature*. 2009; 457(7228):480-4. doi:10.1038/nature07540
67. John GK, Mullin GE. The gut microbiome and obesity. *Current Oncology Reports*. 2016; 18(7):45. doi:10.1007/s11912-016-0528-7
68. Montan PD, Sourlas A, Olivero J, Silverio D, Guzman E, Kosmas CE. Pharmacologic therapy of obesity: Mechanisms of action and cardiometabolic effects. *Annals of Translational Medicine*. 2019; 7(16):393. doi:10.21037/atm.2019.07.27
69. Guidelines (2013) for managing overweight and obesity in adults. *Obesity*. 2014; 22(S2):i-xvi. doi:<https://doi.org/10.1002/oby.20818>
70. Otten JJ, Jones KE, Littenberg B, Harvey-Berino J. Effects of television viewing reduction on energy intake and expenditure in overweight and obese adults: A randomized controlled trial. *Archives of Internal Medicine*. 2009; 169(22):2109-15. doi:10.1001/archinternmed.2009.430

71. Patel DK, Stanford FC. Safety and tolerability of new-generation anti-obesity medications: A narrative review. *Postgraduate Medicine*. 2018; 130(2):173-82. doi:10.1080/00325481.2018.1435129
72. Jensen MD, Ryan DH, Apovian CM, Ard JD, Comuzzie AG, Donato KA, et al. 2013 aha/acc/tos guideline for the management of overweight and obesity in adults: A report of the american college of cardiology/american heart association task force on practice guidelines and the obesity society. *Circulation*. 2014; 129(25 Suppl 2):S102-38. doi:10.1161/01.cir.0000437739.71477.ee
73. Garvey WT, Mechanick JI, Brett EM, Garber AJ, Hurley DL, Jastreboff AM, et al. American association of clinical endocrinologists and american college of endocrinology comprehensive clinical practice guidelines for medical care of patients with obesity. *Endocrine Practice*. 2016; 22 Suppl 3:1-203. doi:10.4158/ep161365.GI
74. Yumuk V, Tsigos C, Fried M, Schindler K, Busetto L, Micic D, et al. European guidelines for obesity management in adults. *Obesity Facts*. 2015; 8(6):402-24. doi:10.1159/000442721
75. Giruzzi N. Plenity (oral superabsorbent hydrogel). *Clinical Diabetes*. 2020; 38(3):313-4. doi:10.2337/cd20-0032
76. Chakhtoura M, Haber R, Ghezzawi M, Rhayem C, Tcheroyan R, Mantzoros CS. Pharmacotherapy of obesity: An update on the available medications and drugs under investigation. *EClinicalMedicine*. 2023; 58:101882. doi:10.1016/j.eclinm.2023.101882
77. Enright C, Thomas E, Saxon DR. An updated approach to antiobesity pharmacotherapy: Moving beyond the 5% weight loss goal. *Journal of the Endocrine Society*. 2023; 7(3) doi:10.1210/jendso/bvac195
78. (FDA) FaDA. Fda requests the withdrawal of the weight-loss drug belviq, belviq xr (lorcaserin) from the market. <https://www.fda.gov/drugs/fda-drug-safety-podcasts/fda-requests-withdrawal-weight-loss-drug-belviq-belviq-xr-lorcaserin-market#:~:text=On%20February%2013%2C%202020%20FDA,an%20increased%20occurrence%20of%20cancer>. 2020; Accessed 17 September 2022
79. Adams TD, Davidson LE, Litwin SE, Kim J, Kolotkin RL, Nanjee MN, et al. Weight and metabolic outcomes 12 years after gastric bypass. *New England Journal of Medicine*. 2017; 377(12):1143-55. doi:10.1056/NEJMoa1700459
80. Jakobsen GS, Småstuen MC, Sandbu R, Nordstrand N, Hofsø D, Lindberg M, et al. Association of bariatric surgery vs medical obesity treatment with long-term medical complications and obesity-related comorbidities. *The Journal of the American Medical Association*. 2018; 319(3):291-301. doi:10.1001/jama.2017.21055
81. Chumakova-Orin M, Vanetta C, Moris DP, Guerron AD. Diabetes remission after bariatric surgery. *World Journal of Diabetes*. 2021; 12(7):1093-101. doi:10.4239/wjd.v12.i7.1093
82. Singh AK, Singh R, Kota SK. Bariatric surgery and diabetes remission: Who would have thought it? *Indian Journal of Endocrinology and Metabolism*. 2015; 19(5):563-76. doi:10.4103/2230-8210.163113

83. Lautenbach A, Stoll F, Mann O, Busch P, Huber TB, Kielstein H, et al. Long-term improvement of chronic low-grade inflammation after bariatric surgery. *Obesity Surgery*. 2021; 31(7):2913-20. doi:10.1007/s11695-021-05315-y
84. Lau E, Belda E, Picq P, Carvalho D, Ferreira-Magalhães M, Silva MM, et al. Gut microbiota changes after metabolic surgery in adult diabetic patients with mild obesity: A randomised controlled trial. *Diabetology & Metabolic Syndrome*. 2021; 13(1):56. doi:10.1186/s13098-021-00672-1
85. Ulker İ, Yildiran H. The effects of bariatric surgery on gut microbiota in patients with obesity: A review of the literature. *Bioscience of Microbiota, Food and Health*. 2019; 38(1):3-9. doi:10.12938/bmfh.18-018
86. Ser HL, Letchumanan V, Goh BH, Wong SH, Lee LH. The use of fecal microbiome transplant in treating human diseases: Too early for poop? *Frontiers in Microbiology*. 2021; 12:519836. doi:10.3389/fmicb.2021.519836
87. Zhang Z, Mocanu V, Cai C, Dang J, Slater L, Deehan EC, et al. Impact of fecal microbiota transplantation on obesity and metabolic syndrome—a systematic review. *Nutrients*. 2019; 11(10) doi:10.3390/nu11102291
88. Napolitano M, Covasa M. Microbiota transplant in the treatment of obesity and diabetes: Current and future perspectives. *Frontiers in Microbiology*. 2020; 11:590370. doi:10.3389/fmicb.2020.590370
89. Ridaura VK, Faith JJ, Rey FE, Cheng J, Duncan AE, Kau AL, et al. Gut microbiota from twins discordant for obesity modulate metabolism in mice. *Science*. 2013; 341(6150):1241214. doi:doi:10.1126/science.1241214
90. Vrieze A, Van Nood E, Holleman F, Salojärvi J, Kootte RS, Bartelsman JF, et al. Transfer of intestinal microbiota from lean donors increases insulin sensitivity in individuals with metabolic syndrome. *Gastroenterology*. 2012; 143(4):913-6.e7. doi:10.1053/j.gastro.2012.06.031
91. (FDA) FaDA. Fecal microbiota for transplantation: Safety alert - risk of serious adverse events likely due to transmission of pathogenic organisms. <https://www.fda.gov/safety/medical-product-safety-information/fecal-microbiota-transplantation-safety-alert-risk-serious-adverse-events-likely-due-transmission>. 2020; Accessed 18 September 2022
92. Reyes-Farias M, Fos-Domenech J, Serra D, Herrero L, Sánchez-Infantes D. White adipose tissue dysfunction in obesity and aging. *Biochemical Pharmacology*. 2021; 192:114723. doi:<https://doi.org/10.1016/j.bcp.2021.114723>
93. Whitehead A, Krause FN, Moran A, MacCannell ADV, Scragg JL, McNally BD, et al. Brown and beige adipose tissue regulate systemic metabolism through a metabolite interorgan signaling axis. *Nature Communications*. 2021; 12(1):1905. doi:10.1038/s41467-021-22272-3
94. van Marken Lichtenbelt W. Brown adipose tissue and the regulation of nonshivering thermogenesis. *Current Opinion in Clinical Nutrition & Metabolic Care*. 2012; 15(6):547-52. doi:10.1097/MCO.0b013e3283599184

95. Lee P, Swarbrick MM, Ho KKY. Brown adipose tissue in adult humans: A metabolic renaissance. *Endocrine Reviews*. 2013; 34(3):413-38. doi:10.1210/er.2012-1081
96. Cypess AM, Kahn CR. The role and importance of brown adipose tissue in energy homeostasis. *Current opinion in pediatrics*. 2010; 22(4):478-84. doi:10.1097/MOP.0b013e32833a8d6e
97. Sun Y, Chen S, Zhang X, Pei M. Significance of cellular cross-talk in stromal vascular fraction of adipose tissue in neovascularization. *Arteriosclerosis, Thrombosis, and Vascular Biology*. 2019; 39(6):1034-44. doi:10.1161/atvbaha.119.312425
98. Reddy P, Lent-Schochet D, Ramakrishnan N, McLaughlin M, Jialal I. Metabolic syndrome is an inflammatory disorder: A conspiracy between adipose tissue and phagocytes. *Clinica Chimica Acta*. 2019; 496:35-44. doi:<https://doi.org/10.1016/j.cca.2019.06.019>
99. Małodobra-Mazur M, Cierzniak A, Pawełka D, Kaliszewski K, Rudnicki J, Dobosz T. Metabolic differences between subcutaneous and visceral adipocytes differentiated with an excess of saturated and monounsaturated fatty acids. *Genes (Basel)*. 2020; 11(9) doi:10.3390/genes11091092
100. Ros Pérez M, Medina-Gómez G. Obesity, adipogenesis and insulin resistance. *Endocrinología y Nutrición (English Edition)*. 2011; 58(7):360-9. doi:<https://doi.org/10.1016/j.endoen.2011.05.004>
101. Wondmkun YT. Obesity, insulin resistance, and type 2 diabetes: Associations and therapeutic implications. *Diabetes, metabolic syndrome and obesity : targets and therapy*. 2020; 13:3611-6. doi:10.2147/DMSO.S275898
102. Al-Goblan AS, Al-Alfi MA, Khan MZ. Mechanism linking diabetes mellitus and obesity. *Diabetes, metabolic syndrome and obesity : targets and therapy*. 2014; 7:587-91. doi:10.2147/DMSO.S67400
103. Bryant NJ, Govers R, James DE. Regulated transport of the glucose transporter glut4. *Nature Reviews Molecular Cell Biology*. 2002; 3(4):267-77. doi:10.1038/nrm782
104. Shepherd PR, Kahn BB. Glucose transporters and insulin action--implications for insulin resistance and diabetes mellitus. *The New England Journal of Medicine*. 1999; 341(4):248-57. doi:10.1056/nejm199907223410406
105. Makki K, Froguel P, Wolowczuk I. Adipose tissue in obesity-related inflammation and insulin resistance: Cells, cytokines, and chemokines. *ISRN Inflammation*. 2013; 2013:139239. doi:10.1155/2013/139239
106. Martínez-Sánchez N. There and back again: Leptin actions in white adipose tissue. *International Journal of Molecular Sciences*. 2020; 21(17):6039.
107. Makki K, Froguel P, Wolowczuk I. Adipose tissue in obesity-related inflammation and insulin resistance: Cells, cytokines, and chemokines. *International Scholarly Research Network Journals (ISRN) Inflammation*. 2013; 2013:139239. doi:10.1155/2013/139239

108. Tsao C-H, Shiao M-Y, Chuang P-H, Chang Y-H, Hwang J. Interleukin-4 regulates lipid metabolism by inhibiting adipogenesis and promoting lipolysis. *Journal of lipid research*. 2014; 55(3):385-97. doi:10.1194/jlr.M041392
109. Lin S-Y, Yang C-P, Wang Y-Y, Hsiao C-W, Chen W-Y, Liao S-L, et al. Interleukin-4 improves metabolic abnormalities in leptin-deficient and high-fat diet mice. *International Journal of Molecular Sciences*. 2020; 21(12):4451.
110. Yamauchi T, Kamon J, Minokoshi Y, Ito Y, Waki H, Uchida S, et al. Adiponectin stimulates glucose utilization and fatty-acid oxidation by activating amp-activated protein kinase. *Nature Medicine*. 2002; 8(11):1288-95. doi:10.1038/nm788
111. Medina-Urrutia A, Posadas-Romero C, Posadas-Sánchez R, Jorge-Galarza E, Villarreal-Molina T, González-Salazar MDC, et al. Role of adiponectin and free fatty acids on the association between abdominal visceral fat and insulin resistance. *Cardiovascular diabetology*. 2015; 14:20-. doi:10.1186/s12933-015-0184-5
112. Wu H, Ballantyne CM. Metabolic inflammation and insulin resistance in obesity. *Circulation Research*. 2020; 126(11):1549-64. doi:doi:10.1161/CIRCRESAHA.119.315896
113. Hotamisligil GS, Arner P, Caro JF, Atkinson RL, Spiegelman BM. Increased adipose tissue expression of tumor necrosis factor- $\alpha$  in human obesity and insulin resistance. *Journal of Clinical Investigation*. 1995; 95(5):2409-15. doi:10.1172/jci117936
114. Uysal KT, Wiesbrock SM, Marino MW, Hotamisligil GS. Protection from obesity-induced insulin resistance in mice lacking  $\text{tnf-}\alpha$  function. *Nature*. 1997; 389(6651):610-4. doi:10.1038/39335
115. Paz K, Hemi R, LeRoith D, Karasik A, Elhanany E, Kanety H, et al. A molecular basis for insulin resistance. Elevated serine/threonine phosphorylation of  $\text{irs-1}$  and  $\text{irs-2}$  inhibits their binding to the juxtamembrane region of the insulin receptor and impairs their ability to undergo insulin-induced tyrosine phosphorylation. *Journal of Biological Chemistry*. 1997; 272(47):29911-8. doi:10.1074/jbc.272.47.29911
116. Fried SK, Bunkin DA, Greenberg AS. Omental and subcutaneous adipose tissues of obese subjects release interleukin-6: Depot difference and regulation by glucocorticoid. *The Journal of Clinical Endocrinology and Metabolism*. 1998; 83(3):847-50. doi:10.1210/jcem.83.3.4660
117. Ito A, Suganami T, Miyamoto Y, Yoshimasa Y, Takeya M, Kamei Y, et al. Role of  $\text{mapk phosphatase-1}$  in the induction of monocyte chemoattractant protein-1 during the course of adipocyte hypertrophy \*. *Journal of Biological Chemistry*. 2007; 282(35):25445-52. doi:10.1074/jbc.M701549200
118. Christiansen T, Richelsen B, Bruun JM. Monocyte chemoattractant protein-1 is produced in isolated adipocytes, associated with adiposity and reduced after weight loss in morbid obese subjects. *The International Journal of Obesity*. 2005; 29(1):146-50. doi:10.1038/sj.ijo.0802839
119. Tilg H, Moschen AR. Adipocytokines: Mediators linking adipose tissue, inflammation and immunity. *Nature Reviews Immunology*. 2006; 6(10):772-83. doi:10.1038/nri1937

120. Yadav A, Kataria MA, Saini V, Yadav A. Role of leptin and adiponectin in insulin resistance. *Clinica Chimica Acta*. 2013; 417:80-4. doi:10.1016/j.cca.2012.12.007
121. Frühbeck G, Catalán V, Rodríguez A, Gómez-Ambrosi J. Adiponectin-leptin ratio: A promising index to estimate adipose tissue dysfunction. Relation with obesity-associated cardiometabolic risk. *Adipocyte*. 2018; 7(1):57-62. doi:10.1080/21623945.2017.1402151
122. Izquierdo AG, Crujeiras AB, Casanueva FF, Carreira MC. Leptin, obesity, and leptin resistance: Where are we 25 years later? *Nutrients*. 2019; 11(11) doi:10.3390/nu11112704
123. Banks WA, Farr SA, Salameh TS, Niehoff ML, Rhea EM, Morley JE, et al. Triglycerides cross the blood-brain barrier and induce central leptin and insulin receptor resistance. *International Journal of Obesity*. 2018; 42(3):391-7. doi:10.1038/ijo.2017.231
124. Chaves C, Kay T, Anselmo J. Early onset obesity due to a mutation in the human leptin receptor gene. *Endocrinology, Diabetes & Metabolism Case Reports*. 2022; 2022 doi:10.1530/edm-21-0124
125. Berger C, Heyne HO, Heiland T, Dommel S, Höfling C, Guiu-Jurado E, et al. A novel compound heterozygous leptin receptor mutation causes more severe obesity than in *lepr<sup>db/db</sup>* mice. *Journal of Lipid Research*. 2021; 62:100105. doi:<https://doi.org/10.1016/j.jlr.2021.100105>
126. Chen H, Charlat O, Tartaglia LA, Woolf EA, Weng X, Ellis SJ, et al. Evidence that the diabetes gene encodes the leptin receptor: Identification of a mutation in the leptin receptor gene in *db/db* mice. *Cell*. 1996; 84(3):491-5. doi:10.1016/s0092-8674(00)81294-5
127. Wabitsch M, Funcke JB, Lennerz B, Kuhnle-Krahl U, Lahr G, Debatin KM, et al. Biologically inactive leptin and early-onset extreme obesity. *The New England Journal of Medicine*. 2015; 372(1):48-54. doi:10.1056/NEJMoa1406653
128. Lubis AR, Widia F, Soegondo S, Setiawati A. The role of *socs-3* protein in leptin resistance and obesity. *Acta Medica Indonesiana*. 2008; 40(2):89-95.
129. White CL, Whittington A, Barnes MJ, Wang Z, Bray GA, Morrison CD. Hf diets increase hypothalamic *ptp1b* and induce leptin resistance through both leptin-dependent and - independent mechanisms. *American Journal of Physiology-Endocrinology and Metabolism*. 2009; 296(2):E291-9. doi:10.1152/ajpendo.90513.2008
130. Mark AL, Correia MLG, Rahmouni K, Haynes WG. Selective leptin resistance: A new concept in leptin physiology with cardiovascular implications. *Journal of Hypertension*. 2002; 20(7):1245-50.
131. Rahmouni K. Differential control of the sympathetic nervous system by leptin: Implications for obesity. *Clinical and Experimental Pharmacology and Physiology*. 2007; 34 Suppl(s1):S8-s10. doi:10.1111/j.1440-1681.2007.04760.x
132. Mark AL. Selective leptin resistance revisited. *American Journal of Physiology-Regulatory, Integrative and Comparative Physiology*. 2013; 305(6):R566-81. doi:10.1152/ajpregu.00180.2013



133. Pizzagalli MD, Bensimon A, Superti-Furga G. A guide to plasma membrane solute carrier proteins. *The FEBS Journal*. 2021; 288(9):2784-835. doi:10.1111/febs.15531
134. Hediger MA, Clémenton B, Burrier RE, Bruford EA. The abcs of membrane transporters in health and disease (slc series): Introduction. *Molecular Aspects of Medicine*. 2013; 34(2-3):95-107. doi:10.1016/j.mam.2012.12.009
135. Schumann T, König J, Henke C, Willmes DM, Bornstein SR, Jordan J, et al. Solute carrier transporters as potential targets for the treatment of metabolic disease. *Pharmacological Reviews*. 2020; 72(1):343-79. doi:10.1124/pr.118.015735
136. Zhang J, Xu Y, Li D, Fu L, Zhang X, Bao Y, et al. Review of the correlation of lat1 with diseases: Mechanism and treatment. *Frontiers in Chemistry*. 2020; 8 doi:10.3389/fchem.2020.564809
137. O'Brien A, Loftus RM, Pisarska MM, Tobin LM, Bergin R, Wood NAW, et al. Obesity reduces mtorc1 activity in mucosal-associated invariant t cells, driving defective metabolic and functional responses. *The Journal of Immunology*. 2019; 202(12):3404-11. doi:10.4049/jimmunol.1801600
138. Scalise M, Galluccio M, Console L, Pochini L, Indiveri C. The human slc7a5 (lat1): The intriguing histidine/large neutral amino acid transporter and its relevance to human health. *Frontiers in Chemistry*. 2018; 6:243. doi:10.3389/fchem.2018.00243
139. Fernandes SA, Demetriades C. The multifaceted role of nutrient sensing and mtorc1 signaling in physiology and aging. *Frontiers in Aging*. 2021; 2 doi:10.3389/fragi.2021.707372
140. Liu GY, Sabatini DM. Mtor at the nexus of nutrition, growth, ageing and disease. *Nature Reviews Molecular Cell Biology*. 2020; 21(4):183-203. doi:10.1038/s41580-019-0199-y
141. Bik-Multanowski M, Madetko-Talowska A, Betka I, Swieczka E, Didycz B, Orchel-Szastak K, et al. Carriership of the rs113883650/rs2287120 haplotype of the slc7a5 (lat1) gene increases the risk of obesity in infants with phenylketonuria. *Molecular Genetics and Metabolism Reports*. 2020; 25:100640. doi:10.1016/j.ymgmr.2020.100640
142. Bik-Multanowski M, Didycz B, Bik-Multanowska K. Management precautions for risk of obesity are necessary among infants with pku carrying the rs113883650 variant of the lat1 gene: A cross-sectional study. *PLoS One*. 2022; 17(2):e0264084. doi:10.1371/journal.pone.0264084
143. Jyotsana N, Ta KT, DelGiorno KE. The role of cystine/glutamate antiporter slc7a11/xct in the pathophysiology of cancer. *Frontiers in Oncology*. 2022; 12 doi:10.3389/fonc.2022.858462
144. Koppula P, Zhang Y, Zhuang L, Gan B. Amino acid transporter slc7a11/xct at the crossroads of regulating redox homeostasis and nutrient dependency of cancer. *Cancer Communications*. 2018; 38(1):12. doi:10.1186/s40880-018-0288-x
145. Jin C, Zhang P, Zhang M, Zhang X, Lv L, Liu H, et al. Inhibition of slc7a11 by sulfasalazine enhances osteogenic differentiation of mesenchymal stem cells by modulating bmp2/4 expression and suppresses bone loss in ovariectomized mice. *Journal of Bone and Mineral Research*. 2017; 32(3):508-21. doi:10.1002/jbmr.3009

146. Zhao X, Si L, Bian J, Pan C, Guo W, Qin P, et al. Adipose tissue macrophage-derived exosomes induce ferroptosis via glutathione synthesis inhibition by targeting slc7a11 in obesity-induced cardiac injury. *Free Radical Biology and Medicine*. 2022; 182:232-45. doi:<https://doi.org/10.1016/j.freeradbiomed.2022.02.033>
147. Jersin RÅ, Tallapragada DSP, Madsen A, Skartveit L, Fjære E, McCann A, et al. Role of the neutral amino acid transporter slc7a10 in adipocyte lipid storage, obesity, and insulin resistance. *Diabetes*. 2021; 70(3):680-95. doi:10.2337/db20-0096
148. Ali AT, Hochfeld WE, Myburgh R, Pepper MS. Adipocyte and adipogenesis. *European Journal of Cell Biology*. 2013; 92(6-7):229-36. doi:10.1016/j.ejcb.2013.06.001
149. Ambele MA, Dhanraj P, Giles R, Pepper MS. Adipogenesis: A complex interplay of multiple molecular determinants and pathways. *International Journal of Molecular Sciences*. 2020; 21(12) doi:10.3390/ijms21124283
150. Audano M, Pedretti S, Caruso D, Crestani M, De Fabiani E, Mitro N. Regulatory mechanisms of the early phase of white adipocyte differentiation: An overview. *Cellular and Molecular Life Sciences*. 2022; 79(3):139. doi:10.1007/s00018-022-04169-6
151. Ahmad B, Serpell CJ, Fong IL, Wong EH. Molecular mechanisms of adipogenesis: The anti-adipogenic role of amp-activated protein kinase. *Frontiers in Molecular Biosciences*. 2020; 7 doi:10.3389/fmolb.2020.00076
152. Dani C, Pfeifer A. The complexity of pdgfr signaling: Regulation of adipose progenitor maintenance and adipocyte-myofibroblast transition. *Stem Cell Investigation*. 2017; 4:28-. doi:10.21037/sci.2017.04.02
153. Wang QA, Song A, Chen W, Schwalie PC, Zhang F, Vishvanath L, et al. Reversible de-differentiation of mature white adipocytes into preadipocyte-like precursors during lactation. *Cell Metabolism*. 2018; 28(2):282-8.e3. doi:10.1016/j.cmet.2018.05.022
154. Zang L, Kothan S, Yang Y, Zeng X, Ye L, Pan J. Insulin negatively regulates dedifferentiation of mouse adipocytes in vitro. *Adipocyte*. 2020; 9(1):24-34. doi:10.1080/21623945.2020.1721235
155. de Winter TJJ, Nusse R. Running against the wnt: How wnt/ $\beta$ -catenin suppresses adipogenesis. *Frontiers in Cell and Developmental Biology*. 2021; 9 doi:10.3389/fcell.2021.627429
156. Grünberg JR, Elvin J, Paul A, Hedjazifar S, Hammarstedt A, Smith U. Ccn5/wisp2 and metabolic diseases. *Journal of Cell Communication and Signaling*. 2018; 12(1):309-18. doi:10.1007/s12079-017-0437-z
157. Lefterova MI, Zhang Y, Steger DJ, Schupp M, Schug J, Cristancho A, et al. Ppargamma and c/ebp factors orchestrate adipocyte biology via adjacent binding on a genome-wide scale. *Genes & Development*. 2008; 22(21):2941-52. doi:10.1101/gad.1709008
158. Gustafson B, Hammarstedt A, Hedjazifar S, Hoffmann JM, Svensson PA, Grimsby J, et al. Bmp4 and bmp antagonists regulate human white and beige adipogenesis. *Diabetes*. 2015; 64(5):1670-81. doi:10.2337/db14-1127

159. Longo M, Raciti GA, Zatterale F, Parrillo L, Desiderio A, Spinelli R, et al. Epigenetic modifications of the zfp/znf423 gene control murine adipogenic commitment and are dysregulated in human hypertrophic obesity. *Diabetologia*. 2018; 61(2):369-80. doi:10.1007/s00125-017-4471-4
160. Hammarstedt A, Hedjazifar S, Jenndahl L, Gogg S, Grünberg J, Gustafson B, et al. Wisp2 regulates preadipocyte commitment and ppar $\gamma$  activation by bmp4. *Proceedings of the National Academy of Sciences of the United States of America*. 2013; 110(7):2563-8. doi:10.1073/pnas.1211255110
161. de Moura e Dias M, dos Reis SA, da Conceição LL, Sediya CMNdO, Pereira SS, de Oliveira LL, et al. Diet-induced obesity in animal models: Points to consider and influence on metabolic markers. *Diabetology & Metabolic Syndrome*. 2021; 13(1):32. doi:10.1186/s13098-021-00647-2
162. Lang P, Hasselwander S, Li H, Xia N. Effects of different diets used in diet-induced obesity models on insulin resistance and vascular dysfunction in c57bl/6 mice. *Scientific Reports*. 2019; 9(1):19556. doi:10.1038/s41598-019-55987-x
163. Kleinert M, Clemmensen C, Hofmann SM, Moore MC, Renner S, Woods SC, et al. Animal models of obesity and diabetes mellitus. *Nature Reviews Endocrinology*. 2018; 14(3):140-62. doi:10.1038/nrendo.2017.161
164. Kleinert M, Clemmensen C, Hofmann SM, Moore MC, Renner S, Woods SC, et al. Animal models of obesity and diabetes mellitus. *Nature Reviews Endocrinology*. 2018; 14(3):140-62. doi:10.1038/nrendo.2017.161
165. Kowalski GM, Kraakman MJ, Mason SA, Murphy AJ, Bruce CR. Resolution of glucose intolerance in long-term high-fat, high-sucrose-fed mice. *Journal of Endocrinology*. 2017; 233(3):269-79. doi:10.1530/joe-17-0004
166. Avtanski D, Pavlov VA, Tracey KJ, Poretsky L. Characterization of inflammation and insulin resistance in high-fat diet-induced male c57bl/6j mouse model of obesity. *Animal Models and Experimental Medicine*. 2019; 2(4):252-8. doi:<https://doi.org/10.1002/ame2.12084>
167. Hostalek U. Global epidemiology of prediabetes - present and future perspectives. *Clinical Diabetes and Endocrinology*. 2019; 5(1):5. doi:10.1186/s40842-019-0080-0
168. Khan RMM, Chua ZJY, Tan JC, Yang Y, Liao Z, Zhao Y. From pre-diabetes to diabetes: Diagnosis, treatments and translational research. *Medicina (Kaunas, Lithuania)*. 2019; 55(9):546. doi:10.3390/medicina55090546

## Chapter 3. *Slc7a8* deletion is protective against diet-induced obesity and attenuates lipid accumulation in multiple organs

Reabetswe R. Pitere<sup>1</sup>, Marlene B. van Heerden<sup>2</sup>, Michael S. Pepper<sup>1</sup> and Melvin A. Ambele<sup>1,2</sup>

1. Institute for Cellular and Molecular Medicine, Department of Immunology, and SAMRC Extramural Unit for Stem Cell Research and Therapy, Faculty of Health Sciences, University of Pretoria, Pretoria 0001, South Africa
2. Department of Oral Pathology and Oral Biology, School of Dentistry, Faculty of Health Sciences, University of Pretoria, Pretoria 0001, South Africa

This chapter is presented in the final published format in the *Biology* journal. The article is accessible from: <https://doi.org/10.3390/biology11020311>.

The screenshot displays the PubMed interface for the article. At the top, the NIH National Library of Medicine logo is visible, along with a search bar and a 'Log in' button. Below the search bar, the PubMed logo and a search button are present. The article title is prominently displayed: ***Slc7a8* Deletion Is Protective against Diet-Induced Obesity and Attenuates Lipid Accumulation in Multiple Organs**. The authors listed are Reabetswe R Pitere<sup>1</sup>, Marlene B van Heerden<sup>2</sup>, Michael S Pepper<sup>1</sup>, and Melvin A Ambele<sup>1,2</sup>. The article is identified as a 'Free PMC article'. On the right side, there are buttons for 'Cite' and 'Collections', and a 'SHARE' section with social media icons for Twitter, Facebook, and LinkedIn. The abstract text is partially visible at the bottom: 'Adipogenesis, through adipocyte hyperplasia and/or hypertrophy, leads to increased adiposity, giving'.

### 3.1 Abstract

Adipogenesis, through adipocyte hyperplasia and/or hypertrophy, leads to increased adiposity, giving rise to obesity. A genome-wide transcriptome analysis of in vitro adipogenesis in human adipose-derived stromal/stem cells identified *SLC7A8* (Solute Carrier Family 7 Member 8) as a potential novel mediator. The current study has investigated the role of *SLC7A8* in adipose tissue biology using a mouse model of diet-induced obesity. *Slc7a8* knockout (KO) and wildtype (WT) C57BL/6J mice were fed either a control diet (CD) or a high-fat diet (HFD) for 14 weeks. On the HFD, both WT and KO mice (WTHFD and KOHFD) gained significantly more weight than their CD counterparts. However, KOHFD gained significantly less weight than WTHFD. KOHFD had significantly reduced levels of glucose intolerance compared with those observed in WTHFD. KOHFD also had significantly reduced adipocyte mass and hypertrophy in inguinal, mesenteric, perigonadal, and brown adipose depots, with a corresponding decrease in macrophage infiltration. Additionally, KOHFD had decreased lipid accumulation in the liver, heart, gastrocnemius muscle, lung, and kidney. This study demonstrates that targeting *Slc7a8* protects against diet-induced obesity by reducing lipid accumulation in multiple organs and suggests that if targeted, has the potential to mitigate the development of obesity-associated comorbidities.

### 3.2 Introduction

Obesity is characterised by an excess accumulation of adipose tissue when energy intake exceeds energy expenditure. The expansion of adipose tissue in obesity occurs either through adipocyte hyperplasia or hypertrophy. The result is dysfunctional adipose tissue mainly due to adipocyte hypertrophy, which leads to adverse metabolic consequences and chronic inflammation<sup>1</sup>. The distribution of adipose tissue in obesity plays an important role in the development of obesity-associated comorbidities. Accumulation of fat in intra-abdominal depots (visceral depots) gives rise to insulin resistance and is also associated with an increased risk of cardiovascular diseases<sup>2</sup>. Subcutaneous white adipose tissue (WAT) is the most common adipose tissue in healthy lean individuals and serves as a metabolic sink for excess lipid storage<sup>3</sup>. Brown adipose tissue takes up fatty acids from the circulation to generate heat, which helps to clear plasma triglycerides thereby reducing the accumulation of lipid in visceral depots<sup>4</sup>. In obesity, where the storage capacity of adipose tissue is exceeded either due to an inability to produce new adipocytes (limited hyperplasia) or to expand further (limited hypertrophy), excess fat is redistributed to peripheral organs such as the liver and skeletal muscle which increases the risk of metabolic-associated syndromes such as hyperglycaemia, hyperinsulinemia, atherosclerosis, dyslipidemia and systemic inflammation<sup>3,5</sup>. Hypertrophy in brown adipose tissue (BAT) may impair its function in acting as a sink for excess blood glucose and clearance of free fatty acids from circulation, thereby contributing to the development of insulin resistance and hyperlipidemia in obesity<sup>3</sup>. Therefore, mitigating adipocyte hypertrophy in both WAT and BAT depots is paramount to improving metabolic health.

Inflammation is a key consequence of adipose tissue expansion that occurs during weight gain and contributes to the development of chronic low-grade systemic inflammation seen in obesity. This expansion of adipose tissue is characterized by increased infiltration of immune cells, with a predominance (around 60%) of macrophages, in response to chemokines that are produced by hypertrophic adipocytes<sup>6</sup>. The majority are derived from circulating monocytes with a small proportion coming from the proliferation of adipose tissue resident macrophages<sup>7</sup>. Tissue resident macrophages present in normal or lean adipose tissue are of the M2 anti-inflammatory macrophage phenotype that express markers such as mannose receptor (CD206) and are thought to be responsible for maintaining tissue homeostasis<sup>8</sup>. Macrophage infiltration in adipose tissue

appears as crown-like clusters which is believed to signify an immune response to dying or dead adipocytes<sup>9</sup>. These infiltrating macrophages undergo a phenotypic switch to a M1 pro-inflammatory phenotype<sup>10</sup>.

In addressing obesity, several studies have suggested countering the process of fat cell formation (adipogenesis) to combat obesity development. These have led to several molecular determinants being described as playing an important role in adipogenesis<sup>11</sup>. Except for PPAR $\gamma$ <sup>12-13</sup>, molecular determinants of adipogenesis have proven to be of limited clinical utility. Therefore, more research is needed to identify new molecular determinants of adipogenesis which could play a role in obesity development and as serve potential therapeutic targets. We have previously undertaken a comprehensive unbiased transcriptomic analysis of human adipose-derived stromal/stem cells undergoing adipogenesis and identified several novel genes and transcription factors with a possible role in this process<sup>14-15</sup>. One of the novel genes identified was *SLC7A8* (Solute Carrier Family 7 Member 8), not previously described in the context of adipogenesis and/or obesity, that was significantly upregulated in the early phase of adipogenesis and declined significantly as the process progresses<sup>14</sup>. This suggested a role for this gene in the early stages of adipogenesis as a potential driver of adiposity and consequently obesity.

The *SLC7A8* gene encodes a large neutral amino acid transporter small subunit 2 (LAT2) with 535 amino acids and it is located on 14q11.2<sup>16-17</sup>. The gene is highly expressed in the kidneys and intestines<sup>17</sup>. Mutations in *SLC7A8* have been implicated in age-related hearing loss<sup>18</sup> and aminoaciduria<sup>19</sup>. Furthermore, *SLC7A8* has been reported to be highly expressed in oestrogen receptor-positive breast cancer<sup>20</sup> and has also been previously shown to be implicated in cataract formation when defective<sup>21</sup>. Since *SLC7A8* has not been described in the context of obesity or adipogenesis, the aim of this study was to investigate the functional role of *SLC7A8* in weight gain/obesity and lipid accumulation in various tissues and organs (such as perigonadal, mesenteric, inguinal subcutaneous, and interscapular brown adipose tissues and the liver, kidneys, heart, brain, lungs, and gastrocnemius muscle) using a mouse model of diet-induced obesity. Macrophage infiltration profiling in some of these tissues (i.e., perigonadal, mesenteric, inguinal subcutaneous, and interscapular brown adipose tissues and the liver, kidneys, and gastrocnemius muscle) was also performed.

### 3.3 Materials and methods

#### 3.3.1 Animals

This study was approved by the Research Ethics Committee, Faculty of Health Sciences and the Animal Ethics Committee, University of Pretoria (Ref. No.: 474/2019).

*Slc7a8* heterozygous (B6.129P2-Slc7a8tm1Dgen/J, #005842) C57BL/6J and inbred wildtype C57BL/6J mating pairs obtained from The Jackson Laboratory (Jackson Laboratory, Bar Harbour, ME, USA) were used to generate *Slc7a8* wildtype (WT) and knockout (KO) genotypes. Genotypes were confirmed by PCR (supplementary methods S1). Both WT and KO mice were fed either a high-fat diet (HFD; D12492) or control diet (CD; D12450J) from Research Diets, Inc. (*New Brunswick, New Jersey, United States of America*) for a period of 14 weeks, with termination time points at weeks 5 and 14. Weekly measurements of weight, food consumption and calorie intake were done. Unless otherwise stated, the nomenclature used for the different genotypes on either a CD or HFD for 14 weeks will be WTCD (wildtype mice on control CD), WTHFD (wildtype mice on HFD), KOCD (*Slc7a8* Knockout mice on control CD) and KOHFD (*Slc7a8* knockout mice on HFD).

#### Glucose tolerance and insulin sensitivity tests

Glucose tolerance tests (GTT) and insulin sensitivity tests (IST) were performed in both KO and WT mice prior to introducing them to either CD or HFD. Mice were fasted for 4 hours, and the baseline glucose concentration measured. A 45% D-(+)- glucose solution (G8769) (*Sigma-Aldrich, St. Louis, Missouri, United States of America*) was then administered interperitoneally at 1.5 mg/g body weight and an insulin solution (*Sigma-Aldrich, St. Louis, Missouri, United States of America*) at 0.8mU/g body weight for GTT and IST, respectively. Blood from the tail vein was used to measure glucose concentration at 15, 30, 60, 90 and 120 minutes using an Accu-Check Instant Blood Glucose Meter (*Roche Diagnostics, Basel, Switzerland*).

#### 3.3.2 Histology and immunohistochemistry of mouse tissues and organs

Mice on either CD or HFD were euthanised at week 5 and 14 followed by the collection of white adipose tissue from the inguinal (iWAT), perigonadal (pWAT) and mesenteric (mWAT) depots; interscapular brown adipose tissue (BAT); and liver, kidneys, heart, brain, lungs, and



gastrocnemius muscle. A 10% formalin fixed paraffin embedded (FFPE) tissue sections were processed for histological analysis.

FFPE tissue sections were cut using a microtome and baked at 62°C for 20 minutes followed by haematoxylin and eosin (H&E) staining using a Leica Autostainer XL (*Leica Microsystems, Wetzlar, Germany*). Slides were mounted with DPX (distyrene, plasticiser, xylene) and imaged using an Axiocam 305 color microscope camera (*ZEISS, Oberkochen, Germany*) and ZEN 2.6 blue edition software (*ZEISS*).

Immunohistochemical analysis of macrophages was performed as previously described<sup>22</sup>. Briefly, tissue sections were stained with F4/80 rat anti mouse antibody clone A3-1 (*Bio-Rad Laboratories, Sandton, Johannesburg, South Africa*). FFPE sections were baked overnight at 54°C, followed by dewaxing in xylene. The sections were then hydrated through a series of ethanol concentrations, rinsed with distilled water and treated with 3% hydrogen peroxide for 5 minutes at 37°C. Heat-induced epitope retrieval was performed in citrate buffer pH 6,1 (*Dako Target Retrieval Solution S1699, Dako, Carpinteria, California, United States of America*) using a 2100 Retriever Unit (*Electron Microscopy Sciences, Hatfield, Pennsylvania, United States of America*). The sections were rinsed in PBS/Tween buffer and treated with 5% Normal Goat Serum (Dako X0907) for 30 minutes after which they were incubated overnight at 4°C with a 1:25 dilution of F4/80 monoclonal rat anti-mouse antibody BM8 (#14-4801-82) (*Thermo Fisher Scientific*) or 1:100 F4/80 rat anti mouse antibody clone A3-1 (*Bio-Rad Laboratories, Sandton, Johannesburg, South Africa*). The sections were rinsed in PBS/Tween buffer before incubating for 60 min in 1:200 goat anti-rat IgG (H+L) antibody conjugated to horseradish peroxidase (HRP) (#31470) (*Invitrogen, Thermo Fisher Scientific*). The slides were then developed in 3,3' diaminobenzidine (DAB) chromogen to visualise F4/80 protein staining. All images were taken and analysed at 20x magnification.

### 3.3.3 Statistical and image analyses

Images from H&E and immunohistochemical staining were analysed using ImageJ Fiji (<https://imagej.nih.gov/ij/download.html>) or Aperio ImageScope version 12.4.3.5008 software (*Leica Biosystems, Wetzlar, Germany*). Morphometric analysis of the various tissue sections was estimated by measuring the diameter of at least 120 cells distributed across the tissue viewed on a single microscope slide. Semi-quantitative analysis of F4/80 staining using ImageJ Fiji was done

according to the protocol described by Crowe and Jue, 2019<sup>23</sup> to quantify macrophages in the tissues.

Statistical analyses were conducted using GraphPad Prism 5 (*GraphPad Software, San Diego, California*). Values are expressed as mean  $\pm$  SEM. One-way ANOVA followed by Bonferroni corrections was used to compare means between three or more categories. When comparing two means, a two-tailed unpaired Student's t-test was used. Two-way ANOVA with Bonferroni corrections was used where necessary. Statistically significant results are indicated as \* $P < 0.05$ , \*\* $P < 0.01$ , \*\*\* $P < 0.001$ .

### 3.4 Results

#### 3.4.1 Deficiency in *Slc7a8* protects against diet-Induced Obesity

WT and KO mice gained significantly more weight at 14 weeks on HFD than did WTCD ( $p < 0.05$  to  $p < 0.001$ ) and KOCD ( $p < 0.05$  to  $p < 0.001$ ), respectively (Figure 3-1a). No significant differences were observed between WT and KO mice on CD. Interestingly, KOHFD gained significantly ( $p < 0.05$  to  $p < 0.001$ ) less weight than WTHFD, which was evident from week 3 (Figure 3-1a). Significant weight gain in WTHFD was associated with significantly larger ( $p < 0.001$ ) iWAT, pWAT, mWAT, BAT, and liver compared with WTCD and KOHFD. Only the pWAT of KOHFD was significantly larger than in KOCD14 (Figure 3-1d). WTHFD and KOHFD mice appeared visibly larger in size when compared to their respective lean counterparts (Figure S3-1). Total food consumption of WTHFD was significantly greater than that of WTCD ( $p < 0.001$ ) and KOHFD ( $p < 0.01$ ) (Figure 3-1b). Energy intake increased significantly between WTCD and WTHFD ( $p < 0.01$  at week 5 and  $p < 0.001$  from week 6 to week 14) and between KOCD and KOHFD ( $p < 0.05$  at week 3,  $p < 0.01$  at week 4, and  $p < 0.001$  from week 5 to 14) (Figure 3-1c). A significant difference ( $p < 0.001$ ) in cumulative caloric intake was observed between WTHFD and KOHFD from week 9 to week 14. No significant differences in calorie intake were seen between KOCD and WTCD.

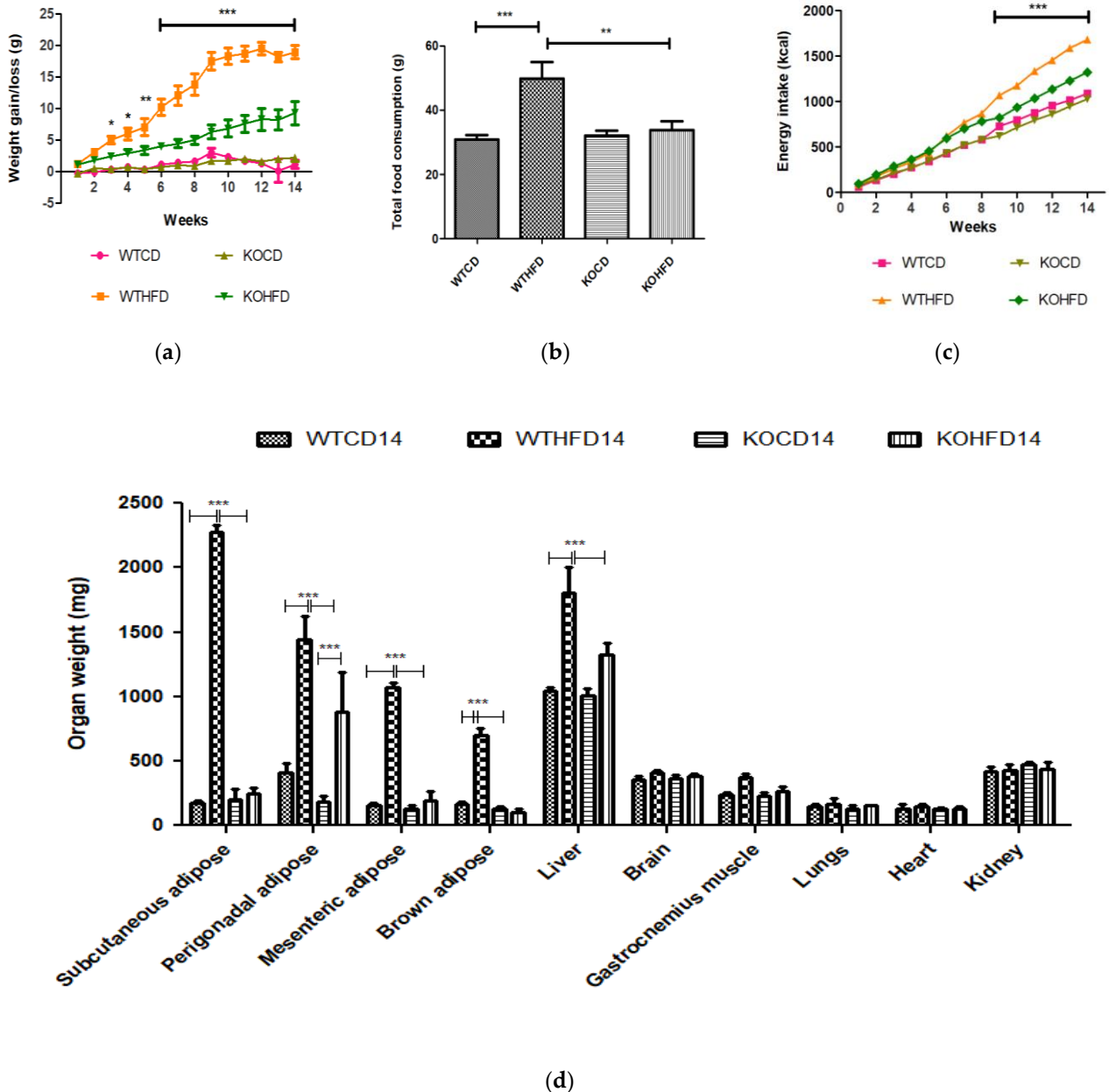


**Figure 3-1: Effect of *Slc7a8* deletion on body weight and caloric intake.** (a) WTHFD gained significantly more weight throughout the 14-week period starting from week 2 than did WTCD ( $p < 0.05$  to  $p < 0.001$ ). KOHFD gained significantly more weight than KOCD ( $p < 0.05$ ). The difference in weight gain between WTHFD and KOHFD was significant starting in week 3, with the  $p$ -value decreasing gradually from  $p < 0.05$  to  $p < 0.001$ . WTCD and KOCD showed no differences in weight. (b) Total cumulative food consumption was significantly greater in WTHFD than in WTCD ( $p < 0.001$ ) and KOHFD ( $p < 0.01$ ). Energy intake increased significantly (from  $p < 0.01$  at week 5 to  $p < 0.001$  from week 6 to week 14) between WTCD and WTHFD. (c) A significant difference ( $p < 0.001$ ) in caloric intake was observed between WTHFD and KOHFD from week 11 to week 14. Comparisons between KOCD and KOHFD revealed significant differences in calorie intake, with  $p < 0.05$  at week 3,  $p < 0.01$  at week 4, and  $p < 0.001$  from week 5 to 14. No significant differences in caloric intake were seen between KOCD and WTCD. (d) WTHFD showed significantly larger ( $p < 0.001$ ) iWAT, pWAT, mWAT, BAT, and liver compared to WTCD and KOHFD. Week 1–5:  $N = 18$  for WTCD, WTHFD, and KOHFD and  $N = 17$  for KOCD; week 6–8:  $N = 12$  for WTCD, WTHFD, and KOHFD and  $N = 11$  for KOCD; week 9–12:  $N = 6$  for WTCD, WTHFD, and KOHFD and  $N = 5$  for KOCD; week 13–14:  $N = 5$  for WTCD, WTHFD, and KOCD and  $N = 6$  for KOHFD. \* $p < 0.05$ , \*\*  $p < 0.01$ , \*\*\*  $p < 0.001$ .

### 3.4.2 Deficiency in *Slc7a8* has no effect on glucose and insulin metabolism but significantly improves glucose tolerance when on HFD

WT and KO mice showed no difference in metabolism of exogenous glucose (Figure 3-2a,b) or insulin (Figure 3-2c,d) prior to introducing them to the experimental diets. However, significantly elevated glucose levels ( $p < 0.01$ ) were observed for the KO mice at 30 min.

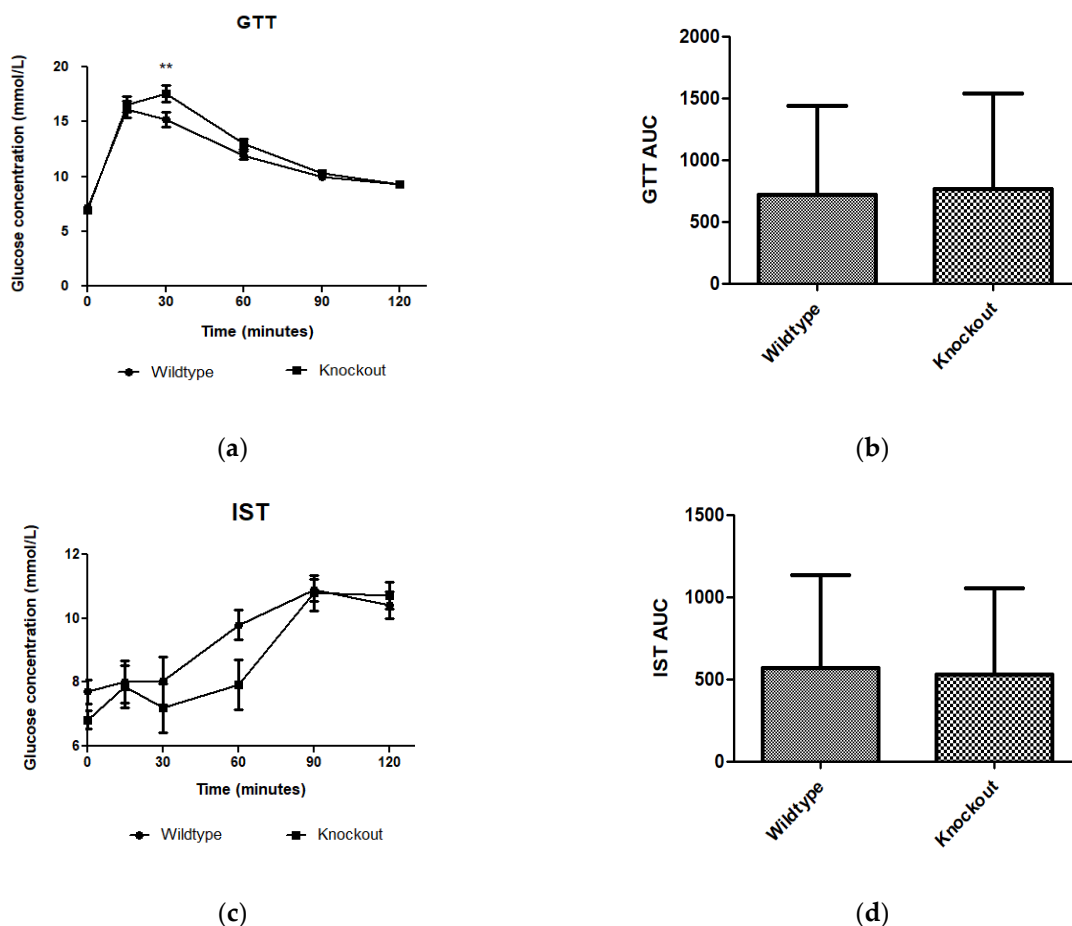


**Figure 3-2: Effect of genotype on glucose tolerance and insulin sensitivity tests.** GTT and IST were conducted before introducing the C57BL/6J wildtype and *Slc7a8* knockout mice to CD or HFD. (a,c) No significant differences were observed in GTT or IST between the WT and KO mice except for significantly higher glucose levels ( $p < 0.01$ ) observed for the KO mice at 30 min with the GTT. (b,d) No significant differences were observed between the areas under the curve (AUCs) for WT and KO mice during GTT and IST. GTT: N = 47 for WT and N = 48 for KO; IST: N = 47 for WT and N = 44 for KO. \*\* $p < 0.01$ .

After 5 weeks on experimental diets, no significant difference was observed in glucose metabolism between WT and KO on either the CD or HFD (Figure 3-3a,b). However, at 14 weeks, WTHFD had significantly higher glucose levels than KOHFD and WTCD starting from 30 min (Figure 3-3c). Although WTHFD had a larger AUC than KOHFD and WTCD, this was not statistically significant (Figure 3-3d). No significant differences were observed between the AUCs of WTCD5, WTHFD5,

KOCD5, and KOHFD5 when compared to their 14-week counterparts (WTCD14, WTHFD14, KOCD14, and KOHFD14; Figure 3-3b,d).

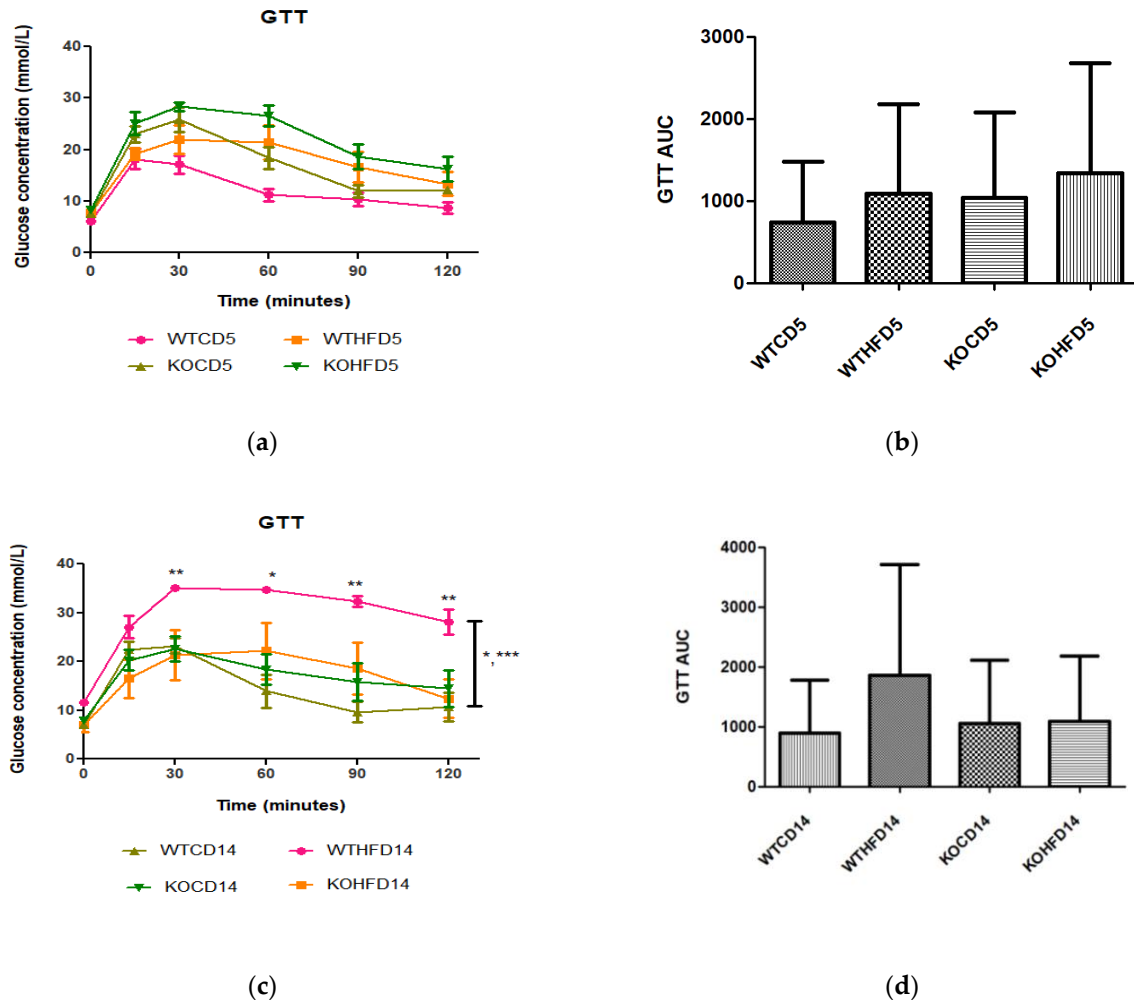
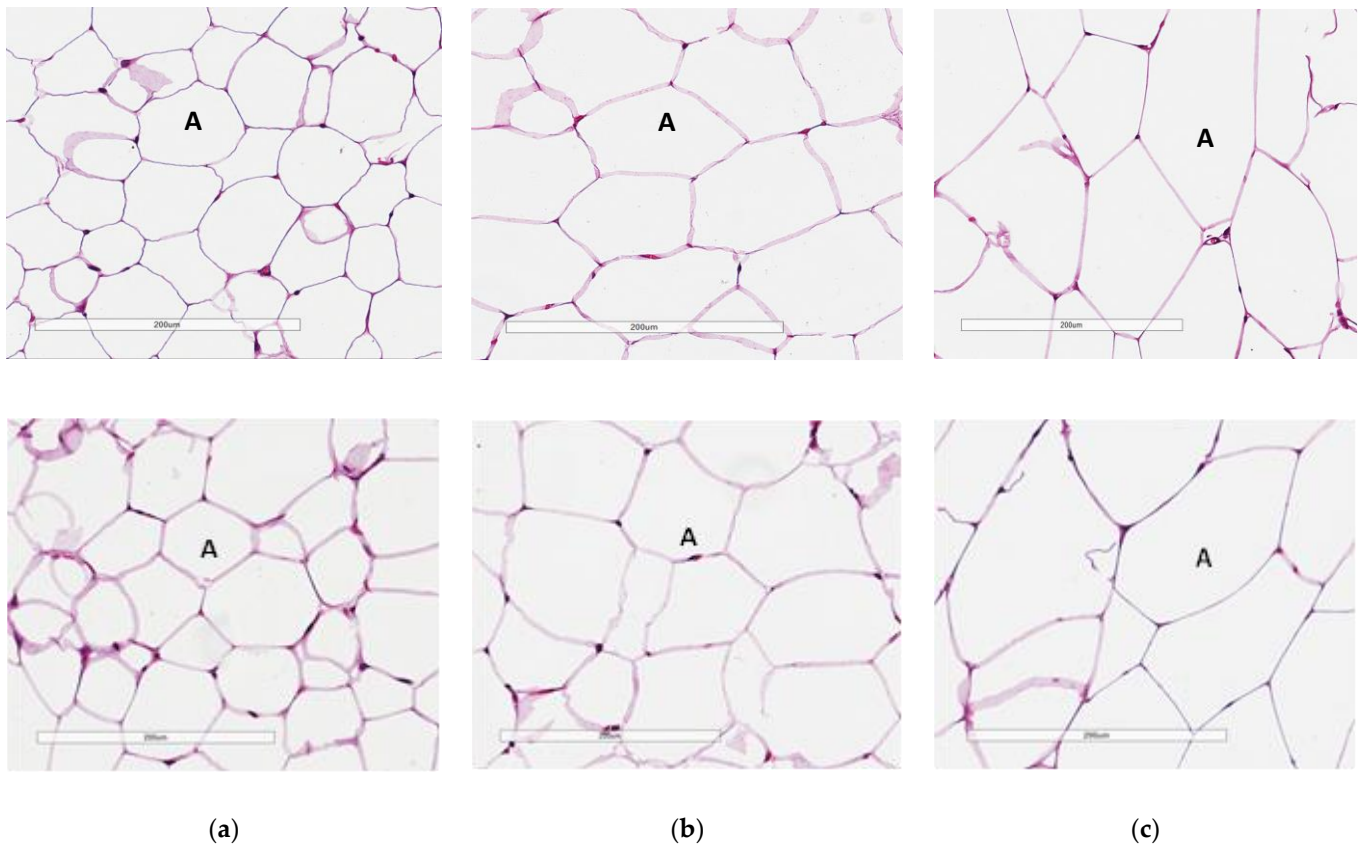


**Figure 3-3: Glucose tolerance and insulin sensitivity tests of animals on experimental diet.** (a) No significant differences were observed after experimental feeding between WT and KO mice on either CD or HFD at 5 weeks. (c) WTHFD showed significantly higher glucose levels than KOHFD ( $p < 0.05$ ,  $0.01$ ) and WTCD ( $p < 0.05$ ,  $0.001$ ) at 14 weeks. (b,d) No significant differences were observed between WTCD5, WTHFD5, KOCD5, and KOHFD5 and their respective 14-week counterparts.  $N = 6$  for WTCD5, WTHFD5, KOCD5, KOHFD5, WTCD14, WTHFD14, and KOCD14 and  $N = 5$  for KOHFD14. \* $p < 0.05$ , \*\* $p < 0.01$ , \*\*\* $p < 0.001$ .

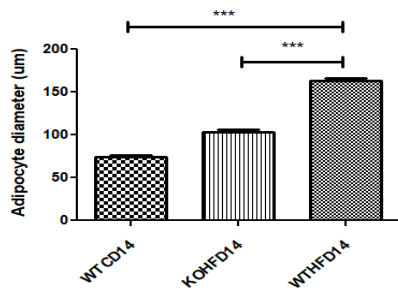
### 3.4.3 *Slc7a8* deletion attenuates adipocyte hypertrophy in white and brown adipose depots

Two representative microscopic images of each adipose tissue depot are depicted in Figure 4. The pWAT from WTCD (Figure 3-4a) and KOHFD (Figure 3-4b) had significantly smaller ( $p < 0.001$ ) adipocytes (A) than did WTHFD (Figure 3-4c), as indicated in Figure 3-4d. The number of adipocytes per field was significantly higher in WTCD ( $p < 0.001$ ) and KOHFD ( $p < 0.05$ ) than in WTHFD (Figure 3-4e). The iWAT in WTHFD (Figure 3-4h) had a significant increase ( $p < 0.001$ )

(Figure 3-4i) in adipocyte hypertrophy compared with that in KOHFD (Figure 3-4g) and WTCD (Figure 3-4f). Similarly, a significant increase ( $p < 0.001$ ) was observed in the adipocyte size of mWAT from WTHFD (Figure 4m) in comparison with those from KOHFD (Figure 3-4l) and WTCD (Figure 3-4k), Figure 3-4n. The number of adipocytes per field was significantly lower in the mWAT ( $p < 0.01$ ) (Figure 3-4j) and iWAT ( $p < 0.001$ ) (Figure 3-4o) of WTHFD than in those of WTCD, as well as in the mWAT ( $p < 0.01$ ) and iWAT ( $p < 0.001$ ) of WTHFD than in those of KOHFD. Lipid droplet accumulation was greater in the BAT of WTHFD (Figure 3-4r) than in that of WTCD (Figure 3-4p) and KOHFD (Figure 3-4q). Additionally, as early as 5 weeks on the experimental diet, adipocyte hypertrophy was greater in WTHFD than in KOHFD and WTCD in pWAT, mWAT, and iWAT, and larger lipid droplets were observed in the BAT of WTHFD (Figure S3-2).

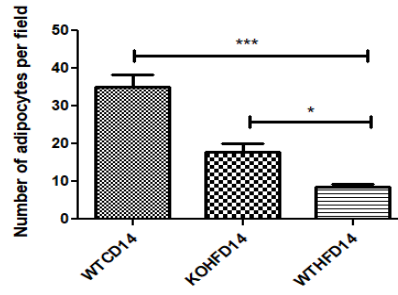


14 weeks perigonadal adipose

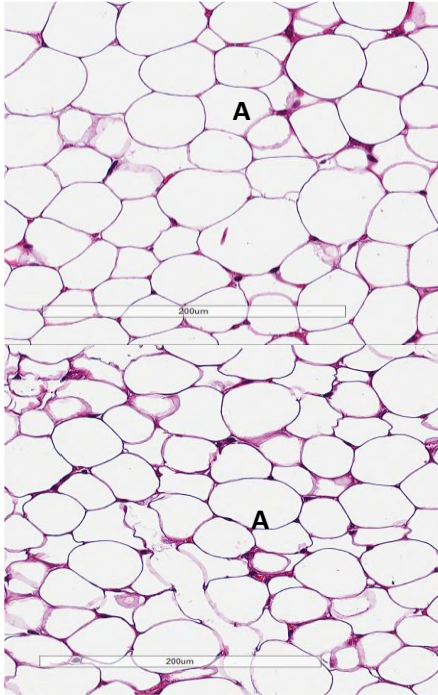


(d)

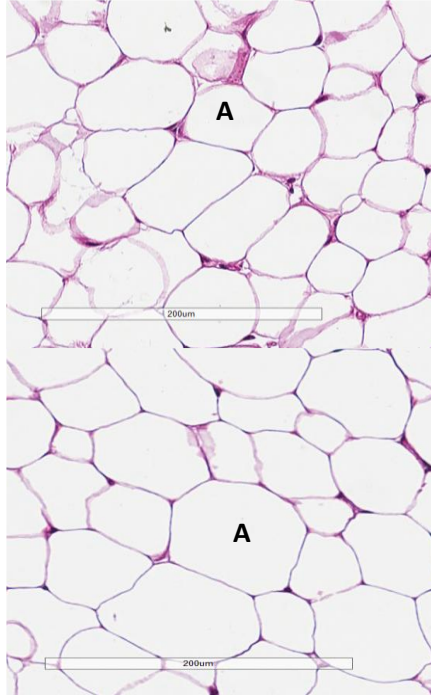
14 weeks perigonadal adipose



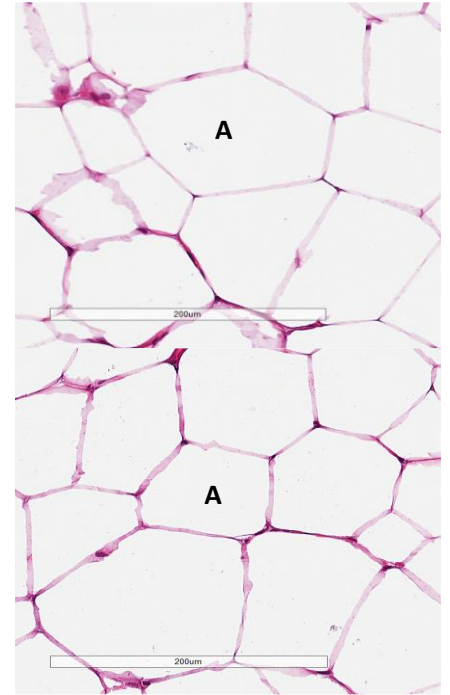
(e)



(f)

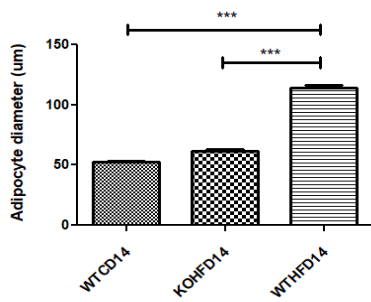


(g)



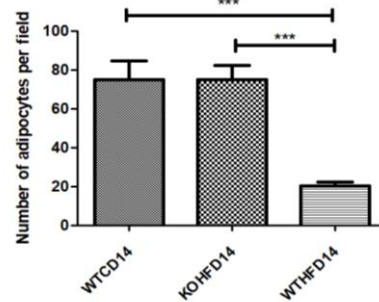
(h)

14 weeks inguinal subcutaneous adipose

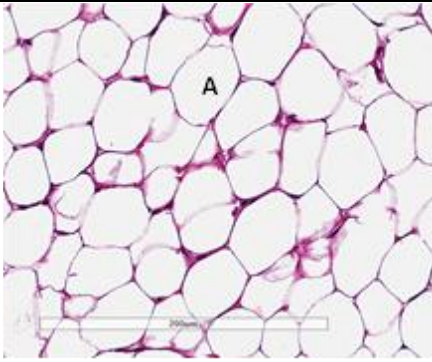


(i)

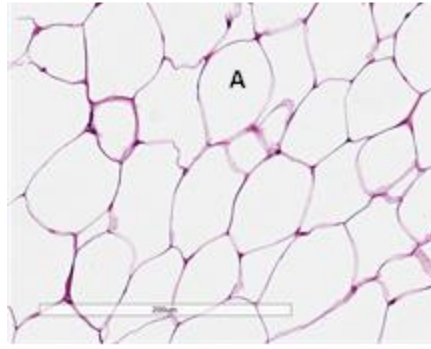
14 weeks inguinal subcutaneous adipose



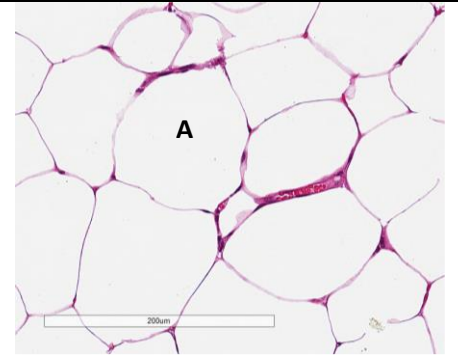
(j)



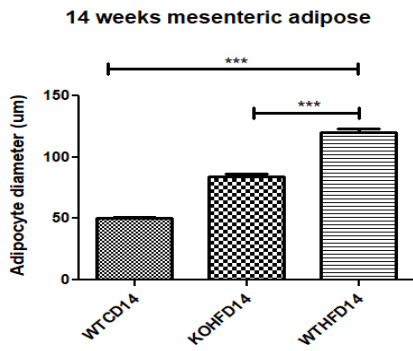
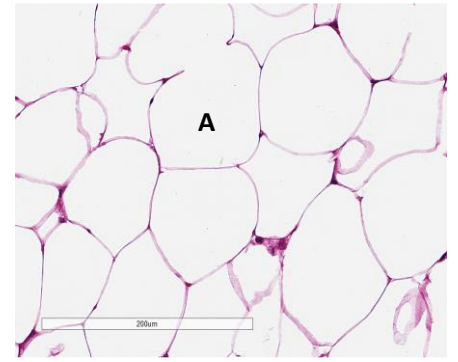
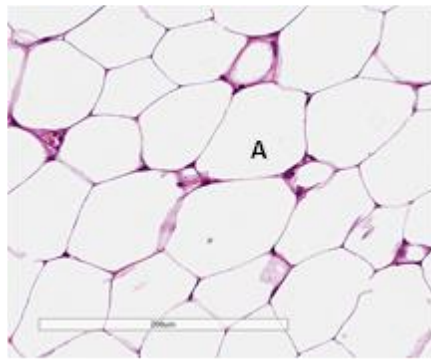
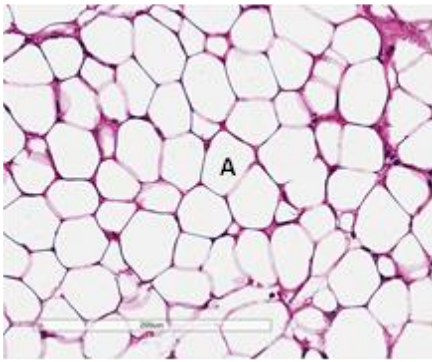
(k)



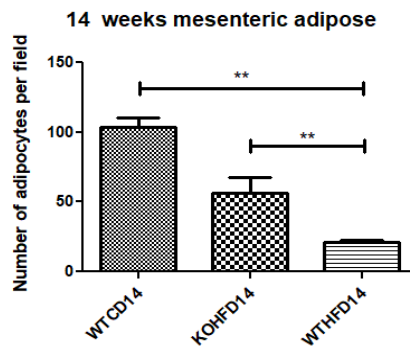
(l)



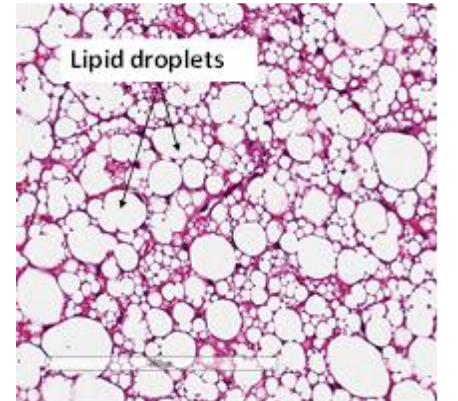
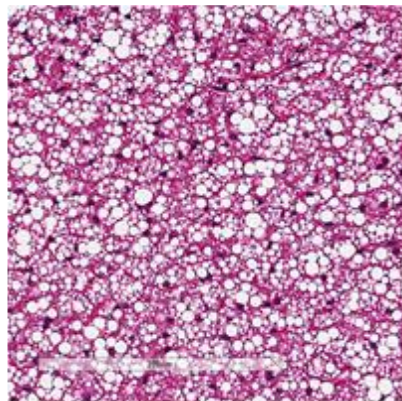
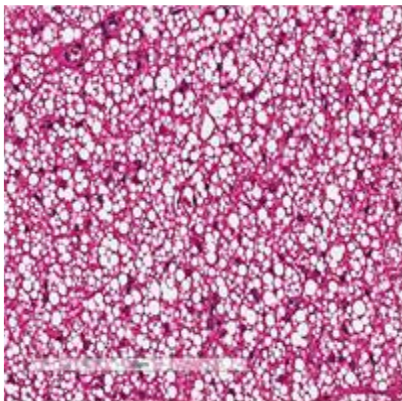
(m)



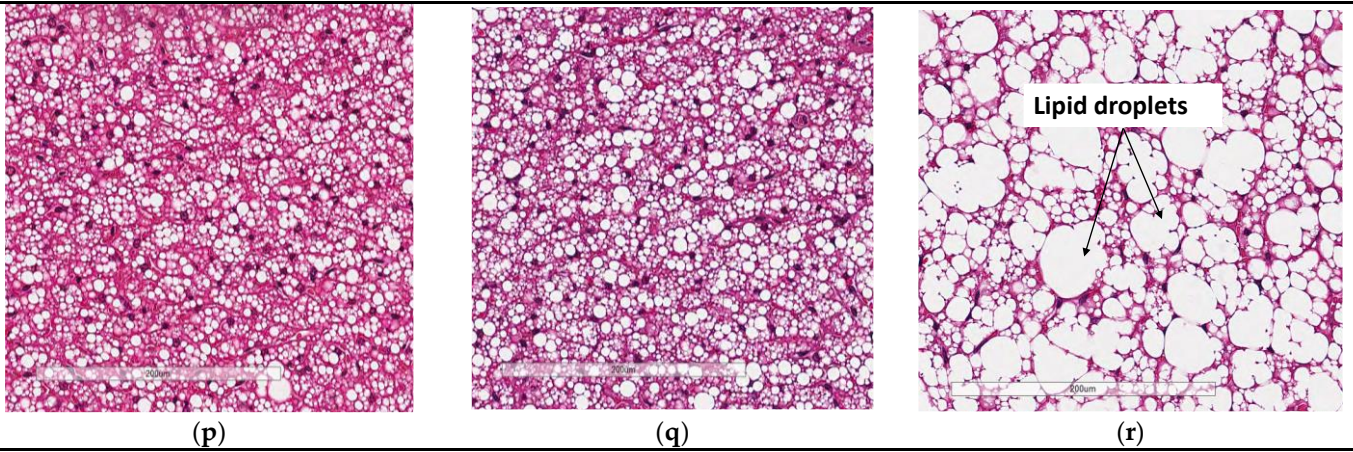
(n)



(o)



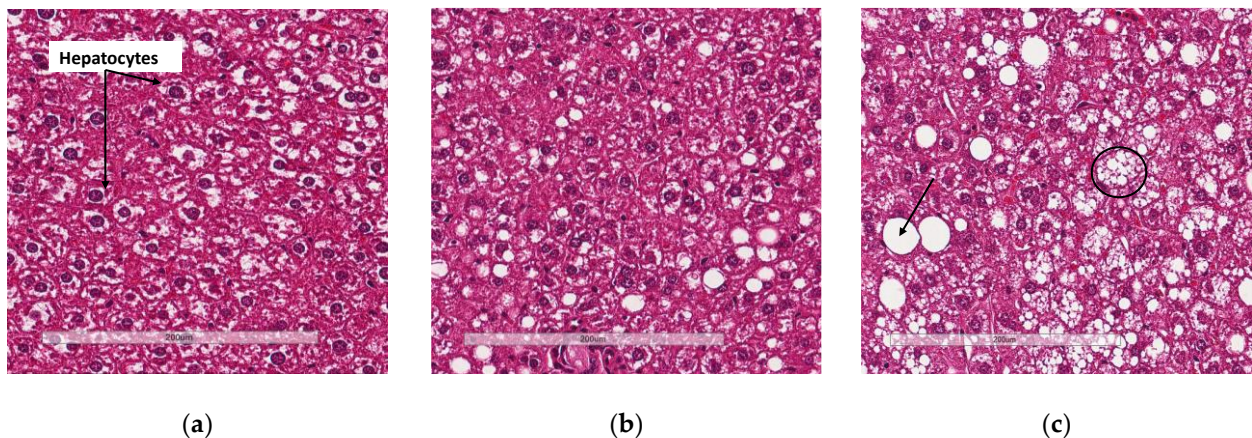




**Figure 3-4: Adipocyte size distribution across the various adipose tissue depots.** H&E-stained sections of perigonadal WAT (pWAT) (d) revealed that the WTHFD (c) had significantly larger ( $p < 0.001$ ), adipocytes than WTCD (a) and KOHFD (b). The number of adipocytes per field was significantly smaller in WTHFD than KOHFD ( $p < 0.05$ ) and WTCD ( $p < 0.001$ ), (e). Similarly, adipocyte diameter of WTHFD (h), of inguinal subcutaneous WAT (iWAT) was significantly greater ( $p < 0.001$ ), (i), than that of WTCD (f), and KOHFD (g). Conversely, the number of adipocytes per view was significantly lower ( $p < 0.001$ ) in WTHFD compared to WTCD, (m) and KOHFD, (j). Significant ( $p < 0.001$ ) adipocyte hypertrophy (n) was also observed in mWAT of WTHFD, (m), compared to WTCD, (m) and KOHFD, (l). Additionally, significantly ( $p < 0.01$ ) fewer adipocytes were viewed per field in WTHFD compared to WTCD and KOHFD, (o). Sections of the BAT revealed that WTCD (p), and KOHFD (q), had smaller lipid droplets compared to those observed in WTHFD (r). Magnification = 20X, Scale bar = 200  $\mu\text{m}$ . Key: A = adipocyte. N = 120 adipocytes

#### 3.4.4 Deletion of *Slc7a8* reduces liver steatosis in diet-induced obese mice

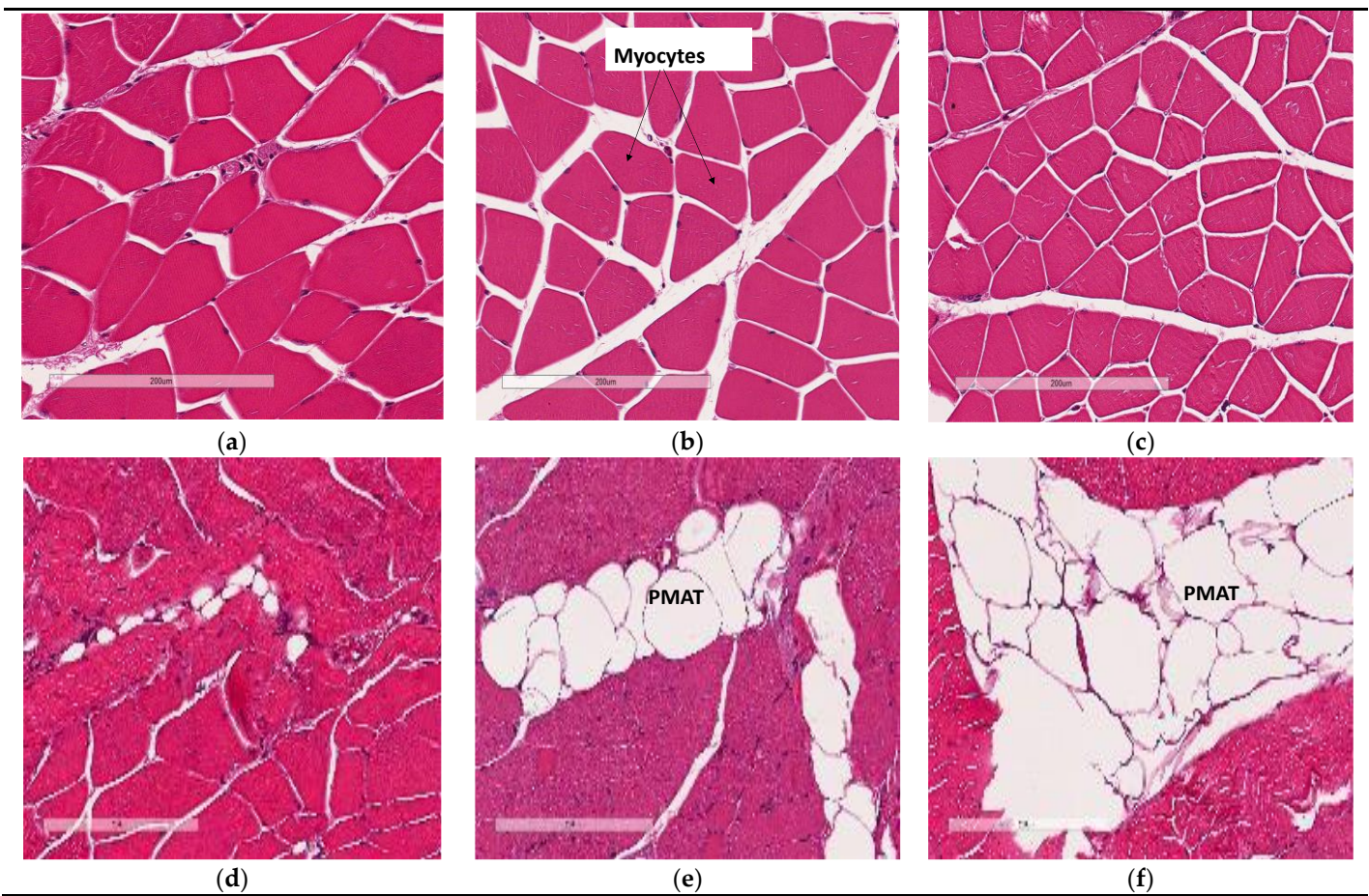
Liver sections from WTHFD (Figure 3-5c) showed lipid accumulation, which could be categorised as microvesicular (circled, Figure 3-5c) and macrovesicular (indicated in black arrow, 3-Figure 5c) steatosis. This phenomenon was absent in liver sections of WTCD (Figure 5a), while macrovesicular steatosis observed in KOHFD (Figure 3-5b) had smaller lipid droplets than that in WTHFD (Figure S3-3).

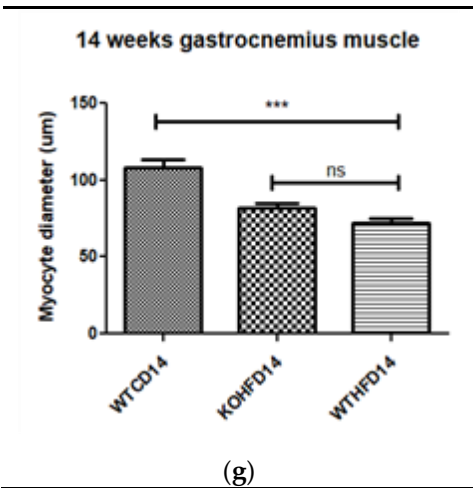


**Figure 3-5: Lipid accumulation in the liver.** H&E-stained liver sections showed the presence of micro- and macrovesicular steatosis in WTHFD (c), which was reduced in KOHFD (b) and absent in WTCD (a). Magnification = 20x. Scale bar = 200  $\mu\text{m}$ .

### 3.4.5 Deficiency in *Slc7a8* decreases lipid accumulation in gastrocnemius muscle

Skeletal muscle myocyte atrophy was observed in WTHFD (Figure 3-6c), which had significantly smaller myocytes ( $p < 0.001$ ) (Figure 3-6g) than WTCD (Figure 3-6a). The deletion of *Slc7a8* increased myocyte size in KOHFD (Figure 3-6b) compared to WTHFD (Figure 3-6g). Accumulation of perimuscular adipose tissue (PMAT) (Figure 3-6f) was greater in WTHFD than in KOHFD (Figure 3-6e) and WTCD (Figure 3-6d). At week 5, the KOHFD had significantly larger myocytes ( $p < 0.001$ ) and less adipose tissue than WTHFD (Figure S3-4).

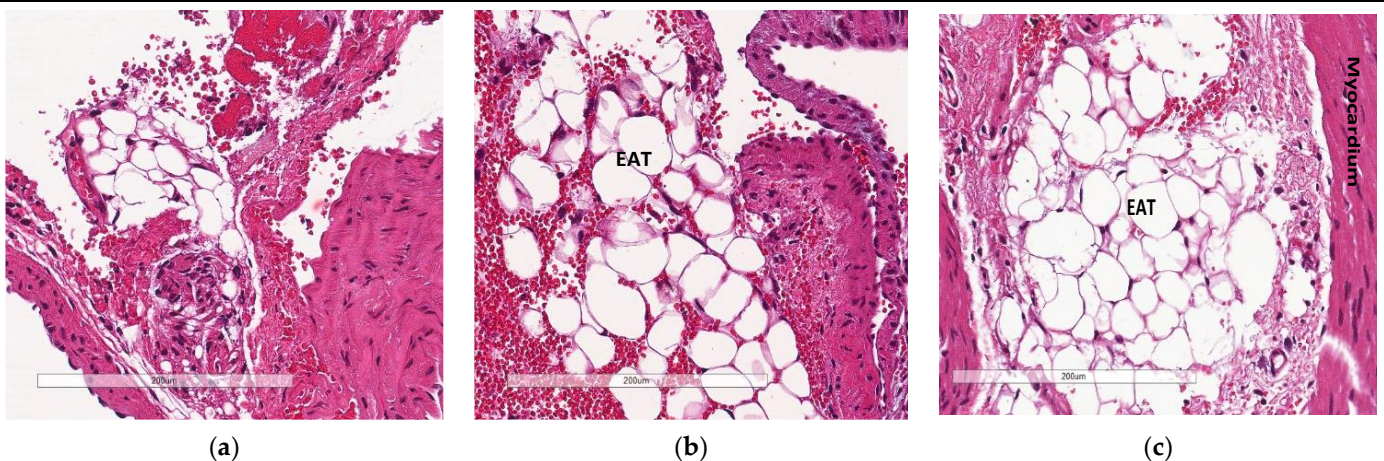


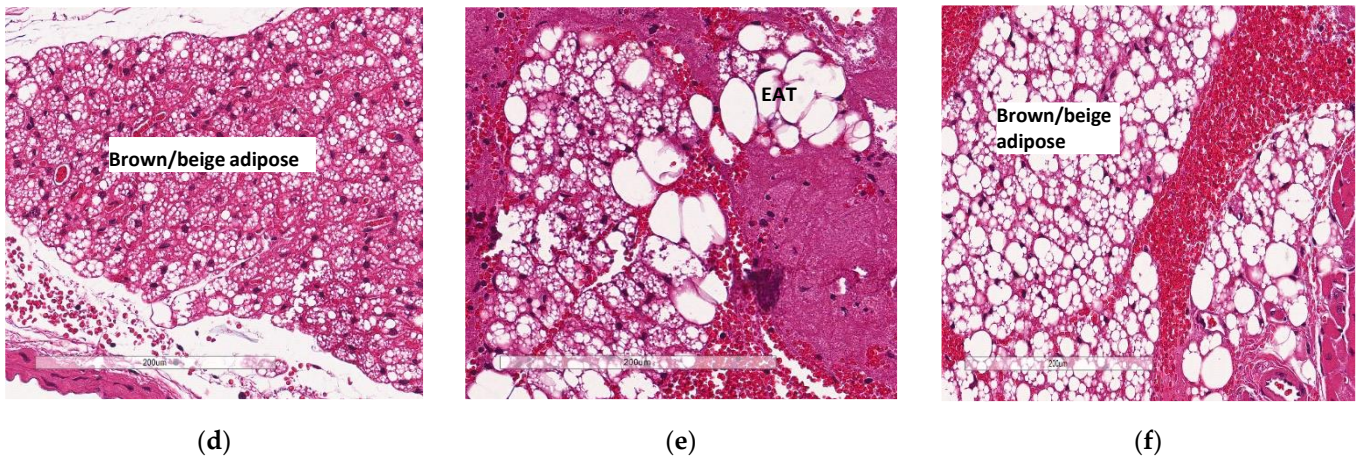


**Figure 3-6: Effect of *Slc7a8* deletion on adipose tissue accumulation and myocyte atrophy in gastrocnemius muscle.** Myocyte atrophy was observed in WTHFD (c) when compared to WTCD (a) and KOHFD (b). WTHFD had significantly smaller ( $p < 0.001$ ) (g) myocytes than WTCD. Greater perimuscular adipose tissue (PMAT) accumulation was seen in WTHFD (f) than in WTCD (d) and KOHFD (e).  $N = 120$  myocytes. \*\*\* $p < 0.001$ .

### 3.4.6 Deficiency in *Slc7a8* reduces accumulation of epicardial adipose tissue

The increase in the accumulation of epicardial adipose tissue (EAT—white adipose tissue) observed in WTHFD (Figure 3-7c) compared to WTCD (Figure 3-7a) was decreased following the deletion of *Slc7a8*, KOHFD (Figure 3-7b). Larger lipid droplets were observed in the brown/beige adipose tissue (a property of epicardial adipose tissue) in WTHFD (Figure 3-7f) than in that in WTCD (Figure 3-7d) and KOHFD (Figure 3-7e).

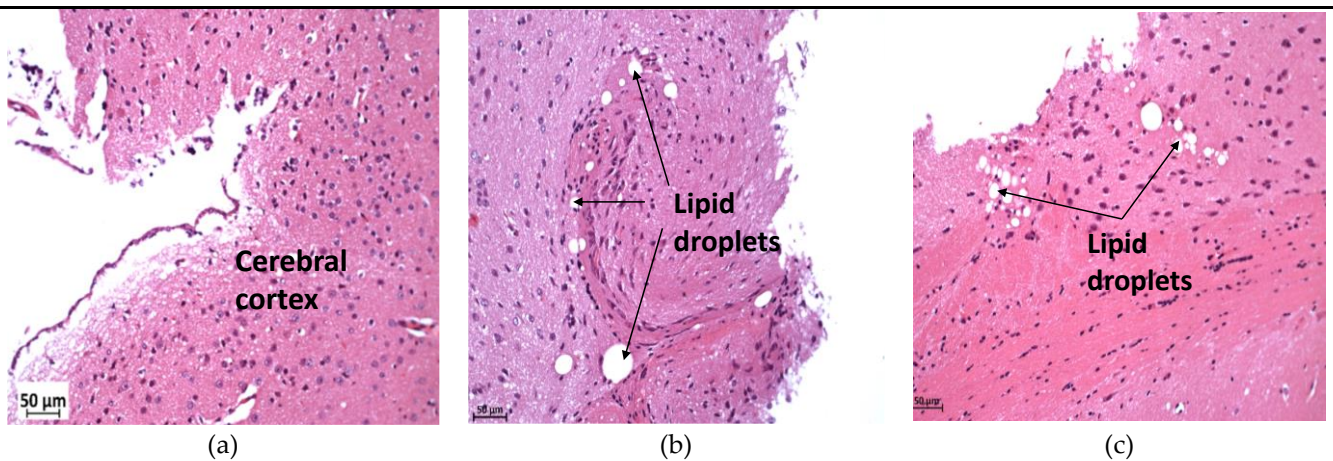




**Figure 3-7: Effect of *Slc7a8* on epicardial adipose tissue accumulation in the heart.** H&E-stained heart sections showed a greater accumulation of epicardial adipose tissue, seen as a brown/beige adipose depot, in the WTHFD (c) compared to WTCD (a) and KOHFD (b). The images demonstrate that the WTHFD (f) mice had more connective tissue (cardiac muscle fibres) than WTCD (d) and KOHFD (e). Magnification = 20×. Scale bar = 200 μm.

### 3.4.7 Deficiency in *Slc7a8* reduces lipid accumulation in the ganglion layer in diet-induced obese mice

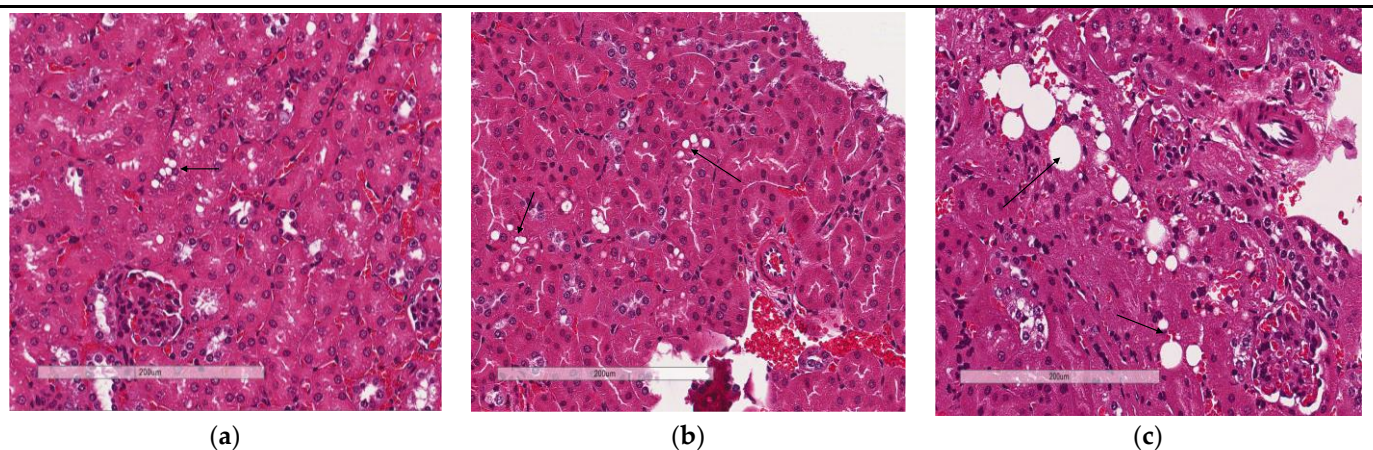
In the cerebral cortex, lipid droplets were seen in KOHFD (Figure 3-8b) and WTHFD (Figure 3-8a), but not in WTCD (Figure 3-8c).



**Figure 3-8: Effect of *Slc7a8* deletion on lipid droplet accumulation in brain tissue.** H&E-stained sections of brain tissue showed lipid droplets in the cerebral cortices of KOHFD (b) and WTHFD (c) that were not seen in that of WTCD (a). Magnification = 20×. Scale bar = 50 μm.

### 3.4.8 Deficiency in *Slc7a8* reduces lipid accumulation in the kidney

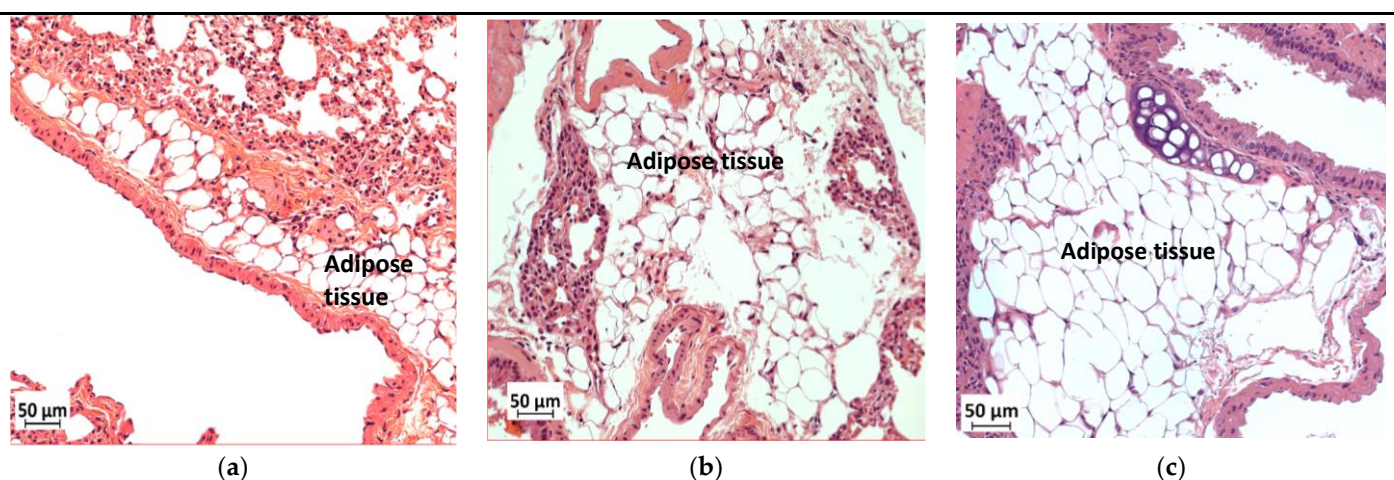
Lipid droplet accumulation was reduced in KOHFD (Figure 3-9b) to the level observed in WTCD (Figure 3-9a). WTHFD showed visibly larger lipid droplets (Figure 3-9c).



**Figure 3-9: Effect of *Slc7a8* deletion on lipid accumulation in the kidneys.** H&E-stained sections showed that accumulation of lipids (black arrows) was greater in WTHFD (c) than in WTCD (a) and KOHFD (b). Magnification = 20×. Scale bar = 200 µm.

### 3.4.9 Deficiency in *Slc7a8* reduces adipose tissue accumulation in the lungs

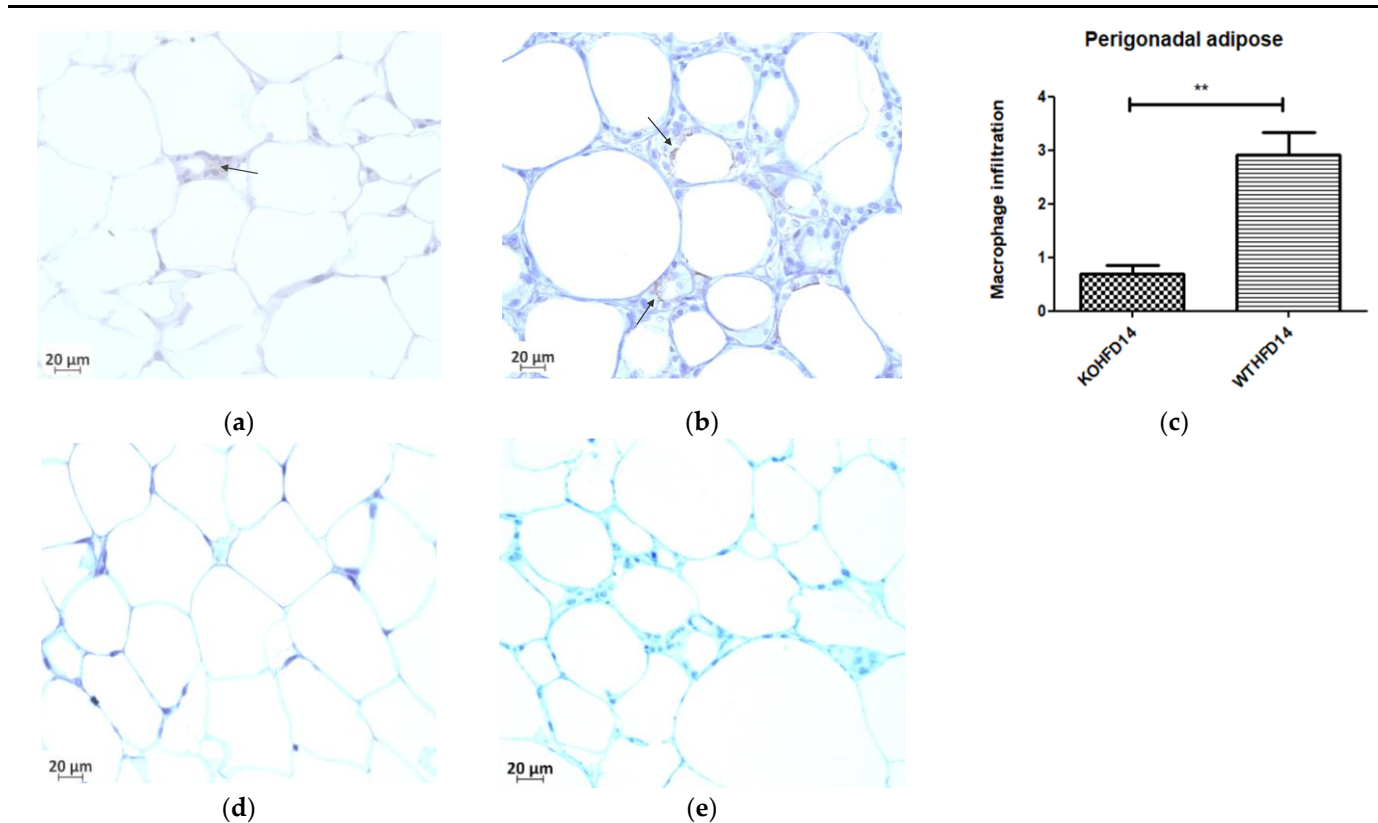
Histological analysis of the lungs showed greater accumulation of adipose tissue in WTHFD (Figure 3-10c) than in WTCD (Figure 3-10a). The accumulation of adipose tissue in DIO appeared to be reduced in KOHFD (Figure 3-10b). Lipid accumulation in the lungs was observed as early as week 5, with more adipose tissue in WTHFD and KOHFD than in WTCD (Figure S3-5).



**Figure 3-10: Effect of *Slc7a8* deletion on lipid accumulation in the lungs.** H&E-stained lung sections showed the accumulation of adipose tissue in the lungs, which was greater in WTHFD (c) than in KOHFD (b) and WTCD (a). Magnification = 20×. Scale bar = 50 µm.

### 3.4.10 Deficiency in *Slc7a8* reduces white adipose tissue inflammation in DIO

Immunohistochemical staining for F4/80, a mouse macrophage marker, was performed to assess the presence of macrophages in pWAT, mWAT, iWAT and brown adipose tissue. Deletion of *Slc7a8* significantly decreased macrophage infiltration (indicated by black arrows) in the pWAT (Figure 3-11c;  $p < 0.01$ ), mWAT (Figure 3-11h;  $p < 0.05$ ), and iWAT (Figure 3-11k;  $p < 0.01$ ) of KOHFD (Figure 3-11a,f,i) compared with those of WTHFD (Figure 3-11b,g,j). No significant difference was observed in the brown adipose macrophage inflammation profile (Figure 3-11n) between WTHFD (Figure 3-11m) and KOHFD (Figure 3-11l). Figure 3-11d,e shows the negative controls for KOHFD and WTHFD, respectively, in perigonadal adipose tissue.



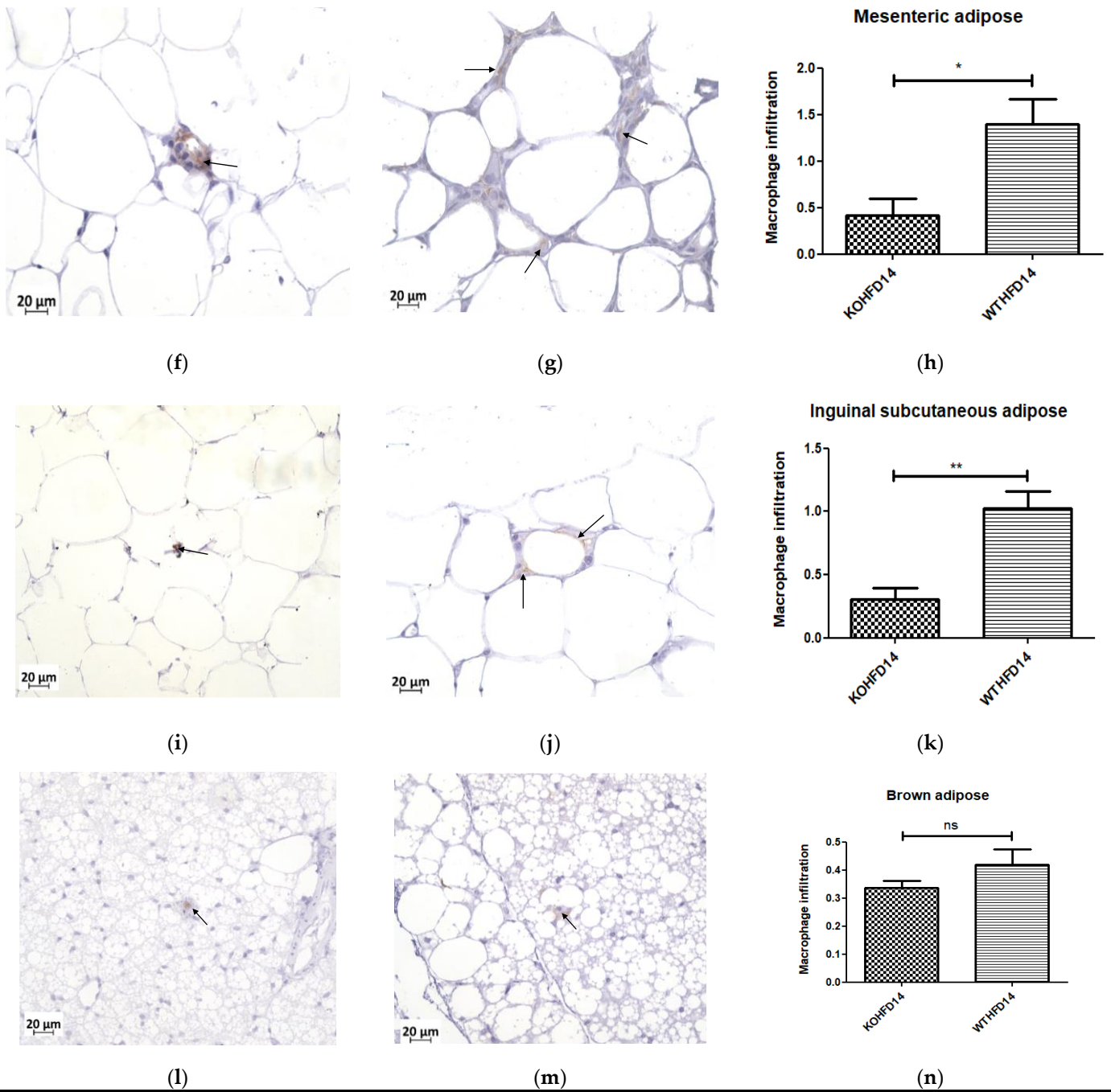


**Figure 3-11: Effect of *Slc7a8* deletion on macrophage infiltration in adipose tissue.** KOHFD (a) showed a significant decrease in macrophage infiltration (indicated by black arrows) in pWAT ( $p < 0.01$ ), (c) compared to WTHFD (b). (d,e) represent the negative controls for KOHFD and WTHFD, respectively, in perigonadal adipose tissue. A significant decrease in macrophage infiltration in mWAT ( $p < 0.05$ ) (h) was observed in KOHFD (f) compared to WTHFD (g). A significant decrease in macrophage infiltration in iWAT ( $p < 0.01$ ) (k) was observed in KOHFD (i) compared to WTHFD (j). No significant differences in macrophage infiltration in brown adipose tissue (n) were observed between KOHFD (l) and WTHFD (m). Magnification = 40 $\times$ . Scale bar = 20  $\mu$ m. N = 5 fields. \* $p < 0.05$ , \*\* $p < 0.01$ .

### 3.4.11 Deficiency in *Slc7a8* reduces inflammation in the liver

Deficiency in *Slc7a8* resulted in a significant ( $p < 0.05$ ) (Figure 3-12c) reduction in macrophages in the liver from KOHFD, Figure 3-12a, compared to WTHFD (Figure 3-12b). Figure 3-12d,e show negative control staining of KOHFD and WTHFD, respectively; no staining for macrophages was detected in these controls.

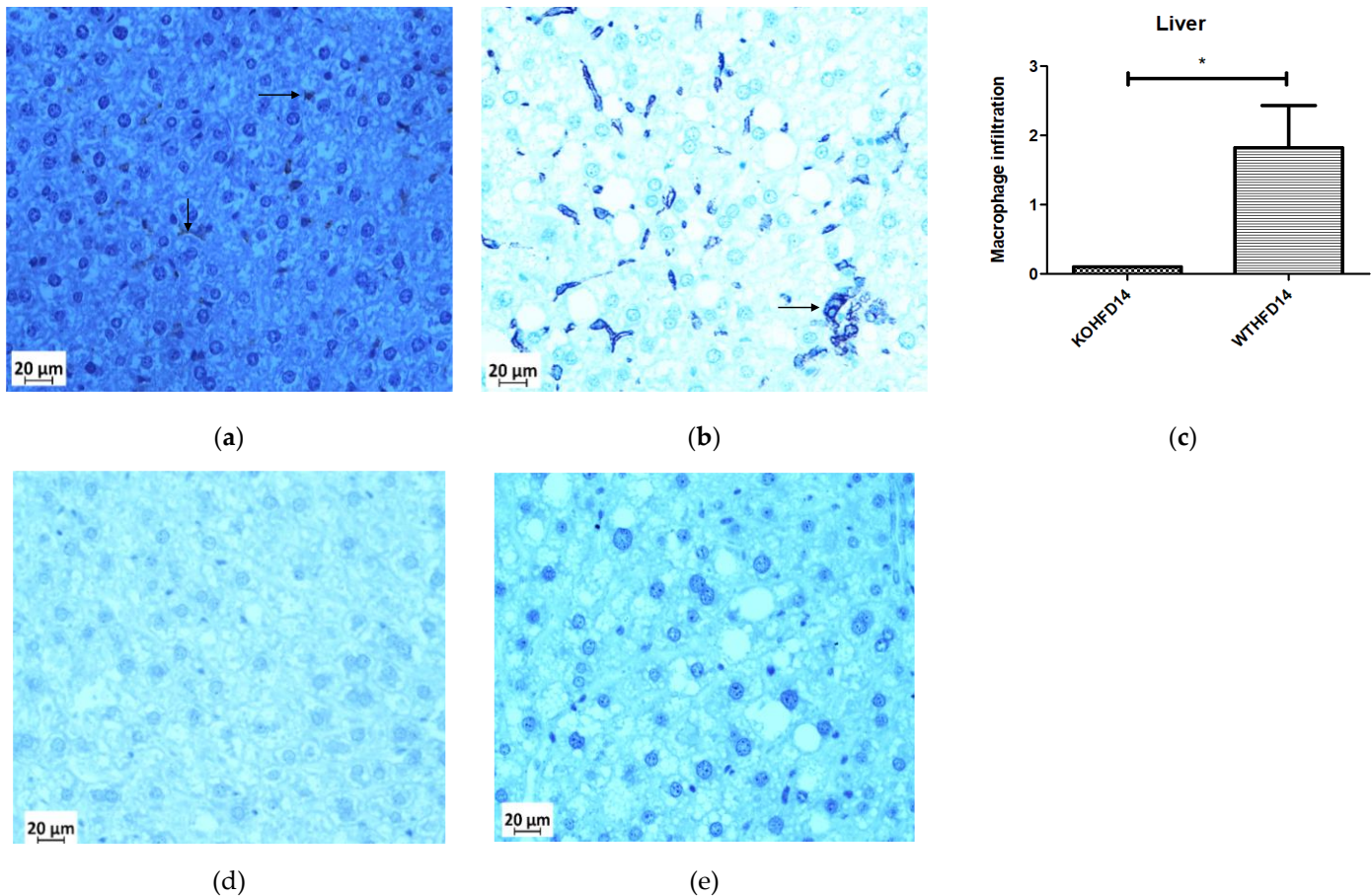


**Figure 3-12: Effect of *Slc7a8* deletion on the presence of macrophages in the liver.** WTHFD (b) had significantly greater infiltration ( $p < 0.05$ ) (c) of macrophages than KOHFD, (a). Negative controls for KOHFD (d) and WTHFD (e); no macrophages were detected. Magnification = 40 $\times$ . Scale bar = 20  $\mu$ m. N = 10 fields. \*  $p < 0.05$ .

### 3.4.12 Deficiency in *Slc7a8* has no effect on the presence of macrophages in the kidney or gastrocnemius muscle in DIO

The presence of macrophages in the kidney of KOHFD (Figure 3-13a) and WTHFD (Figure 3-13b) was similar (Figure 3-13c). This observation was the same for the gastrocnemius muscle of KOHFD



(Figure 3-13d) and WTHFD (Figure 3-13e), with no statistical difference in macrophage profile between them (Figure 3-13f).

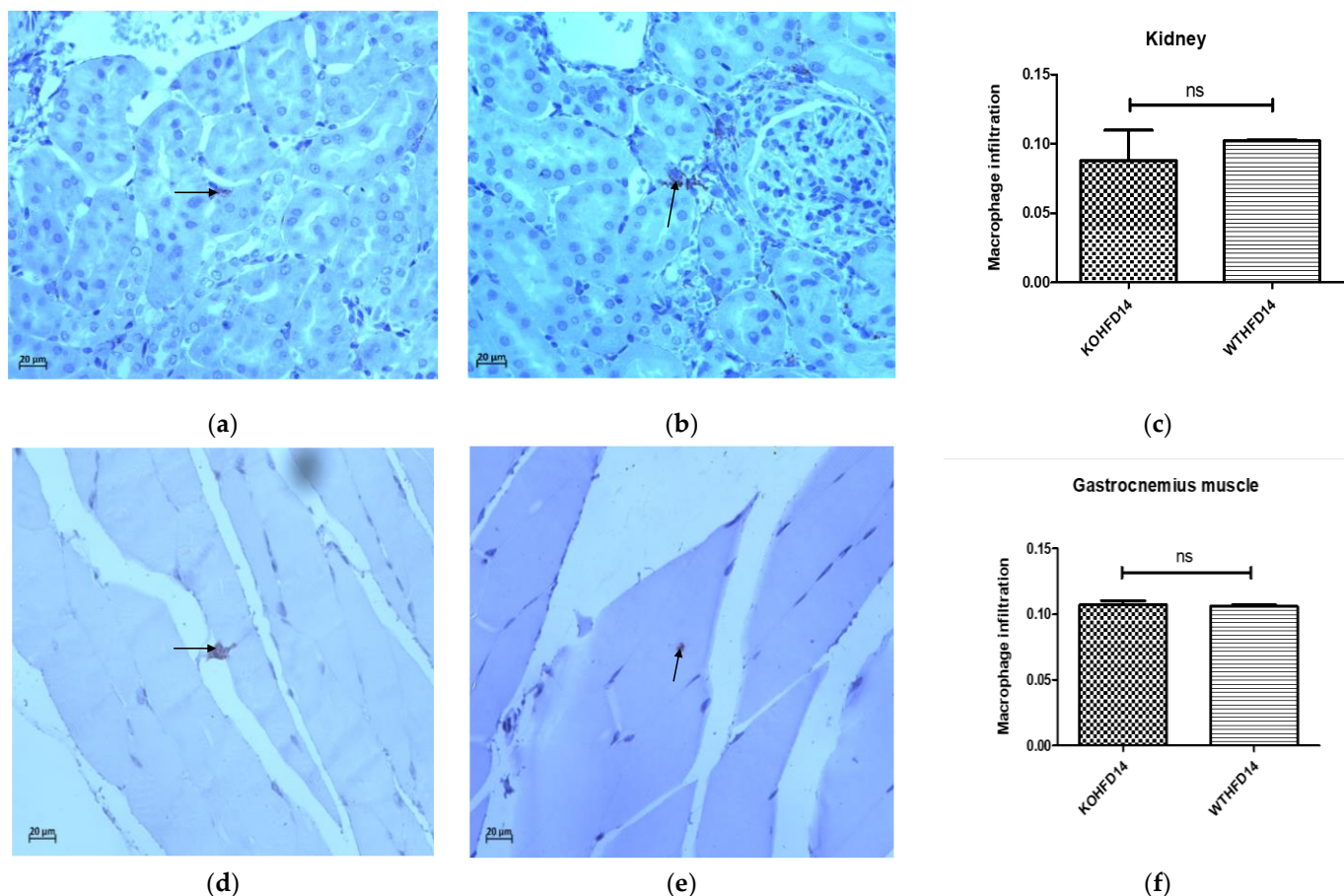


**Figure 3-13: Effect of *slc7a8* on macrophage infiltration profiles of the kidney and gastrocnemius muscle.** KOHFD (a) had slightly fewer macrophages infiltrating into the kidney (c) than WTHFD (b). However, no significant differences were noted between KOHFD and WTHFD. No significant differences (f) were observed in infiltration between the gastrocnemius muscles of KOHFD (d) and WTHFD (e). Magnification = 40×. Scale bar = 20 µm. N = 5 fields.

### 3.5 Discussion

Obesity is characterised by excessive accumulation of adipose tissue and is associated with the development of metabolic syndromes affecting many organs and tissues in the body. The search for molecular factors that play a role in attenuating lipid accumulation in conditions such as diet-induced obesity is paramount to identifying good candidates for therapeutic interventions that mitigate the development of obesity associated comorbidities. Studies of adipogenesis in human-derived stromal/stem cells in vitro have served as an excellent model for identifying molecular factors with a potential role in adipocyte formation and lipid accumulation/metabolism<sup>11,14</sup>. This

study investigated the role of a previously identified novel human adipogenic gene, SLC7A8<sup>14</sup> in diet-induced obesity, and its effect on adipose tissue accumulation in different organs and tissues. To achieve this, *slc7a8* knockout (KO) and wildtype (WT) C57BL/6 mice were fed either a HFD or nutrient matched CD for 14 weeks followed by the analyses of different parameters.

Weight gain, food, and caloric intake between WTCD and KOCD were similar, indicating that *Slc7a8* deletion had no effect on food intake, caloric consumption, or weight gain on a normal diet. WTHFD gained significantly more weight ( $p < 0.001$ ) than WTCD starting from week 3 (Figure 3-1a), with a significantly higher caloric intake ( $p < 0.01$  to  $p < 0.001$ ) than WTCD (Figure 3-1c). Total food consumption was not significantly different during the 14-week period except at week 8, where food consumption in WTHFD was significantly higher ( $p < 0.05$ ). This indicates that the occurrence of diet-induced obesity was due to an increase in caloric intake when on HFD. Interestingly, the *Slc7a8*-deficient genotype on HFD (KOHFD) gained significantly less weight ( $p < 0.05$  to  $p < 0.001$ ) than the WTHFD starting from week 3 (Figure 3-1a). This suggests that *Slc7a8* deletion was protective against diet-induced obesity. The significant decrease in weight gain in KOHFD was accompanied by significantly lower tissue mass of iWAT, mWAT, pWAT, BAT, and liver compared with those in WTHFD (Figure 3-1d). Strikingly, it was observed that KOHFD gained significantly more weight ( $p < 0.05$  to  $p < 0.001$ ) than KOCD from week 8, and this corresponded to a significantly larger pWAT in KOHFD than in KOCD (Figure 3-1d). This indicates that weight gain by KOHFD was due to pWAT expansion and suggests that pWAT was the primary site of lipid accumulation in the KO phenotype.

BAT in WTHFD (Figure 3-4r) displayed enlarged lipid droplets compared with those in WTCD (Figure 3-4p). A recent study showed that following 20 weeks of feeding mice on an HFD, lipid accumulation did not influence the function of brown adipose tissue. However, the authors speculated that if the period of HFD feeding were to be extended, a malfunction of BAT would be observed in obese mice<sup>24</sup>. We observed in the current study that KOHFD (Figure 3-4q) attenuated adipocyte hypertrophy and lipid accumulation in BAT. This suggests that *Slc7a8* deletion could be protective against the long-term effects of BAT hypertrophy and malfunctioning caused by DIO.

Furthermore, it was observed that WTHFD had a significantly greater caloric intake than KOHFD (Figure 3-1c) while food consumption was similar, except at week 11, when a significant difference ( $p < 0.05$ ) was observed. It is possible that the deletion of *Slc7a8* regulated weight gain on HFD by

burning calories quicker than WTHFD, since both KOHFD and WTHFD had similar caloric intake up to week 8 (Figure 3-1c), but as early as week 5, adipocyte hypertrophy was already significantly greater in WTHFD than in KOHFD (Figure S3-2). Additionally, food and caloric intake was similar between KO and WT on a normal diet, with differences observed only on HFD; this could suggest satiety in KOHFD, as caloric intake significantly decreased after week 8 (Figure 3-1c).

Adipose tissue expansion in obesity is commonly associated with conditions such as hyperglycaemia, impaired glucose tolerance, and insulin resistance<sup>25</sup>. To investigate the effect of *Slc7a8* deletion on the metabolism of exogenous glucose and insulin, GTT and IST were performed on all animals (KO and WT) prior to introducing them to an experimental diet (Figure 3-2a,b). Importantly, there was no significant difference between the KO and WT mice for either test. This shows that the deletion of *Slc7a8* had no effect on their ability to metabolise glucose and insulin efficiently. However, significantly higher levels of blood glucose were seen in KO mice at 30 min of the GTT (Figure 3-2a), which later returned to normal, without any change in the AUC between KO and WT (Figure 3-2b). Both WTCD and KOCD at 5 and 14 weeks showed similar trends in glucose metabolism (Figure 3-3a,c), with no difference in the AUC (Figure 3-2b,d), suggesting that glucose metabolism was unaltered in *slc7a8*-deficient mice on a normal diet. Under conditions of DIO, WTHFD showed significantly higher levels of glucose intolerance than WTCD, and this effect was significantly improved in KOHFD, with blood glucose levels returning to baseline levels at the end of the GTT (Figure 3-3c). This demonstrated that *Slc7a8* deletion significantly improved glucose metabolism in DIO.

WTHFD showed significantly larger adipocytes in the pWAT, mWAT, and iWAT (Figure 3-4) than WTCD. The adipose tissue hypertrophy in WTHFD may increase susceptibility to hyperglycaemia. In an obese phenotype, insulin signalling is usually impaired, which results in reduced glucose uptake by muscles and thus increased glucose levels in the circulation<sup>26</sup>. pWAT was significantly larger ( $p < 0.001$ ) than iWAT and mWAT in WTHFD (Figure S3-6), which may be suggestive of pWAT being the main site of lipid accumulation in this group, as was observed in the KO group. Abdominal/visceral obesity is critical to the development of metabolic syndrome, and accumulation of adipose tissue in the abdomen correlates with metabolic syndrome more than lipid accumulation in the subcutaneous depot<sup>27</sup>. The larger pWAT in WTHFD may thus have been responsible for the glucose intolerance observed in these mice. Lipid accumulation in the liver

presented as microvesicular steatosis (characterised by small lipid droplets in the cytoplasm of hepatocytes) and macrovesicular steatosis (large lipid droplets) (Figure 3-5), which are both important in the development of nonalcoholic fatty liver disease (NAFLD)<sup>28-29</sup>, and were observed in WTHFD but not in WTCD. The presence of lipid droplets in WTHFD liver could be due to the redistribution of excess lipid to peripheral organs such as the liver or muscles seen in the obese phenotype, when the storage capacity of adipose tissue is exceeded<sup>3,5</sup>. The liver has previously been reported to be the major site for storage of free-fatty acids (FFA) released from white adipose tissue in an obese phenotype<sup>30</sup>. Furthermore, the vast majority of hepatic triglycerides in obese individuals with NAFLD are from FFA released from adipose tissue<sup>31</sup>. The observations made in our study indicate that KOHFD attenuates both macrovesicular and microvascular steatosis seen in WTHFD, suggesting that *Slc7a8* deletion could be protective against NAFLD in DIO.

DIO is often associated with the recruitment and accumulation of macrophages in adipose depots. The F4/80 antibody is a marker for macrophages in mouse tissues<sup>10,32</sup> and was utilised in this study. Adipose tissues from obese WTHFD mice showed significantly more macrophages, which indicates increased inflammation when compared to KOHFD (Figure 3-11). Thus, *Slc7a8* deletion significantly improves the inflammatory profile of adipose tissues in DIO. The liver tissue sections in WTHFD showed significantly elevated levels of macrophages. The observed histopathological changes in liver which occur due to DIO were improved by *Slc7a8* deletion in KOHFD (Figure 3-12).

Apart from metabolic syndromes that are associated with excess adipose tissue accumulation, obese individuals are also prone to developing pulmonary disorders such as chronic obstructive pulmonary disease (COPD) or asthma<sup>33</sup>. In DIO, the lungs of WTHFD showed an increase in adipose tissues accumulation which was reduced in KOHFD (Figure 3-10). A previous study showed that accumulation of adipose tissue in the lungs increased with an individual's body mass index (BMI)<sup>34</sup>. Additionally, an increase in adipose tissue affects the structure of the lungs, resulting in the blockage of airways and causing inflammation which ultimately gives rise to pulmonary disease<sup>33-34</sup>. We observed that the deletion of *Slc7a8* attenuates adipose tissue accumulation in DIO, and this could mitigate the development of obesity associated lung pathologies.

DIO resulted in a significant reduction in gastrocnemius muscle myocyte size in WTHFD compared to WTCD, and the deletion of *Slc7a8* decreased this effect of DIO (KOHFD) on myocytes size (Figure 3-6g). Additionally, peri-muscular adipose tissue accumulation, which was observed to increase in

muscle of WTHFD, decreased in KOHFD (Figure 3-6e,f). Peri-muscular adipose tissue has previously been shown to promote age- and obesity-related muscle atrophy by increasing muscle senescence<sup>35</sup>. Hence, a decrease in lipid accumulation due to *Slc7a8* deletion in our study suggests an improvement in DIO associated muscular disease. Conversely, there was no significant difference in the gastrocnemius muscle macrophage profile between WTHFD and KOHFD.

The development of cardiovascular diseases is associated with an increase in adiposity<sup>36</sup>. In DIO, the heart of WTHFD showed greater accumulation of epicardial adipose tissue, which was found to decrease in the absence of *Slc7a8*, KOHFD (Figure 3-7). Epicardial adipose tissue is located between the myocardium and epicardium and has properties of brown or beige adipose tissue. It is important for maintaining energy homeostasis and thermoregulation of the heart<sup>37</sup>. However, accumulation of epicardial adipose tissue is associated with increasing BMI and poses a risk for the development of cardiovascular disease<sup>36</sup>.

Renal injury and disease have been associated with obesity and studies in mice have documented renal morphological changes due to HFD<sup>22,41</sup>. An accumulation of lipid droplets in the kidneys was observed in DIO in WTHFD, suggesting that an increase in body weight could contribute to renal abnormalities. Lipid accumulation was reduced in KOHFD (Figure 3-9), suggesting that *Slc7a8* deletion may improve kidney health in DIO.

### **3.6 Conclusions**

This study has demonstrated that deletion of *Slc7a8* in mice is protective against DIO by significantly reducing adipose tissue mass and lipid accumulation in multiple organs and tissues, and results in improved glucose tolerance in diet-induced obesity. Furthermore, our histological findings revealed that the negative effects of DIO on different organs and tissues are improved with *Slc7a8* deletion, suggesting that this gene may contribute to the development of some obesity-associated comorbidities. Overall, the results from this study suggest that *Slc7a8* might be a potential therapeutic target for controlling DIO, as well as for mitigating the development of some of the pathophysiological conditions associated with obesity. Nevertheless, further studies will be required to provide additional knowledge on how *Slc7a8* regulates plasma parameters such as hormones, lipids, and the cytokine inflammatory profile in DIO to reduce lipid accumulation in multiple organs and tissues.

## 3.7 Supplementary data

### 3.7.1 Supplementary methods

#### 3.7.1.1 *S1: Genotyping of mice*

Genomic DNA was extracted from tail biopsy of mouse pups using the KAPA Mouse Genotyping Kit (*Wilmington, Massachusetts, United States of America*) and the KAPA Express Extract Protocol. The extractions were performed in a volume of 100 µl and was set up as follows: 88 µl PCR-grade water, 10 µl of 10X KAPA Extract Express buffer, 2 µl of 1 U/µl KAPA Express Extract enzyme and approximately 2 mm of mouse tail tissue. Enzymatic lysis was performed in the Applied Biosystems 9700 thermal cycler (*Foster City, California, United States of America*) at 75°C for 10 minutes and enzyme inactivation at 95°C for 5 minutes. The DNA extracts were subsequently diluted 10-fold in 10 mM TRIS-HCL (pH 8.5).

To determine the wildtype, heterozygous and knockout *SLC7A8* genotypes, the following gene-specific primer sequences were used: 5'-CAAATGCCAGCTGTCCTGACCTCAC-3' forward primer for the wildtype allele, 5'-GGGTGGGATTAGATAAATGCCTGCTCT-3' forward primer for the knockout allele and 5'-CAGACTTAGGGATGGTGACGCCTAG-3' for the common reverse primer. All oligonucleotides used in the study were synthesised by Integrated DNA Technologies (*Coralville, Iowa, United States of America*). The PCR reaction mixture consisted of 6.5 µl of PCR-grade water, 12.5 µl of the KAPA2G Fast Genotyping buffer, 1.25 µl of both the 10 µM wildtype forward primer and 10 µM knockout forward primer, 2.5 µl of 10 µM common reverse primer and 1 µl of the diluted DNA extract. The PCR amplifications were performed in a total volume of 25 µl and cycled in the ABI Applied Biosystems 9700 thermal cycler. The thermal cycling conditions used were as such: 95°C for 3 minutes followed by 95°C for 15 seconds, 60°C for 15 seconds, 72°C for 15 seconds and a final extension for 2 minutes at 72°C. After amplification, 10 µl of each amplicon was separated on a 2% agarose gel alongside a Thermo Scientific FastRuler Low Range DNA ladder (*Waltham, Massachusetts, United States of America*). Electrophoresis was performed in 1 x TAE (diluted from UltraPure 10 x TAE buffer (*ThermoFischer Scientific, Waltham, Massachusetts, United States of America*)) at 120V for 40 minutes. The gel was stained with Ethidium Bromide Solution, Molecular Grade (*Promega, Madison, Wisconsin, United States of America*) and viewed under UV light using the Molecular Imager Gel Doc XR System (*Bio-Rad, Hercules, California,*

*United States of America*). The expected amplicon sizes were 206bp for the wildtype allele and 390bp for the knockout allele. Only wildtype and knockout mice for the *SLC7A8* gene were used in the study.

### 3.7.2 Supplementary figures

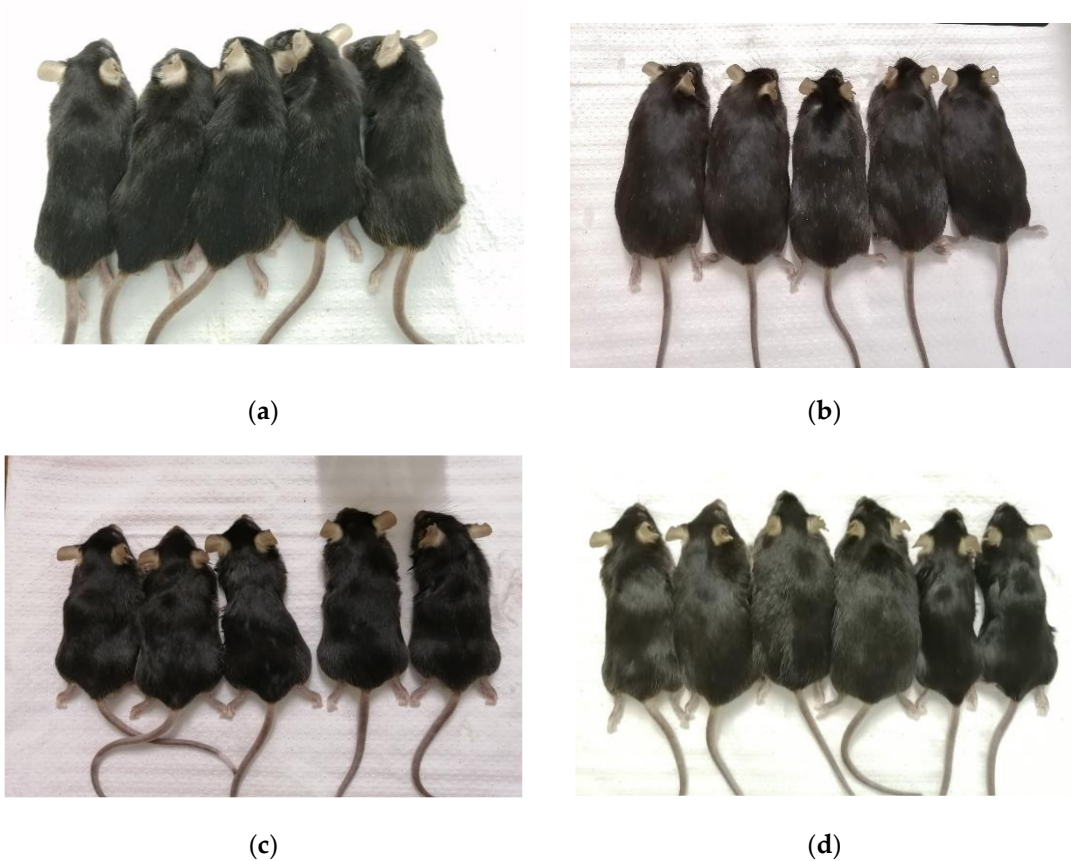
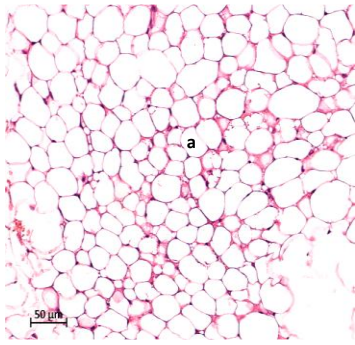
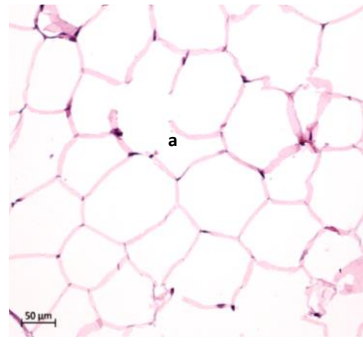


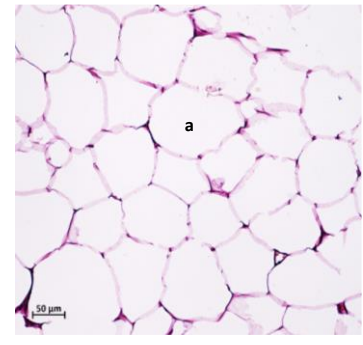
**Figure S3-1: Mice used in the study.** (a) Represents KOCD14 mice. (b) KOHFD14 mice (c) WTCD14 mice (d) WTHFD14 mice. The images demonstrate that KOHFD14 and WTHFD14 mice are larger in size than their control diet counterparts, KOCD14 and WTCD14, respectively.



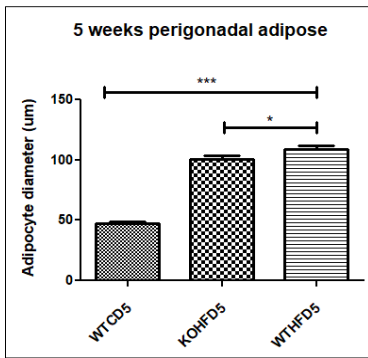
(a)



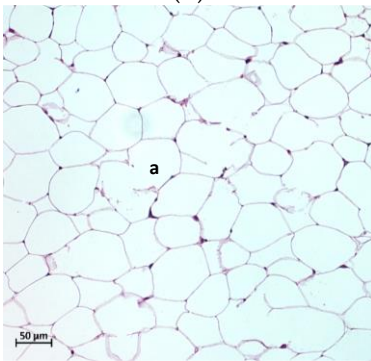
(b)



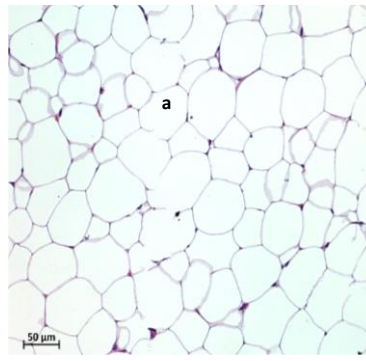
(c)



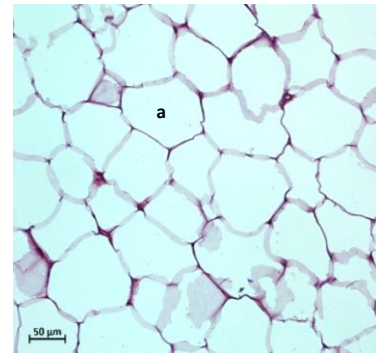
(d)



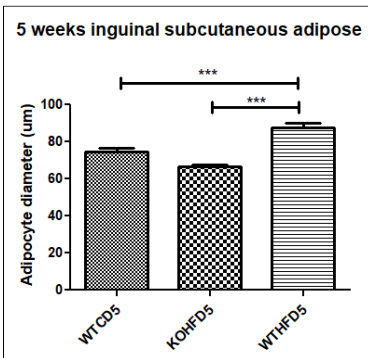
(e)



(f)

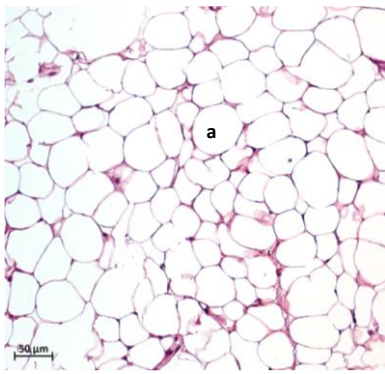


(g)

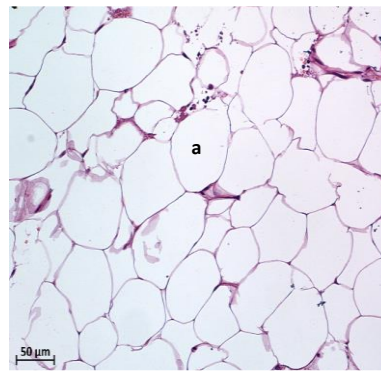


(h)

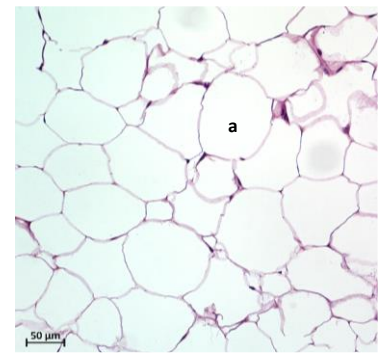




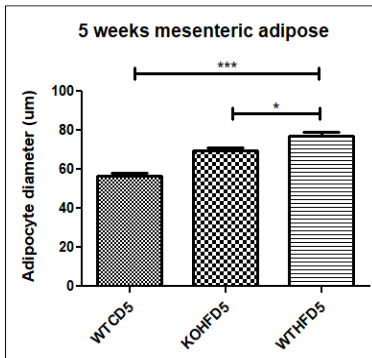
(i)



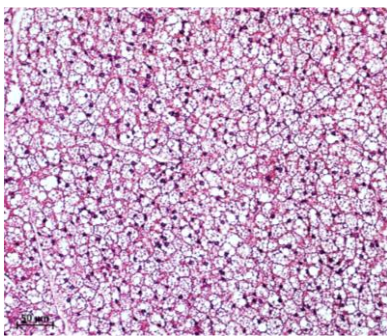
(j)



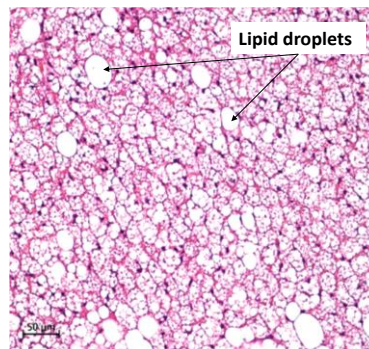
(k)



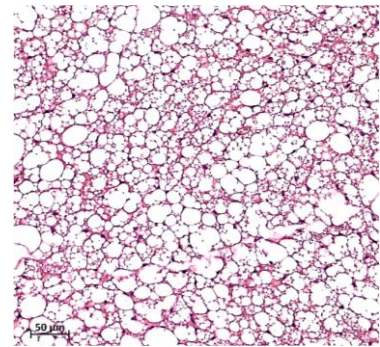
(l)



(m)

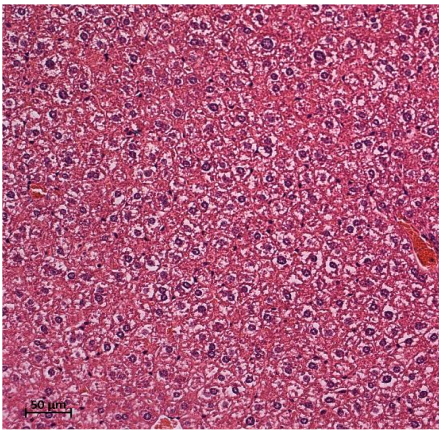


(n)

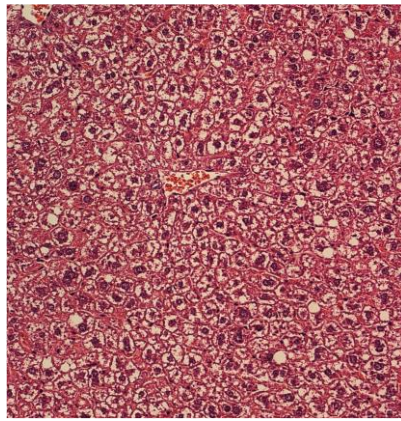


(o)

**Figure S3-2: Adipocyte hypertrophy at 5 weeks.** Adipocyte diameter of WTHFD, c, in pWAT was significantly larger than WTCD, a ( $p < 0.001$ ) and KOHFD, b ( $p < 0.05$ ). In iWAT, WTHFD, g, adipocyte hypertrophy was significantly greater ( $p < 0.05$ ) than WTCD, e and KOHFD, f. WTHFD, k in mWAT showed significantly larger adipocytes than WTCD, i ( $p < 0.001$ ) and KOHFD, j ( $p < 0.05$ ). Accumulation of enlarged lipid droplets were observed in WTHFD, o than WTCD, m and KOHFD, n.



(a)

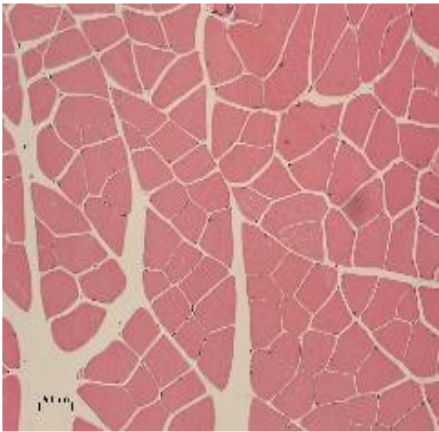


(b)

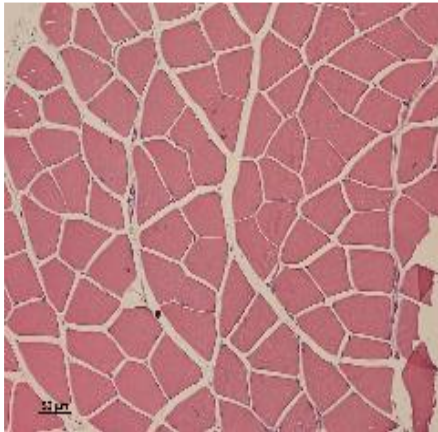


(c)

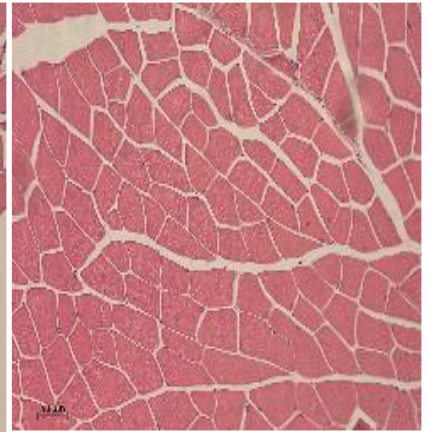
**Figure S3-3: Lipid droplets in the liver at 5 weeks.** WTHFD, c, and KOHFD, b, had lipid droplets in the tissue, while none were observed in WTCD, a.



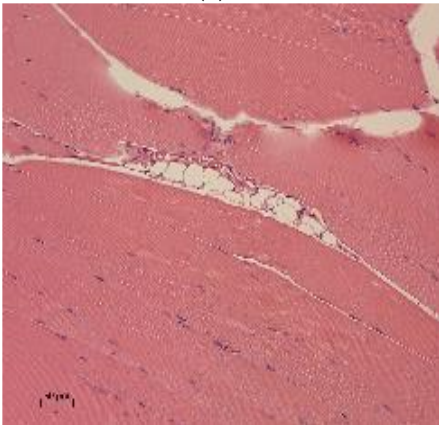
(a)



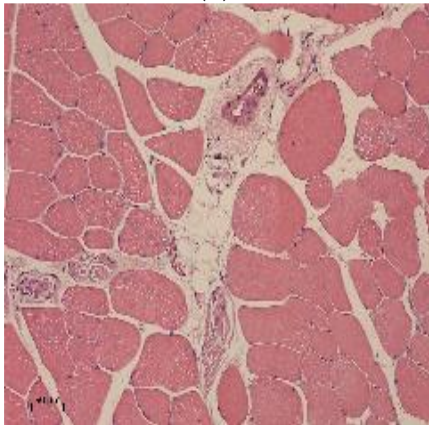
(b)



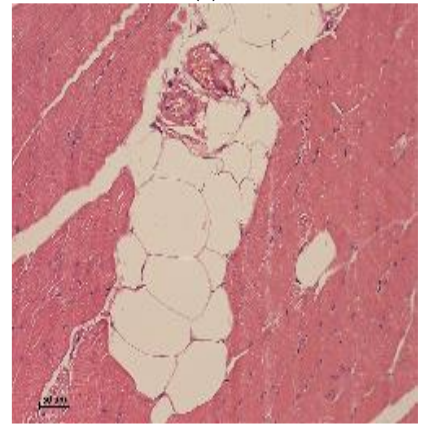
(c)



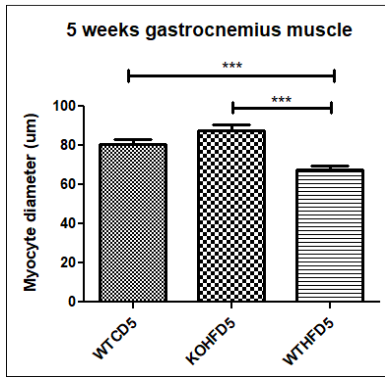
(d)



(e)

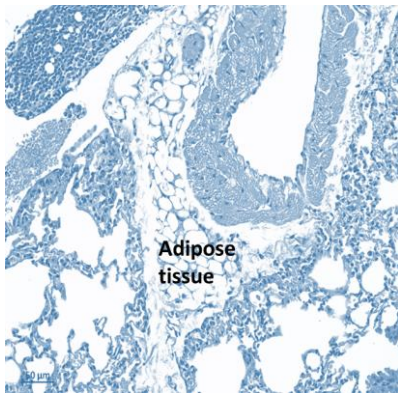


(f)

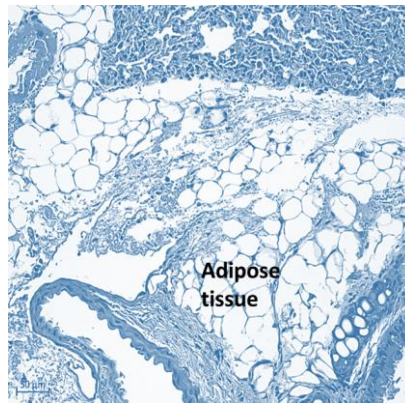


(g)

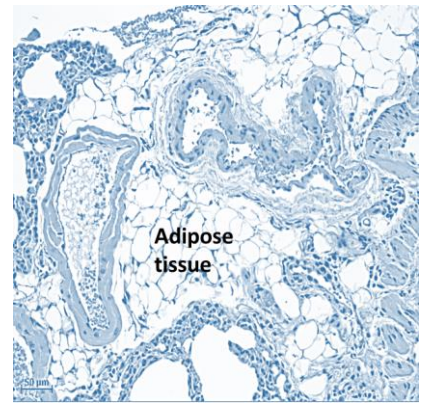
**Figure S3-4: Myocyte sizes at 5 weeks.** Significantly larger myocytes ( $p < 0.001$ ), g, were observed in the WTCD, a, and KOHFD, b, in comparison to those in the WTHFD, c. The distribution of peri-muscular adipose tissue shows that greater accumulation of the adipose was observed in WTHFD, f, compared to WTCD, d and KOHFD, e.



(a)

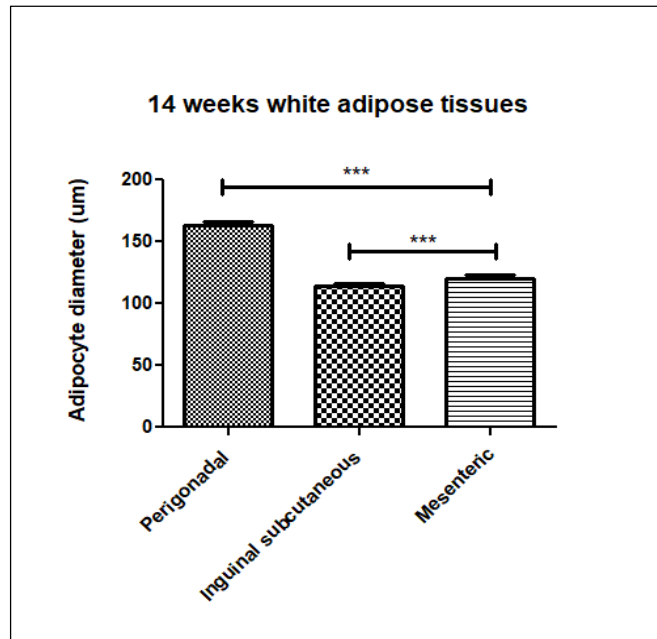


(b)



(c)

**Figure S3-5: Accumulation of adipose tissue in the lungs.** Greater accumulation was observed in WTHFD, c, and KOHFD, b, in comparison to WTCD, a.



(a)

**Figure S3-6: Adipocyte diameter in the various adipose tissue depot.** (a) Perigonadal adipose tissue in WTHFD is significantly larger ( $p < 0.001$ ) than inguinal and mesenteric adipose tissues.

### 3.8 References

1. Goossens GH, Blaak EE. Adipose tissue dysfunction and impaired metabolic health in human obesity: A matter of oxygen? *Frontiers in endocrinology*. 2015; 6:55-. doi:10.3389/fendo.2015.00055
2. Lee CM, Huxley RR, Wildman RP, Woodward M. Indices of abdominal obesity are better discriminators of cardiovascular risk factors than bmi: A meta-analysis. *J Clin Epidemiol*. 2008; 61(7):646-53. doi:10.1016/j.jclinepi.2007.08.012
3. Chait A, den Hartigh LJ. Adipose tissue distribution, inflammation and its metabolic consequences, including diabetes and cardiovascular disease. *Frontiers in Cardiovascular Medicine*. 2020; 7:22. doi:10.3389/fcvm.2020.00022
4. Cannon B, Nedergaard J. Brown adipose tissue: Function and physiological significance. *Physiological Reviews*. 2004; 84(1):277-359. doi:10.1152/physrev.00015.2003
5. Björntorp P. "Portal" adipose tissue as a generator of risk factors for cardiovascular disease and diabetes. *Arteriosclerosis: An Official Journal of the American Heart Association, Inc*. 1990; 10(4):493-6. doi:doi:10.1161/01.ATV.10.4.493
6. Weisberg SP, McCann D, Desai M, Rosenbaum M, Leibel RL, Ferrante AW, Jr. Obesity is associated with macrophage accumulation in adipose tissue. *J Clin Invest*. 2003; 112(12):1796-808. doi:10.1172/jci19246
7. Haase J, Weyer U, Immig K, Klöting N, Blüher M, Eilers J, et al. Local proliferation of macrophages in adipose tissue during obesity-induced inflammation. *Diabetologia*. 2014; 57(3):562-71. doi:10.1007/s00125-013-3139-y
8. Bourlier V, Zakaroff-Girard A, Miranville A, De Barros S, Maumus M, Sengenès C, et al. Remodeling phenotype of human subcutaneous adipose tissue macrophages. *Circulation*. 2008; 117(6):806-15. doi:10.1161/circulationaha.107.724096
9. Murano I, Barbatelli G, Parisani V, Latini C, Muzzonigro G, Castellucci M, et al. Dead adipocytes, detected as crown-like structures, are prevalent in visceral fat depots of genetically obese mice. *J Lipid Res*. 2008; 49(7):1562-8. doi:10.1194/jlr.M800019-JLR200
10. Lumeng CN, Deyoung SM, Bodzin JL, Saltiel AR. Increased inflammatory properties of adipose tissue macrophages recruited during diet-induced obesity. *Diabetes*. 2007; 56(1):16-23. doi:10.2337/db06-1076
11. Ambele MA, Dhanraj P, Giles R, Pepper MS. Adipogenesis: A complex interplay of multiple molecular determinants and pathways. *International Journal of Molecular Sciences*. 2020; 21(12) doi:10.3390/ijms21124283
12. Hauner H. The mode of action of thiazolidinediones. *Diabetes Metab Res Rev*. 2002; 18 Suppl 2:S10-5. doi:10.1002/dmrr.249

13. Diamant M, Heine RJ. Thiazolidinediones in type 2 diabetes mellitus: Current clinical evidence. *Drugs*. 2003; 63(13):1373-405. doi:10.2165/00003495-200363130-00004
14. Ambele MA, Dessels C, Durandt C, Pepper MS. Genome-wide analysis of gene expression during adipogenesis in human adipose-derived stromal cells reveals novel patterns of gene expression during adipocyte differentiation. *Stem Cell Research & Therapy* 2016; 16(3):725-34. doi:10.1016/j.scr.2016.04.011
15. Ambele MA, Pepper MS. Identification of transcription factors potentially involved in human adipogenesis in vitro. *Mol Genet Genomic Med*. 2017; 5(3):210-22. doi:10.1002/mgg3.269
16. Bassi MT, Sperandeo MP, Incerti B, Bulfone A, Pepe A, Surace EM, et al. Slc7a8, a gene mapping within the lysinuric protein intolerance critical region, encodes a new member of the glycoprotein-associated amino acid transporter family. *Genomics*. 1999; 62(2):297-303. doi:10.1006/geno.1999.5978
17. Rossier G, Meier C, Bauch C, Summa V, Sordat B, Verrey F, et al. Lat2, a new basolateral 4f2hc/cd98-associated amino acid transporter of kidney and intestine \*. *Journal of Biological Chemistry*. 1999; 274(49):34948-54. doi:10.1074/jbc.274.49.34948
18. Espino Guarch M, Font-Llitjos M, Murillo-Cuesta S, Errasti-Murugarren E, Celaya AM, Giroto G, et al. Mutations in I-type amino acid transporter-2 support slc7a8 as a novel gene involved in age-related hearing loss. *Elife*. 2018; 7 doi:10.7554/eLife.31511
19. Braun D, Wirth EK, Wohlgemuth F, Reix N, Klein MO, Gruters A, et al. Aminoaciduria, but normal thyroid hormone levels and signalling, in mice lacking the amino acid and thyroid hormone transporter slc7a8. *Biochemical Journal*. 2011; 439(2):249-55. doi:10.1042/BJ20110759
20. El Ansari R, Alfarsi L, Craze ML, Masisi BK, Ellis IO, Rakha EA, et al. The solute carrier slc7a8 is a marker of favourable prognosis in er-positive low proliferative invasive breast cancer. *Breast Cancer Research and Treatment*. 2020; 181(1):1-12. doi:10.1007/s10549-020-05586-6
21. Knöpfel EB, Vilches C, Camargo SMR, Errasti-Murugarren E, Stäubli A, Mayayo C, et al. Dysfunctional lat2 amino acid transporter is associated with cataract in mouse and humans. *Frontiers in Physiology*. 2019; 10(688) doi:10.3389/fphys.2019.00688
22. Dhanraj P, van Heerden MB, Pepper MS, Ambele MA. Sexual dimorphism in changes that occur in tissues, organs and plasma during the early stages of obesity development. *Biology*. 2021; 10(8) doi:10.3390/biology10080717
23. Crowe AR, Yue W. Semi-quantitative determination of protein expression using immunohistochemistry staining and analysis: An integrated protocol. *Bio Protoc*. 2019; 9(24) doi:10.21769/BioProtoc.3465
24. Alcalá M, Calderon-Dominguez M, Bustos E, Ramos P, Casals N, Serra D, et al. Increased inflammation, oxidative stress and mitochondrial respiration in brown adipose tissue from obese mice. *Scientific Reports*. 2017; 7(1):16082. doi:10.1038/s41598-017-16463-6

25. Alberti KG, Eckel RH, Grundy SM, Zimmet PZ, Cleeman JI, Donato KA, et al. Harmonizing the metabolic syndrome: A joint interim statement of the international diabetes federation task force on epidemiology and prevention; national heart, lung, and blood institute; american heart association; world heart federation; international atherosclerosis society; and international association for the study of obesity. *Circulation*. 2009; 120(16):1640-5. doi:10.1161/CIRCULATIONAHA.109.192644
26. Martyn JA, Kaneki M, Yasuhara S. Obesity-induced insulin resistance and hyperglycemia: Etiologic factors and molecular mechanisms. *Anesthesiology*. 2008; 109(1):137-48. doi:10.1097/ALN.0b013e3181799d45
27. Nathalie Esser SL-P, Jacques Piette, Andre' J. Scheen, Nicolas Paquot. Inflammation as a link between obesity, metabolic syndrome and type 2 diabetes. *Diabetes Research and Clinical Practice*. 2014; 105:141 – 50. doi:<http://dx.doi.org/10.1016/j.diabres.2014.04.006>
28. Tandra S, Yeh MM, Brunt EM, Vuppalanchi R, Cummings OW, Ünalp-Arida A, et al. Presence and significance of microvesicular steatosis in nonalcoholic fatty liver disease. *Journal of Hepatology*. 2011; 55(3):654-9. doi:10.1016/j.jhep.2010.11.021
29. Brunt EM. Pathology of fatty liver disease. *Modern Pathology*. 2007; 20(1):S40-S8. doi:10.1038/modpathol.3800680
30. Kabir M, Catalano KJ, Ananthnarayan S, Kim SP, Citters GWV, Dea MK, et al. Molecular evidence supporting the portal theory: A causative link between visceral adiposity and hepatic insulin resistance. *American Journal of Physiology-Endocrinology and Metabolism*. 2005; 288(2):E454-E61. doi:10.1152/ajpendo.00203.2004
31. Donnelly KL, Smith CI, Schwarzenberg SJ, Jessurun J, Boldt MD, Parks EJ. Sources of fatty acids stored in liver and secreted via lipoproteins in patients with nonalcoholic fatty liver disease. *Journal of Clinical Investigation*. 2005; 115(5):1343-51. doi:10.1172/jci23621
32. van der Heijden RA, Sheedfar F, Morrison MC, Hommelberg PP, Kor D, Kloosterhuis NJ, et al. High-fat diet induced obesity primes inflammation in adipose tissue prior to liver in c57bl/6j mice. *Aging (Albany NY)*. 2015; 7(4):256-68. doi:10.18632/aging.100738
33. Bianco A, Nigro E, Monaco ML, Matera MG, Scudiero O, Mazzarella G, et al. The burden of obesity in asthma and copd: Role of adiponectin. *Pulmonary Pharmacology & Therapeutics*. 2017; 43:20-5. doi:10.1016/j.pupt.2017.01.004
34. Elliot JG, Donovan GM, Wang KCW, Green FHY, James AL, Noble PB. Fatty airways: Implications for obstructive disease. *European Respiratory Journal*. 2019; 54(6) doi:10.1183/13993003.00857-2019
35. Zhu S, Tian Z, Torigoe D, Zhao J, Xie P, Sugizaki T, et al. Aging- and obesity-related perimuscular adipose tissue accelerates muscle atrophy. *PLoS One*. 2019; 14(8):e0221366. doi:10.1371/journal.pone.0221366

36. Aitken-Buck HM, Moharram M, Babakr AA, Reijers R, Van Hout I, Fomison-Nurse IC, et al. Relationship between epicardial adipose tissue thickness and epicardial adipocyte size with increasing body mass index. *Adipocyte*. 2019; 8(1):412-20. doi:10.1080/21623945.2019.1701387
37. Iacobellis G. Aging effects on epicardial adipose tissue. *Frontiers in Aging*. 2021; 2(12) doi:10.3389/fragi.2021.666260
38. Hinderer S, Schenke-Layland K. Cardiac fibrosis – a short review of causes and therapeutic strategies. *Advanced Drug Delivery Reviews*. 2019; 146:77-82. doi:<https://doi.org/10.1016/j.addr.2019.05.011>
39. Suthahar N, Meijers WC, Silljé HHW, de Boer RA. From inflammation to fibrosis-molecular and cellular mechanisms of myocardial tissue remodelling and perspectives on differential treatment opportunities. *Current Heart Failure Reports*. 2017; 14(4):235-50. doi:10.1007/s11897-017-0343-y
40. Thomas TP, Grisanti LA. The dynamic interplay between cardiac inflammation and fibrosis. *Frontiers in Physiology*. 2020; 11:529075. doi:10.3389/fphys.2020.529075
41. Deji N, Kume S, Araki S, Soumura M, Sugimoto T, Isshiki K, et al. Structural and functional changes in the kidneys of high-fat diet-induced obese mice. *American Journal of Physiology-Renal Physiology*. 2009; 296(1):F118-26. doi:10.1152/ajprenal.00110.2008



## **Chapter 4. Investigating the possible mechanism of *Slc7a8* deletion on the prevention of adipocyte hypertrophy and its effect on plasma metabolite levels**

Reabetswe R. Pitere<sup>1</sup>, Michael S. Pepper<sup>1</sup>, Melvin A. Ambele<sup>1,2</sup>

<sup>1</sup>Institute for Cellular and Molecular Medicine, Department of Immunology and SAMRC Extramural Unit for Stem Cell Research and Therapy, Faculty of Health Sciences, University of Pretoria, Pretoria 0001, South Africa

<sup>2</sup>Department of Oral and Maxillofacial Pathology, School of Dentistry, Faculty of Health Sciences, University of Pretoria, Pretoria 0001, South Africa

This chapter is presented in manuscript format currently under review in Genes (Manuscript ID: genes-2302882; under review).

#### 4.1 Abstract

The expansion of adipose tissue through adipocyte hypertrophy leads to obesity. We previously showed that *Slc7a8* knockout (KO) in mice protects against diet-induced obesity and attenuates adipocyte hypertrophy in different lipid depots. Here we investigated the possible mechanisms of reduced adipocyte hypertrophy by (a) lipid transport and metabolism and (b) plasma metabolites. The results in KO mice showed that attenuation of adipocyte hypertrophy in the perigonadal (pWAT) and brown adipose tissues (BAT) occurs through increased lipolysis, in addition to browning (in BAT), and by passive or slow lipid uptake in the mesenteric adipose tissue (mWAT). The reduced adipocyte hypertrophy in KO mice led to significantly lower and higher leptin and adiponectin levels, respectively compared with WT. Furthermore, KO mice had significantly lower levels of the proinflammatory cytokines IL- $\alpha$ , IP-10, KC, IL-7 and MIP-1 $\alpha$ , and significantly higher levels of the anti-inflammatory cytokine IL-5 when compared with WT. This study effectively demonstrates a possible fat depot-specific mechanism of adipocyte hypertrophy reduction in KO with a corresponding improvement in plasma metabolic profile and a reduction in inflammatory state during obesity development.

## 4.2 Introduction

Adipose tissue is an active endocrine organ which is fundamental in mediating intracellular signalling resulting in the synthesis and secretion of various fatty acids, lipids and adipokines<sup>1</sup>. Obesity, which is a consequence of expanding and dysfunctional adipose tissue, is important in the development of metabolic syndromes<sup>2-3</sup>. The primary role of white adipose tissue is to store lipids and release them during fasting periods<sup>4</sup>. However, when there is constant lipid influx, adipocytes become hypertrophic<sup>5</sup>. Both adipocyte hypertrophy (increase in cell size) and adipocyte hyperplasia (increase in cell number) lead to adipose tissue expansion with the former being the main contributor to adipose tissue expansion and dysfunction in obesity<sup>4-5</sup>. Adipocyte hypertrophy in various adipose depots (subcutaneous or visceral) has serious metabolic consequences in disease development<sup>6</sup>. Subcutaneous adipose tissue (SAT) makes up most of the adipose tissue, accounting for approximately 80%<sup>7</sup>. It acts as a reservoir for excess lipid storage and when storage capacity is exceeded due to reduced hyperplasia or increased hypertrophy, lipids are stored in ectopic sites such as liver or skeletal muscle<sup>6</sup>. Visceral adipose tissue (VAT), also considered as a type of ectopic fat, is important in the onset of visceral obesity. Hypertrophy of VAT increases susceptibility to the development of metabolic syndrome including hyperinsulinaemia, dysglycaemia, dyslipidaemia and systemic inflammation<sup>6,8</sup>.

Over the past two decades, a tremendous amount of research has been conducted on adipogenesis to identify potential mediators and/or drivers of lipid accumulation during adipocyte hypertrophy or hyperplasia<sup>9-13</sup>. A study by Ambele et al. (2016) investigated the transcriptome of human adipose-derived stromal cells undergoing adipogenesis and identified Solute Carrier Family 7 Member 8 (*SLC7A8*) as a potentially novel gene involved in this process but which had not previously been described either in the context of adipogenesis or obesity.<sup>9</sup> *SLC7A8* encodes a large neutral amino acid transporter small subunit (LAT2) protein which transports small and large neutral amino acids across the cell membrane<sup>14</sup>. Moreover, LAT2 is essential in amino acid exchange and reabsorption of neutral amino acids<sup>15-16</sup>. Functional studies of *Slc7a8* in a mouse model of diet-induced obesity showed that a deficiency in this gene significantly protects against diet-induced obesity with a significant attenuation of adipocyte hypertrophy in various adipose depots<sup>17</sup>.

Additionally, the deletion of this gene was found to reduce lipid accumulation and storage in non-lipid storage organs like the liver<sup>17</sup> which can potentially produce liver steatosis and insulin resistance. Overall, the results demonstrated that *Slc7a8* plays an important role in obesity development.

Furthermore, various proteins secreted by adipose tissue such as fatty acid binding protein 4 (FABP4) for example, have been associated to the development of metabolic disorders such as obesity, insulin resistance, hypertension, and dyslipidaemia<sup>18-19</sup>. FABP4 interacts with other proteins such as cluster of differentiation 36 (CD36) to facilitate fatty acid transport, import and metabolism<sup>20</sup>. The expression of *FABP4* is regulated by peroxisome proliferator-activated receptor- $\gamma$  (PPAR $\gamma$ ) and CCAAT/enhancer-binding protein alpha (C/EBP $\alpha$ )<sup>21</sup>. PPAR $\gamma$  and C/EBP $\alpha$  are vital in controlling the differentiation of adipocyte precursor cells into mature adipocytes<sup>3,22-24</sup>. Expression patterns of PPAR and C/EBP can be correlated to the pathogenesis of obesity<sup>25-26</sup>. Genes involved in lipolysis such as adipocyte triglyceride lipase (*ATGL*), which has a high specificity for triglycerides, are important in regulating fatty acid storage and release from adipocytes<sup>27</sup>. Reduced expression of *ATGL* has been associated with adipocyte hypertrophy in obese subjects<sup>28</sup>. Adipocyte hypertrophy is important in adipose tissue inflammation as it induces the activity of pro-inflammatory cytokines and chemokines during obesity development, as well as macrophage infiltration<sup>29-31</sup>.

Cytokines act as signalling molecules to regulate pro- and anti-inflammatory function, while chemokines are proteins in the cytokine family whose function is to induce the migration of immune cells such as leukocytes<sup>29-31</sup>. Adipokines (cytokines which are secreted by adipose tissue) play an important role in low-grade chronic inflammation associated with obesity<sup>32</sup>. Leptin is a hormone primarily produced by adipocytes and its function is to regulate reproduction, appetite, body weight and metabolism<sup>32-33</sup>. Leptin levels in circulation correspond to the amount of energy stored and total body fat, and are therefore elevated in obese individuals<sup>1</sup>. In obesity however, energy homeostasis is not well regulated due to the inability of the brain to respond effectively to leptin signals, thereby leading to leptin resistance in obese individuals<sup>34</sup>. The subcutaneous adipose depot has been shown to be the major source of leptin in circulation<sup>33,35</sup>. Adiponectin, like leptin is mainly synthesised by adipose tissue and is involved in regulating glucose homeostasis and lipid metabolism<sup>36</sup>.

Adiponectin levels are inversely correlated to adiposity, and levels of adiponectin are reduced significantly in individuals with obesity<sup>36</sup>.

It has been shown that IL-6 may act as an anti-inflammatory cytokine by promoting the production of interleukin-10 (IL-10), a phenomenon which has been observed in female mice during the early stages of diet-induced obesity (DIO)<sup>37</sup>. The relationship between inflammation and obesity is supported by the high levels of circulating proinflammatory cytokines in obese individuals<sup>32,38</sup>. An inflammatory response in metabolic cells such as adipocytes can be triggered by an accumulation of cholesterol in the bloodstream, leading to a perturbation of metabolic homeostasis<sup>39</sup>. The observed trend is that total cholesterol increases with increasing body mass index (BMI), and thus obese individuals tend to have higher cholesterol levels in comparison to their leaner counterparts<sup>39-40</sup>. In an *Slc7a8* knockout model, a decrease in macrophage infiltration into different adipose depots was observed, thus suggesting a decrease in local inflammation when compared with the wildtype counterpart under condition of DIO<sup>17</sup>.

To provide a better understanding of the role of *Slc7a8* in the development obesity at the molecular level, this study investigated the possible mechanism of reduced adipocyte hypertrophy by lipid transport in various adipose depots of *Slc7a8* deficient mice under condition of DIO and its overall effect on plasma metabolic profile in this phenotype. The goal is that targeting adipocyte hypertrophy may provide long lasting beneficial effects in combating obesity and some of its associated metabolic disorders.

## **4.3 Materials and Methods**

### **4.3.1 Animal model**

The animal model, experimental diet, housing and care are similar to those previously described<sup>17</sup>, with minor modifications. The heterozygous and wildtype *SLC7A8* (*Slc7a8*<sup>tm1Dgen</sup>) C57BL/6J mice strain mating pair were sourced from The Jackson Laboratory (*Bar Harbor, Maine, United States of America*) and were used to generate *SLC7A8* wildtype (WT) and knockout (KO) genotypes. The genotypes were confirmed using standard PCR. The study was approved by the Research Ethics Committee, Faculty of Health Sciences and the Animal

Ethics Committee, Faculty of Veterinary Sciences, University of Pretoria (Ref. No.: 474/2019). Both the WT and KO mice were fed on either a high-fat diet (HFD; D12492) or control diet (CD; D12450J) sourced from Research Diets, Inc. (*New Brunswick, New Jersey, United States of America*), for a period of 5 and 14 weeks, and thereafter mice were euthanised at the respective weeks using isoflurane Isofor (*Safeline Pharmaceuticals, Weltevreden Park, Johannesburg, South Africa*) and cardiac puncture was performed to collect blood samples. Blood was collected into EDTA tubes and immediately centrifuged at 21.1 x g for 10 minutes to collect plasma, which was stored at -80°C until it was used for analyses. The nomenclature used for the different genotypes on either a CD or HFD is WTCD (wildtype mice on control CD), WTHFD (wildtype mice on HFD), and KOHFD (knockout mice on HFD).

#### 4.3.2 RNA isolation and RT-qPCR

Total RNA was isolated from the perigonadal, mesenteric and brown adipose tissues<sup>17</sup> of 14-week WTCD, KOHFD and WTHFD mice using the E.Z.N.A.<sup>®</sup> Total RNA kit (*Omega Bio-Tek Inc., Georgia, United States of America*) according to the manufacturer's recommendations. The integrity of the RNA was assessed using the Agilent 2200 TapeStation (*Agilent Technologies, California, United States of America*) following the manufacturer's instructions. cDNA synthesis was done using the SensiFAST cDNA synthesis kit (*Bioline, London, United Kingdom*), with 1µg RNA input of perigonadal and mesenteric adipose tissues (pWAT and mWAT, respectively), and 200ng RNA input of brown adipose tissue (BAT) as BAT had lower RNA concentrations in comparison to WAT. Three biological replicates and two technical replicates were used for each tissue isolated from mice of the different genotypes. The thermal cycling conditions were performed in an Applied Biosystems 9700 thermal cycler (*Applied Biosystems, Waltham, Massachusetts, United States of America*) in a total reaction volume of 20µl. RT-qPCR was carried out in the QuantStudio 6 Real-Time PCR System (*Thermo Fisher Scientific, Waltham, Massachusetts, United States of America*) using TaqMan<sup>®</sup> Fast Advanced Master Mix and TaqMan<sup>®</sup> Gene Expression assays (*Thermo Fisher Scientific*). The following commercial probes were used: *Pparγ* (Mm00440940\_m1), *Fabp4* (Mm00445878\_m1), *Cd36* (Mm00432403\_m1), *Atgl/Pnpla2* (Mm00503040\_m1), *Ucp1* (Mm01244861\_m1) and *Gapdh* (Mm99999915\_g1) (*Thermo Fisher Scientific, Waltham, Massachusetts, United States of America*). A total of 100 ng cDNA was used in a final volume

of 20µl. The comparative CT method was used, and the thermal cycling conditions were set to the instrument standard protocol with the following conditions: uracil-DNA glycosylase activation at 50°C for 2 minutes, polymerase activation at 95°C for 10 minutes, 40 cycles of denaturation at 95°C for 15 seconds and annealing and extension at 60°C for 1 minute. The delta delta CT ( $2^{-\Delta\Delta Ct}$ ) method was used to quantify the fold change (FC) expression of each gene.

#### 4.3.3 Measurement of plasma hormones and lipid

Plasma leptin, adiponectin, and cholesterol concentrations were quantified as previously described<sup>37</sup> using the following commercially available kits: Mouse/Rat Leptin Quantikine ELISA kit (MOB00B; *R&D Systems, Minneapolis, Minnesota, United States of America*), Mouse Adiponectin/Acrp30 Quantikine ELISA kit (MRP300; *R&D Systems, Minneapolis, Minnesota, United States of America*), and Cholesterol Assay HDL and LDL/VLDL kit (ab65390; *Abcam Cambridge, United Kingdom*) as described in the manufacturer's manual. For the leptin and adiponectin assays, diluent was added to each well, followed by the addition of samples. The plates were incubated for 2 and 3 hours, respectively. Mouse leptin or adiponectin conjugate was added to the wells and incubated for 1 hour, followed by a substrate solution (which produces a blue colour which can be measured on the microplate reader) and then a stop solution (to stop the colour development). For the cholesterol assay, samples and Total Cholesterol reaction mix were added to each well and incubated for 60 minutes at 37°C. For leptin and adiponectin, the plates were read at 450nm using a BioTek PowerWaveX microplate reader (*BioTek, Winooski, Vermont, United States of America*). A standard curve was generated using the Quantikine kit standards. Total cholesterol was measured using a Luminescence Spectrometer LS50 (*PerkinElmer, Waltham, Massachusetts, United States of America*) with excitation and emission (Ex/Em) set at 535/587nm.

#### 4.3.4 Measurement of plasma chemokines and cytokines

Chemokines and cytokines in plasma were quantified using the Milliplex® MAP Mouse Cytokine/Chemokine Magnetic Bead Panel-Premixed 25-plex (MCYTOMAG-70K-PMX; *The Merck Group, Darmstadt, Germany*) according to the manufacturer's recommendations as

previously described<sup>37</sup>. The 25 measured chemokines and cytokines are as follows: granulocyte colony stimulating factor (G-CSF), granulocyte-macrophage colony stimulating factor (GM-CSF), interferon gamma (IFN- $\gamma$ ), interleukins (IL-1 $\alpha$ , IL-1 $\beta$ , IL-2, IL-4, IL-5, IL-6, IL-7, IL-9, IL-10, IL-12 (p40), IL-12 (p70), IL-13, IL-15, IL-17), interferon- $\gamma$  inducible protein 10 (IP-10), tumor necrosis factor alpha (TNF- $\alpha$ ), monocyte chemoattractant protein 1 (MCP-1), keratinocyte chemoattractant (KC) macrophage inflammatory protein 1 alpha (MIP-1 $\alpha$ ), macrophage inflammatory protein 1 beta (MIP-1 $\beta$ ), macrophage inflammatory protein 2 (MIP-2), regulated on activation normal T cell expressed and secreted (RANTES). To prepare the assay, the plate was incubated with wash buffer for 10 minutes at room temperature. Following removal of the wash buffer, the sample wells were filled with assay buffer and 25 $\mu$ L of sample was added. The premixed beads were subsequently added, and the plate was sealed and allowed to incubate overnight at 4°C. The following day, the plate was washed to remove unbound beads and then incubated with detection antibodies. This was followed by the addition of Streptavidin-Phycoerythrin solution and a 30-minute incubation at room temperature. The plate was washed, and beads were resuspended with sheath fluid. 100 $\mu$ L of the resuspended beads were used and the plate was run on the Bio-Plex 200 System (*Bio-Rad Laboratories, Hercules, California, United States of America*).

#### 4.3.5 Statistical analysis

Statistical analyses were conducted using GraphPad Prism 5 (*GraphPad Software, San Diego, California*). Values are expressed as mean  $\pm$  SEM. Mann-Whitney t-test was used to compare means of two groups. Statistically significant results are represented as \*P<0.05, \*\*P<0.01, \*\*\*P<0.001.

## 4.4 Results

### 4.4.1 Expression of genes involved in lipid metabolism and adipogenesis across various adipose tissue depots

In comparison to WTCD, the pWAT of WTHFD showed no change in the expression of *Ppar $\gamma$*  (FC 1.1), which is the master regulator of adipogenesis, or the lipolytic enzyme *Atgl* (FC 1.0),



that has a high specificity for triglycerides and plays a key role in lipid droplet degradation in adipocytes, (Figure 4- 1A). However, expression of *PparY* regulated lipid transporter genes *Fabp4* (FC 3.1) and *Cd36* (FC 3.1) increased while *Ucp1* was not expressed in the pWAT of either WTHFD and WTCD (Figure 4-1A). The *Slc7a8* deletion (KOHFD) led to high expression of *PparY* (FC 14.0), *Cd36* (FC 13.6), *Fabp4* (FC 14.5), and a remarkably high level of *Atgl* (FC 158.3) in pWAT, but still *Ucp1* was not expressed (Figure 4-1D). In the mWAT of WTHFD, there was no expression of *Atgl*, *Ucp1* or *PparY*, while *Cd36* (FC 93.1) and *Fabp4* (FC 94.1) were increased (Figure 4-1B). Deletion of *Slc7a8* (KOHFD) markedly downregulated *Cd36* (FC 0.1) and *Fabp4* (FC 0.1), with no detectable expression of *Atgl*, *PparY* or *Ucp1* (Figure 4-1E). BAT in WTHFD showed high expression of *PparY* (FC 17.1), *Ucp1* (FC 98.9), *Cd36* (FC 15.7), *Fabp4* (FC 95.2) and *Atgl* (FC 3.6) (Figure 4-1C). Meanwhile, deletion of *Slc7a8* (KOHFD) led to subtle changes in *PparY* (FC 0.9) and *Ucp1* (FC 1.3), while *Fabp4* (FC 2.4), *Cd36* (FC 14.1) and *Atgl* (FC 5.9) all increased (Figure 4-1F).

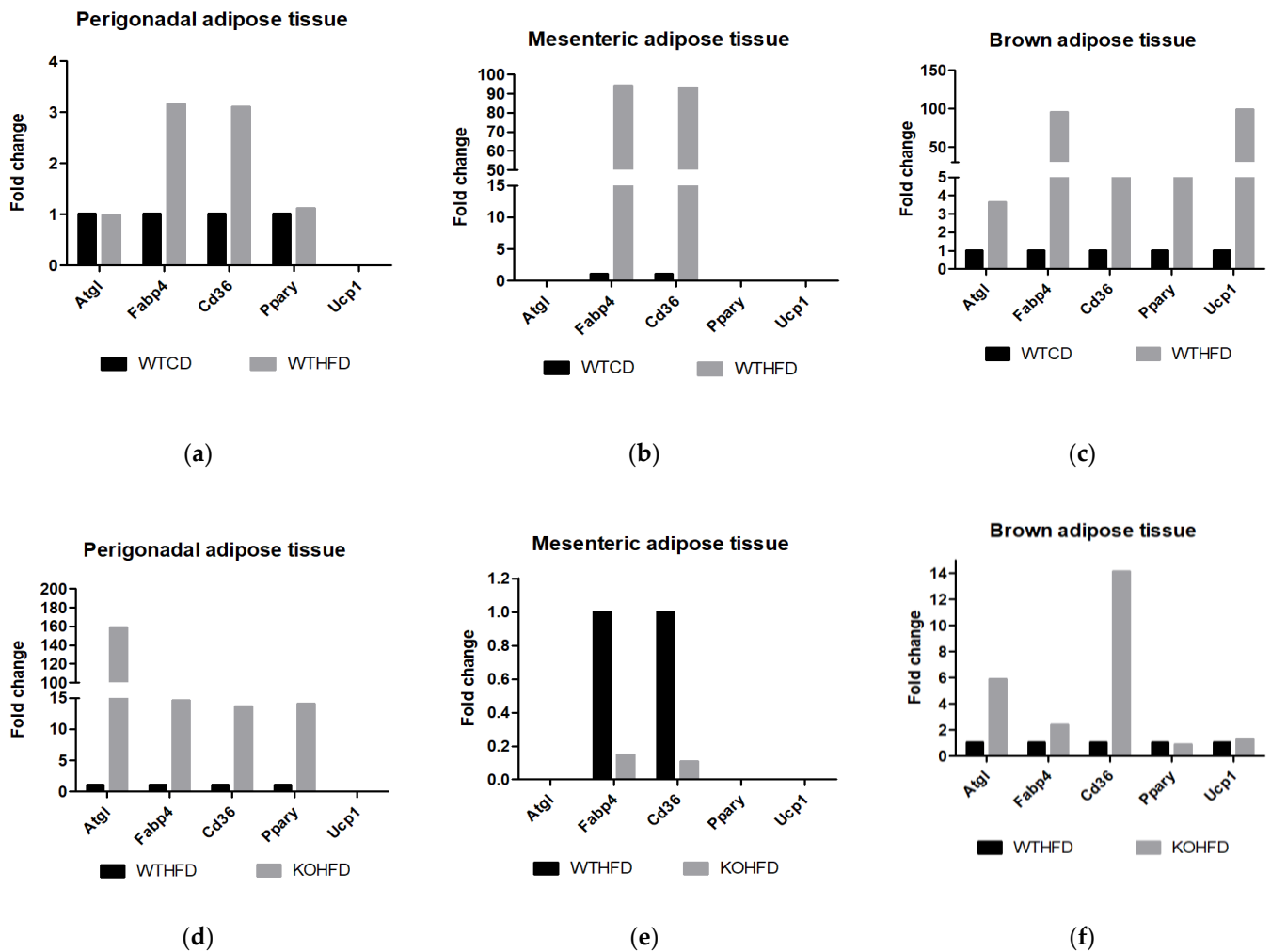


**Figure 4-1: Effect of *Slc7a8* deletion on gene expression profiles in perigonadal, mesenteric and brown adipose depots.** (a) Expression of *Atgl*, *Fabp4*, *Cd36*, *Pparγ* and *Ucp1* in the perigonadal adipose tissue of WTHFD compared with WTCD, (d) and in KOHFD compared with WTHFD. *Ucp1* (a and d) was not expressed in WTCD, WTHFD or KOHFD. (e) The expression of *Fabp4* and *Cd36* was higher in mWAT of WTHFD compared with WTCD, and KOHFD. (b and e) *Ucp1*, *Atgl* and *Pparγ* were not expressed in WTCD, WTHFD or KOHFD. (c) The expression of *Fabp4*, *Cd36*, *Pparγ*, *Atgl* and *Ucp1* was higher in brown adipose tissue of WTHFD in comparison to WTCD, (f) while *Atgl*, *Cd36*, *Fabp4* and *Ucp1* expression was higher in KOHFD compared with WTHFD. (N=3 for all experimental groups).

#### 4.4.2 Plasma leptin

Plasma leptin levels in animals on HFD were significantly higher ( $p < 0.05$ ) as early as week 5 (WTHFD5) when compared with controls, WTCD5, and the deletion of *Slc7a8* reduces the high plasma leptin level (KOHFD5), although to a level that is not statistically significant (Figure 4-2). Prolonged feeding on either diet from week 5 to 14 showed no significant change in plasma leptin levels in animals on CD (WTCD5 and WTCD14), while the levels increased significantly ( $p < 0.05$ ) in animals on HFD (WTHFD5 and WTHFD14). The deletion of *Slc7a8* resulted in a slight increase in leptin levels from weeks 5 to 14 on HFD (KOHFD5 and KOHFD14) but most importantly, it significantly decreased ( $p < 0.05$ ) leptin levels compared with WTHFD14. WTHFD14 had significantly higher ( $p < 0.05$ ) leptin levels than WTCD14 (Figure 4-2).

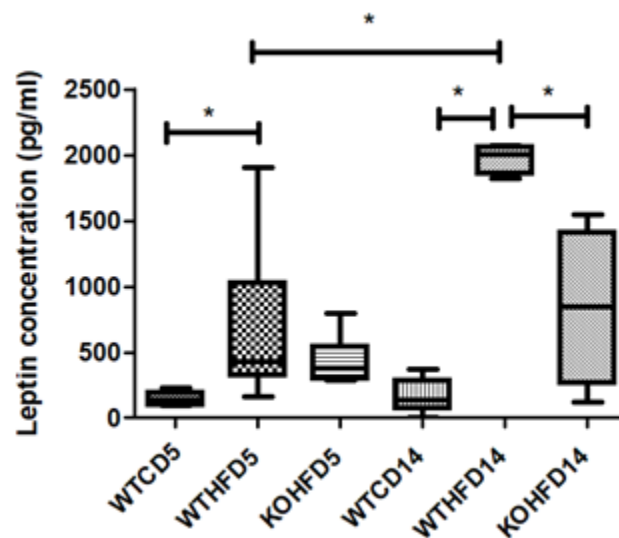


**Figure 4-2: Effect of *Slc7a8* deletion on plasma leptin concentrations.** Leptin levels observed between WTCD5 and WTHFD5 were significantly different ( $p < 0.05$ ) while no significant changes were observed between KOHFD5 and WTHFD5 or during prolonged feeding in WTCD (WTCD5 and WTCD14) and KOHFD (KOHFD5 and KOHFD14). However, prolonged feeding for 14 weeks significantly increased ( $p < 0.05$ ) leptin levels in WTHFD (WTHFD5 and WTHFD14), which was significantly reduced ( $p < 0.05$ ) when *Slc7a8* was deleted (WTHFD14 and KOHFD14). Experimental feeding for 14 weeks displayed a significant difference ( $p < 0.05$ ) between WTCD14 and WTHFD14. N=4 for KOHFD14 and WTHFD14; N=5 for WTCD14; N=6 for WTCD5, KOHFD5 and WTHFD5.

#### 4.4.3 Plasma adiponectin

Adiponectin levels in plasma did not change significantly in WT animals on the different diets (WTCD5 and WTHFD5) or between WTHFD5 and KOHFD5. However, under prolonged feeding for 14 weeks on the respective diets, adiponectin levels significantly decreased in both WTCD (WTCD5 and WTCD14;  $p < 0.05$ ) and WTHFD (WTHFD5 and WTHFD14;  $p < 0.01$ ) but not in KOHFD (KOHFD5 and KOHFD14), which showed a slight increase (Figure 4-3). Contrary to the decrease in adiponectin levels observed in WTHFD14, the deletion of *Slc7a8* (KOHFD14) led to a significant increase ( $p < 0.05$ ) in adiponectin (Figure 4-3).

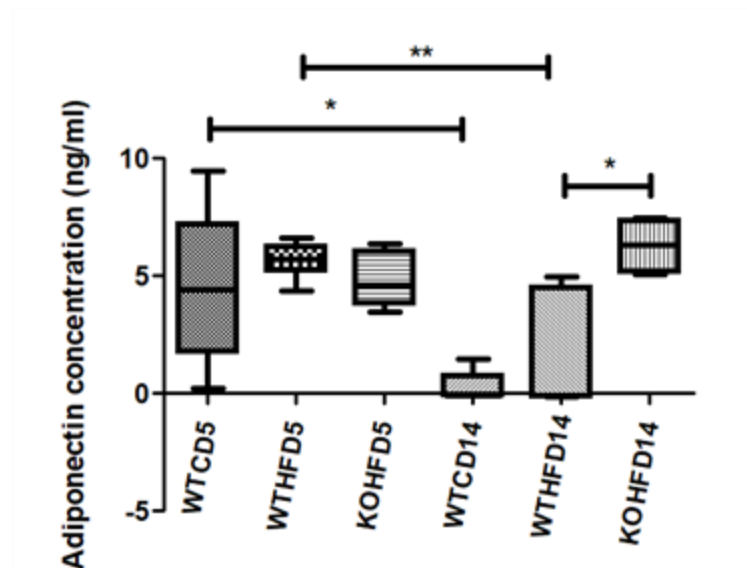


**Figure 4-3: Effect of *Slc7a8* deletion on plasma adiponectin levels.** There was no significant difference in adiponectin levels between WTCD5 and WTHFD5, or between WTHFD5 and KOHFD5. Adiponectin levels significantly decreased under prolonged feeding for 14 weeks in WTCD14 and WTHFD14 compared with their respective counterparts on week 5. Meanwhile, there was a slight increase in adiponectin with prolonged feeding of KOHFD14. The deletion of *Slc7a8* (KOHFD14) significantly increased adiponectin levels during prolonged feeding on HFD compared with WTHFD14. N=4 for KOHFD14; N=5 for WTCD5, WTCD14 and WTHFD14; N=6 for WTHFD5 and KOHFD5.

#### 4.4.4 Plasma total cholesterol

Analysis of plasma total cholesterol levels showed that there were no significant differences between WTCD and WTHFD, or between KOHFD and WTHFD at week 5 (Figure 4-4).

Although there was a slight but non-significant increase in total cholesterol after prolonged feeding for 14 weeks in all experimental groups (WTCD14, WTHFD14 and KOHFD14), there was still no significant difference between WTCD14 and WTHFD14 or between WTHFD14 and KOHFD14 (Figure 4-4).

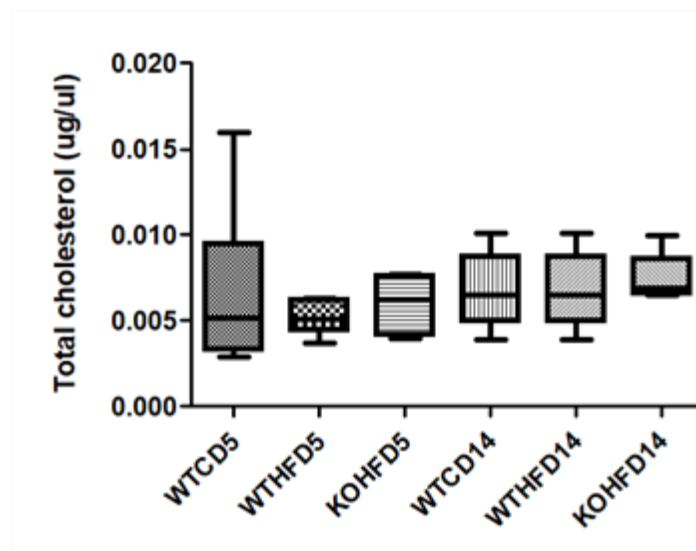


**Figure 4-4: Effect of *Slc7a8* deletion on plasma total cholesterol concentrations.** Total cholesterol levels did not significantly change WTCD and WTHFD at 5 or 14 weeks, even though there was a slight increase at week 14. Total cholesterol in KOHFD was slightly higher than WTHFD at both weeks 5 and 14, although this was not statistically significant. N=6 for WTCD5, WTHFD5 and KOHFD5; N=5 for, WTCD14, KOHFD14 and WTHFD14.

#### 4.4.5 Effect of *Slc7a8* deletion on the kinetics of cytokine and chemokine production as measured in plasma

The effect of DIO on plasma cytokine levels was evaluated at two time points over a period of 14 weeks. Table S1 indicates the various cytokines and the concentrations that were determined across the various groups in the 14-week period. Cytokines levels were measured in 5 different animals in each experimental group (WTCD, WTHFD and KOHFD) at both weeks 5 and 14. However, it is important to note that due to inherent biological variability between individual animals, not all the animals in the same experimental group had detectable levels of cytokines in plasma and as a result the number of animals with

detectable plasma levels of each cytokine may differ in each experimental group. However, the number of animals with detectable levels of each cytokine measured in all experimental groups was at least 3 (n=3), unless otherwise stated. Of the 25 different cytokines/chemokines analysed, GM-CSF, IL-1 $\beta$ , IL-12 p70, IL-15 and MCP-1 were not detectable in plasma in any of the experimental groups.

For IL-1 $\alpha$  and IP-10, there was no significant change in concentration at week 5 when comparing WTCD5 and WTHFD5 and between KOHFD5 and WTHFD5 (Figure 4-5a,b). Prolonged feeding increased IL-1 $\alpha$  and IP-10 levels in all experimental groups at week 14 compared with their respective counterparts in week 5, with that in WTHFD14 showing a significant increase (p<0.05). Deletion of *Slc7a8* slightly reduced IL-1 $\alpha$  and IP-10 levels under prolonged DIO compared with wildtype controls (KOHFD14 vs WTHFD14) (Figure 4-5a,b).

KC levels were significantly lower (p<0.05) in WTHFD5 compared with WTCD5 but did not change between KOHFD5 and WTHFD5. Experimental feeding for 14 weeks increased KC levels across all experimental groups and significantly so in WTHFD14 (p<0.01) and KOHFD14 (p<0.05) when compared their respective 5-week counterparts. At week 14, the KC levels in WTHFD14 were significantly higher (p<0.05) compared with WTCD14, while the deletion of *Slc7a8* (KOHFD14) reduced KC levels when compared with WTHFD14, but not significantly (Figure 4-5c).

MIP2 plasma concentrations were measured in WTCD5 and KOHFD5 but were not detectable in WTHFD5 which seemed to increase only later as was measured at 14 weeks post experimental feeding (Figure 4-5d). KOHFD14 showed slightly higher MIP2 levels when compared with WTHFD14, which was not significant. MIP2 levels were similar between WTCD14 vs WTHFD14, and WTHFD14 vs KOHFD14. However, WTCD14 showed significantly elevated MIP2 levels (p<0.05) compared with WTCD5 (Figure 4-5d).

There were no significant differences in RANTES levels between WTCD5 and WTHFD5, or between KOHFD5 and WTHFD5, although KOHFD5 showed higher levels than WTHFD5. Following 14 weeks of experimental feeding, RANTES levels in WTCD (WTCD14 vs WTCD5) and KOHFD (KOHFD14 vs KOHFD5) did not change significantly, while they increased in

WTHFD from 5 to 14 weeks, albeit not significantly. Deletion of *Slc7a8* (KOHFD14) did not alter RANTES levels (WTHFD14) (Figure 4-5e).

INF- $\gamma$  was not detected in WTCD14 or WTHFD14 (Figure 4-5f). No significant differences were seen in INF- $\gamma$  between the WTCD5 and WTHFD5 at week 5, but INF- $\gamma$  was higher in KOHFD5 compared with WTHFD5 although not significantly (Figure 4-5f).

The kinetics of IL-2 production increased proportionately across all experimental groups from week 5 to 14, although this was not statistically significant (Figure 4-5g). Furthermore, the IL-2 concentrations between WTCD and WTHFD as well as WTHFD and KOHFD were similar at both week 5 and week 14 (Figure 4-5g).

The IL-6 concentrations did not change between WTCD5 and WTHFD5 but increased in KOHFD5 compared with WTHFD5 albeit not statistically significant (Figure 4-5h). Prolonged feeding led to an increase of IL-6 levels in WTCD14 and WTHFD14 but not in KOHFD14 which showed a decrease compared with their respective week 5 counterparts. However, there was no change in IL-6 levels between KOHFD14 and WTHFD14 (Figure 4-5h).

IL-7 concentrations were slightly high in WTHFD5 compared with WTCD5 and were similar in KOHFD5 and WTHFD5 (Figure 4-5i). Prolonged feeding led to significantly increased IL-7 levels in WTCD14 ( $p < 0.05$ ), and increased levels in WTHFD14 but not in KOHFD14. KOHFD14 had reduced IL-7 levels compared with WTHFD14 (Figure 4-5i).

IL-9 concentrations increased from week 5 to 14 in all the experimental groups although this was not statistically significant (Figure 4-5j). The deletion of *Slc7a8* led to higher levels of IL-9 at week 5 (KOHFD5) compared with WTHFD5. IL-9 was not detected in WTCD after 5 weeks but increased to measurable levels at week 14 on experimental feeding. No significant changes in IL-9 levels were observed between KOHFD14 and WTHFD14 (Figure 4-5j).

The levels of IL-12 p40 did not significantly change from week 5 to 14 in any of the experimental groups. However, IL-12 p40 concentration was lower in WTHFD than WTCD and higher in KOHFD compared with WTHFD both at weeks 5 and 14 (Figure 4-5k).

There was a slight increase in IL-17 cytokine production in WTCD and WTHFD from week 5 to 14 while that of KOHFD did not change (Figure 4-5l). The deletion of *Slc7a8* increased IL-17 in KOHFD5 compared with WTHFD5 but remained stable even after prolonged feeding at week 14, while it increased in WTHFD14 (Figure 4-5l).

MIP-1 $\alpha$  concentrations were elevated in WTHFD5 compared with WTCD5 and significantly elevated ( $p < 0.05$ ) when compared with KOHFD5 (Figure 4-5m). WTCD14 and KOHFD14 MIP-1 $\alpha$  levels were higher than their week 5 counterparts, while WTHFD14 displayed lower MIP-1 $\alpha$  levels than WTHFD5. Meanwhile, deletion of *Slc7a8* (KOHFD) resulted in slightly lower MIP-1 $\alpha$  levels in KOHFD14 than WTHFD14 (Figure 4-5m).

MIP-1 $\beta$  concentrations in WTCD5 were greater than in WTHFD5 (Figure 4-5n). WTCD14, WTHFD14 and KOHFD14 had higher MIP-1 $\beta$  levels in comparison to their 5-week counterparts. MIP-1 $\beta$  concentrations were reduced in KOHFD14 compared with WTHFD14 (Figure 4-5n).

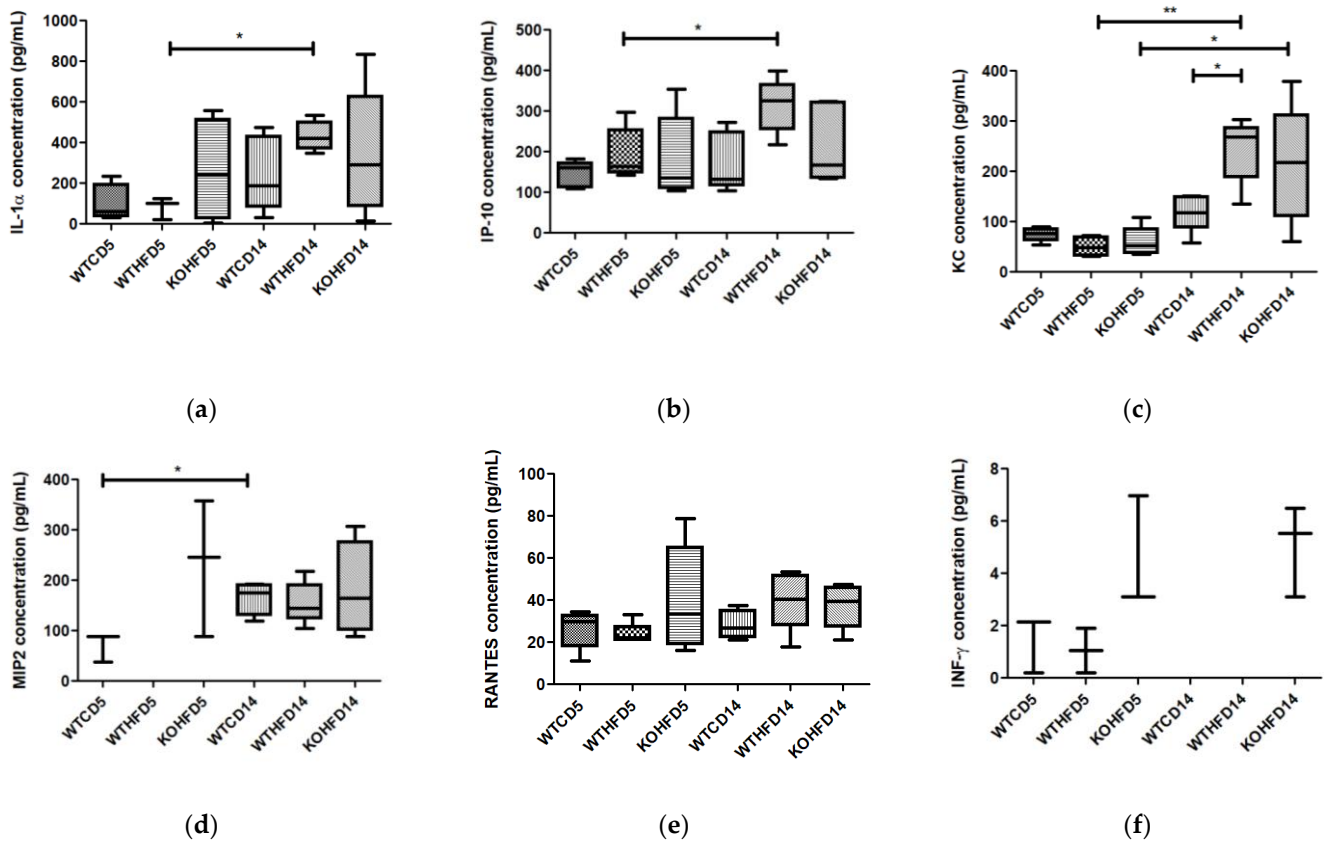
TNF- $\alpha$  was not detected in WTCD5 and WTHFD5 but increased to detectable levels after 14 weeks on experimental feeding in WTCD14 and WTHFD14, while higher concentrations of TNF- $\alpha$  in KOHFD5 decreased after prolonged feeding in KOHFD14 (Figure 4-5o). The kinetics of IL-4 production from week 5 to 14 in WTHFD and KOHFD did not change except for the WTCD which increased significantly ( $p < 0.05$ ) on week 14 (Figure 4-5p).

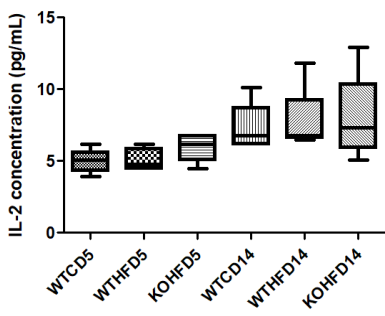
IL-5 production from week 5 to 14 significantly increased ( $p < 0.05$ ) in WTCD, while the observed increase in KOHFD14 and decrease in WTHFD14 compared with their 5-week counterparts were not statistically significant. Deletion of *Slc7a8* significantly increased IL-5 ( $p < 0.05$ ) in KOHFD14 compared with WTHFD14 (Figure 4-5q).

IL-10 levels were similar in all experimental groups between week 5 and 14, except for KOHFD that showed much higher levels at week 5 (KOHFD5) compared with WTHFD5 and KOHFD14 (Figure 4-5r), which is similar to the pattern of IL-6 levels measured in these experimental groups (Figure 4-5h). There was no change in IL-10 levels between KOHFD14 and WTHFD14 (Figure 4-5r).

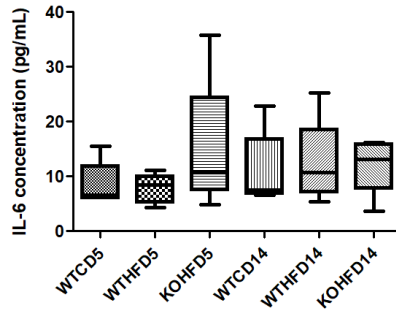


IL-13 levels were lower in WTHFD5 compared with WTCD5 and KOHFD5. At week 14, WTCD14, WTHFD14 and KOHFD14, IL-13 levels were higher, although not significantly, compared with their week 5 counterparts. (Figure 4-5s). The deletion of *Slc7a8* (KOHFD14) resulted in higher IL-13 levels than WTHFD14 (Figure 4-5s). The concentration of G-CSF was higher in WTHFD5 when compared with WTCD5, with no significant differences between WTHFD5 and KOHFD5. WTCD14 had elevated levels of G-CSF in comparison to WTCD5, while G-CSF was lower in WTHFD14 compared with WTHFD5. KOHFD14 had higher G-CSF levels in comparison to WTHFD14 (Figure 4-5t).

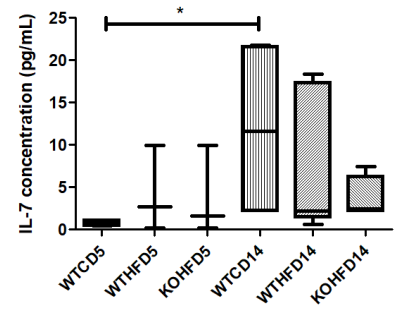




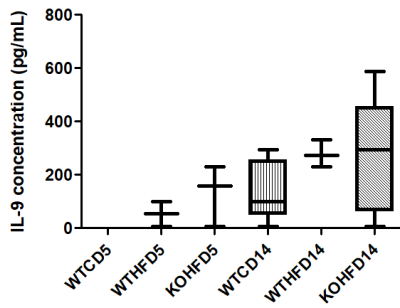
(g)



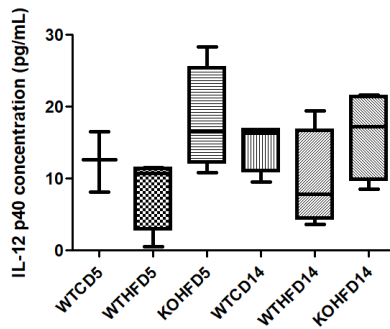
(h)



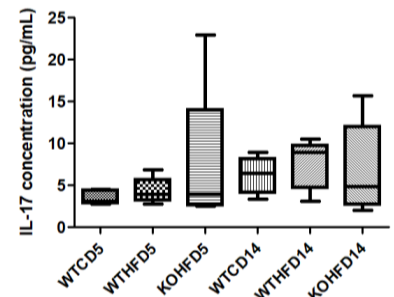
(i)



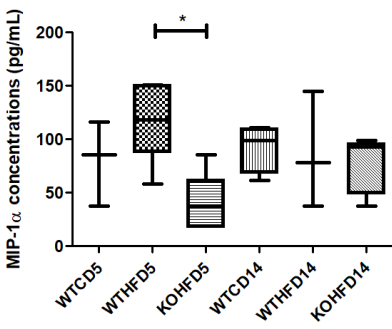
(j)



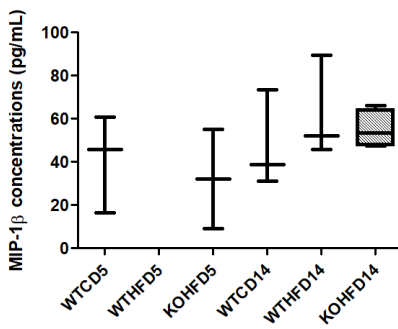
(k)



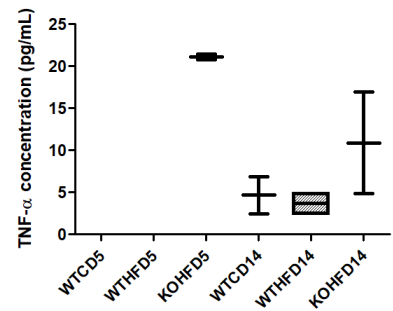
(l)



(m)



(n)



(o)

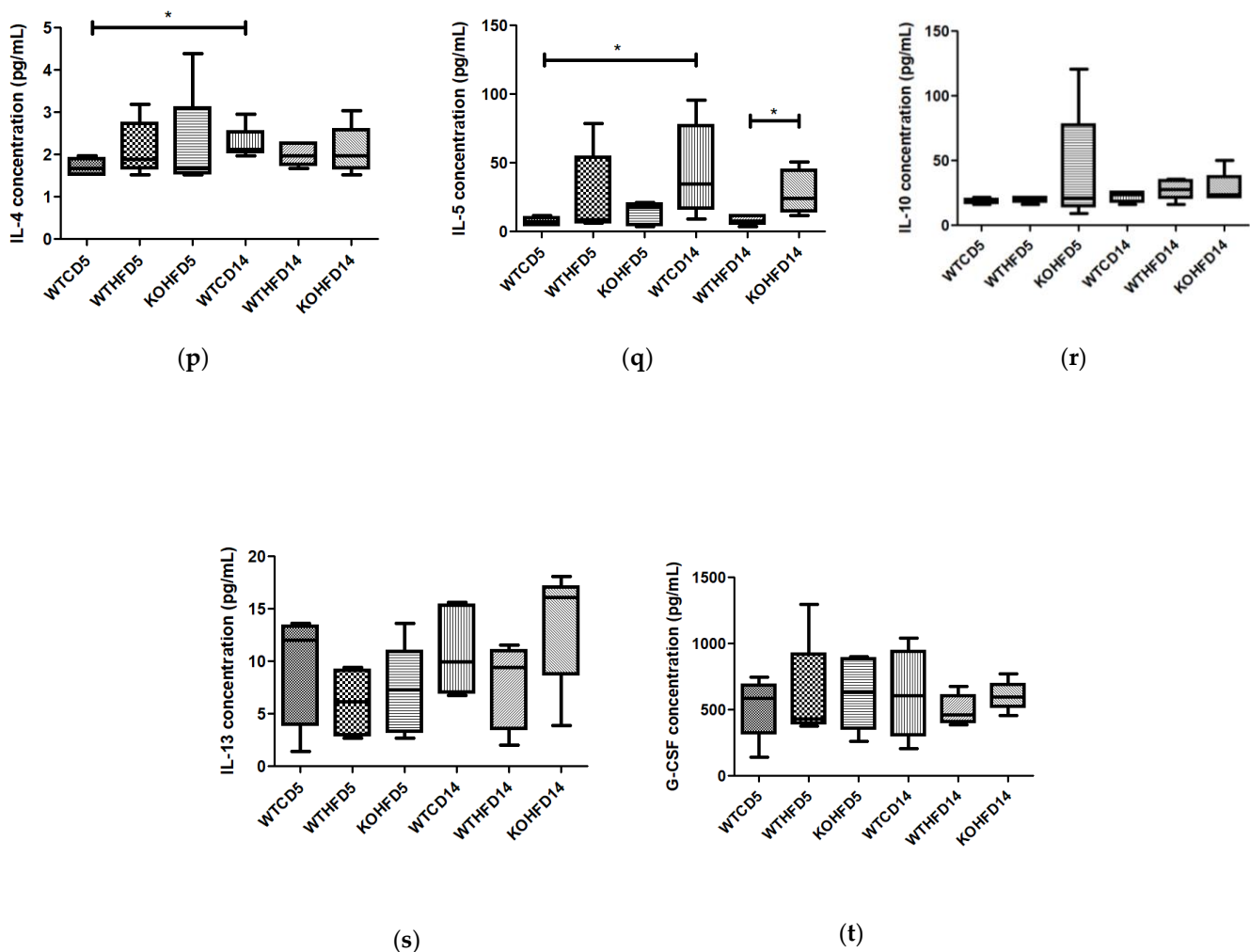


**Figure 4-5: Effect of *Slc7a8* deletion on plasma cytokine production.** (a) IL-1 $\alpha$  increased from week 5 to 14 in WTCD, WTHFD and KOHFD with only WTHFD14 being statistically significant ( $p < 0.05$ ). (b) IP-10 showed a significant increase ( $p < 0.05$ ) only in WTHFD from week 5 to 14, however, KOHF14 was lower than WTHFD14. (c) KC significantly increased in WTHFD ( $p < 0.001$ ) and KOHFD ( $p < 0.05$ ) from week 5 to 14 but did not change between KOHFD14 and WTHFD14. (d) MIP2 increased significantly ( $p < 0.05$ ) from week 5 to 14 only in WTCD, however, the levels in KOHFD14 and WTHFD14 did not differ. (e) RANTES increased significantly ( $p < 0.05$ ) from week 5 to 14 only in WTHFD, meanwhile the levels in KOHFD and WTHFD were similar. (f) INF- $\gamma$  levels did not change much from week 5 to 14 in KOHFD while WTCD14 and WTHFD14 had no detectable plasma levels ( $N=2$  for WTHFD5). (g) IL-2 levels increased from week 5 to 14 in WTCD, WTHFD and KOHFD but none were statistically significant. (h) IL-6 levels increased from week 5 to 14 in WTCD and WTHFD, while decreasing in KOHFD from week 5 to 14. (i) IL-7 levels increased from 5 to 14, with higher levels in WTCD14 and WTHFD14 but no change in KOHFD14. KOHFD14 IL-7 levels were reduced in WTHFD14. (j) IL-9 concentrations increased in WTCD, WTHFD and KOHFD from week 5 to 14 ( $N=2$  for WTHFD5). (k) IL-12 p40 levels were not significantly different from week 5 to 14 in all experimental groups. (l) A slight increase in IL-17 cytokine production was observed in WTCD and WTHFD from week 5 to 14 while that of KOHFD did not change. (m) At 5 weeks, MIP-1  $\alpha$  was significantly elevated ( $p < 0.05$ ) in WTHFD compared with KOHFD. From 5 to 14 weeks, there was no change in the MIP1- $\alpha$  concentrations of WTCD, reduction in WTHFD and an increase in KOHFD. (n) The MIP-1 $\beta$  concentrations increased in WTCD, KOHFD and WTHFD from 5 to 14 weeks, while MIP-1 $\beta$  was undetectable in WTCD5 ( $N=2$  for KOHFD5). (o) TNF- $\alpha$  was not detected in WTCD5 and WTHFD5 but increased to detectable levels in WTCD14 and WTHFD14 respectively, while TNF- $\alpha$  increased from WTCD5 to WTCD14 ( $N=2$  for KOHFD5). (p) IL-4 did not significantly change from week 5 to 14 in WTHFD and KOHFD, but WTCD14 levels increased significantly ( $p < 0.05$ ) compared with WTCD5. (q) IL-5 in WTCD14 increased significantly ( $p < 0.05$ ) when compared with WTCD5, while at week 14, IL-5 levels in KOHFD14 were significantly higher ( $p < 0.05$ ) compared with WTHFD14. (r) No significant changes in IL-10 levels were observed between WTCD and WTHFD, while IL-10 reduced from KOHFD5 to KOHFD14. (s) IL-13 levels increased in WTCD, WTHFD and KOHFD from week 5 to week 14. (t) G-CSF levels were increased in WTCD, reduced in WTHFD, and remained similar in KOHFD from 5 to 14 week.

## 4.5 Discussion

A high expression of *PparY*, *Cd36* and *Fabp4* with no detectable expression in *Ucp1* observed in pWAT of WTHFD suggests that adipocyte hypertrophy seen in WTHFD resulted from increased lipid uptake due to adipogenesis (Figure 4-1A) while reduced adipocyte hypertrophy in pWAT of KOHFD may be due to increased lipolysis by *Atgl* lipolytic activity. A previous study showed that the development of obesity in mice on HFD was as a result of adipocyte hypertrophy in white adipose depots caused by a low expression of ATGL<sup>28</sup>. The mWAT in WTHFD did not express *PparY*, *Ucp1* or *Atgl*, while there was an increase in *Fabp4* and *Cd36* (Figure 4-1B) suggesting that adipocyte hypertrophy in this phenotype is due to an increase of lipid uptake via lipid transporters independent of adipogenesis. Similarly, mWAT in KOHFD did not express *PparY*, *Ucp1* or *Atgl*, while there was a decrease in the expression of *Fabp4* and *Cd36* (Figure 4-E) compared with WTHFD, indicating that reduced adipocyte hypertrophy in KOHFD could be from a decrease in lipid uptake because of the very low expression levels of lipid transporters. These results suggest that *Atgl* lipolytic activity is important in regulating lipid fluxes in perigonadal tissue as opposed to the mesenteric depot as previously observed in other studies<sup>41-42</sup>.

BAT in WTHFD showed very high expression of *Ucp1* and *Fabp4*, followed by *PparY* and *Cd36*, then *Atgl* (Figure 4-1C), suggesting adipocyte hypertrophy of BAT in WTHFD could be due to lipid uptake by *Fabp4* and *Cd36* through adipogenesis but with limited lipolysis. Conversely, BAT in KOHFD showed no change in *PparY* expression with a slight increase in *Ucp1*, while *Cd36*, *Fabp4* and *Atgl* were even higher (Figure 4-1F) than in WTHFD, suggesting that attenuation of adipocyte hypertrophy in BAT could be both by increasing lipolysis and browning activity. Moreover, in KOHFD, *Atgl* was higher than *Fabp4* which is indicative of higher lipolysis than lipid uptake, resulting in reduced adipocyte hypertrophy in the brown adipose depot. The expression of *Ucp1* was slightly higher in *Slc7a8* deficient animals compared with the wildtype counterparts on HFD which indicates an induction of diet-induced thermogenesis due to an increase in energy expenditure in response to high-caloric intake, which has been previously reported<sup>43-44</sup>. Previous studies have proposed that defective diet-induced thermogenesis may increase predisposition to obesity, and therefore improving thermogenesis may induce weight loss<sup>45-47</sup>. It is therefore possible that increased

thermogenic capacity and lipolytic activity are possible mechanisms through which adipocyte hypertrophy is limited in BAT of *Slc7a8* deficient mice during period of diet induced obesity (KOHD). In summary, our molecular data suggest the mechanism of attenuation of adipocyte hypertrophy in KOHD is depot dependent and differs between the pWAT, mWAT and BAT.

The impact of reduced adipocyte hypertrophy in *Slc7a8* deficient mice (KOHD) on plasma metabolites was evaluated at weeks 5 and 14, and then compared with the wildtype counterparts (WTHD) at the same time points. Plasma leptin levels increases from 5 to 14 weeks and were only significant in WTHD ( $p < 0.01$ ) but not in KOHD. The increase in plasma leptin levels correspond to the increase in weight gain previously observed in both KOHD and WTHD from 5 to 14 weeks, which was significantly higher in WTHD compared with KOHD<sup>17</sup>. Previous research has also demonstrated an increase in leptin levels with increasing adiposity<sup>32,34</sup>. Leptin levels in DIO often suggest the presence of leptin resistance whereby despite sufficient levels of leptin, it does not pass the blood-brain barrier to regulate appetite<sup>34</sup>. In addition, high levels of leptin are correlated with insulin resistance<sup>35</sup>. Importantly, at week 14, leptin levels in KOHD14 were significantly lower ( $p < 0.01$ ) than in WTHD14 (Figure 4-2). The significant reduction in leptin concentration in KOHD14 may suggest the lack of *Slc7a8* is protective against the early onset of leptin resistance in DIO.

Plasma adiponectin concentrations decreased significantly from weeks 5 to 14 in WTHD ( $P < 0.01$ ) and WTCD ( $P < 0.05$ ) while it increased in KOHD, but not significantly (Figure 4-3). The results obtained in WTHD animals are consistent with previous findings which indicate that adiponectin levels decrease with increasing body mass<sup>32,36</sup>. Adiponectin has been shown to improve insulin sensitivity and it is postulated that sensitivity is improved by adiponectin regulating lipid and glucose homeostasis<sup>36,48</sup>. Decreased adiponectin levels in circulation have been shown to correlate with insulin resistance<sup>48</sup>, which may imply that the WTHD in this study are highly susceptible to developing insulin resistance. Furthermore, WTCD14 had significantly lower ( $p < 0.05$ ) adiponectin levels than WTCD5. A previous study showed that lower adiponectin levels correlated to increasing BMI<sup>49</sup>. This, however, is contrary to our previous findings which showed that weight in the WTCD mice remained similar between weeks 5 and 14<sup>17</sup>. Moreover, other studies have demonstrated that adiponectin levels

increase with age<sup>50-51</sup>. The adiponectin paradox has been described which associates high adiponectin to increasing age and development of disease, but the underlying mechanisms are currently unknown<sup>51-52</sup>. Taking the existing paradox into consideration, it would be imperative to conduct more studies in the future which explain the reduction in the adiponectin levels in an older, lean, and presumably healthy subject such as WTCD14. Finally, significantly higher ( $P < 0.05$ ) plasma adiponectin levels were measured in KOHFD14 compared with WTHFD14, is a positive indicator to show that deficiency in *Slc7a8* can significantly improve plasma adiponectin levels to regulate lipid and glucose metabolism in DIO, thereby protecting against the development of insulin resistance. Together, leptin and adiponectin levels measured in *Slc7a8* knockout phenotype showed great promise in targeting the function of this gene/protein in combating the early onset of insulin resistance and the development of T2D in condition of DIO.

Levels of total plasma cholesterol increased from week 5 to 14 in both *Slc7a8* deficient (KOHFD) and wildtype (WTHFD) mice (Figure 4-4). People with obesity are reported to have elevated total cholesterol levels when compared with the lean counterparts<sup>40,53</sup>. Furthermore, obesity is often correlated with high levels of low-density lipoprotein (LDL), referred to as bad cholesterol, and low high-density lipoprotein (HDL), so-called good cholesterol. In an obesity phenotype, an increase in triglycerides and disruptions in cholesterol metabolism may provoke inflammation in adipocytes<sup>39-40</sup>. However, we did not assess the levels of LDL and HDL cholesterol in this study, but it would be important to understand the distribution of these metabolites in KOHFD compared with WTHFD.

Cytokines inflammatory profile of *Slc7a8* deficient mice in DIO were measured both at week 5 and 14 (Figure 4-5). The proinflammatory cytokines GM-CSF, IL-1 $\beta$ , IL-12 p70, IL-15 and MCP-1 were not detected in the plasma of either KOHFD and WTHFD, thus, suggesting that these cytokines may not play an active role during weight gain in DIO, or the 14-week period is not sufficient to produce detectable levels of these cytokine in plasma. The proinflammatory cytokines IL- $\alpha$ , IP-10 and KC were significantly elevated in WTHFD14 mice, suggesting a proinflammatory milieu in wildtype animals during weight gain which may contribute to the pathophysiology of obesity. Importantly, these cytokines were greatly reduced in KOHFD14, indicative of a protective effect against chronic inflammation during

weight gain in *Slc7a8* deficient animals. The proinflammatory cytokines, RANTES, IL-6, IL-7, MIP-1 $\alpha$  and MIP-1 $\beta$  were also higher in WTHFD14 than in KOHFD14. These cytokines showed weak but consistent correlation with the obesity phenotype (WTHFD). The reduction of these cytokines in KOHFD14 suggests a reduced inflammatory state. Furthermore, it could be possible that a longer experimental period of more than 14 weeks may be required to show a strong and significant association of reduced inflammation in *Slc7a8* deficient animals. Animals deficient in *Slc7a8* (KOHFD14) had significantly higher IL-5 levels, in addition to high IL-13 and G-CSF plasma levels compared with WTHFD14. These cytokines have been shown to have anti-inflammatory properties<sup>54-55</sup> and therefore, the high concentration in the plasma confers a beneficial anti-inflammatory response to weight gain in DIO in *Slc7a8* deficient animals.

This study has provided some suggestions into the mechanistic role of *Slc7a8* in adipocyte hypertrophy and its effect on plasma metabolites level, however, this data should be interpreted with caution due to some limitations of the study such as the absence of western blot experiments to confirm protein expression of the reported genes. Furthermore, *Slc7a8* being a solute transporter, protein expression to investigate the involvement of mTOR activation and/or PPAR $\gamma$ /Akt signalling pathways in *Slc7a8* mediated function was not performed and should therefore be considered in future studies to establish the detailed molecular signalling mechanism through which *Slc7a8* mediate lipid transport and metabolism in adipose tissues for possible intervention to curb obesity development.

#### **4.6 Conclusions**

This study has demonstrated that the possible mechanism of lipid transport and attenuation of hypertrophy in adipose tissues in *Slc7a8* deficient phenotype is fat-depot dependent and results to a beneficial effect in this phenotype by improving the plasma metabolic profiles of leptin and adiponectin. Additionally, a decrease in the proinflammatory cytokines IL- $\alpha$ , IP-10, KC, IL-7 and MIP-1 $\alpha$ , and a decrease in the IL-5 anti-inflammatory cytokine is suggestive of a decrease in cytokine-mediated inflammation which is normally associated with the pathophysiology of obesity development.

## 4.7 Supplementary data

Table S4-1: The concentration (pg/ml) of plasma cytokines in WTCD, WTHFD and KOHFD at 5 and 14 weeks of experimental feeding.

	WTCD14	WTHFD14	KOHFD14	WTCD5	WTHFD5	KOHFD5
<b>GM-CSF</b>	-	-	57.24 (N=1)	-	-	-
<b>INF-<math>\gamma</math></b>	3.12 (N=2)	6.50 (N=1)	5.05 $\pm$ 1.01 (N=3)	1.50 $\pm$ 0.65 (N=3)	1.05 $\pm$ 0.86 (N=2)	4.41 $\pm$ 1.29 (N=3)
<b>IL-1<math>\alpha</math></b>	244.00 $\pm$ 81.80 (N=5)	433.60 $\pm$ 31.48 (N=5)	344.60 $\pm$ 140.00 (N=5)	98.31 $\pm$ 46.33 (N=4)	82.64 $\pm$ 31.98 (N=3)	261.70 $\pm$ 128.50 (N=4)
<b>IL-1<math>\beta</math></b>	0.86 $\pm$ 0.59 (N=2)	2.48 $\pm$ 1.68 (N=3)	6.92 $\pm$ 6.08 (N=2)	-	0.25 (N=1)	0.64 $\pm$ 0.39 (N=3)
<b>IL-2</b>	7.31 $\pm$ 0.74 (N=5)	7.71 $\pm$ 1.03 (N=5)	7.98 $\pm$ 1.32 (N=5)	4.99 $\pm$ 0.37 (N=5)	5.10 $\pm$ 0.34 (N=5)	5.96 $\pm$ 0.42 (N=5)
<b>IL-4</b>	2.27 $\pm$ 0.18 (N=5)	2.01 $\pm$ 0.12 (N=5)	2.10 $\pm$ 0.26 (N=5)	1.71 $\pm$ 0.09 (N=5)	2.14 $\pm$ 0.29 (N=5)	2.20 $\pm$ 0.55 (N=5)
<b>IL-5</b>	44.48 $\pm$ 15.14 (N=5)	8.70 $\pm$ 1.46 (N=5)	28.59 $\pm$ 7.11 (N=5)	7.48 $\pm$ 1.39 (N=5)	26.10 $\pm$ 13.82 (N=5)	13.57 $\pm$ 3.62 (N=5)
<b>IL-6</b>	11.00 $\pm$ 3.05 (N=5)	12.44 $\pm$ 3.40 (N=5)	12.13 $\pm$ 2.24 (N=5)	8.54 $\pm$ 1.81 (N=5)	7.82 $\pm$ 1.16 (N=5)	14.96 $\pm$ 5.37 (N=5)
<b>IL-7</b>	11.82 $\pm$ 5.56 (N=4)	7.97 $\pm$ 3.88 (N=5)	3.64 $\pm$ 1.27 (N=4)	0.84 $\pm$ 0.18 (N=4)	3.22 $\pm$ 2.32 (N=4)	3.93 $\pm$ 3.03 (N=3)
<b>IL-9</b>	142.30 $\pm$ 49.81 (N=5)	279.8 $\pm$ 29.26 (N=3)	267.00 $\pm$ 98.05 (N=5)	159.61 (N=1)	53.53 $\pm$ 47.18 (N=2)	132.70 $\pm$ 66.52 (N=3)
<b>IL-10</b>	22.34 $\pm$ 1.80 (N=5)	27.76 $\pm$ 3.40 (N=5)	28.71 $\pm$ 5.40 (N=5)	18.61 $\pm$ 0.91 (N=5)	20.10 $\pm$ 1.02 (N=5)	41.17 $\pm$ 20.29 (N=5)
<b>IL-12 (p40)</b>	14.77 $\pm$ 1.77 (N=4)	9.70 $\pm$ 3.41 (N=4)	16.18 $\pm$ 3.12 (N=4)	12.44 $\pm$ 2.41 (N=3)	8.39 $\pm$ 2.64 (N=4)	18.08 $\pm$ 3.68 (N=4)



	<b>WTCD14</b>	<b>WTHFD14</b>	<b>KOHFD14</b>	<b>WTCD5</b>	<b>WTHFD5</b>	<b>KOHFD5</b>
<b>IL-12 (p70)</b>	-	-	-	-	-	123.31 (N=1)
<b>IL-13</b>	10.95 ± 1.89 (N=5)	7.73 ± 1.80 (N=5)	13.57 ± 2.52 (N=5)	9.79 ± 2.82 (N=4)	6.11 ± 1.66 (N=4)	7.17 ± 1.92 (N=5)
<b>IL-15</b>	621.3 ± 66.98 (N=2)	251.0 ± 123.8 (N=2)	103.82 (N=1)	-	857.84 (N=1)	150.36 (N=1)
<b>IL-17</b>	6.23 ± 0.98 (N=5)	7.58 ± 1.31 (N=5)	6.88 ± 2.45 (N=5)	3.57 ± 0.38 (N=5)	4.38 ± 0.69 (N=5)	7.48 ± 3.90 (N=5)
<b>IP-10</b>	173.60 ± 32.24 (N=5)	313.20 ± 29.43 (N=5)	216.60 ± 43.26 (N=5)	146.50 ± 14.24 (N=5)	194.3 ± 28.27 (N=5)	184.90 ± 46.17 (N=5)
<b>KC</b>	118.90 ± 16.70 (N=5)	244.50 ± 29.03 (N=5)	213.20 ± 52.19 (N=5)	75.01 ± 6.21 (N=5)	50.46 ± 8.38 (N=5)	59.94 ± 13.03 (N=5)
<b>MCP-1</b>	-	8.98 ± 3.86 (N=2)	41.84 ± 13.05 (N=3)	-	-	32.84 (N=1)
<b>MIP-1α</b>	92.50 ± 11.02 (N=4)	87.16 ± 31.19 (N=3)	76.77 ± 11.71 (N=5)	80.03 ± 22.78 (N=3)	118.90 ± 16.70 (N=5)	39.57 ± 12.41 (N=5)
<b>MIP-1β</b>	47.93 ± 13.02 (N=3)	62.49 ± 13.65 (N=3)	55.12 ± 4.314 (N=4)	40.99 (N=3)	22.05 (N=1)	32.09 (N=2)
<b>MIP-2</b>	165.70 ± 16.44 (N=4)	155.40 ± 18.38 (N=5)	181.20 ± 46.48 (N=4)	71.66 (N=3)	-	231.14 (N=3)
<b>RANTES</b>	28.45 ± 2.96 (N=5)	40.08 ± 6.21 (N=5)	37.38 ± 4.69 (N=5)	26.40 ± 4.08 (N=5)	23.94 ± 2.34 (N=5)	40.50 ± 11.35 (N=5)
<b>TNF-α</b>	4.69 ± 2.22 (N=2)	3.68 ± 0.70 (N=4)	10.92 ± 6.04 (N=2)	-	2.47 (N=1)	21.13 (N=2)
<b>G-CSF</b>	621.20 ± 149.80 (N=5)	499.10 ± 50.98 (N=5)	606.10 ± 49.77 (N=5)	520.30 ± 102.80 (N=5)	613.80 ± 173.10 (N=5)	623.80 ± 122.00 (N=5)

## 4.8 References

1. Frühbeck G, Catalán V, Rodríguez A, Gómez-Ambrosi J. Adiponectin-leptin ratio: A promising index to estimate adipose tissue dysfunction. Relation with obesity-associated cardiometabolic risk. *Adipocyte*. 2018; 7(1):57-62. doi:10.1080/21623945.2017.1402151
2. Tang P, Virtue S, Goie JYG, Png CW, Guo J, Li Y, et al. Regulation of adipogenic differentiation and adipose tissue inflammation by interferon regulatory factor 3. *Cell Death & Differentiation*. 2021; 28(11):3022-35. doi:10.1038/s41418-021-00798-9
3. Longo M, Zatterale F, Naderi J, Parrillo L, Formisano P, Raciti GA, et al. Adipose tissue dysfunction as determinant of obesity-associated metabolic complications. *International Journal of Molecular Sciences*. 2019; 20(9):2358.
4. Torres N, Vargas-Castillo AE, Tovar AR. Adipose tissue: White adipose tissue structure and function. In: Caballero B, Finglas PM, Toldrá F, editors. *Encyclopedia of food and health*. Oxford: Academic Press; 2016. p. 35-42.
5. Haczeyni F, Bell-Anderson KS, Farrell GC. Causes and mechanisms of adipocyte enlargement and adipose expansion. *Obesity Reviews*. 2018; 19(3):406-20. doi:10.1111/obr.12646
6. Chait A, den Hartigh LJ. Adipose tissue distribution, inflammation and its metabolic consequences, including diabetes and cardiovascular disease. *Frontiers in Cardiovascular Medicine*. 2020; 7:22. doi:10.3389/fcvm.2020.00022
7. Reddy P, Lent-Schochet D, Ramakrishnan N, McLaughlin M, Jialal I. Metabolic syndrome is an inflammatory disorder: A conspiracy between adipose tissue and phagocytes. *Clinica Chimica Acta*. 2019; 496:35-44. doi:<https://doi.org/10.1016/j.cca.2019.06.019>
8. Wang QA, Tao C, Gupta RK, Scherer PE. Tracking adipogenesis during white adipose tissue development, expansion and regeneration. *Nature Medicine*. 2013; 19(10):1338-44. doi:10.1038/nm.3324
9. Ambele MA, Dessels C, Durandt C, Pepper MS. Genome-wide analysis of gene expression during adipogenesis in human adipose-derived stromal cells reveals novel patterns of gene expression during adipocyte differentiation. *Stem Cell Research & Therapy* 2016; 16(3):725-34. doi:10.1016/j.scr.2016.04.011
10. Ambele MA, Pepper MS. Identification of transcription factors potentially involved in human adipogenesis in vitro. *Molecular Genetics & Genomic Medicine*. 2017; 5(3):210-22. doi:<https://doi.org/10.1002/mgg3.269>

11. Ambele MA, Dhanraj P, Giles R, Pepper MS. Adipogenesis: A complex interplay of multiple molecular determinants and pathways. *International Journal of Molecular Sciences*. 2020; 21(12) doi:10.3390/ijms21124283
12. Pyrina I, Chung K-J, Michailidou Z, Koutsilieris M, Chavakis T, Chatzigeorgiou A. Fate of adipose progenitor cells in obesity-related chronic inflammation. *Frontiers in Cell and Developmental Biology*. 2020; 8 doi:10.3389/fcell.2020.00644
13. Liu F, He J, Wang H, Zhu D, Bi Y. Adipose morphology: A critical factor in regulation of human metabolic diseases and adipose tissue dysfunction. *Obesity Surgery*. 2020; 30(12):5086-100. doi:10.1007/s11695-020-04983-6
14. Rossier G, Meier C, Bauch C, Summa V, Sordat B, Verrey F, et al. Lat2, a new basolateral 4f2hc/cd98-associated amino acid transporter of kidney and intestine \*. *Journal of Biological Chemistry*. 1999; 274(49):34948-54. doi:10.1074/jbc.274.49.34948
15. Pineda M, Fernández E, Torrents D, Estévez R, López C, Camps M, et al. Identification of a membrane protein, lat-2, that co-expresses with 4f2 heavy chain, an l-type amino acid transport activity with broad specificity for small and large zwitterionic amino acids. *Journal of Biological Chemistry*. 1999; 274(28):19738-44. doi:10.1074/jbc.274.28.19738
16. Park SY, Kim JK, Kim IJ, Choi BK, Jung KY, Lee S, et al. Reabsorption of neutral amino acids mediated by amino acid transporter lat2 and tat1 in the basolateral membrane of proximal tubule. *Archives of Pharmacal Research*. 2005; 28(4):421-32. doi:10.1007/bf02977671
17. Pitere RR, van Heerden MB, Pepper MS, Ambele MA. Slc7a8 deletion is protective against diet-induced obesity and attenuates lipid accumulation in multiple organs. *Biology*. 2022; 11(2):311.
18. Li HL, Wu X, Xu A, Hoo RL. A-fabp in metabolic diseases and the therapeutic implications: An update. *International Journal of Molecular Sciences*. 2021; 22(17) doi:10.3390/ijms22179386
19. Saito N, Furuhashi M, Koyama M, Higashiura Y, Akasaka H, Tanaka M, et al. Elevated circulating fabp4 concentration predicts cardiovascular death in a general population: A 12-year prospective study. *Scientific Reports*. 2021; 11(1):4008. doi:10.1038/s41598-021-83494-5
20. Gyamfi J, Yeo JH, Kwon D, Min BS, Cha YJ, Koo JS, et al. Interaction between cd36 and fabp4 modulates adipocyte-induced fatty acid import and metabolism in breast cancer. *Nature Partner Journals (NPJ) Breast Cancer*. 2021; 7(1):129. doi:10.1038/s41523-021-00324-7
21. Trojnar M, Patro-Małyśza J, Kimber-Trojnar Ź, Leszczyńska-Gorzela B, Mosiewicz J. Associations between fatty acid-binding protein 4—a proinflammatory adipokine and insulin resistance, gestational and type 2 diabetes mellitus. *Cells*. 2019; 8(3):227.

22. Audano M, Pedretti S, Caruso D, Crestani M, De Fabiani E, Mitro N. Regulatory mechanisms of the early phase of white adipocyte differentiation: An overview. *Cellular and Molecular Life Sciences*. 2022; 79(3):139. doi:10.1007/s00018-022-04169-6
23. Ghaben AL, Scherer PE. Adipogenesis and metabolic health. *Nature Reviews Molecular Cell Biology*. 2019; 20(4):242-58. doi:10.1038/s41580-018-0093-z
24. Ali AT, Hochfeld WE, Myburgh R, Pepper MS. Adipocyte and adipogenesis. *European Journal of Cell Biology*. 2013; 92(6-7):229-36. doi:10.1016/j.ejcb.2013.06.001
25. Darwish NM, Gouda W, Almutairi SM, Elshikh MS, Morcos GNB. Pparg expression patterns and correlations in obesity. *Journal of King Saud University - Science*. 2022; 34(6):102116. doi:<https://doi.org/10.1016/j.jksus.2022.102116>
26. Rodríguez-Acebes S, Palacios N, Botella-Carretero JI, Olea N, Crespo L, Peromingo R, et al. Gene expression profiling of subcutaneous adipose tissue in morbid obesity using a focused microarray: Distinct expression of cell-cycle- and differentiation-related genes. *BioMed Central (BMC) Medical Genomics*. 2010; 3(1):61. doi:10.1186/1755-8794-3-61
27. Trites MJ, Clugston RD. The role of adipose triglyceride lipase in lipid and glucose homeostasis: Lessons from transgenic mice. *Lipids in Health and Disease*. 2019; 18(1):204. doi:10.1186/s12944-019-1151-z
28. Li J, Gong L, Liu S, Zhang Y, Zhang C, Tian M, et al. Adipose hnr protects against diet-induced obesity and insulin resistance. *Nature Communications*. 2019; 10(1):2375. doi:10.1038/s41467-019-10348-0
29. Zatterale F, Longo M, Naderi J, Raciti GA, Desiderio A, Miele C, et al. Chronic adipose tissue inflammation linking obesity to insulin resistance and type 2 diabetes. *Frontiers in Physiology*. 2020; 10 doi:10.3389/fphys.2019.01607
30. Michailidou Z, Gomez-Salazar M, Alexaki VI. Innate immune cells in the adipose tissue in health and metabolic disease. *Journal of Innate Immunity*. 2022; 14(1):4-30. doi:10.1159/000515117
31. Pei-Chi C, Po-Shiuan H. The role of adipocyte hypertrophy and hypoxia in the development of obesity-associated adipose tissue inflammation and insulin resistance. In: Jan Oxholm G, editor. *Adiposity*. Rijeka: IntechOpen; 2017. p. Ch. 7.
32. Tilg H, Moschen AR. Adipocytokines: Mediators linking adipose tissue, inflammation and immunity. *Nature Reviews Immunology*. 2006; 6(10):772-83. doi:10.1038/nri1937
33. Yadav A, Kataria MA, Saini V, Yadav A. Role of leptin and adiponectin in insulin resistance. *Clinica Chimica Acta*. 2013; 417:80-4. doi:10.1016/j.cca.2012.12.007
34. Izquierdo AG, Crujeiras AB, Casanueva FF, Carreira MC. Leptin, obesity, and leptin resistance: Where are we 25 years later? *Nutrients*. 2019; 11(11) doi:10.3390/nu11112704

35. Martínez-Sánchez N. There and back again: Leptin actions in white adipose tissue. *International Journal of Molecular Sciences*. 2020; 21(17):6039.
36. Nguyen TMD. Adiponectin: Role in physiology and pathophysiology. *International journal of preventive medicine*. 2020; 11:136-. doi:10.4103/ijpvm.IJPVM\_193\_20
37. Dhanraj P, van Heerden MB, Pepper MS, Ambele MA. Sexual dimorphism in changes that occur in tissues, organs and plasma during the early stages of obesity development. *Biology*. 2021; 10(8):717.
38. Makki K, Froguel P, Wolowczuk I. Adipose tissue in obesity-related inflammation and insulin resistance: Cells, cytokines, and chemokines. *International Scholarly Research Network Journals (ISRN) Inflammation*. 2013; 2013:139239. doi:10.1155/2013/139239
39. Curley S, Gall J, Byrne R, Yvan-Charvet L, McGillicuddy F. Metabolic inflammation in obesity – at the crossroads between fatty acid and cholesterol metabolism. *Molecular Nutrition & Food Research*. 2020; 65:1900482. doi:10.1002/mnfr.201900482
40. Gostynski M, Gutzwiller F, Kuulasmaa K, Döring A, Ferrario M, Grafnetter D, et al. Analysis of the relationship between total cholesterol, age, body mass index among males and females in the who monica project. *International Journal of Obesity*. 2004; 28(8):1082-90. doi:10.1038/sj.ijo.0802714
41. Wueest S, Yang X, Liu J, Schoenle EJ, Konrad D. Inverse regulation of basal lipolysis in perigonadal and mesenteric fat depots in mice. *American Journal of Physiology-Endocrinology and Metabolism*. 2012; 302(1):E153-60. doi:10.1152/ajpendo.00338.2011
42. Yang X, Lu X, Lombès M, Rha GB, Chi YI, Guerin TM, et al. The g(0)/g(1) switch gene 2 regulates adipose lipolysis through association with adipose triglyceride lipase. *Cell Metabolism*. 2010; 11(3):194-205. doi:10.1016/j.cmet.2010.02.003
43. Nedergaard J, Cannon B. Diet-induced thermogenesis: Principles and pitfalls. In: Guertin DA, Wolfrum C, editors. *Brown adipose tissue: Methods and protocols*. New York, NY: Springer US; 2022. p. 177-202.
44. Dieckmann S, Strohmeier A, Willershäuser M, Maurer SF, Wurst W, Marschall S, et al. Susceptibility to diet-induced obesity at thermoneutral conditions is independent of ucp1. *American Journal of Physiology-Endocrinology and Metabolism*. 2022; 322(2):E85-E100. doi:10.1152/ajpendo.00278.2021
45. Levin BE, Sullivan AC. Regulation of thermogenesis in obesity. *International Journal of Obesity*. 1984; 8 Suppl 1:159-80.
46. de Jonge L, Bray GA. The thermic effect of food and obesity: A critical review. *Obesity Research*. 1997; 5(6):622-31. doi:10.1002/j.1550-8528.1997.tb00584.x

47. Yamazaki T, Ikaga R, Li D, Nakae S, Tanaka S. A novel method for measuring diet-induced thermogenesis in mice. *MethodsX*. 2019; 6:1950-6. doi:<https://doi.org/10.1016/j.mex.2019.08.016>
48. Medina-Urrutia A, Posadas-Romero C, Posadas-Sánchez R, Jorge-Galarza E, Villarreal-Molina T, González-Salazar MDC, et al. Role of adiponectin and free fatty acids on the association between abdominal visceral fat and insulin resistance. *Cardiovascular diabetology*. 2015; 14:20-. doi:10.1186/s12933-015-0184-5
49. Baker JF, Newman AB, Kanaya A, Leonard MB, Zemel B, Miljkovic I, et al. The adiponectin paradox in the elderly: Associations with body composition, physical functioning, and mortality. *The Journals of Gerontology: Series A*. 2018; 74(2):247-53. doi:10.1093/gerona/gly017
50. Muratsu J, Kamide K, Fujimoto T, Takeya Y, Sugimoto K, Taniyama Y, et al. The combination of high levels of adiponectin and insulin resistance are affected by aging in non-obese old peoples. *Frontiers in Endocrinology*. 2022; 12 doi:10.3389/fendo.2021.805244
51. Walowski CO, Herpich C, Enderle J, Braun W, Both M, Hasler M, et al. Analysis of the adiponectin paradox in healthy older people. *Journal of Cachexia, Sarcopenia and Muscle*. 2023; 14(1):270-8. doi:<https://doi.org/10.1002/jcsm.13127>
52. Menzaghi C, Trischitta V. The adiponectin paradox for all-cause and cardiovascular mortality. *Diabetes*. 2018; 67(1):12-22. doi:10.2337/dbi17-0016
53. Veghari G, Sedaghat M, Maghsodlo S, Banihashem S, Moharloe P, Angizeh A, et al. The association between abdominal obesity and serum cholesterol level. *International Journal of Applied and Basic Medical Research*. 2015; 5(2):83-6. doi:10.4103/2229-516x.157150
54. Zhang JM, An J. Cytokines, inflammation, and pain. *International Anesthesiology Clinics*. 2007; 45(2):27-37. doi:10.1097/AIA.0b013e318034194e
55. Lee Y, Song YS, Fang CH, So BI, Park JY, Joo HW, et al. Anti-obesity effects of granulocyte-colony stimulating factor in otsuka-long-evans-tokushima fatty rats. *PLoS One*. 2014; 9(8):e105603. doi:10.1371/journal.pone.0105603

## **Chapter 5. Inhibition of SLC7A8 function decreased adipogenic differentiation capacity of human adipose derived stromal/stem cell**

Reabetswe R. Pitere<sup>1</sup>, Michael S. Pepper<sup>1</sup>, Melvin A. Ambele<sup>1,2</sup>

<sup>1</sup>Institute for Cellular and Molecular Medicine, Department of Immunology and SAMRC Extramural Unit for Stem Cell Research and Therapy, Faculty of Health Sciences, University of Pretoria, Pretoria 0001, South Africa

<sup>2</sup>Department of Oral and Maxillofacial Pathology, School of Dentistry, Faculty of Health Sciences, University of Pretoria, Pretoria 0001, South Africa

The chapter has been prepared in the format of a manuscript.

## 5.1 Abstract

Adipose tissue expansion through adipogenesis can lead to adverse metabolic and health consequences. Solute Carrier Family 7 Member 8 (*SLC7A8*) is a potential mediator of adipogenesis, and gene deletion studies have shown its absence to be protective against diet-induced obesity, adipocyte hypertrophy and to improve metabolic parameters. Thus, the current study investigated the effect of inhibiting *SLC7A8* function with 2-Aminobicyclo-(2,2,1)-heptane-2-carboxylic acid (BCH) treatment at different time points in the early stages of adipogenic differentiation in human adipocyte-derived stromal cells (ASCs) on adipogenesis *in vitro*. Inhibition of *SLC7A8* function on days 0 and 3 of adipogenic induction led to a reduction in lipid droplet formation in the adipocytes when compared with the untreated induced cells and this was statistically significant ( $p < 0.05$ ) when *SLC7A8* function was inhibited on day 0. Additionally, the reduction in lipid droplet formation in these cells corresponded to the downregulation of *PPARY*, *FABP4*, *CD36* and *SLC7A8*, thereby suggesting inhibition of *SLC7A8* function suppressed adipogenesis. *PRDM16* expression was similar in day 0 treated and untreated induced cells but was much higher on day 3 treated cells suggesting an increase in browning activity. This shows the inhibition of *SLC7A8* function on days 0 and 3 post-induction led to decrease in white adipogenesis in addition to increase browning activity in day 3 treated cells. The results demonstrate that *SLC7A8* plays a vital role in the early stages of adipogenesis in terms of browning activity, white adipogenic differentiation capacity and in determining the overall phenotype of the mature adipocyte.



## 5.2 Introduction

Obesity is associated with an increased risk of severe health consequences. An imbalance in energy homeostasis, wherein calorie consumption exceeds energy expenditure, can result in obesity development<sup>1</sup>. During a positive energy balance, adipose tissue expands to accommodate the excess energy<sup>1</sup>. In obesity, the size of adipocytes increases due to an accumulation of excess triglycerides making it to become larger as a result of storing more fat, a process known as hypertrophy<sup>2</sup>. However, when the adipose tissue reaches its maximum capacity to store fat, it becomes dysfunctional and can lead to the development of metabolic disorders such as insulin resistance, type 2 diabetes, and cardiovascular disease<sup>2-3</sup>. Adipose tissue expansion during obesity can also be due to formation on new adipocytes and thus, increased number of adipocytes; this is known as hyperplasia or adipogenesis<sup>2-3</sup>.

Adipogenesis is the process by which adipocyte precursor cells (preadipocytes) differentiate into mature adipocytes<sup>3</sup>. Several transcription factors are needed for successful adipogenic differentiation to produce mature and functional adipocytes<sup>3</sup>. Peroxisome proliferator-activated receptor gamma (PPAR $\gamma$ ) is the master regulator of adipogenesis and without its expression, the precursor cells are incapable of becoming adipocytes<sup>3-4</sup>. CCAAT/enhancer binding protein alpha (C/EBP $\alpha$ ) is another important transcription factor in adipogenesis, and it promotes the expression of PPAR $\gamma$ <sup>4</sup>. In addition to PPAR $\gamma$  and C/EBP $\alpha$ , many other genes involve in lipid metabolism and transport play an important role in the formation of a mature adipocyte phenotype<sup>3,5-6</sup>. Various studies have been conducted to aid our understanding of adipogenesis and to identify other important genes that may be involved in this process<sup>4,7-9</sup>. The Solute Carrier Family 7 Member 8 (SLC7A8) is one of those novel genes identified with no previous role in adipogenesis<sup>10</sup>. Functional studies in a mouse model showed knockout of *Slc7a8* significantly protects against diet induced obesity and reduce adipocyte hypertrophy at different fat depots<sup>11</sup>. Thus, suggesting *Slc7a8* could play an important role obesity development through lipid metabolism and adipocyte formation.

*SLC7A8* encodes a LAT2 protein, which is a sodium-independent transporter of small and large neutral amino acids across the cellular membrane<sup>12-13</sup>. The amino acids transported by LAT2 include alanine, threonine, cysteine, tryptophan, leucine, and tyrosine<sup>13-14</sup>. Amino acids are important in synthesising proteins which are vital in various cellular processes such as cell growth and proliferation<sup>1,15</sup>. Various studies have shown that dietary manipulation and restriction of

certain amino acids affects energy homeostasis and may be important in reducing body weight<sup>16-18</sup>. Increased levels of circulating branched-chained amino acids (BCAAs) such as tryptophan and leucine have been reported in obese subjects, while decreased intake of BCAAs was shown to promote weight loss<sup>18-20</sup>. A previous study showed that the quantity of BCAAs was higher in mature adipocytes in comparison to preadipocytes and that catabolism of BCAA was important in fuelling adipogenic differentiation<sup>21</sup>. Considering that some of the BCAA transported by LAT2 such as leucine and tryptophan have been reported to play a role in body weight and adipogenesis, it would be important to understand how the inhibition of SLC7A8/LAT2 function in adipose derived stromal/stem cells affect adipocyte formation through the process of adipogenesis.

2-Aminobicyclo-(2,2,1)-heptane-2-carboxylic acid (BCH) is an inhibitor of L-type amino neutral amino acid (LNAA) transporters including LAT2<sup>22</sup>. Its mode of inhibition is by depleting amino acids in the cell or reducing the uptake of LNAA such as leucine into cells by reducing glutamine efflux which is key in regulating the uptake of leucine, and thus depriving cells of amino acids which are required for insulin signalling, protein synthesis, cell growth and proliferation<sup>22-23</sup>. In this study, we investigated the effect of BCH inhibition of SLC7A8/LAT2 function in ASCs on adipogenesis *in vitro* and if the timing of inhibition in the early stages of adipogenesis is important to the overall process.

### **5.3 Materials and methods**

#### **5.3.1 Ethics statement**

The study was approved by the Faculty of Health Sciences Research Ethics Committee, University of Pretoria, South Africa (reference number 474/2019).

#### **5.3.2 Adipocyte isolation**

Adipocyte-derived stromal cells (ASCs) were isolated from human subcutaneous adipose tissue from individuals undergoing liposuction as described<sup>24</sup>, with some modifications. The cells used in the study were previously cryopreserved in liquid nitrogen at the Institute for Cellular and Molecular Medicine (ICMM), University of Pretoria and were thawed before use. Three different ASC cultures were used in the study with each culture derived from a single individual. The ASC

cultures were A270620-01A P5F1, A280621-01B P4F1 and A280621-01R P5F1. The nomenclature/labelling of cultures are described in Figure 5-1.

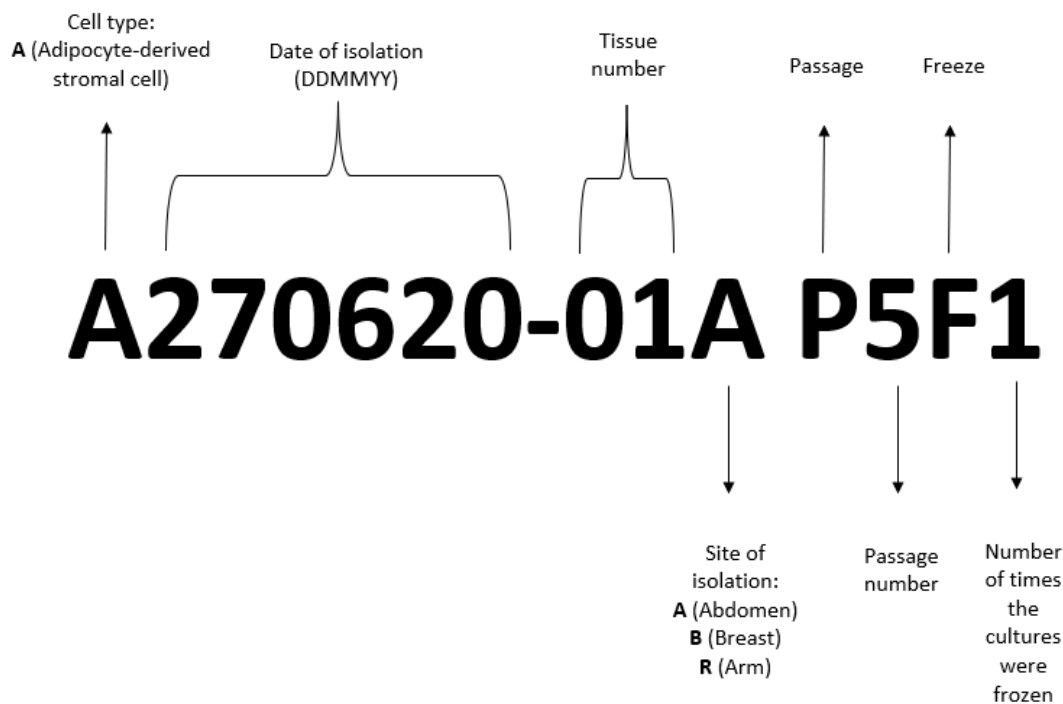


**Figure 5-1: Nomenclature of adipocyte-derived stromal cell (ASC) cultures.** The nomenclature represents how ASC cultures are labelled at the Institute for Cellular and Molecular Medicine, University of Pretoria.

#### 1.1.1.1 Adipocyte expansion, characterisation, and differentiation

The ASCs were cultured in a T75 flask, in complete culture medium which comprised of Dulbecco's Modified Eagle's Medium (DMEM) (GIBCO, Thermo Fisher Scientific, Massachusetts, United States), 2% penicillin/streptomycin (pen/strep) (GIBCO, Thermo Fisher Scientific, Massachusetts, United States) and 10% foetal bovine serum (FBS) (GIBCO, Thermo Fisher Scientific, Massachusetts, United States), and incubated at 37°C in 5% CO<sub>2</sub> Forma CO<sub>2</sub> water jacketed 3111TF incubator (Thermo Fisher Scientific, Massachusetts, United States) until 80-90% confluent. Once confluent, the cells were dissociated from the wells using 0.25% trypsin EDTA (GIBCO, Thermo Fisher Scientific, Massachusetts, United States) for 10 minutes at 37°C. This was followed by deactivating the trypsin-EDTA with 2mL complete DMEM (equivalent to medium in the plate wells). The suspension was centrifuged at 300xg for 5 minutes, and the resulting pellet was resuspended

in DMEM and used for isolation. Immunophenotypic analysis of the ASCs was performed using flow cytometry. A 100µl of the resuspended pellet was incubated with 5µl of each of the monoclonal antibodies (mouse anti-human CD73-PB450, CD105-PE, CD90-FITC, CD34-PC7, CD-36 APC, CD44 APC-AF750 and CD45-KO525 (*Beckman Coulter, Brea, United States*) and incubated for 15 minutes at 37°C. The antibodies were quantified on a CytoFlex Flow Cytometer (*Beckman Coulter, Brea, United States*) and analysed on the Kaluza version 2.1 Analysis Software (*Beckman Coulter, Brea, United States*). To prepare the cells for differentiation, ASCs were seeded at 5000 cells/cm<sup>2</sup> in 6-well plates and grown to approximately 90% confluency. For adipogenic induction, the cells were washed twice with phosphate-buffered saline (PBS)/2% pen/strep and cultured with adipogenic medium which constituted of complete DMEM, 10µg/mL human insulin (*GIBCO, Thermo Fisher Scientific, Massachusetts, United States*), 1µM dexamethasone, 0.5M 3-isobutylmethylxanthine (*GIBCO, Thermo Fisher Scientific, Massachusetts, United States*) and 200µM indomethacin (*Sigma-Aldrich, Missouri, United States*).

#### 5.3.2.1 BCH treatment of ASC undergoing adipogenesis

ASCs were cultured in adipogenic medium and treated with 100µl of BCH (*Sigma-Aldrich, Missouri, United States*) dissolved in 1N ammonium hydroxide (NH<sub>4</sub>OH) for a period of 72 hours (3 days). Following treatment, the ASCs were washed twice with PBS/2% pen/strep to remove the BCH treatment and then re-cultured in adipogenic medium only. The BCH treatment was done at different timepoints as illustrated on Figure 5-2: Three days before adipogenic induction (-3DI BCH) (Figure 5-2A), on day 0 of adipogenic induction (DOI BCH) (Figure 5-2B) and three days after induction (+3DI BCH) (Figure 5-2C). Control experiments include ASCs grown in adipogenic medium without BCH treatment (Figure 5-2D), and non-induced ASCs grown in the complete DMEM (Figure 2E). Adipogenic differentiation for all cells was for a period of 21 days. Following differentiation, the cells were dissociated using 0.25% trypsin EDTA (*GIBCO, Thermo Fisher Scientific, Massachusetts, United States*) for 10 minutes at 37°C. This was followed by deactivating the trypsin-EDTA with 2mL complete DMEM (equivalent to medium in the plate wells). The suspension was centrifuged at 300xg for 5 minutes, and the resulting pellet was used for RNA isolation.

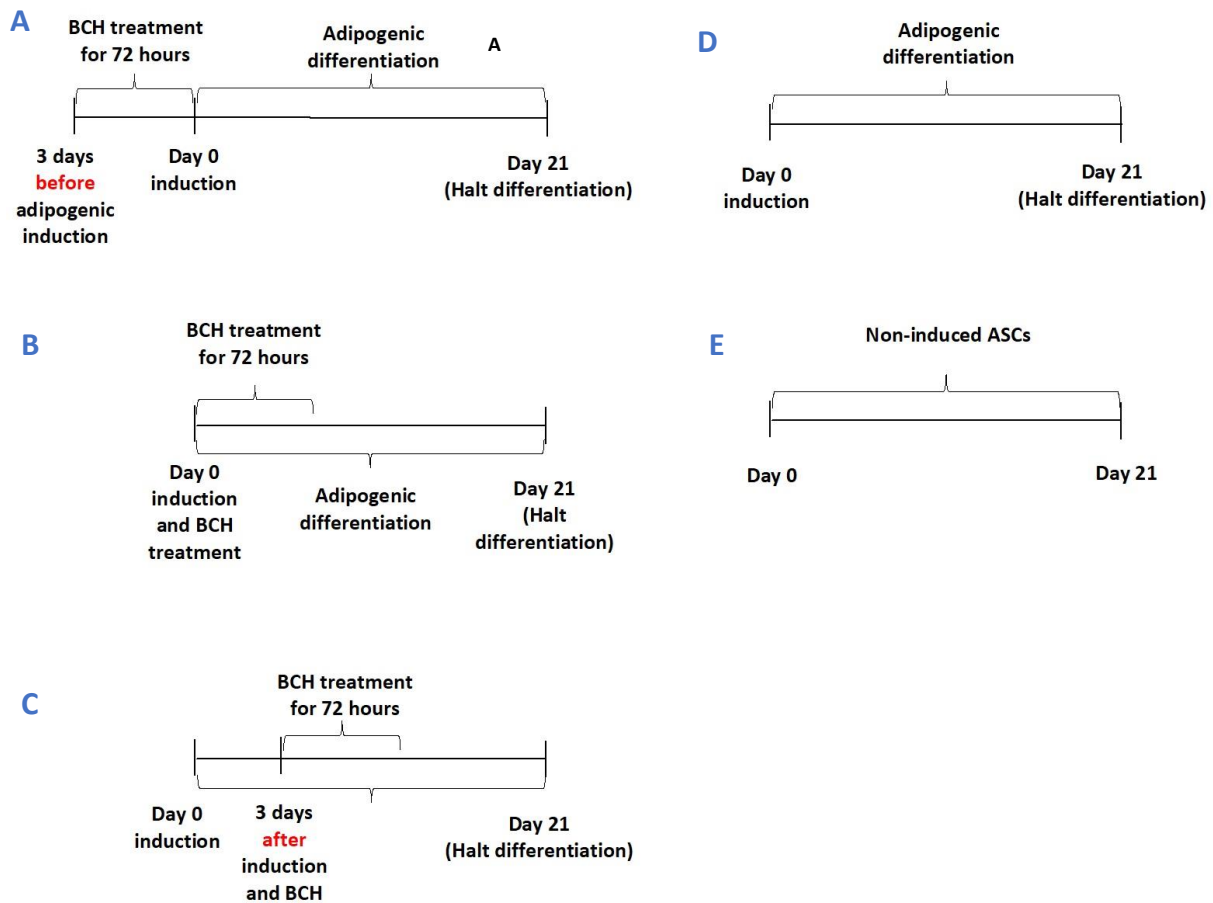


**Figure 5-2: Inhibition of SLC7A8 function with BCH treatment in differentiating ASCs.** ASCs undergoing adipogenic differentiation were treated at different timepoints: 3 days before adipogenic induction, A; on day 0 of induction, B and 3 days after induction, C. Controls include adipogenic induced ASCs without BCH treatment, D and non-induced ASCs cultured in normal growth medium, E.

### 5.3.3 Microscopy imaging of differentiated adipocyte

Microscopy was used to confirm lipid droplet accumulation during adipogenesis in both the induced and non-induced cells. All cells were stained with 2.5µg/mL of 4', 6-diamino-2-phenylindole, dihydrochloride (DAPI) (*Life Technologies, Thermo Fisher Scientific, California, United States*) overnight at 37°C for nucleus detection. The next day, the cells were stained with 50 ng/mL of Nile Red (*Life Technologies, Thermo Fisher Scientific, California, United States*) and incubated for 20 minutes to stain lipid droplets. Following incubation, the plates were washed twice with PBS/2% pen/strep and viewed on the AxioVert A1 inverted fluorescence microscope (*Carl Zeiss AG, Jena Germany*) using an AxioCam ICm 1 camera (*Carl Zeiss AG, Jena Germany*) on the Zen Blue 2.3 software (*Carl Zeiss AG, Jena Germany*). The images were captured at 5X and 20X magnification.

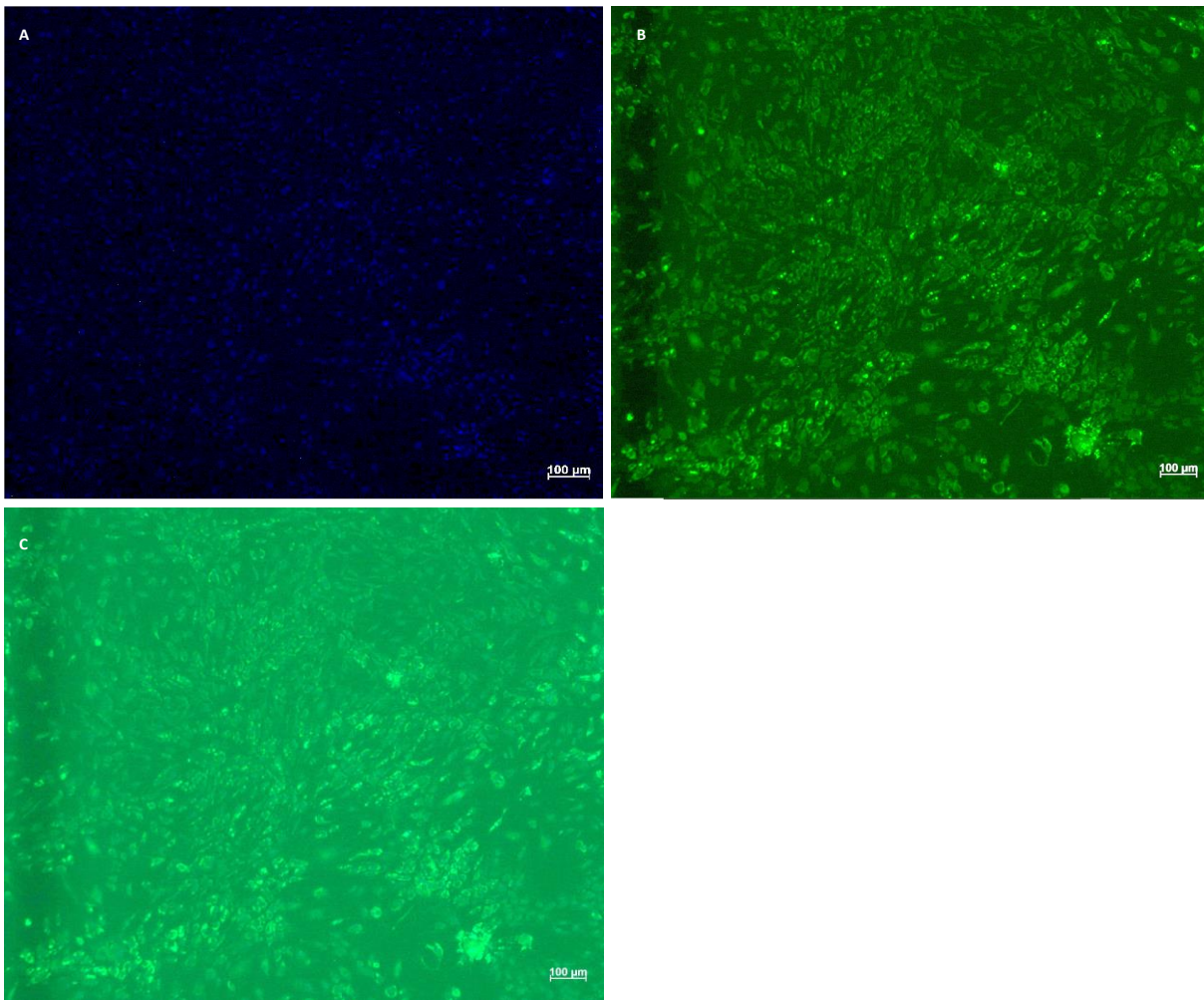


**Figure 5-3: The fluorescent microscopy images of the differentiated adipocytes.** A representative image of only the stained nuclei, A, that of the lipid droplets, B, and the adipocyte with both the nuclei and lipid droplets, C. Magnification = 5X, scale bar = 100µM.

The images captured on 5X magnification with only the formation of lipid droplets (Figure 5-3B) were used on ImageJ Fiji (<https://imagej.nih.gov/ij/download.html>) to semi-quantitatively analyse the lipid droplets. Analysis and quantification were performed according to the protocol described by Adomshick et al., 2020<sup>25</sup>. Ten different images captured across the microscope slide were used for analysis. The analysis was performed as follows:

1. Upload image to ImageJ by selecting “File”, and then “Open”.
2. Convert the colour image to grayscale by selecting “Image”, “Type” and then “8-bit”.
3. Convert the grayscale image to a binary image by selecting “Image”, “Adjust” and “Threshold”.

- a. The threshold setting is important to separate pixels according to the object of interest from the background signal<sup>26</sup>.
  - b. The threshold is manually selected between the minimum value of 0 and maximum value of 255, depending on the signal intensity.
  - c. The threshold settings used were “Default” and “B&W” (black and white) colours.
  - d. Once the threshold settings have been established, select “Apply”.
4. To analyse, select “Analyze”, then “Analyze Particles” using the default settings; “Size: 0-Infinity” and “Circularity: 0.00-1.00”, then Select “OK”.
  5. To count, select “Analyze” then “Measure”.

#### 5.3.4 RNA isolation and RT-qPCR

Total cellular RNA was isolated after 21 days of adipogenic induction from the induced ASCs treated with BCH, induced ASCs treated with NH<sub>4</sub>OH (without BCH), induced and non-induced ASCs in complete DMEM. RNA isolation was performed using the E.Z.N.A.<sup>®</sup> Total RNA kit (*Omega Bio-Tek Inc., Georgia, United States*) in accordance with the manufacturer’s instructions. The integrity of the RNA was assessed using the Agilent 2200 TapeStation (*Agilent Technologies, California, United States of America*) following the manufacturer’s instructions. The cDNA was synthesised using 1µg RNA with the SensiFAST cDNA synthesis kit (*Bioline, London, United Kingdom*). The concentration and purity of the cDNA was determined using the Nanodrop ND-1000 Spectrophotometer (*ThermoFischer Scientific Waltham, Massachusetts, United States of America*). PCR reactions were prepared in a total reaction volume of 20µl using the CelGREEN Universal qPCR mix (*Celtic Molecular Diagnostics, Cape Town, South Africa*), with primer concentrations of 10µM and cDNA concentration of 100ng/µl. The primer sequences used for specific gene target were purchased from IDT Oligos (*Integrated DNA Technologies, Iowa, United States*) and are as follows: *PPARY* (forward: 5’-CGTGGATCTCTCCGTAAT-3’; reverse: 5’-TGGATCTGTTCTTGTGAATG-3’), *FABP4* (forward: 5’-ATCAACCACCATAAAGAGAAA-3’; reverse: 5’-AACTTCAGTCCAGGTCAA-3’), *SLC7A8* (forward: 5’-GTAGCCCTGAAGAAAGAGATCG-3’; reverse: 5’-ATTCTCCAGCACTCCCTTTG-3’), *PRDM16* (forward: 5’-CAGCACGGTGAAGCCATTC-3’; reverse: 5’-GCGTGCATCCGCTTGTG-3’), *GUSB* (forward: 5’-GATCGCTCACACCAAATC-3’; reverse: 5’-TCGTGATACCAAGAGTAGTAG-3’), *TBP* (forward: 5’-CCGAAACGCCGAATATAA-3’; reverse: 5’-

GGACTGTTCTTCACTCTTG-3') and *YWHAZ* (forward: 5'-TGACATTGGGTAGCATTAAAC-3'; reverse: 5'-GCACCTGACAAATAGAAAGA-3'). RT-qPCR was performed in the LightCycler 480 II (*Roche, Basel, Switzerland*) under the following PCR conditions: denaturation at 95°C for 5 minutes and 45 PCR cycles at 95°C for 30 seconds, 62°C for 30 seconds, and 72°C for 30 seconds. The Ct values obtained after amplification were used to quantify the fold expression of each gene using the delta delta CT ( $2^{-\Delta\Delta Ct}$ ) method. The Ct values for *PPARY*, *FABP4*, *CD36*, *SLC7A8* and *PRDM16* were normalised using the Ct values of the reference genes; *GUSB*, *TBP* and *YWHAZ*. Thereafter, the untreated induced cells were normalised to the noninduced cells. For both treatment time points on day 0 and day 3, BCH treated induced cells were normalised to the NH<sub>4</sub>OH treatment induced cells.

#### 5.3.5 Statistical analysis

The statistical analyses were conducted using GraphPad Prism 5 (*GraphPad Software Inc., San Diego, United States*). All the values are expressed as mean  $\pm$  SEM. A paired t-test was used to compare means between two categories. The results which statistically significant are indicated as \* $p < 0.05$ , \*\* $p < 0.01$ , \*\*\* $p < 0.001$ .

## 5.4 Results

### 5.4.1 ASC characterisation and adipocyte differentiation

ASCS were positive for CD105, CD44, CD90 and CD73 (Figure 5-4A), whilst negative for CD45, CD36 and CD34 (Figure 5-4B)<sup>27-28</sup>. The red peaks on the graphs are indicative of the unstained ASCs which act as the negative control while the green bars represent the ASCs stained with the antibodies. A shift of the green peaks to the right from the red peaks indicate positive staining and antibody binding to the epitopes (Figure 5-4).



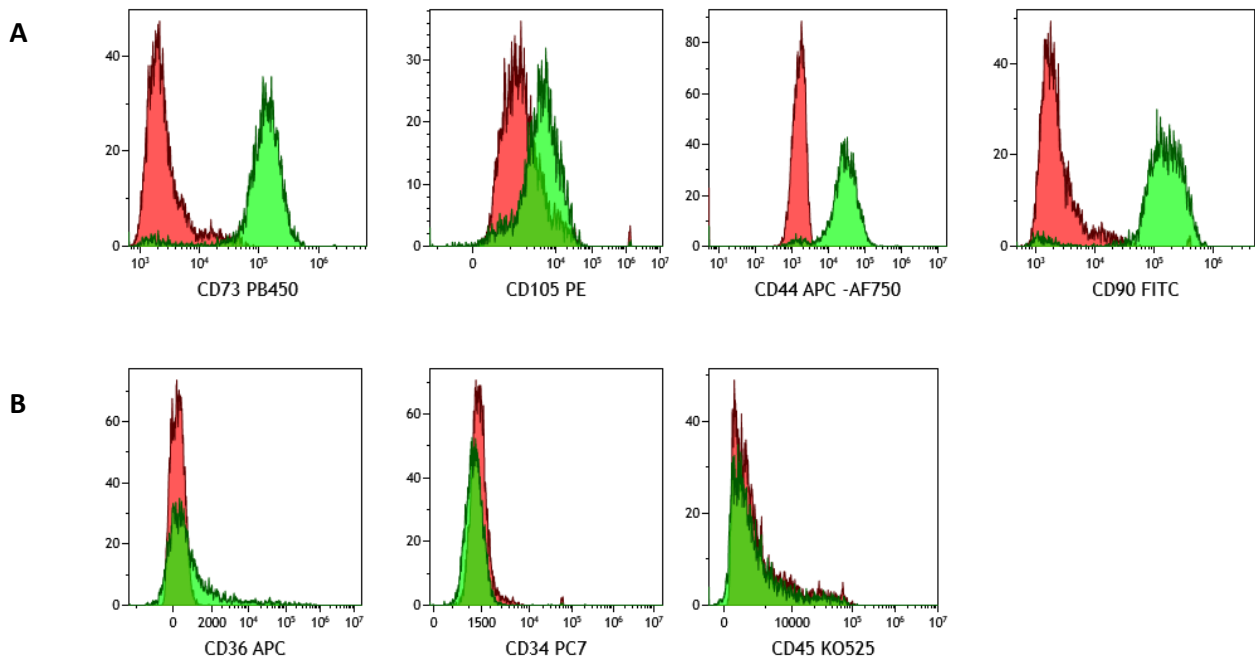


**Figure 5-4: Immunophenotype data of the ASCs.** The ASCs were positive for the CD73, CD105, CD44 and CD90 while negative for CD36, CD34 and CD45.

Following the 21-day induction period, the ASCs were successfully induced into adipocytes, with lipid droplet formation observed in induced cells but not in the non-induced ASCs (Figure 5-5). The cells treated with BCH three days prior to induction (Figure 5-5A), and cells treated only with  $\text{NH}_4\text{OH}$  (Figure 5-5B) differentiated and formed lipid droplets. Similar results were observed in the cells treated with BCH and  $\text{NH}_4\text{OH}$  on the day of induction (Figures 5-5C and 5-5D, respectively), and three days after induction (Figures 5-5E and 5-5F, respectively). The formation of lipid droplets was seen in the differentiated cells which were induced in the absence of BCH or  $\text{NH}_4\text{OH}$  treatment (Figure 4G), while the non-induced cells lacking the lipid droplets are illustrated on Figure 5-5H.

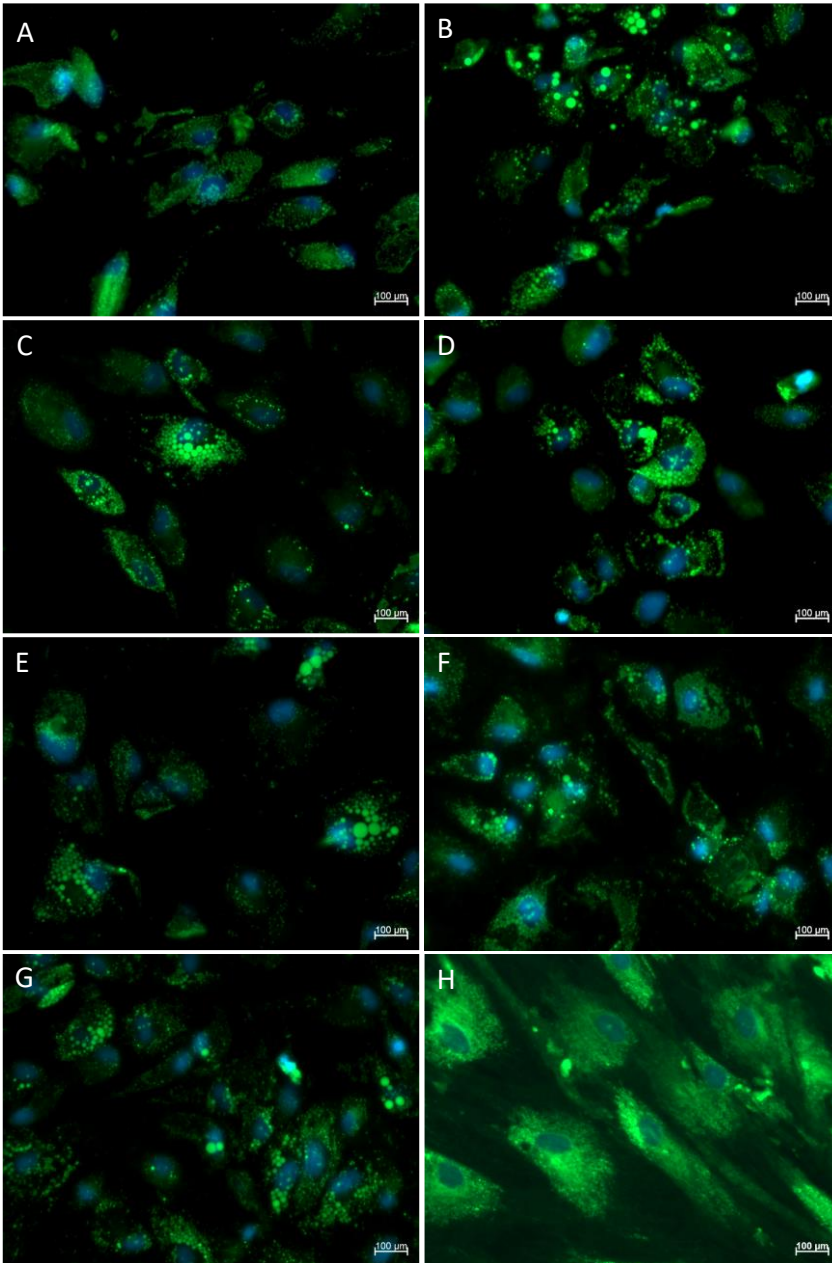


**Figure 5-5: Microscopic images of ASCs differentiated into adipocytes.** The images were captured 21 days after inducing ASCs to differentiate into adipocytes. BCH and NH<sub>4</sub>OH treated cells 3 days before induction are shown in A and B, respectively. BCH and NH<sub>4</sub>OH treated cells on day 0 of induction are represented by C and D, respectively. Three days post induction, the cells treated with BCH and NH<sub>4</sub>OH are shown in E and F, respectively. G is representative of the control induced cells which were neither treated with BCH nor NH<sub>4</sub>OH, while H represents non-induced cells. Magnification= 20X, scale bar = 100μM.

#### 5.4.2 Semi-quantification of lipid droplet formation

The number of lipid droplets formed after 21 days of adipogenic differentiation did not differ significantly when comparing DOI BCH with -3D1 BCH ( $p=0.34$ ), or +3DI BCH ( $p=0.59$ ). However, there was a significant difference in lipid droplet formation between DOI BCH and the untreated

induced cells ( $p < 0.05$ ). Furthermore, there was no significant difference in lipid droplet accumulation when comparing -3DI BCH with +3DI BCH ( $p = 0.33$ ), -3DI BCH and untreated induced cells ( $p = 0.68$ ), and +3DI BCH and untreated induced ( $p = 0.10$ ). The untreated induced cells had more lipid droplets compared with the BCH treated cells (Figure 5-6).

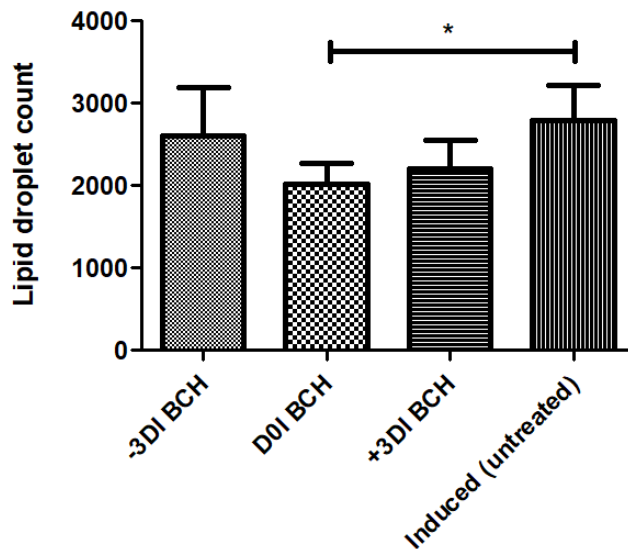


**Figure 5-6: Semi-quantification of number of lipid droplets formed in differentiated adipocytes.** The amount of lipid droplets formed in the adipocytes did not differ between D0I BCH and -3DI BCH ( $p = 0.34$ ), D0I and +3DI BCH ( $p = 0.59$ ), -3DI BCH and +3DI BCH ( $p = 0.33$ ), -3DI BCH and untreated induced ( $p = 0.38$ ), and +3DI BCH and untreated induced ( $p = 0.10$ ) and were statistically different between D0I BCH and the untreated induced cells ( $p < 0.05$ ),  $N = 3$  for -3DI BCH, D0I BCH, +3DI BCH and untreated induced. \* $p < 0.05$ .

#### 5.4.3 RT-qPCR

On day 21 of differentiation, the expression of *PPARY*, *FABP4*, *CD36* and *SLC7A8* was lower in the D0I BCH and +3DI BCH when compared with the untreated induced cells (Figure 5-7A, B, C & D, respectively). *PPARY* expression was lower in D0I BCH ( $p = 0.18$ ) and +3DI BCH ( $p = 0.20$ ) when compared with the untreated induced cells, and  $p = 3.20$  between D0I BCH and +3DI BCH (Figure 5-7A). D0I BCH expressed more *FABP4* than +3DI BCH ( $p = 0.46$ ) while *FABP4* was decreased in D0I BCH (0.20) and +3DI BCH ( $p = 0.19$ ) when compared with the untreated induced cells (Figure 5-7B). D0I BCH *CD36* expression was higher ( $p = 0.70$ ) than in +3DI BCH and the expression of D0I BCH ( $p = 0.39$ ) and +3DI BCH ( $p = 0.36$ ) was reduced in comparison to the untreated induced cells (Figure 5-7C). *SLC7A8* expression was similar between D0I BCH and +3DI BCH ( $p = 0.91$ ), and D0I BCH

( $p=0.24$ ) and +3DI BCH ( $p=0.47$ ) *SLC7A8* expression was lower than that observed in the untreated induced cells (Figure 5-7D). *PRDM16* expression was higher in +3DI BCH compared with DOI BCH ( $p=0.51$ ) and the untreated induced ( $p=0.36$ ) cells.  $P=0.91$  between DOI BCH and untreated induced (Figure 5-7E).

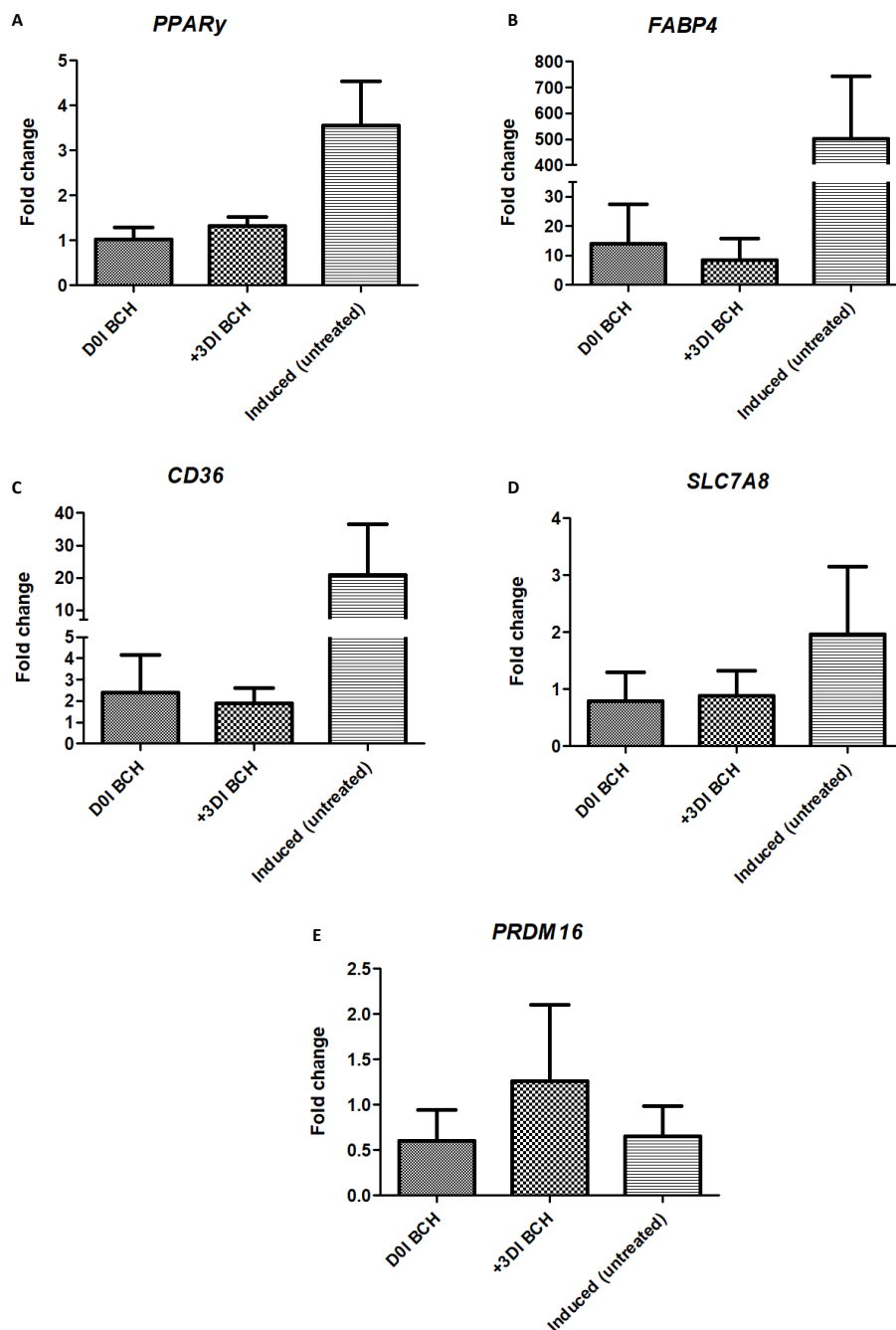


**Figure 5-7: Gene expression in adipogenic differentiated BCH-treated ASCs.** PPAR $\gamma$ ; A, FABP4; B, CD36; C and SLC7A8; D was higher in the untreated induced cells compared with the BCH treated cells. PRDM16 was higher in the +3DI BCH cells compared with the DOI and the untreated induced cells, E. N=3 for DOI BCH, +3DI BCH and induced (untreated).

## 5.5 Discussion

The prevalence of obesity continues to increase worldwide. Efforts to identify genes and proteins that are important in obesity to serve as potential therapeutic targets for alleviating the burden of disease are of paramount importance. Studies in our group have led to the identification of *Slc7a8* gene as important player in adipogenesis and functional studies has shown the deletion of this in a murine model significantly protects against diet induced obesity<sup>11</sup>. This study investigated the role of SLC7A8 in the early stages of adipogenesis by inhibiting its function with BCH treatment and semi-quantitatively analyse the overall effect on the formation of adipocytes. Additionally, the timing of inhibition of SLC7A8 function on the overall differentiation process was investigated.

To ensure that differentiation was successful and lipid droplets had formed in the differentiated cells (Figures 5-6A-G), non-induced cells (Figure 5-6H) which were grown in complete medium without adipogenic components were included in the study. The non-induced cells are illustrated by an auto-fluorescent signal on the cytoskeleton, with no formation of lipid droplets and adipocytes. Further analysis of differentiated cells showed that BCH treatment on the day of induction (DOI BCH) or 3 days post-induction (+3DI BCH) led to a decrease in lipid droplet accumulation in adipocytes which was significantly lower ( $p < 0.05$ ) SLC7A8 function was inhibited on the same day of adipogenic induction (DOI BCH). The inhibition of SLC7A8 function 3 days before induction (-3DI BCH) still led to similar amount of lipid droplets formed compared with those in the untreated induced cells (Figure 5-6). This suggests that the function of SLC7A8 protein is important for adipogenic differentiation and the inhibition of function to decrease adipogenesis is only effective when the differentiation process has been initiated. Moreover, the yield in lipid droplet formation appears to be greatly affected when SLC7A8 function is inhibited on day 0 than on day 3.

The expression of *PPARY* was downregulated in DOI BCH and +3DI BCH treated cells when compared with the untreated cells (Figure 5-7A). *PPARY* is the master regulator of adipogenesis and is a vital component in the differentiation of preadipocytes to mature adipocytes<sup>3-4</sup>. This indicates that SLC7A8 inhibition led to decrease expression of *PPARY*, resulting in a reduction in adipogenic differentiation potential of preadipocytes. This can be seen by the decrease in lipid droplet accumulation in the adipocytes formed in the BCH treated cells (Figures 5-7A, C and E) versus the untreated induced cells (Figure 5-7G). The expression of *FABP4* was downregulated in

both +3DI BCH and DOI BCH cells compared with untreated induced cells (Figure 5-7B). FABP4 is highly expressed in adipocytes and it is highly induced during adipogenic differentiation<sup>29</sup>. It is important in maintaining adipocyte homeostasis and regulating adipogenesis by interacting with *PPARY*<sup>30-31</sup>. Furthermore, it interacts with proteins such as CD36 to transport, import and metabolise lipids<sup>30,32</sup>. The expression of *CD36* was also downregulated in DOI BCH and +3DI BCH compared with untreated induced cells (Figure 5-7C). CD36 was previously showed to promote the differentiation of preadipocytes into mature adipocytes and its expression was upregulated following adipocyte differentiation<sup>33</sup>. Another study showed an increase in CD36 expression correlated with an increase in FABP4, and that CD36 interacts directly with FABP4 to facilitate fatty acid import, transport and metabolism<sup>34</sup>. These results demonstrates that the inhibition of SLC7A8 function in the early stages of differentiation greatly decreased lipid uptake and accumulation by downregulating lipid transporters (*FABP4* and *CD36*). The expression of *SLC7A8* was reduced in the +3DI BCH and DOI BCH in comparison to the untreated induced cells (Figure 5-7D). A previous study has shown that *PPARY* and the amino acid transporters L-type amino acid transporter 1 (LAT1) and LAT2/SLC7A8 have a relationship that is directly proportional in the human placenta<sup>29</sup>. The study demonstrated that *PPARY* stimulates LAT1 and LAT2, and when the expression of *PPARY* protein was downregulated, the expression of both LAT1 and LAT2 reduced<sup>29</sup>. Thus, the results corroborate with findings in this study where inhibition of SLC7A8 function with BCH treatment led to the downregulation of *PPARY* and *SLC7A8*. *PRDM16* expression was upregulated in the +3DI BCH cells when compared with the DOI BCH cells, and the untreated induced cells (Figure 5-7E) that both had similar expression levels. *PRDM16* induces thermogenesis and it is responsible for browning white adipose tissue<sup>35</sup>. In the brown and beige adipose tissues, *PRDM16* is highly expressed and it is a crucial component in maintaining proper structure and function of brown adipose phenotype<sup>35</sup>. Knockdown or knockout of *Prdm16* was shown to diminish the expression of brown adipose phenotype, without preventing overall adipogenesis<sup>36-37</sup>. Our results demonstrate that inhibiting SLC7A8 function in ASCs induced to undergo adipogenic differentiation such as in +3DI BCH cells promotes browning in addition to decreasing overall adipogenesis.

Overall, the results suggest that the amino acids transported by SLC7A8 are required for the differentiation of preadipocytes and that timing is critical to the function of SLC7A8 in the early stages of adipogenic differentiation as inhibition of function can only decrease adipogenesis (DOI

BCH) or could decrease adipogenesis while at the same time promote white adipose tissue browning (+3DI BCH), which will be more beneficial in combating obesity.

## 5.6 References

1. Xiao F, Guo F. Impacts of essential amino acids on energy balance. *Molecular Metabolism*. 2022; 57:101393. doi:10.1016/j.molmet.2021.101393
2. Chait A, den Hartigh LJ. Adipose tissue distribution, inflammation and its metabolic consequences, including diabetes and cardiovascular disease. *Frontiers in Cardiovascular Medicine*. 2020; 7:22. doi:10.3389/fcvm.2020.00022
3. Ghaben AL, Scherer PE. Adipogenesis and metabolic health. *Nature Reviews Molecular Cell Biology*. 2019; 20(4):242-58. doi:10.1038/s41580-018-0093-z
4. Rosen ED, Hsu CH, Wang X, Sakai S, Freeman MW, Gonzalez FJ, et al. C/ebpalpha induces adipogenesis through ppargamma: A unified pathway. *Genes & Development*. 2002; 16(1):22-6. doi:10.1101/gad.948702
5. Longo M, Zatterale F, Naderi J, Parrillo L, Formisano P, Raciti GA, et al. Adipose tissue dysfunction as determinant of obesity-associated metabolic complications. *International Journal of Molecular Sciences*. 2019; 20(9):2358.
6. Ambele MA, Dhanraj P, Giles R, Pepper MS. Adipogenesis: A complex interplay of multiple molecular determinants and pathways. *International Journal of Molecular Sciences*. 2020; 21(12) doi:10.3390/ijms21124283
7. Richon VM, Lyle RE, McGehee RE. Regulation and expression of retinoblastoma proteins p107 and p130 during 3t3-l1 adipocyte differentiation\*. *Journal of Biological Chemistry*. 1997; 272(15):10117-24. doi:<https://doi.org/10.1074/jbc.272.15.10117>
8. Rosen ED, Walkey CJ, Puigserver P, Spiegelman BM. Transcriptional regulation of adipogenesis. *Genes & Development*. 2000; 14(11):1293-307.
9. MacDougald OA, Lane MD. Transcriptional regulation of gene expression during adipocyte differentiation. *Annual Review of Biochemistry*. 1995; 64(1):345-73. doi:10.1146/annurev.bi.64.070195.002021
10. Ambele MA, Dessels C, Durandt C, Pepper MS. Genome-wide analysis of gene expression during adipogenesis in human adipose-derived stromal cells reveals novel patterns of gene expression during adipocyte differentiation. *Stem Cell Research & Therapy* 2016; 16(3):725-34. doi:10.1016/j.scr.2016.04.011
11. Pitere RR, van Heerden MB, Pepper MS, Ambele MA. Slc7a8 deletion is protective against diet-induced obesity and attenuates lipid accumulation in multiple organs. *Biology*. 2022; 11(2):311.
12. Bassi MT, Sperandeo MP, Incerti B, Bulfone A, Pepe A, Surace EM, et al. Slc7a8, a gene mapping within the lysinuric protein intolerance critical region, encodes a new member of the glycoprotein-associated amino acid transporter family. *Genomics*. 1999; 62(2):297-303. doi:<https://doi.org/10.1006/geno.1999.5978>



13. Rossier G, Meier C, Bauch C, Summa V, Sordat B, Verrey F, et al. Lat2, a new basolateral 4f2hc/cd98-associated amino acid transporter of kidney and intestine. *Journal of Biological Chemistry*. 1999; 274(49):34948-54. doi:10.1074/jbc.274.49.34948
14. Pineda M, Fernández E, Torrents D, Estévez R, López C, Camps M, et al. Identification of a membrane protein, lat-2, that co-expresses with 4f2 heavy chain, an I-type amino acid transport activity with broad specificity for small and large zwitterionic amino acids. *Journal of Biological Chemistry*. 1999; 274(28):19738-44. doi:10.1074/jbc.274.28.19738
15. Gwin JA, Church DD, Wolfe RR, Ferrando AA, Pasiakos SM. Muscle protein synthesis and whole-body protein turnover responses to ingesting essential amino acids, intact protein, and protein-containing mixed meals with considerations for energy deficit. *Nutrients*. 2020; 12(8) doi:10.3390/nu12082457
16. Cheng Y, Meng Q, Wang C, Li H, Huang Z, Chen S, et al. Leucine deprivation decreases fat mass by stimulation of lipolysis in white adipose tissue and upregulation of uncoupling protein 1 (ucp1) in brown adipose tissue. *Diabetes*. 2010; 59(1):17-25. doi:10.2337/db09-0929
17. Du Y, Meng Q, Zhang Q, Guo F. Isoleucine or valine deprivation stimulates fat loss via increasing energy expenditure and regulating lipid metabolism in wat. *Amino Acids*. 2012; 43(2):725-34. doi:10.1007/s00726-011-1123-8
18. Xiao F, Du Y, Lv Z, Chen S, Zhu J, Sheng H, et al. Effects of essential amino acids on lipid metabolism in mice and humans. *Journal of Molecular Endocrinology*. 2016; 57(4):223-31. doi:10.1530/jme-16-0116
19. Yu D, Richardson NE, Green CL, Spicer AB, Murphy ME, Flores V, et al. The adverse metabolic effects of branched-chain amino acids are mediated by isoleucine and valine. *Cell Metabolism*. 2021; 33(5):905-22.e6. doi:10.1016/j.cmet.2021.03.025
20. Zhou Z, Yin H, Guo Y, Fang Y, Yuan F, Chen S, et al. A fifty percent leucine-restricted diet reduces fat mass and improves glucose regulation. *Nutrition & Metabolism*. 2021; 18(1):34. doi:10.1186/s12986-021-00564-1
21. Green CR, Wallace M, Divakaruni AS, Phillips SA, Murphy AN, Ciaraldi TP, et al. Branched-chain amino acid catabolism fuels adipocyte differentiation and lipogenesis. *Nature Chemical Biology*. 2016; 12(1):15-21. doi:10.1038/nchembio.1961
22. Kim CS, Cho SH, Chun HS, Lee SY, Endou H, Kanai Y, et al. Bch, an inhibitor of system I amino acid transporters, induces apoptosis in cancer cells. *Biological and Pharmaceutical Bulletin*. 2008; 31(6):1096-100. doi:10.1248/bpb.31.1096
23. Nicklin P, Bergman P, Zhang B, Triantafellow E, Wang H, Nyfeler B, et al. Bidirectional transport of amino acids regulates mtor and autophagy. *Cell*. 2009; 136(3):521-34. doi:10.1016/j.cell.2008.11.044
24. Multilineage cells from human adipose tissue: Implications for cell-based therapies. *Tissue Engineering*. 2001; 7(2):211-28. doi:10.1089/107632701300062859

25. Adomshick V, Pu Y, Veiga-Lopez A. Automated lipid droplet quantification system for phenotypic analysis of adipocytes using cellprofiler. *Toxicology Mechanisms and Methods*. 2020; 30(5):378-87. doi:10.1080/15376516.2020.1747124
26. Rasband WS. Imagej, u.S. National Institutes of Health. 1997-2018; Bethesda, Maryland, USA(<https://imagej.nih.gov/ij/>, 1997-2018.)
27. Mollentze J. In vitro osteogenic differentiation of mesenchymal stem cells. Institute for Cellular and Molecular Medicine, Department of Immunology, University of Pretoria. 2022; Master's dissertation
28. Murdoch C. Asc immunophenotyping and differentiation data. Institute for Cellular and Molecular Medicine, University of Pretoria. 2020;
29. Furuhashi M, Saitoh S, Shimamoto K, Miura T. Fatty acid-binding protein 4 (fabp4): Pathophysiological insights and potent clinical biomarker of metabolic and cardiovascular diseases. *Clinical Medicine Insights: Cardiology*. 2014; 8(Suppl 3):23-33. doi:10.4137/cmc.S17067
30. Trojnar M, Patro-Małyśza J, Kimber-Trojnar Ż, Leszczyńska-Gorzela B, Mosiewicz J. Associations between fatty acid-binding protein 4—a proinflammatory adipokine and insulin resistance, gestational and type 2 diabetes mellitus. *Cells*. 2019; 8(3):227.
31. Prentice KJ, Saksi J, Hotamisligil GS. Adipokine fabp4 integrates energy stores and counterregulatory metabolic responses. *Journal of Lipid Research*. 2019; 60(4):734-40. doi:<https://doi.org/10.1194/jlr.S091793>
32. Gyamfi J, Yeo JH, Kwon D, Min BS, Cha YJ, Koo JS, et al. Interaction between cd36 and fabp4 modulates adipocyte-induced fatty acid import and metabolism in breast cancer. *Nature Partner Journals (NPJ) Breast Cancer*. 2021; 7(1):129. doi:10.1038/s41523-021-00324-7
33. Christiaens V, Van Hul M, Lijnen HR, Scroyen I. Cd36 promotes adipocyte differentiation and adipogenesis. *Biochimica et Biophysica Acta (BBA) - General Subjects*. 2012; 1820(7):949-56. doi:<https://doi.org/10.1016/j.bbagen.2012.04.001>
34. Gyamfi J, Yeo JH, Kwon D, Min BS, Cha YJ, Koo JS, et al. Interaction between cd36 and fabp4 modulates adipocyte-induced fatty acid import and metabolism in breast cancer. *npj Breast Cancer*. 2021; 7(1):129. doi:10.1038/s41523-021-00324-7
35. Ishibashi J, Seale P. Functions of prdm16 in thermogenic fat cells. *Temperature (Austin)*. 2015; 2(1):65-72. doi:10.4161/23328940.2014.974444
36. Harms MJ, Ishibashi J, Wang W, Lim HW, Goyama S, Sato T, et al. Prdm16 is required for the maintenance of brown adipocyte identity and function in adult mice. *Cell Metabolism*. 2014; 19(4):593-604. doi:10.1016/j.cmet.2014.03.007
37. Seale P, Kajimura S, Yang W, Chin S, Rohas LM, Uldry M, et al. Transcriptional control of brown fat determination by prdm16. *Cell Metabolism*. 2007; 6(1):38-54. doi:10.1016/j.cmet.2007.06.001

## Chapter 6. General discussion and conclusion

### 6.1 Discussion

The prevalence of obesity is expected to increase over the next few years affecting approximately 18% of men and more than 21% of women by the year 2025, while affecting over 250 million children and adolescents by 2030<sup>1-2</sup>. The fundamental cause of obesity is excessive consumption of calories and reduced energy expenditure, resulting in adipose tissue expansion arising from an increase in adipocyte hypertrophy or hyperplasia<sup>3-5</sup>. In an effort to continuously identify genes and transcription factors involved in adipogenesis, *SLC7A8* was identified as a potential early marker of adipogenesis in a transcriptome analysis of human ASCs and was also observed to share common pathways with obesity-related pathophysiological conditions<sup>6</sup>. *SLC7A8* is a transporter of neutral amino acids such as tyrosine, tryptophan and leucine<sup>7</sup>. Solute Carrier proteins such as *SLC7A5*, *SLC7A10* and *SLC7A11* which belong to the same superfamily as *SLC7A8*, have previously been shown to play a role in adipogenesis and/or the onset of obesity<sup>8-11</sup>. A previous study showed that a decrease in amino acid transport by *SLC7A5* resulted in impaired mTORC1 signalling which subsequently led to the metabolic dysregulation observed in obesity<sup>12</sup>. Considering that *SLC7A8* had neither been described in the context of obesity nor adipogenesis, we sought to annotate its functional role in obesity and adipogenesis.

The findings reported in Chapter 3 demonstrated a strong correlation between the presence of the *Slc7a8* gene and obesity, supporting the hypothesis that this gene is involved in obesity development. The results showed that the deletion of *Slc7a8* in mice subjected to conditions of diet-induced obesity led to significant reduction in weight gain ( $p < 0.001$ ), accompanied by significant attenuation of adipocyte hypertrophy in the perigonadal, inguinal subcutaneous, mesenteric and brown adipose depots, reduced lipid accumulation in non-lipid storage tissues and organs (i.e. liver, gastrocnemius muscle, heart, brain, kidney, lungs), improved glucose tolerance, and decreased macrophage infiltration into adipose tissues. Overall, the results obtained clearly demonstrate a role of *Slc7a8* in obesity development, which had not previously been described prior to this study. This important finding on *Slc7a8* role in obesity development led to further investigation in Chapter 4 of the possible molecular mechanisms underlying the prevention of adipocyte hypertrophy in the various adipose tissue depots of *Slc7a8* knockout mice and how the

effect it has on circulating plasma hormones, lipid and cytokines, which are important biochemical parameters that are dysregulated in obesity.

The findings reported in Chapter 4 show that the mechanism of prevention of adipocyte hypertrophy in *Slc7a8* knockout mouse varies across the perigonadal, mesenteric and brown adipose depots. In pWAT and BAT, prevention of adipocyte hypertrophy seemed to occur because of increased lipolytic activity in addition to increased thermogenic activity in BAT, while in mWAT, it was due to reduced lipid uptake into the adipose tissue. Moreover, prevention of adipocyte hypertrophy in the *Slc7a8* knockout phenotype significantly improved metabolic profiles of adiponectin and leptin, while promoting the anti-inflammatory cytokines and decreasing pro-inflammatory cytokines response in obesity development. Thus, targeting *Slc7a8* not only significantly protects against diet induced obesity development through a fat-depot specific mechanism of preventing adipocyte hypertrophy, but also reverses the negative effect of metabolic dysregulation and inflammation profiles that characterize obesity development.

Finally, the effect of inhibiting *SLC7A8* function in ASCs during adipogenic differentiation was assessed in Chapter 5. The results showed inhibition of *SLC7A8* function reduced lipid droplet formation, reduced adipogenic capacity and decreased adipocytes formation in cells induced to undergo adipogenic differentiation. Furthermore, it was observed that the timing of inhibiting *SLC7A8* function during the early stages of adipogenesis seems to be crucial in the way in which it affects the differentiation process. Inhibition of *SLC7A8* function either on day 0 (day of induction) or day 3 post-adipogenic induction led to reduced lipid formation in the mature adipocytes with a corresponding downregulation in *PPARY*, *FABP4* and *CD36* expression when compared with untreated control induced cells. The reduction in lipid accumulation in mature adipocytes was significant when inhibition occurred on day 0 of adipogenic induction. Conversely, the inhibition of *SLC7A8* function in cells prior to them being induced to differentiate did not affect the formation of mature adipocytes as lipid accumulation was similar to that in induced untreated control. This strongly suggest *SLC7A8* function in adipogenesis is critical when the differentiation process has been initiated. Importantly, the inhibition of *SLC7A8* function on day 3 of adipogenic differentiation led to increase in preadipocyte browning activity via the upregulation of *PRDM16*, whose expression levels did not change between day 0 *SLC7A8* inhibition and untreated control differentiated cells. This observation is very significant in targeting *SLC7A8* function in modulating

lipid accumulation as it suggests inhibition of function on day 3 not only decreases adipogenic capacity, but in addition may also increase the formation of beige adipocytes within white adipose depots, thereby mitigating the potential of adipose tissue dysfunction in obesity development.

## **6.2 Conclusion**

Even with an increase in the number of anti-obesity drugs available on the market, the prevalence and incidence of obesity keeps rising globally. Therefore, it is important to continuously search for new molecular targets for anti-obesity drug development. Bearing in mind that obesity is a systemic disease, the current study has demonstrated the potential clinical utility of *SLC7A8* as a suitable therapeutic target for anti-obesity drug development that specifically target the prevention of adipocyte hypertrophy in various fat depots, reduce lipid accumulation in various body tissues and organs while at the same time improving metabolic health and decreasing inflammation that contributes to the pathophysiology of obesity.

## **6.3 Limitations of the study**

1. The study focused mainly on annotating the functional role of *SLC7A8* in obesity development and thus the role of *SLC7A8* in various gene-gene interactions and other molecular pathways was not investigated.
2. Subcutaneous adipose tissue was not included in the study, and it is an important depot in the onset of obesity. Including this tissue would have provided additional knowledge on the possible mechanism of adipocyte hypertrophy prevention in this depot which is primary site for lipid storage in obesity development.
3. Some data lacked statistical support for the differences. To potentially improve this in future, the study duration may be elongated longer than 14 weeks for the mouse studies. For BCH-related studies, a higher concentration or volume can be explored for *SLC7A8* inhibition.

#### 6.4 Future studies

1. To investigate the role of *SLC7A8* in nutrient signalling pathways such as the mTOR signalling pathway which is important in adipose tissue biology and obesity development.
2. To use radiolabelled amino acid uptake assays to characterise the amino acids transported by *SLC7A8* and taken up by adipocytes during adipogenesis.
3. For therapeutic purposes, it will be important to explore miRNA or siRNA knockdown of *SLC7A8* or functional inhibition of the protein in condition of obesity development and to determine whether it would yield similar results as observed in the knockout model. This would aid to inform of the potential of miRNA or siRNA therapeutics for alleviating obesity and/or improving metabolic health.

## 6.5 References

1. Collaboration NCDRF. Trends in adult body-mass index in 200 countries from 1975 to 2014: A pooled analysis of 1698 population-based measurement studies with 19.2 million participants. *Lancet*. 2016; 387(10026):1377-96. doi:10.1016/S0140-6736(16)30054-X
2. World Obesity Federation W. Global atlas on childhood obesity. <https://www.worldobesity.org/membersarea/global-atlas-on-childhood-obesity>. 2022; Accessed 16 May 2022
3. Hill JO, Wyatt HR, Peters JC. The importance of energy balance. *European endocrinology*. 2013; 9(2):111-5. doi:10.17925/EE.2013.09.02.111
4. Longo M, Zatterale F, Naderi J, Parrillo L, Formisano P, Raciti GA, et al. Adipose tissue dysfunction as determinant of obesity-associated metabolic complications. *International Journal of Molecular Sciences*. 2019; 20(9):2358.
5. Chait A, den Hartigh LJ. Adipose tissue distribution, inflammation and its metabolic consequences, including diabetes and cardiovascular disease. *Frontiers in Cardiovascular Medicine*. 2020; 7:22. doi:10.3389/fcvm.2020.00022
6. Ambele MA, Dessels C, Durandt C, Pepper MS. Genome-wide analysis of gene expression during adipogenesis in human adipose-derived stromal cells reveals novel patterns of gene expression during adipocyte differentiation. *Stem Cell Research & Therapy* 2016; 16(3):725-34. doi:10.1016/j.scr.2016.04.011
7. Rossier G, Meier C, Bauch C, Summa V, Sordat B, Verrey F, et al. Lat2, a new basolateral 4f2hc/cd98-associated amino acid transporter of kidney and intestine \*. *Journal of Biological Chemistry*. 1999; 274(49):34948-54. doi:10.1074/jbc.274.49.34948
8. Hediger MA, Cl  men  on B, Burrier RE, Bruford EA. The abcs of membrane transporters in health and disease (slc series): Introduction. *Molecular Aspects of Medicine*. 2013; 34(2-3):95-107. doi:10.1016/j.mam.2012.12.009
9. Pizzagalli MD, Bensimon A, Superti-Furga G. A guide to plasma membrane solute carrier proteins. *The FEBS Journal*. 2021; 288(9):2784-835. doi:10.1111/febs.15531
10. Jin C, Zhang P, Zhang M, Zhang X, Lv L, Liu H, et al. Inhibition of slc7a11 by sulfasalazine enhances osteogenic differentiation of mesenchymal stem cells by modulating bmp2/4 expression and suppresses bone loss in ovariectomized mice. *Journal of Bone and Mineral Research*. 2017; 32(3):508-21. doi:10.1002/jbmr.3009

11. Jersin RÅ, Tallapragada DSP, Madsen A, Skartveit L, Fjære E, McCann A, et al. Role of the neutral amino acid transporter slc7a10 in adipocyte lipid storage, obesity, and insulin resistance. *Diabetes*. 2021; 70(3):680-95. doi:10.2337/db20-0096
12. O'Brien A, Loftus RM, Pisarska MM, Tobin LM, Bergin R, Wood NAW, et al. Obesity reduces mtorc1 activity in mucosal-associated invariant t cells, driving defective metabolic and functional responses. *The Journal of Immunology*. 2019; 202(12):3404-11. doi:10.4049/jimmunol.1801600



# Appendix 1. Research ethics certificate



Faculty of Health Sciences

**Institution:** The Research Ethics Committee, Faculty Health Sciences, University of Pretoria complies with ICH-GCP guidelines and has US Federal wide Assurance.

- FWA 00002557, Approved dd 18 March 2022 and Expires 18 March 2027.
- IORG # IORG0001762 OMB No. 0990-0278 Approved for use through August 31, 2023.

Faculty of Health Sciences **Research Ethics Committee**

16 February 2023

## Approval Certificate Annual Renewal

Dear Ms RR Pitere,

**Ethics Reference No.:** 474/2019 – Line 5

**Title:** The role of Solute Carrier Family 7 Member 8 gene in adipogenesis in vitro and murine model of obesity

The **Annual Renewal** as supported by documents received between 2023-01-18 and 2023-02-15 for your research, was approved by the Faculty of Health Sciences Research Ethics Committee on 2023-02-15 as resolved by its quorate meeting.

Please note the following about your ethics approval:

- Renewal of ethics approval is valid for 1 year, subsequent annual renewal will become due on 2024-02-16.
- Please remember to use your protocol number (474/2019) on any documents or correspondence with the Research Ethics Committee regarding your research.
- Please note that the Research Ethics Committee may ask further questions, seek additional information, require further modification, monitor the conduct of your research, or suspend or withdraw ethics approval.

**Ethics approval is subject to the following:**

- The ethics approval is conditional on the research being conducted as stipulated by the details of all documents submitted to the Committee. In the event that a further need arises to change who the investigators are, the methods or any other aspect, such changes must be submitted as an Amendment for approval by the Committee.

We wish you the best with your research.

Yours sincerely



On behalf of the FHS REC, Dr R Sommers

MBChB, MMed (Int), MPharmMed, PhD

Deputy Chairperson of the Faculty of Health Sciences Research Ethics Committee, University of Pretoria

*The Faculty of Health Sciences Research Ethics Committee complies with the SA National Act 61 of 2003 as it pertains to health research and the United States Code of Federal Regulations Title 45 and 46. This committee abides by the ethical norms and principles for research, established by the Declaration of Helsinki, the South African Medical Research Council Guidelines as well as the Guidelines for Ethical Research: Principles Structures and Processes, Second Edition 2015 (Department of Health)*

Research Ethics Committee  
Room 4-60, Level 4, Tavelopela Building  
University of Pretoria, Private Bag 3323  
Oezha 0031, South Africa  
Tel: +27 (0)12 358 3084  
Email: [depeeka.behari@up.ac.za](mailto:depeeka.behari@up.ac.za)  
[www.up.ac.za](http://www.up.ac.za)

Fakulteit Gesondheidswetenskappe  
Lefapha la Ditsaane ea Maphelo

## Appendix 2. Animal ethics certificate



Faculty of Veterinary Science  
Animal Ethics Committee

21 April 2023

### Approval Certificate Annual Renewal (EXT4)

**AEC Reference No.:** 474/2019 Line 5  
**Title:** The role of Solute Carrier Family 7 Member 8 gene in adipogenesis in vitro and murine model of obesity  
**Researcher:** Ms RR Pitere  
**Student's Supervisor:** Dr MA Ambele

Dear Ms RR Pitere,

The **Annual Renewal** as supported by documents received between 2023-02-24 and 2023-03-27 for your research, was approved by the Animal Ethics Committee on its quorate meeting of 2023-03-27.

Please note the following about your ethics approval:

1. The use of species is approved:

Species	Approved
Mice - C57BL/6J (Not in Use)	96
Samples	Approved
Mouse - Blood and organs Live (Not in Use)	0

2. Ethics Approval is valid for 1 year and needs to be renewed annually by 2024-04-21.
3. Please remember to use your protocol number (474/2019) on any documents or correspondence with the AEC regarding your research.
4. Please note that the AEC may ask further questions, seek additional information, require further modification, monitor the conduct of your research, or suspend or withdraw ethics approval.
5. All incidents must be reported by the PI by email to Ms Marleze Rheeder (AEC Coordinator) within 3 days, and must be subsequently submitted electronically on the application system within 14 days.
6. The committee also requests that you record major procedures undertaken during your study for own-archiving, using any available digital recording system that captures in adequate quality, as it may be required if the committee needs to evaluate a complaint. However, if the committee has monitored the procedure previously or if it is generally can be considered routine, such recording will not be required.

Ethics approval is subject to the following:

- The ethics approval is conditional on the research being conducted as stipulated by the details of all documents submitted to the Committee. In the event that a further need arises to change who the investigators are, the methods or any other aspect, such changes must be submitted as an Amendment for approval by the Committee.

Room 8-13, Arnold Theiler Building, Onderstepoort  
Private Bag X04, Onderstepoort 0110, South Africa  
Tel +27 12 529 8434  
Fax +27 12 529 8321  
Email: marleze.rheeder@up.ac.za

Fakulteit Veeartsenynkunde  
Lefapha la Ditseanse tsa Bongakadinswa

We wish you the best with your research.

Yours sincerely



**Prof. V. Naidoo**  
**CHAIRMAN: UP-Animal Ethics Committee**

---

Room 6-15, Arnold Theiler Building, Onderstepoort  
Private Bag X04, Onderstepoort 0110, South Africa  
Tel +27 12 529 8434  
Fax +27 12 529 8321  
Email: [marieze.rheader@up.ac.za](mailto:marieze.rheader@up.ac.za)

Fakulteit Veterinêre Geneeskunde  
Lefapha la Disanso tsa Bongakredithuwa

**Appendix 3. Biostatistician letter of clearance**

Date: 25 / 2 / 2019

**LETTER OF CLEARANCE FROM THE BIOSTATISTICIAN**

This letter is to confirm that,

Name(s): Miss RANBETSWA PITHEE

from the University of PRETORIA

discussed with me the study titled \_\_\_\_\_

I hereby confirm that I am aware of the project and also undertake to assist, if possible, with the Statistical analysis of the data generated from the project.

The analytical tool(s) that will be used is (are) Descriptive Statistics, ANCOVA, multivariable regression, Logistic regression

to achieve the objective(s) of the study.

Name: PJ Becker (Tel: 012-319-2203)

Signature \_\_\_\_\_  
Research Office,  
Faculty of Health Sciences, UP

BIOSTATISTICS  
Faculty of Health Sciences  
Research Office  
2019 -02- 25  
UNIVERSITY OF PRETORIA

## Appendix 4. Proof of manuscript submission

13/03/2023, 09:53

University of Pretoria Mail - [Genes] Manuscript ID: genes-2302882 - Submission Received



Reabetswe Pitere <u10228188@tuks.co.za>

### [Genes] Manuscript ID: genes-2302882 - Submission Received

1 message

Editorial Office <genes@mdpi.com>

9 March 2023 at 12:25

Reply-To: genes@mdpi.com

To: Reabetswe Pitere <u10228188@tuks.co.za>

Cc: "Reabetswe R. Pitere" <reabetswe.pitere@tuks.co.za>, Michael Sean Pepper <michael.pepper@up.ac.za>, Melvin Ambele <melvin.ambele@up.ac.za>

Dear Ms. Pitere,

Thank you very much for uploading the following manuscript to the MDPI submission system. One of our editors will be in touch with you soon.

Journal name: Genes

Manuscript ID: genes-2302882

Type of manuscript: Article

Title: Investigating the mechanism of Slc7a8 deletion on the prevention of adipocyte hypertrophy and its effect on plasma metabolite levels

Authors: Reabetswe R. Pitere, Michael Sean Pepper, Melvin Ambele \*

Received: 9 March 2023

E-mails: [reabetswe.pitere@tuks.co.za](mailto:reabetswe.pitere@tuks.co.za), [michael.pepper@up.ac.za](mailto:michael.pepper@up.ac.za), [melvin.ambele@up.ac.za](mailto:melvin.ambele@up.ac.za)

You can follow progress of your manuscript at the following link (login required):

[https://susy.mdpi.com/user/manuscripts/review\\_info/9489bd8d8f778a20ea773c5ac41943a5](https://susy.mdpi.com/user/manuscripts/review_info/9489bd8d8f778a20ea773c5ac41943a5)

The following points were confirmed during submission:

1. Genes is an open access journal with publishing fees of 2400 CHF for an accepted paper (see <https://www.mdpi.com/about/apc/> for details). This manuscript, if accepted, will be published under an open access Creative Commons CC BY license (<https://creativecommons.org/licenses/by/4.0/>), and I agree to pay the Article Processing Charges as described on the journal webpage (<https://www.mdpi.com/journal/genes/apc>). See <https://www.mdpi.com/about/openaccess> for more information about open access publishing.

Please note that you may be entitled to a discount if you have previously received a discount code or if your institute is participating in the MDPI Institutional Open Access Program (IOAP), for more information see <https://www.mdpi.com/about/ioap>. If you have been granted any other special discounts for your submission, please contact the Genes editorial office.

2. I understand that:

a. If previously published material is reproduced in my manuscript, I will provide proof that I have obtained the necessary copyright permission. (Please refer to the Rights & Permissions website: <https://www.mdpi.com/authors/rights>).

b. My manuscript is submitted on the understanding that it has not been published in or submitted to another peer-reviewed journal. Exceptions to this rule are papers containing material disclosed at conferences. I confirm that I will inform the journal editorial office if this is the case for my manuscript. I confirm that all authors are familiar with and agree with submission of the contents of the manuscript. The journal editorial office reserves the right to contact all authors to confirm this in case of doubt. I will provide email addresses for all authors and an institutional e-mail address for at least one of the co-authors, and specify the name, address and e-mail for invoicing purposes.

<https://mail.google.com/mail/u/1/?ik=98fab29b31&view=pt&search=all&permthid=thread-f%3A1759885434569665222&siml=msg-f%3A1759885...> 1/2

13/03/2023, 09:53

University of Pretoria Mail - [Genes] Manuscript ID: genes-2302882 - Submission Received

If you have any questions, please do not hesitate to contact the Genes editorial office at [genes@mdpi.com](mailto:genes@mdpi.com)

Kind regards,  
Genes Editorial Office  
St. Alban-Anlage 66, 4052 Basel, Switzerland  
E-Mail: [genes@mdpi.com](mailto:genes@mdpi.com)  
Tel. +41 61 683 77 34  
Fax: +41 61 302 89 18

\*\*\* This is an automatically generated email \*\*\*

<https://mail.google.com/mail/u/1/?ik=98fab29b31&view=pt&search=all&permthid=thread-f%3A1759885434569665222&simpl=msg-f%3A1759885...> 2/2